The Asymmetric Desymmetrisation of *Meso* Compounds

A thesis submitted in partial
fulfilment of the degree of PhD

Benjamin I. Andrews

University of Sheffield
Brook Hill
Sheffield
S3 7HF

September 2000

Abstract

This thesis is concerned with the asymmetric desymmetrisation of *meso* compounds. It commences with an introduction to the areas of two-directional synthesis and asymmetric desymmetrisation. This is followed by a review of asymmetric desymmetrisation of achiral and *meso* compounds, illustrating the power of this technique and the diversity of substrates and reagents that can be employed.

Chapter one details the asymmetric desymmetrisation of centrosymmetric *meso* 2-pyridone [4 + 4]-photodimer derivatives, as a strategy towards the synthesis of functionalised amino acids. The reductive enantioselective desymmetrisation of *N*-Boc tetrahydro photodimer **227** using Corey's oxazaborolidine catalyst **236** was achieved in good yield (76%) and excellent ee (≥97%), representing the first ever asymmetric desymmetrisation of a centrosymmetric compound.

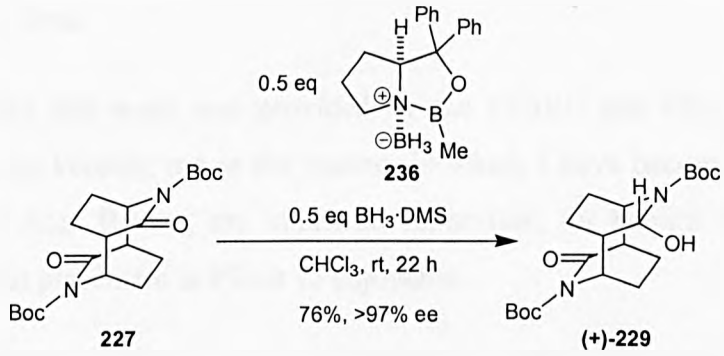

Chapter two details the synthesis and asymmetric desymmetrisation of *meso* decalin diallylc alcohols as part of a strategy towards the synthesis of core structures of bioactive *Celastraceae* sesquiterpenes. The two-directional synthesis of diallylic alcohol **298** (a classical *meso* compound containing a plane of symmetry) was completed and its subsequent desymmetrisation using a novel Zr modified Sharpless asymmetric epoxidation proceeded in reasonable yield (54%) and excellent ee (≥95%).

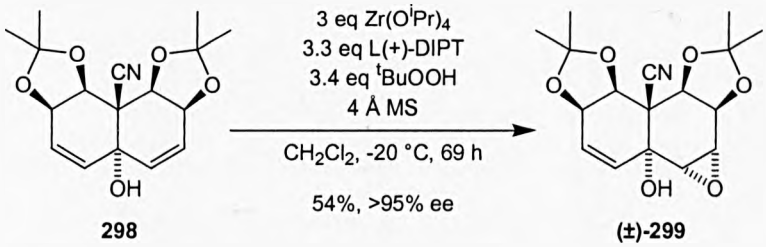

Acknowledgements

First and foremost, I would like to thank my supervisor Dr Alan Spivey for being a constant source of inspiration, motivation, and encouragement over the last few years, to whom I am very grateful.

Thanks also go to members of the Spivey group, past and present; to Dr Steven Woodhead and Matthew Weston for their work towards the synthesis and desymmetrisation of decalin diallylic alcohols, without which my work in this area would not have been possible; to Iain Lingard, an MChem project student, for his help with some of the α-methyl substituted photodimer work; and to all the other members of the group who helped to make E39 and D32/36 a nice environment to work in.

I would also like to thank the numerous staff and technicians in the Department of Chemistry at the University of Sheffield for their 'behind the scenes' work, which made it possible for this chemistry to be done.

Financial support for this work was provided by the EPSRC and Pfizer, and my grateful thanks go to them for keeping me in the manner in which I have become accustomed. I am also grateful to Dr Alan Brown, my industrial supervisor, for helpful discussions and for making my industrial placement at Pfizer so enjoyable.

Thanks also go to Prof Chris Frampton at Roche for his constant enthusiasm in running our x-ray crystal structures, to Chiroscience for their attempts at desymmetrisating the *N*-H photodimer using lactamases, and to Kevin Rushby for his kind permission to use the 'khat' picture from his book *Eating the Flowers of Paradise*, Flamingo, **1998**, ISBN 0006530885.

Finally, I would like to thank my girlfriend Anne Cutting for her love and support over the last four years, and it is to her that this thesis is dedicated.

Ben Andrews

Contents

Abbreviations

Ac	acetyl
acac	acetylacetonate
Ar	aryl
ax	axial
bp	boiling point
BINAL	2,2'-dihydroxy-1,1'-binaphthyl-lithium aluminium hydride
BINAP	2,2'-bis(diphenylphosphino)-1,1'-binaphthyl
BINOL	binaphthol
Boc	*tert*-butyloxycarbonyl
br	broad
Bn	benzyl
BOM	benzyloxymethyl
^{n}Bu	*normal*-butyl
^{t}Bu	*tert*-butyl
Bz	benzoyl
CAN	ceric ammonium nitrate
cat.	catalytic
CBS	Corey-Bakshi-Shibata
Celite™	high grade diatomaceous earth used as a filter aid
cod	cyclooctadiene
CSA	camphorsulfonic acid
d	doublet
dba	dibenzylideneacetone
DBN	1,5-diazabicyclo[4.3.0]non-5-ene
DBU	1,8-diazabicyclo[5.4.0]undec-7-ene
DCC	dicyclohexylcarbodiimide

DCHT	dicyclohexyl tartrate
DDO	dimethyldioxirane
de	Diastereomeric excess
DHQ	dihydroquinine
DIBAL	diisobutylaluminium hydride
DIOP	2,3-*O*-isopropylidine-2,3-dihydroxy-1,4-bis(diphenylphosphino)butane
DIPT	diisopropyl tartrate
DMAP	4-dimethylaminopyridine
DMF	dimethylformamide
DMP	2,2-dimethoxypropane
DMS	dimethylsulfide
DMSO	dimethylsulfoxide
DPP	diphenylphosphinyl
dr	diastereomeric ratio
ee	enantiomeric excess
e.g.	*exempli gratia* (Latin: 'for example')
eq	equatorial
Et	ethyl
i.e.	*id est* (Latin: 'that is')
h	hours
HPLC	high performance liquid chromatography
HMPA	hexamethylphosphoric acid triamide
IPA	isopropyl alcohol
Ipc	isocamphenyl
KHMDS	potassium hexamethyldisilazide
LDA	lithium diisopropylamine
LHMDS	lithium hexamethyldisilazide

mCPBA	*m*-chloroperbenzoic acid
Me	methyl
MEM	(2-methoxyethoxy)methyl
MOM	methoxymethyl
mp	melting point
Ms or mesyl	methanesulfonyl
MS	mass spectrometry
MS	molecular sieves
NBS	*N*-bromosuccinimide
NMO	*N*-methylmorpholine *N*-oxide
NMP	*N*-methylpyrrolidin-2-one
NMR	nuclear magnetic resonance
Nu	nucleophile
Ph	phenyl
PPTS	pyridinium *p*-toluenesulfonate
^{i}Pr	*iso*-propyl
pybox	2,6-bis[4'(*S*)-isopropyloxazolin-2'-yl]pyridine
PYR	diphenylpyrimidine
q	quartet
R_f	retention factor
rt	room temperature
s	singlet
t	triplet
TBAF	tetrabutylammonium fluoride
TBS	*tert*-butyldimethylsilyl
TBDMS	see TBS
Tf or triflate	trifluoromethanesulfonyl

TFA	trifluoroacetic acid
THF	tetrahydrofuran
TLC	thin layer chromatography
TMS	trimethylsilyl
Ts or tosyl	*para*-toluenesulfonyl
UHP	urea-hydrogen peroxide complex

Chapter 1: Asymmetric Desymmetrisation of Achiral or Meso Compounds

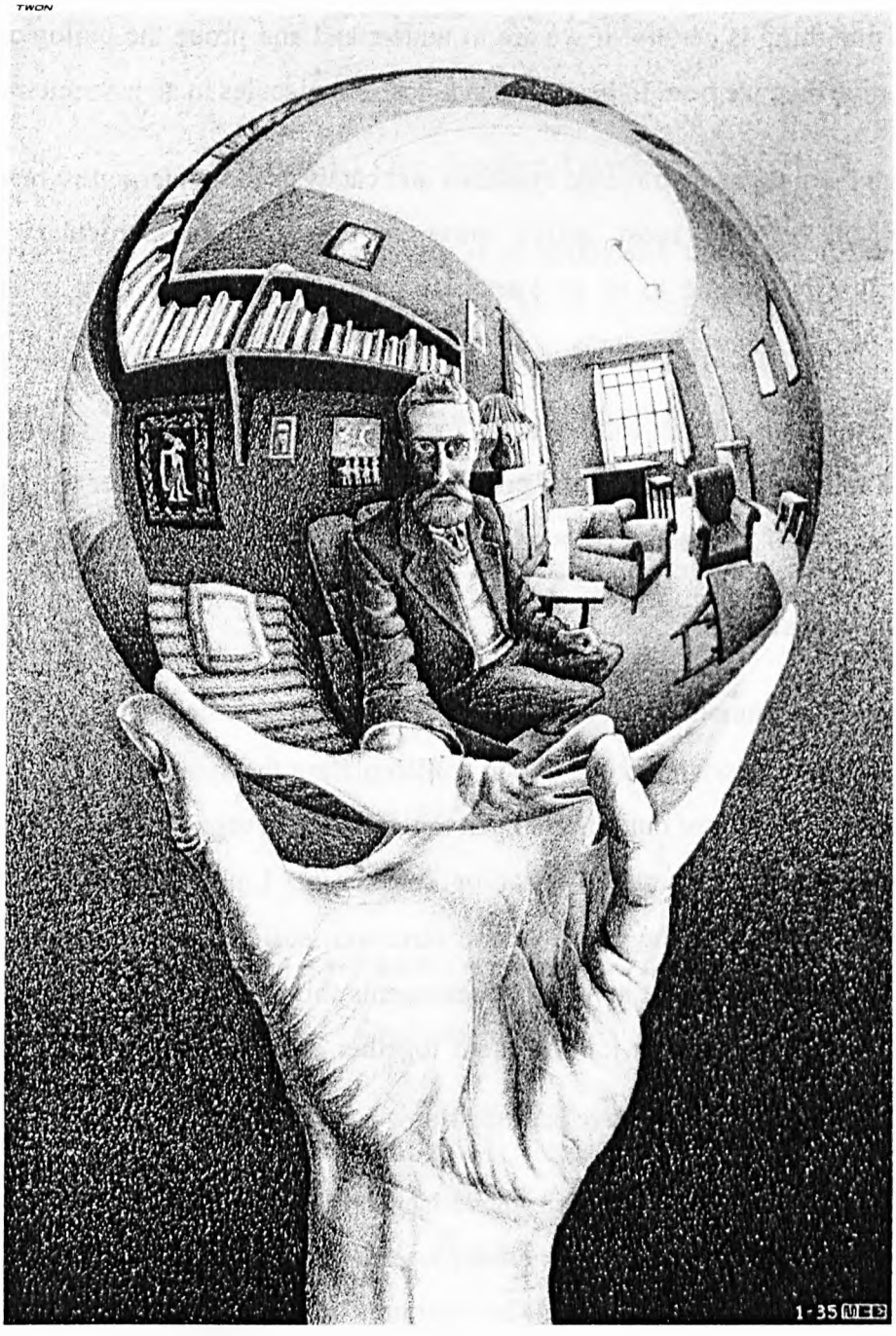

M. C. Escher contemplating the mysteries of symmetry and mirror planes.

Chapter 1: Asymmetric Desymmetrisation of Achiral or Meso Compounds

We live in a chiral Universe. All known forms of life, from the very simplest to the most complex, are composed from optically active molecules. The origin of this chirality is as yet a mystery, but one thing is certain: if we are to understand and probe the biological processes that keep us alive then we need to be able to synthesise molecules in an asymmetric fashion.

In recent years the field of asymmetric synthesis and catalysis has undergone a revolution, and is currently one of the most active areas of research. In particular, asymmetric desymmetrisation is proving to be an extremely powerful strategy for the enantioselective synthesis of complex natural products.

It is the purpose of this chapter to review the technique of asymmetric desymmetrisation and topics related to it, and to illustrate the power of the technique by reference to some of the numerous examples of this method at work.

Two-directional synthesis

Before defining asymmetric desymmetrisation, its original context of two-directional synthesis must first be understood.[1,2] When contemplating the synthesis of long 'chain like' natural products, a number of options are open to the synthetic organic chemist. Classical one-directional synthesis can be either linear or convergent. Linear synthesis, involving the sequential homologation of the chain in one direction, suffers from low efficiency as the yields are in series. Convergent synthesis circumvents this problem by synthesising sections of the molecule in parallel and joining them together at a late stage, resulting in a more efficient process (scheme 1.1).

Linear synthesis

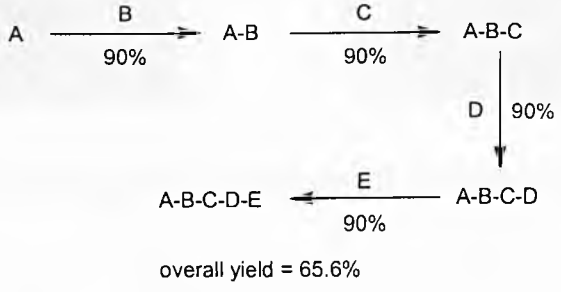

Convergent synthesis

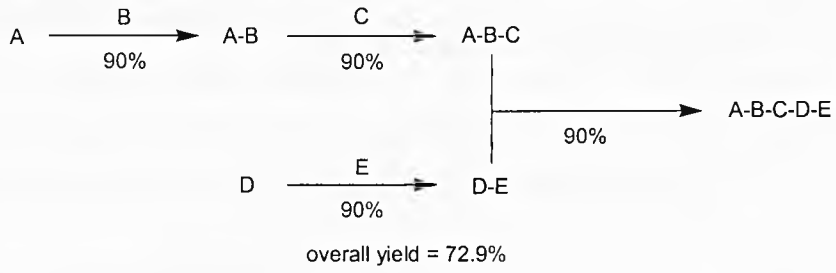

Scheme 1.1 One-directional synthesis

An alternative to the one-directional strategy is to synthesise the chain in two directions, either sequentially or simultaneously. Sequential homologation is no more efficient than linear synthesis. However, simultaneous two-directional synthesis offers significant advantages as it involves fewer synthetic steps and is therefore more efficient (scheme 1.2).

Sequential synthesis

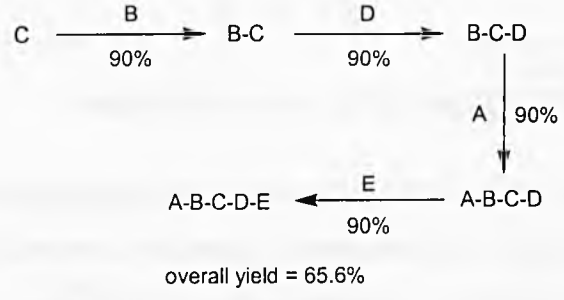

Simultaneous synthesis

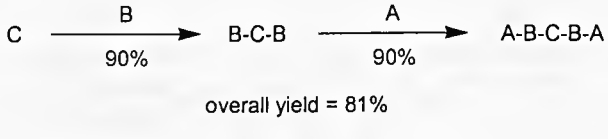

Scheme 1.2 Two-directional synthesis

It is evident that the power of two-directional synthesis lies in the simultaneous synthesis of symmetrical molecules. However, few natural products are completely symmetrical, so there emerges a need to desymmetrise these symmetrical chains, i.e. differentiate between the two chain termini. As a result, the fields of two-directional synthesis and desymmetrisation are intimately linked. Schreiber, in his seminal paper, identifies three classes of molecule that lend themselves to this strategy, and outlines their requirements for two-directional chain synthesis and terminus differentiation.[2] All three classes are elongated using standard synthetic techniques in a simultaneous two-directional fashion. Where they differ is in the

techniques employed to generate new stereocentres and to achieve the final desymmetrisation. With all three classes it is desirable to preserve the symmetry for as long as possible in the synthesis before carrying out the final desymmetrisation.

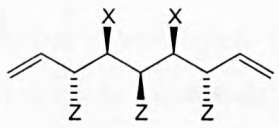

Figure 1.1 Achiral and *meso* chains

Achiral and *meso* chains are elongated with substrate control where new stereocentres are formed, in order to preserve the C_s symmetry. The chain termini of these molecules are enantiotopic and therefore can be differentiated using reagent control (i.e. asymmetric desymmetrisation).

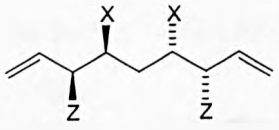

Figure 1.2 C_2 symmetric chains

The elongation of C_2 symmetric chains can proceed with either substrate or reagent control. The chain termini are identical (i.e. homotopic), therefore desymmetrisation can be achieved simply by monofunctionalisation, as altering either of the chain termini gives the same product.

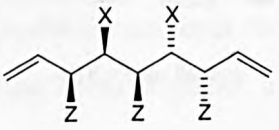

Figure 1.3 Pseudo C_2 symmetric chains

Pseudo C_2 symmetric chains have a central chirotopic (or pseudoasymmetric) carbon which is non-stereogenic. As a result, chain elongation must proceed with reagent control. Desymmetrisation can be achieved by diastereotopic group selection of one terminus over the other.

Of the three classes, the asymmetric desymmetrisation of achiral and *meso* chains finds by far the greatest application in organic chemistry, and this will be the focus of the remainder of this chapter.

Asymmetric desymmetrisation

Asymmetric desymmetrisation can be defined as the enantio (or diastereo) selective loss of symmetry of an achiral or *meso* compound by the use of a chiral reagent or catalyst. To achieve this the reagent must be able to differentiate between two enantiotopic faces or enantiotopic groups. This leads to four possible scenarios (scheme 1.3).

Differentiation of enantiotopic faces

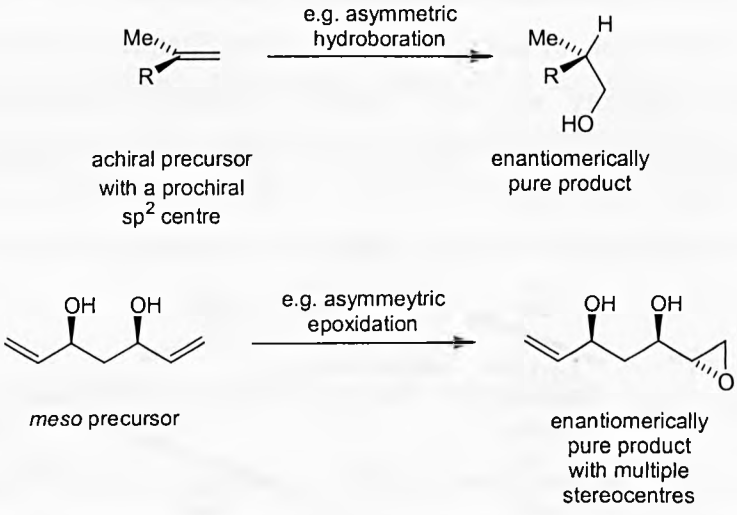

Differentiation of enantiotopic groups

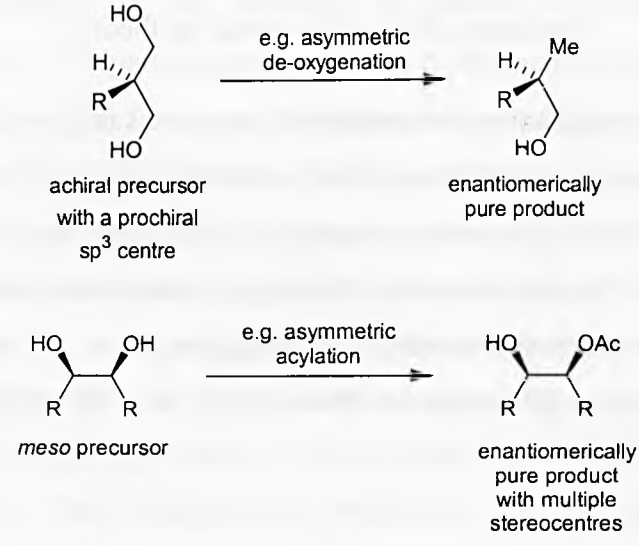

Scheme 1.3 Asymmetric desymmetrisation

It is evident that *meso* compounds offer an advantage over achiral compounds in that multiple stereocentres are established in a single desymmetrisation step. Therefore this strategy is of great significance and utility when synthesising homochiral natural products as the number of

stereocentres is only limited by the complexity of the *meso* compound.

The '*meso* trick'

A very interesting phenomenon is associated with asymmetric desymmetrisation, known as the '*meso* trick'.[3,4] With certain substrates that can react twice with a homochiral reagent, products can be obtained with unusually high levels of enantiomeric purity. This is made possible by the initial asymmetric reaction being coupled with a kinetic resolution, resulting in the increase in enantiomeric excess as the reaction proceeds. The classical example is the asymmetric desymmetrisation of diallylic alcohol **1** by Sharpless asymmetric epoxidation (scheme 1.4). For simplicity we have assumed complete diastereoselectivity in the epoxidation, i.e. only one face of each alkene reacts – which is not far removed from reality.

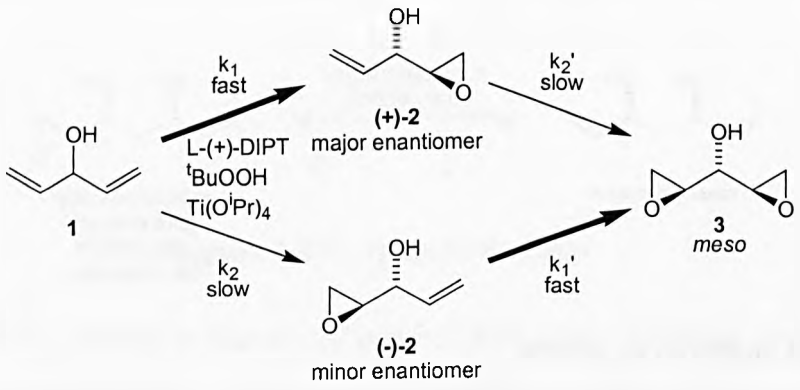

Scheme 1.4 The '*meso* trick' in theory

The initial asymmetric epoxidation produces **(+)-2** in excess (as $k_1 > k_2$). The reaction of the second alkene of the major enantiomer **(+)-2** with the homochiral reagent is very slow, however the second alkene of the minor enantiomer **(-)-2** reacts much faster (as $k_1' > k_2'$) to give *meso* diepoxide **3**. This consumption of the minor enantiomer results in the increase in the ee of **(+)-2** as the reaction proceeds, at the slight expense of the yield. Schrieber has devised a mathematical model to predict these trends, as well as demonstrating them in practice[3] (scheme 1.5).

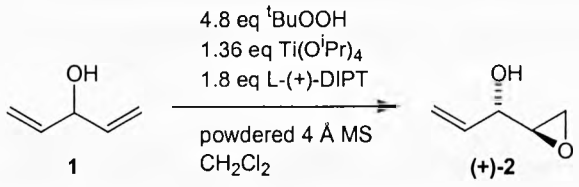

Conditions	% ee	% de
3 h, -25°C	84	92
24 h, -25°C	93	99.7
140 h, -25°C	≥97	>99.7

Scheme 1.5 The '*meso* trick' in practice

This phenomenon is a significant advantage of asymmetric desymmetrisation as it allows for ees to be obtained that are higher than the intrinsic selectivity of the asymmetric reaction employed. Obviously, when desymmetrising advanced intermediates any increase in the ee is of great value, making the asymmetric desymmetrisation of achiral or *meso* compounds a very attractive strategy.

Asymmetric desymmetrisation of achiral or *meso* compounds

This section details some of the many reactions utilised to achieve the asymmetric desymmetrisation of achiral or *meso* compounds, and the numerous substrates on which they have been carried out. It is not intended to be comprehensive, but to serve as an indication of the scope and versatility of this strategy. A handful of reviews on asymmetric desymmetrisation exist[1,2,5-7] (particularly noteworthy is the excellent recent review by Willis) and they should be referred to for a more complete account of this area. Two areas that are covered comprehensively are the asymmetric desymmetrisation of *meso* imides (by reduction) and diallylic alcohols, as they are of paticular relavence to this thesis. Asymmetric desymmetrisation by enzymatic means is not covered, as this is an enormous area in itself. Also, the desymmetrisation of C_2 and pseudo C_2 symmetrical substrates are not covered, as these are not true asymmetric desymmetrisations. Generally, only transformations that achieve enantio or diastereoselectivities of 80% or above are included, unless they are of particular significance. The examples are organised first by the class of substrate desymmetrised and then further subdivided by the reaction employed.

Anhydride and imide substrates

The asymmetric desymmetrisation of achiral or *meso* anhydrides and imides is almost always performed using a chiral nucleophile to distinguish between the two enantiotopic carbonyl

groups. As reaction of the first carbonyl dramatically reduces the reactivity of the second, the enhancement of the ee by the '*meso* trick' is not possible (scheme 1.6).

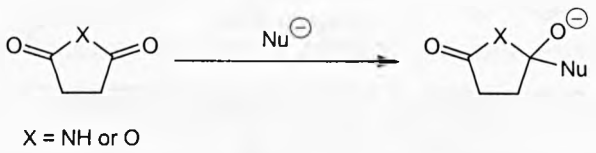

Scheme 1.6

Heathcock has reported the diastereoselective desymmetrisation of a range of prochiral anhydrides **4**.[8,9] The process was diastereo rather than enantioselective as the attack of homochiral alcohol **5** resulted in the production of a pair of diastereomers **6**. Treatment with diazomethane followed by hydrogenolysis yielded the enantiomerically enriched monoesters **7** (scheme 1.7). Perhaps counter-intuitively, the diastereomeric ratio decreased with increasing size of the 4-substituent, suggesting that two or more transition states exist for each diastereomeric combination.

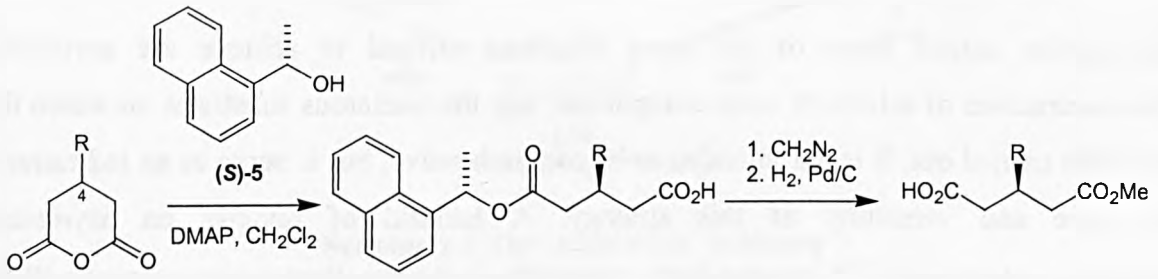

4 **6** **7**

R	OTBS	Me	Et	^{i}Pr	Ph	^{t}Bu
dr	50:1	16:1	14:1	7:1	8:1	1:3

Scheme 1.7

A Ti TADDOLate mediated enantioselective desymmetrisation of bicyclic anhydrides has been developed by Seebach[10] (scheme 1.8). Attack of isopropoxide takes place from the convex face of the molecule with excellent enantiotopic carbonyl selectivity for a number of bicyclic substrates. Substoichiometric amounts of Ti TADDOLate, with stoichiometric amounts of $Al(O^{i}Pr)_3$ also gave good enantiomeric ratios but the reaction times were long (12 to 24 days).

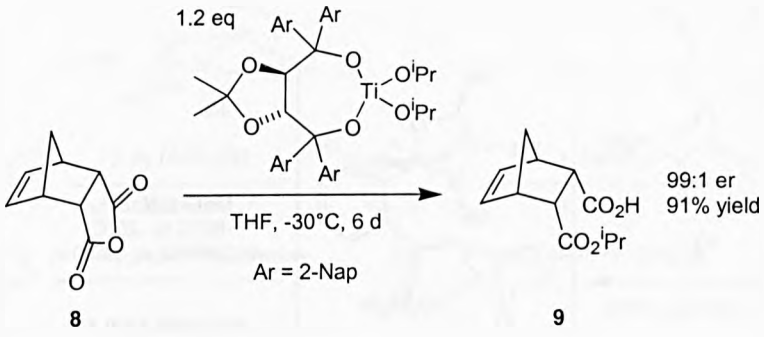

Scheme 1.8

Seebach has also extended this methodology to include *N*-Ms substituted imides[11] (scheme 1.9). The ring-opening proceeded under the same conditions as the anhydride, albeit with slightly lower selectivities.

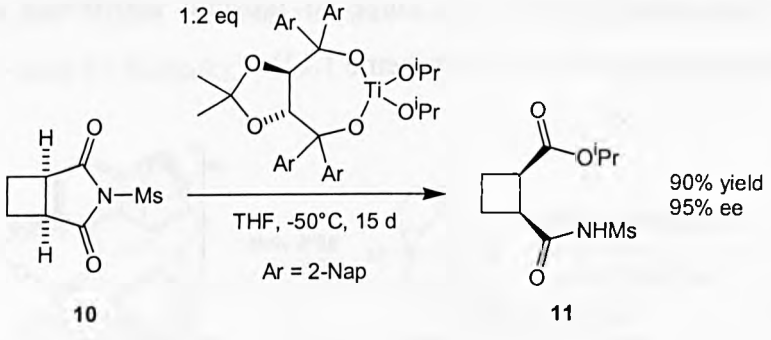

Scheme 1.9

Whereas anhydride desymmetrisation using chiral heteroatom nucleophiles is quite common, the use of carbon nucleophiles is comparatively rare. In connection with their thromboxane agonist programme, Real and co-workers at Bristol-Myers Squibb developed the chiral Grignard desymmetrisation of bicyclic anhydride **12**.[12] Oxazolidine Grignard **13**, from the condensation of ortho-bromobenzaldehyde with (-)-pseudoephedrine, attacks the anhydride in a diastereoselective fashion to give intermediate **14** which, on treatment with methanol and $NaBH_4$, gives lactone **15** in a reasonable yield and excellent ee (scheme 1.10).

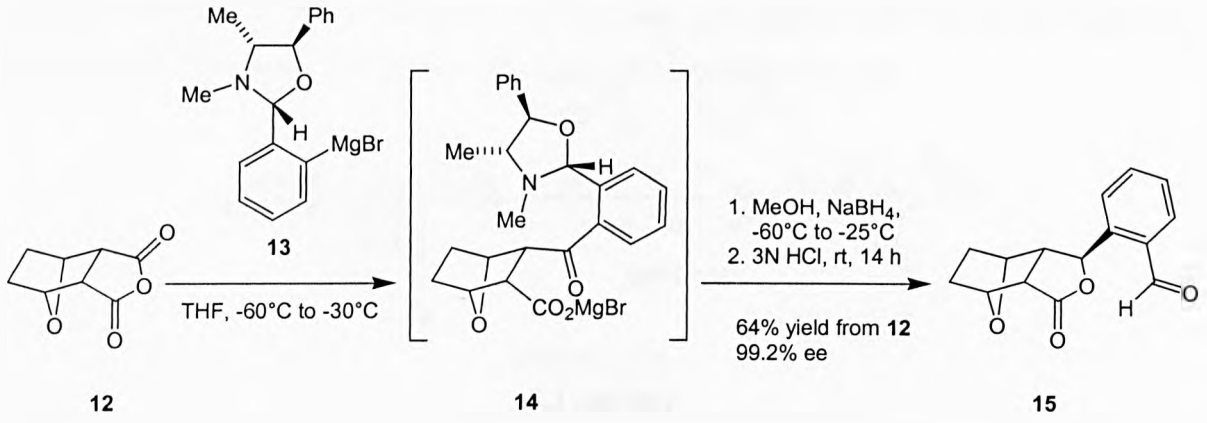

Scheme 1.10

Reductive desymmetrisation of anhydrides and imides can be achieved using homochiral hydride reducing agents. For example, Matsuki has employed Noyori's (*R*)-BINAL-H(ROH) reagent to effect desymmetrisation of a range of bicyclic anhydrides and imides with consistently high enantioselectivities[13,14] (scheme 1.11).

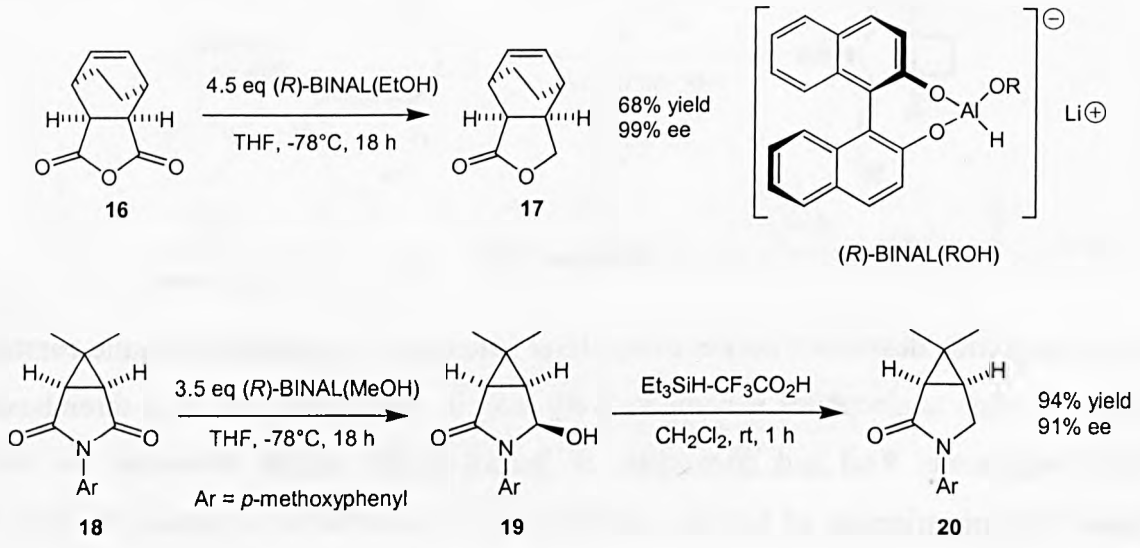

Scheme 1.11

In the case of the imides, the selectivities are slightly lower, and the hydroxylactams have a tendency to epimerise on treatment with acid.

Kang has developed a catalytic enantioselective borane reduction procedure for *meso* imides using chiral thiazincolidine complex **21**.[15,16] For example, enantioselective reduction of imide **22** followed by further reduction and acid catalysed lactonisation of the resulting hydroxylactam **23**, gives lactone **24** in excellent yield and ee (scheme 1.12).

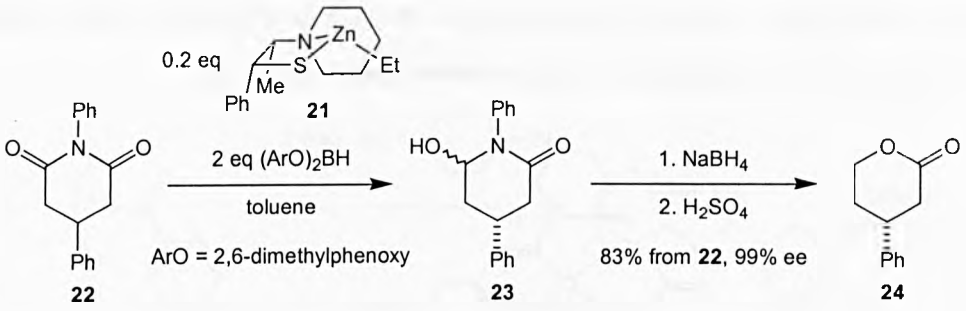

Scheme 1.12

Speckamp has reported the catalytic asymmetric reduction of *N*-alkyl substituted bicyclic imides using Corey's oxazaborolidine catalyst[17,18] (scheme 1.13). Once again, the hydroxylactams are prone to epimerisation, but treatment with acidic ethanol afforded the ethoxylactams in good yield and excellent enantioselectivities. This procedure is noteworthy as *N*-alkyl substituted imides are less reactive towards nucleophilic attack than the *N*-aryl substituted imides used by Matsuki.

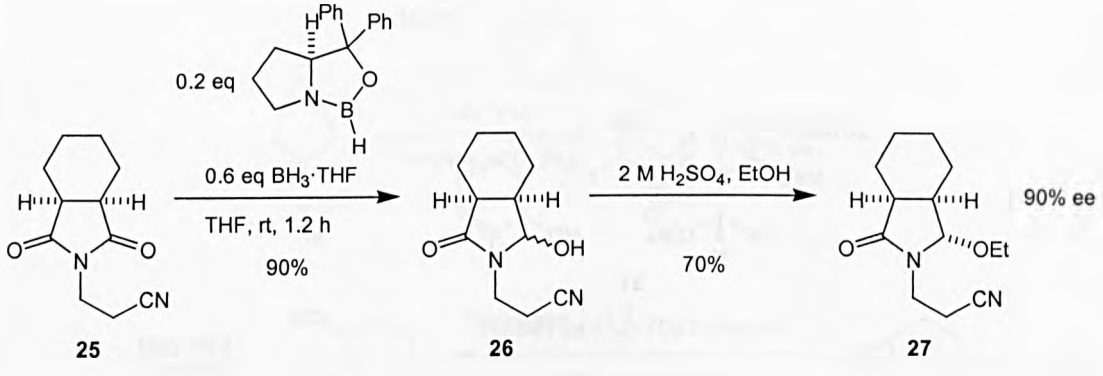

Scheme 1.13

Epoxide and aziridine substrates

The chemistry of these heterocycles can involve nucleophilic opening or deprotonation α or β to the three membered ring, all of which have been exploited to achieve asymmetric desymmetrisation. Once again, due to the nature of these substrates, reaction can only occur once so the '*meso* trick' is not operative.

Achiral and *meso* epoxides have been opened with both heteroatom and carbon nucleophiles, both of which are useful techniques for the synthesis of chiral compounds. Jacobsen has explored the use of Cr(salen) complexes as catalysts for the enantioselective opening of *meso* epoxides with $TMSN_3$[19] (scheme 1.14). Not only is this system extremely catalytically active

and enantioselective, but it has also been shown to operate under solvent free conditions with catalyst recycling without a significant drop in the enantioselectivity.

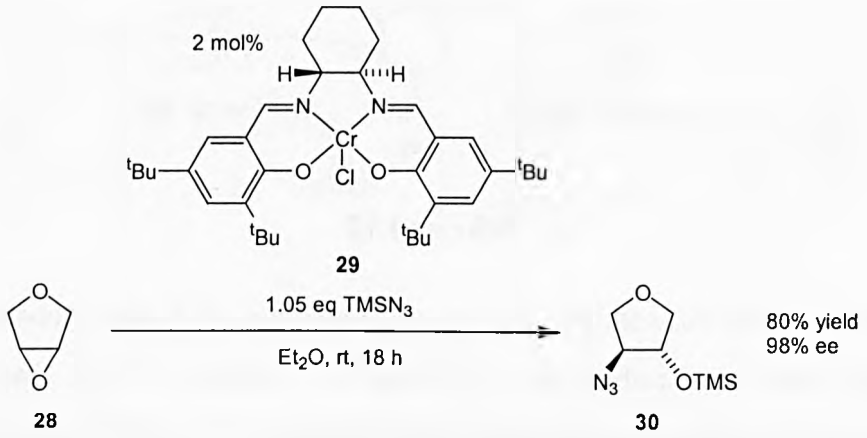

Scheme 1.14

A combinatorial approach towards ligand design has revealed 'peptoid' **31**/Ti(O^{i}Pr)$_4$ complex to be an enantioselective catalyst for the addition of TMSCN to *meso* epoxides[20] (scheme 1.15).

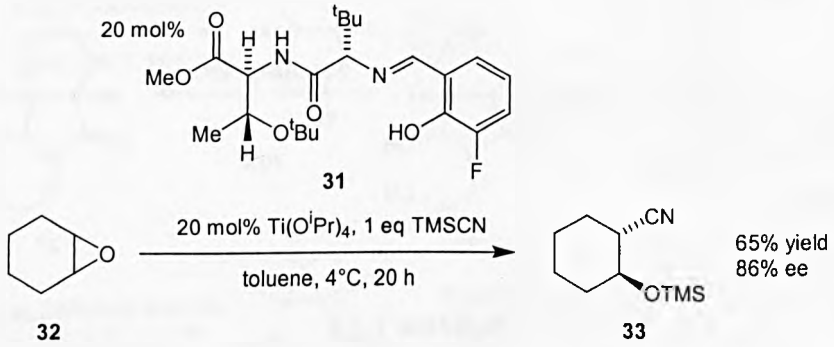

Scheme 1.15

Asymmetric opening of aziridines has been achieved using ^{t}BuPhSH and a catalyst derived from Et_2Zn-dicyclohexyl L-(+)-tartrate[21,22] (scheme 1.16). Attempts to make the reaction catalytic did not affect the yield but reduced the enantioselectivity, giving ees of 78% and 17% with 50 mol% and 20 mol% of catalyst respectively.

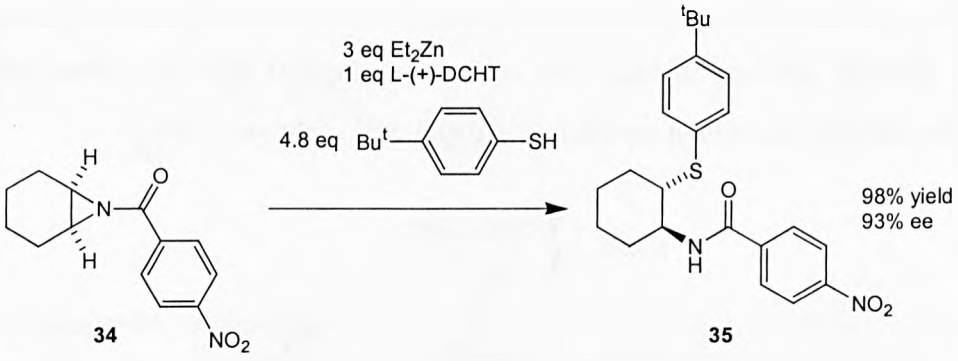

Scheme 1.16

Enantioselective deprotonation of epoxides has been extensively studied and the subject is covered in a number of reviews.[23-27] Isomerisation by deprotonation β to the epoxide can be effected in excellent ee by using homochiral Li-amide bases (scheme 1.17) as shown by Singh.[28,29]

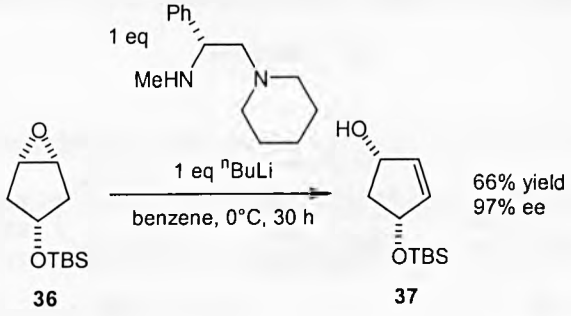

Scheme 1.17

Asami, one of the pioneers in this field, has developed the catalytic enantioselective deprotonation of *meso* epoxides.[30] The deprotonation is performed by chiral Li-amide **38**, which is then regenerated by stoichiometric amounts of less reactive lithium diispropylamide, completing the catalytic cycle (scheme 1.18).

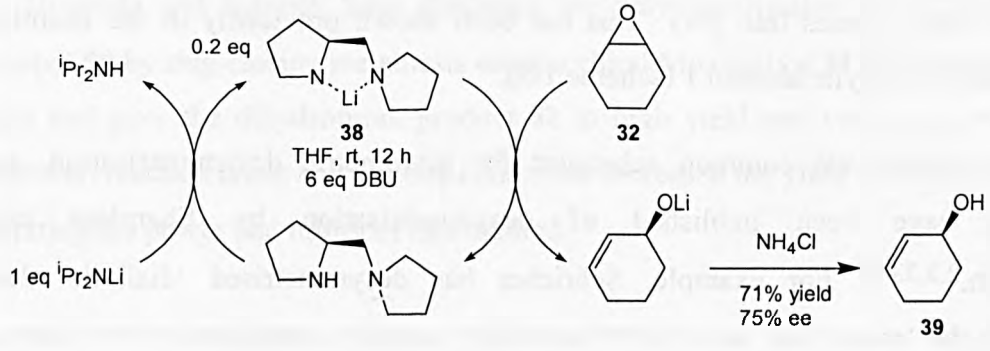

Scheme 1.18

Very recently, Andersson has optimised this procedure and shown that chiral diamine **40** is a remarkable catalyst for the rearrangement of a wide range of *meso* epoxides, affording the corresponding allylic alcohols in excellent yield and ee[31] (scheme 1.19).

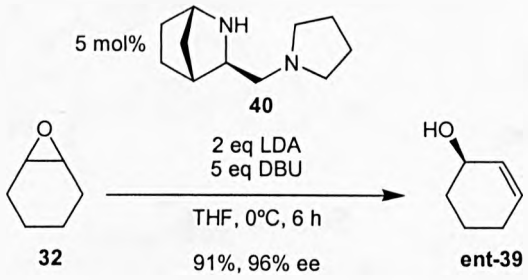

Scheme 1.19

Hodgeson has reported an elegant enantioselective α-deprotonation-rearrangement sequence of *meso* epoxides to give bicyclic alcohols in very good ee.[32] α-Deprotonation of **41** produced a carbene which inserted into a C-H bond across the ring to give cis fused bicycle **42** (scheme 1.20).

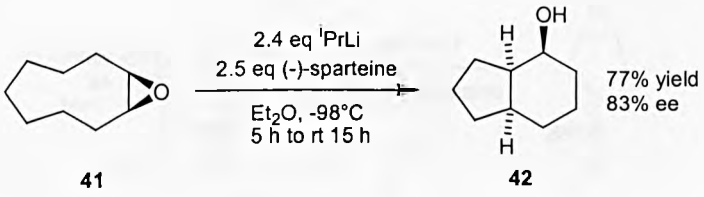

Scheme 1.20

Alkene and diene substrates

Many methods have been used to desymmetrise alkene and diene substrates, almost all of which involve the differentiation of two enantiotopic alkene faces. Unlike the previous two substrate classes, the potential exists with dienes to react twice with a homochiral reagent, and the '*meso* trick' comes into play. This has been shown previously in the enantioselective epoxidation of diallylic alcohol **1** (scheme 1.5).

Diallylic alcohols are common substrates for asymmetric desymmetrisation, and many examples have been published of desymmetrisation by Sharpless asymmetric epxodation.[2,3,33-44] For example, Schrieber has desymmetrised 'diallylic alcohol' **43** exploiting the '*meso* trick' to achieve essentially complete enantioselectivity during studies towards the structure determination of (+)-mycoticins A and B[2] (scheme 1.21).

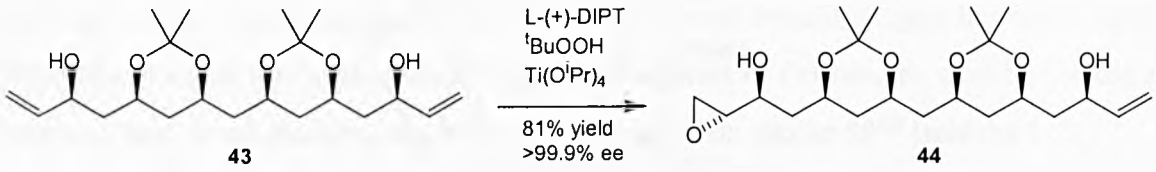

43 44

Scheme 1.21

Sharpless asymmetric aminohydroxylation has been employed to desymmetrise masked diallylic alcohols by Landais.[45] Aminohydroxylation of diene **45** was shown to occur with complete diastereo and regioselectivity and in reasonable yield and enantioselectivity (scheme 1.22).

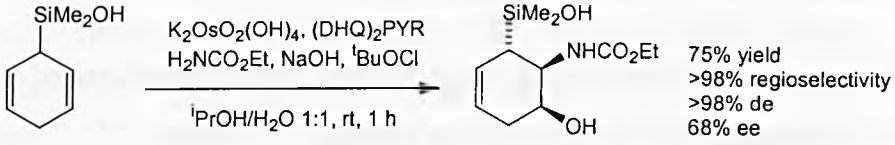

45 46

Scheme 1.22

The intramolecular hydrosilylation of protected diallylic alcohol **47** has long been known.[46] The silane selectively attacks one of the enantiotopic alkenes in preference to the other on treatment with Rh-DIOP complex, and oxidative cleavage of the Si-C bond produces diol **49** with high enantiomeric purity (scheme 1.23).

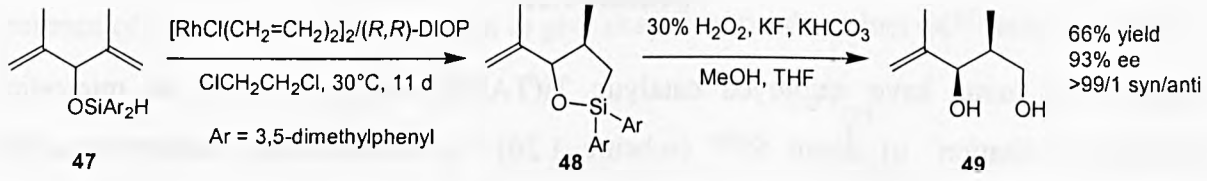

47 48 49

Scheme 1.23

Recently, Hoveyda and Schrock have disclosed the desymmetrisation of allyl substituted diallyl alcohol **50** by ring-closing metathesis using a chiral Mo catalyst **51**.[47] The catalyst was very active and gave the dihydrofuran product **52** in high yield and very high ee (scheme 1.24). However, reaction under solvent free conditions increased the yield and ee even further, thus illustrating the power and utility of this method.

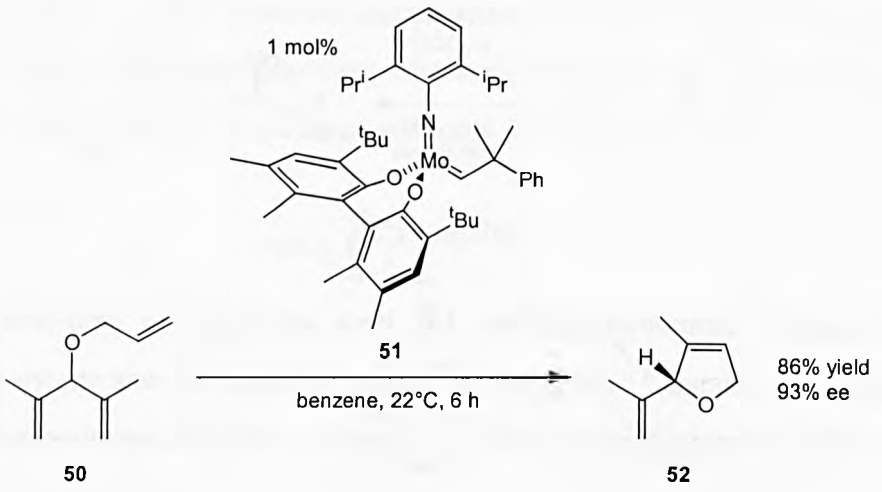

Scheme 1.24

Towards their synthesis of (+)-conduritol E, the Takano group desymmetrised *meso* diene **53** using Sharpless asymmetric dihydroxylation methodology[48] (scheme 1.25). They observed no formation of the doubly dihydroxylated product, indicating that for this substrate the '*meso* trick' was not active.

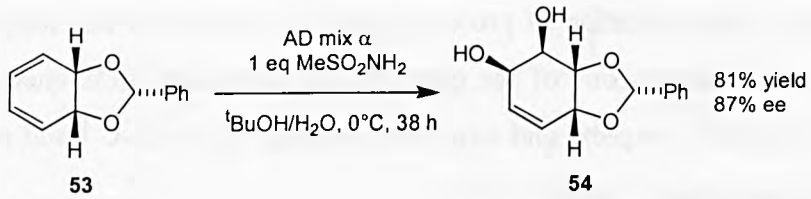

Scheme 1.25

Taguchi and Inoue have employed catalytic Ti(TADDOLate)$_2$ to effect an interesting 'iodocarbocyclisation' of diene **55**[49] (scheme 1.26). Ti(TADDOLate)$_2$ deprotonates the malonate before complexing to it to form a chiral enolate. This then selectively attacks one of the enantiotopic alkenes (activated by I_2) to give carbocycle **56**, which on heating produces bicyclic lactone **57** in excellent yield and ee. Dienes with allyl and homoallyl groups also give comparable enantioselectivities.

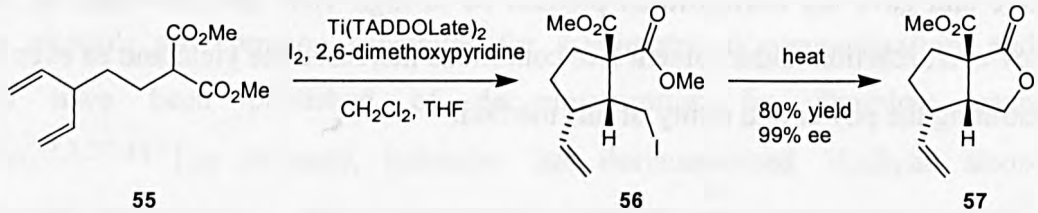

Scheme 1.26

Asymmetric hydroboration using Brown's diisocamphenyl borane reagent has been reported on both alkenes and dienes. As part of their total synthesis of (+)-hirustic acid C, Greene and co-workers performed an enantioselective hydroboration on alkene **58**[50] (scheme 1.27).

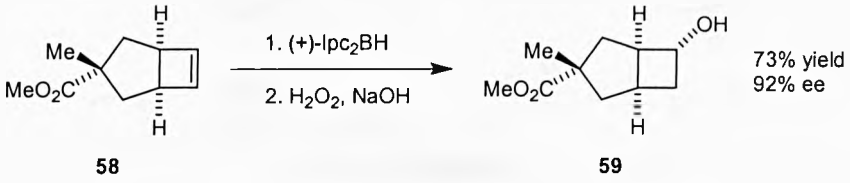

58 **59**

Scheme 1.27

On the other hand, the same reagent has been used to desymmetrise diene **60**, also with excellent enantioselectivity[51,52] (scheme 1.28). The '*meso* trick' is probably at work in this second example, which would explain the slightly higher ee.

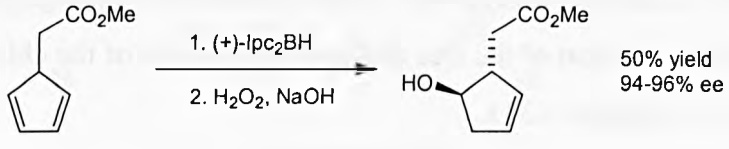

60 **61**

Scheme 1.28

The asymmetric ene reaction is another transformation that has been utilised to desymmetrise both alkenes and dienes. Alkene **62** undergoes reaction with propargyl aldehyde **63** in the presence of (*R*)-BINOL-$TiCl_2$ complex to give desymmetrised product **64**[53] (scheme 1.29).

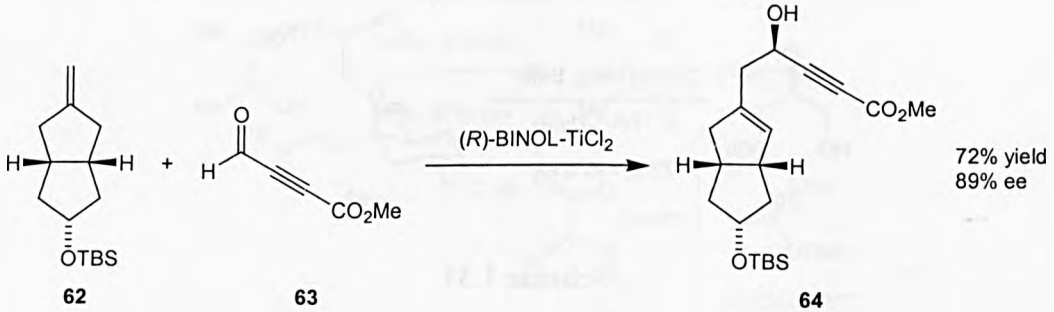

62 **63** **64**

Scheme 1.29

The '*meso* trick' is clearly at work in the catalytic asymmetric ene reaction of diene **65**, producing extremely high enantioselectivities[54] (scheme 1.30).

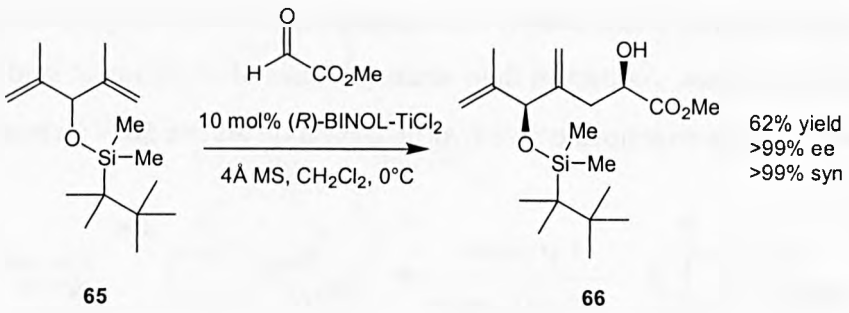

Scheme 1.30

Diol and polyol substrates

For diol and polyol substrates, acetal and acylation chemistry are the main areas exploited to achieve asymmetric desymmetrisation. Early attempts at diol desymmetrisation employed L-menthone to form chiral ketals, usually with reasonable diastereoselectivity (the minor diastereomer can be columned away).[55-57] These ketals then undergo stereoselective ring cleavage followed by protection of the free alcohol and removal of the chiral auxiliary to give desymmetrised diol **70** (scheme 1.31).

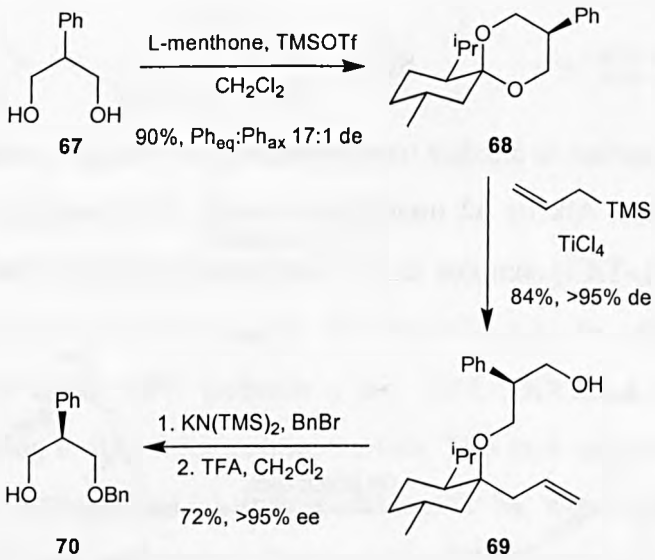

Scheme 1.31

Very recently a procedure employing C_2-symmetric bis-sulfoxide **71** to desymmetrise *meso* diols has been published.[58] The advantage of using a C_2-symmetric auxiliary is that only one product is formed on ketal formation as opposed to the mixture of diastereomers obtained when using chiral auxiliaries lacking symmetry (e.g. L-menthone). Base promoted diastereoselective acetal cleavage followed by alcohol protection and auxiliary removal gave

desymmetrised diol **75** in excellent yield and enantioselectivity (scheme 1.32).

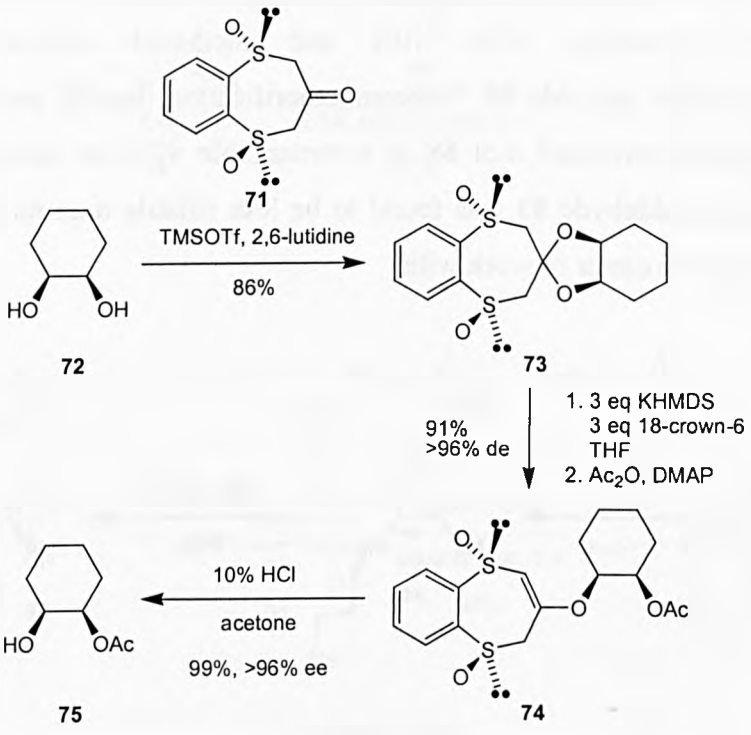

Scheme 1.32

Harada has used a chiral Lewis acid to selectively cleave acetals of *meso* 1,2-diols.[59,60] The chiral Lewis acid **79** facilitates the cleavage of **78** by silyl ketene *S,O*-acetal, with excellent enantioselectivity (scheme 1.33).

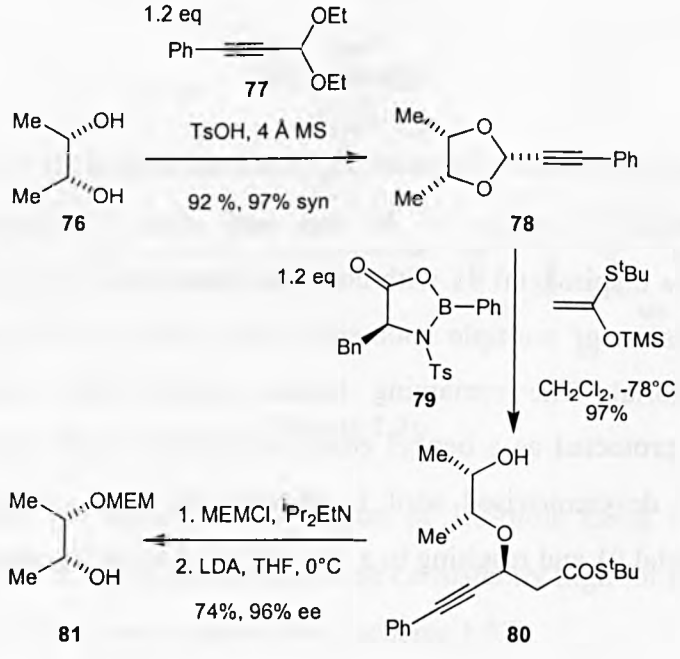

Scheme 1.33

Fujioka has recently published a modification to his *meso* diol desymmetrisation by intramolecular haloetherification of ene acetals.[61,62] Ene acetal **84** was formed as a single diastereomer, and treatment with NBS and methanol effected intramolecular haloetherification to give bromide **85**. Debromoetherification, benzyl protection and acetal cleavage afforded desymmetrised diol **88** in a remarkable 97% ee (scheme 1.34). Phenyl substituted norbornene aldehyde **83** was found to be less volatile than its methyl substituted counterpart and therefore easier to work with.

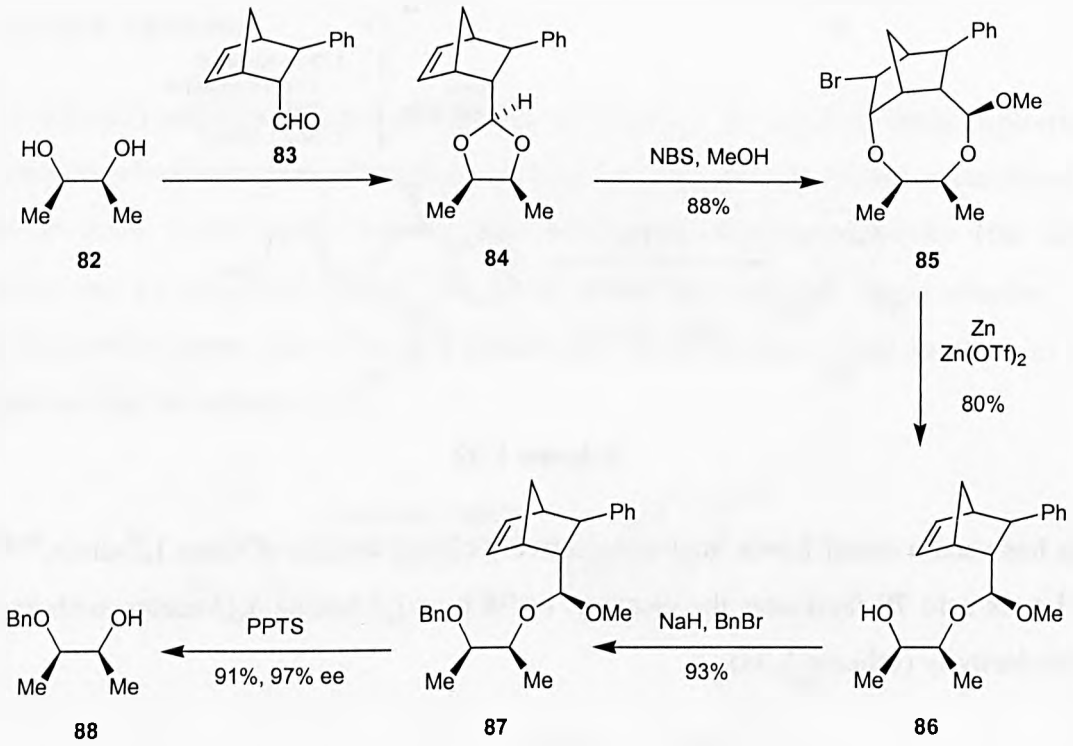

Scheme 1.34

The asymmetric desymmetrisation of glycerol has been accomplished by Ley and co-workers in an ingenious fashion.[63] Reaction of the triol with chiral C_2-symmetric dimethyl bis-dihydropyran **90** gives dispiroketal **91** with complete diastereoselectivity. This selectivity is dictated by the operation of multiple anomeric effects, and the preference of the methyl groups to be equatorial. The remaining hydroxymethyl group adopts an equatorial conformation and is protected as a benzyl ether on treatment with benzyl bromide/sodium hydride. Finally the desymmetrised triol is released by ketal exchange with glycerol, regenerating dispiroketal **91** and resulting in a very efficient recycling process (scheme 1.35).

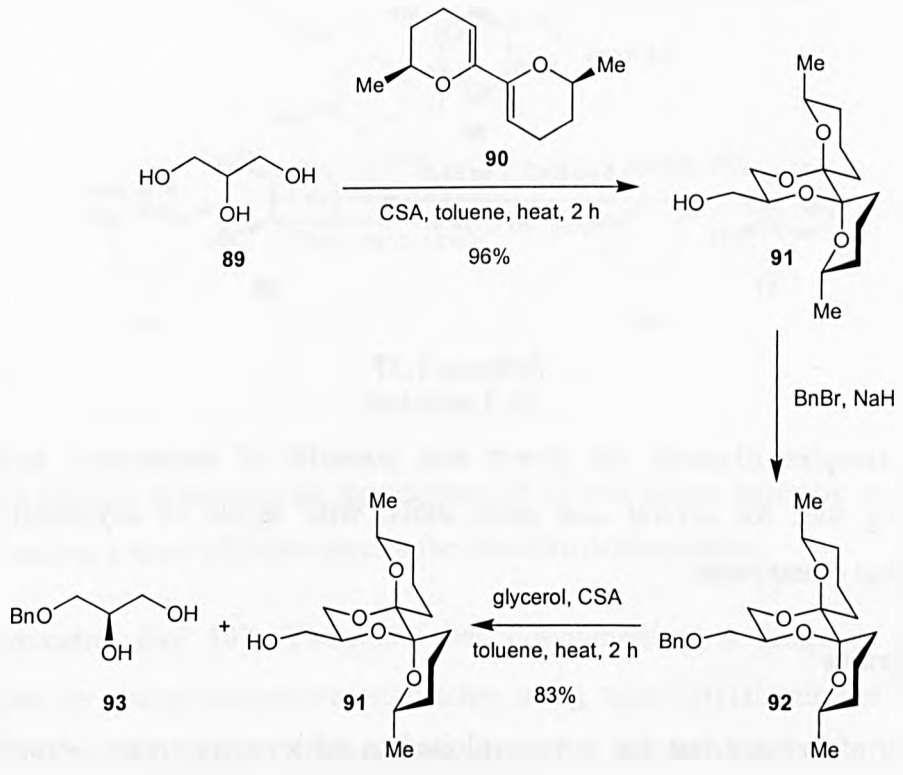

Scheme 1.35

Achiral and *meso* diols can be desymmetrised by asymmetric acylation. Fu has applied his chiral DMAP catalyst **95** to the asymmetric desymmetrisation of diol **94** with remarkable efficiency and selectivity[64] (scheme 1.36). The only drawback to this method is the inability to perform the reaction at lower temperatures due to the high freezing point of the solvent.

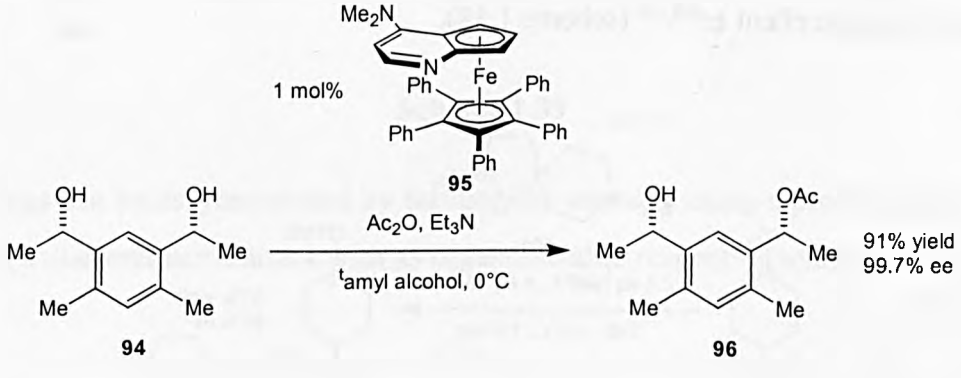

Scheme 1.36

Oriyama has achieved the asymmetric acylation of 1,2-diols using benzoyl chloride and diamine catalyst **98**.[65,66] Enantioselectivities were consistently high for a range of *meso* diols, and catalyst loading levels were extremely low (scheme 1.37).

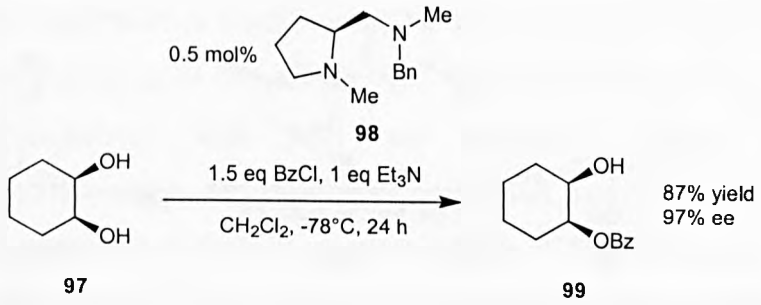

Scheme 1.37

These two examples illustrate the power and potential of asymmetric acylation as a desymmetrising tool for achiral and *meso* diols, with levels of asymmetric induction approaching that of enzymes.

Ketone substrates

The chemistry of ketones that has been exploited to achieve asymmetric desymmetrisation includes enantioselective deprotonation, chiral ketal formation, attack with chiral nucleophiles and ketone rearrangements. With diketone substrates the potential exists for double reaction, therefore the '*meso* trick' can operate.

The enantioselective deprotonation of ketones using chiral bases is a large and mature field,[25,26,67] and several highly selective asymmetric desymmetrisations have emerged from it. For example, Koga has achieved the enantioselective α-deprotonation of substituted cyclohexanones in excellent ee[68,69] (scheme 1.38).

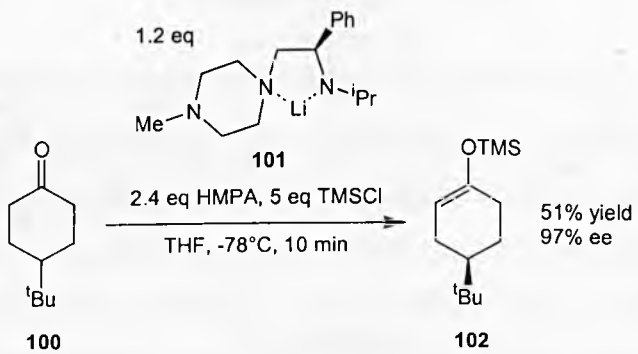

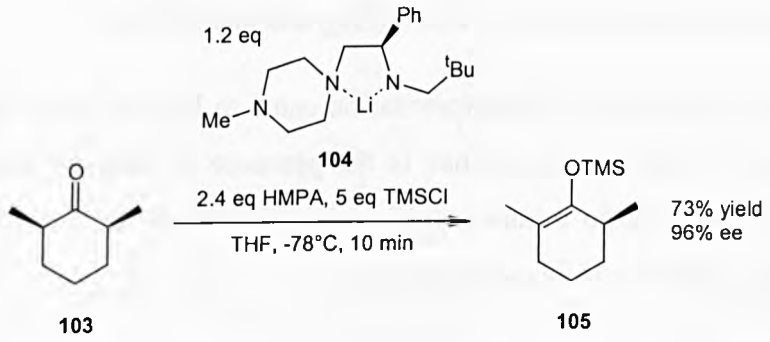

Scheme 1.38

The HMPA is thought to prevent the aggregation of lithium amide bases by co-ordinating to the lithium, making a more efficient species for selective deprotonation.

Using C_2-symmetric diol **107**, Yamamoto has desymmetrised a range of 4-substituted cyclohexanones by diastereoselective enolisation using triisobutylaluminium[70,71] (scheme 1.39). Interestingly, changing the 4-substituent to ethyl or *tert*-butyl did not affect the yields or diastereomeric ratio.

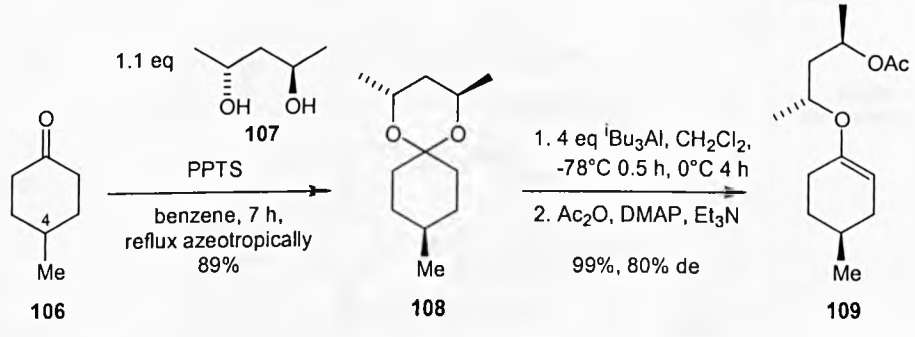

Scheme 1.39

1,2-Diketones can be desymmetrised by forming the enamine using a proline derivative, then performing a diastereofacial attack with an organometallic reagent[72] (scheme 1.40).

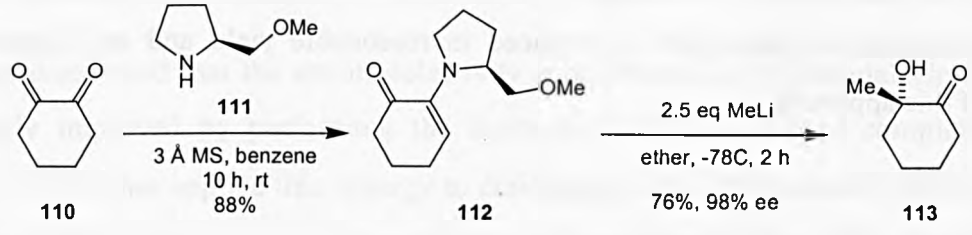

Scheme 1.40

Remarkably, the use of methylmagnesium bromide in place of methyl lithium gives the

opposite enantiomer of hydroxylactone **113** in 67% yield and 95% ee.

An early example of asymmetric desymmetrisation came to light in the 1970s in the context of steroid synthesis. It was discovered that, in the presence of catalytic amounts of proline, triketones such as **114** undergo intramolecular aldol cyclisations to give hydroxyketones in essentially optically pure form[73-75] (scheme 1.41).

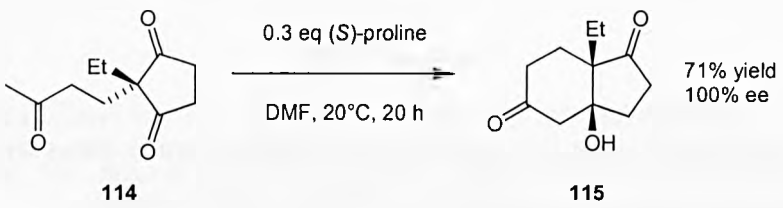

114 **115**

Scheme 1.41

Desymmetrisation by Wittig and Horner-Wadsworth-Emmons type reactions is another strategy that has met with success. Hanessian has used chiral *bis*-phosphonamide **116** to desymmetrise 4-*tert*-butylcyclohexanone **100** in excellent ee[76,77] (scheme 1.42).

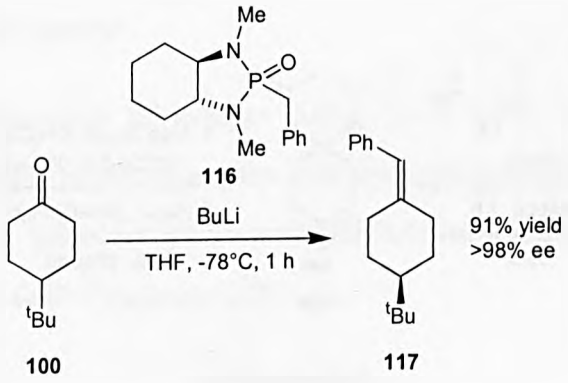

116

100 **117**

Scheme 1.42

Arai and Shioiri have developed a catalytic version of the Horner-Wadsworth-Emmons reaction, using quaternised cinchonine alkaloid **119** as a phase transfer catalyst[78] (scheme 1.43). α,β-Unsaturated ester **120** is produced in reasonable yield and ee, illustrating the potential of this approach.

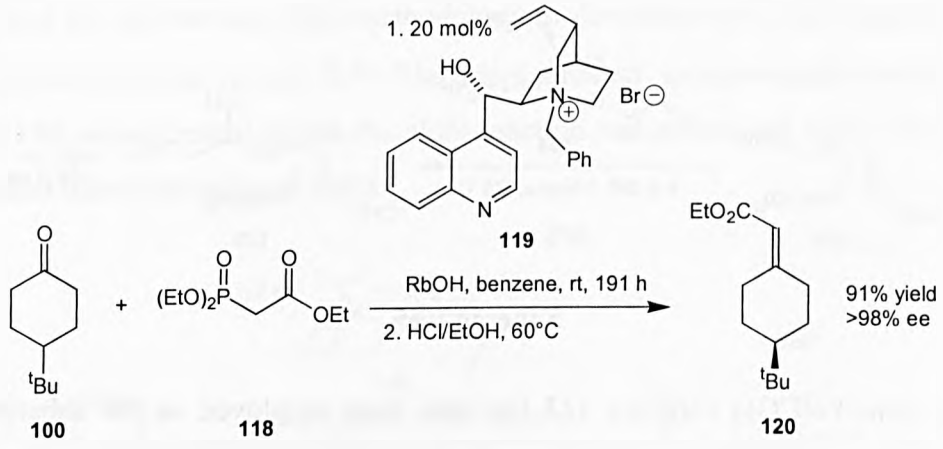

Scheme 1.43

The final example of ketone desymmetrisation was performed by Aubé and co-workers who have achieved the asymmetric Schmidt reaction of 4-*tert*-butylcyclohexanone **100**.[79,80] Treatment with chiral azido alcohol **121** in the presence of a Lewis acid gives ring-expanded lactam **122** as a single diastereomer (scheme 1.44).

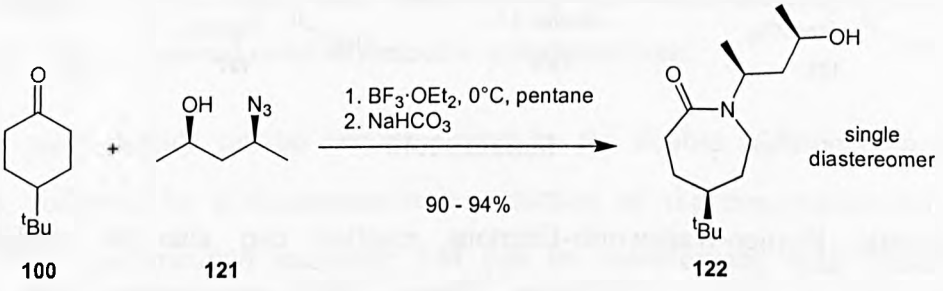

Scheme 1.44

Dialdehyde substrates

All examples of dialdehyde desymmetrisation involve the enantiotopic group and face selective differentiation of the two enantiotopic carbonyl groups by a homochiral nucleophile. As with diketone substrates, the '*meso* trick' is able to operate.

Roush has discovered that the enantioselectivity of allylboration of dienylaldehydes can be significantly improved by performing the reaction on metal carbonyl complexes of the substrate.[81,82] He has applied this strategy to dialdehyde **123** to give alcohol **125** in excellent ee (scheme 1.45). The selectivity is thought to arise from a dipole effect of the metal carbonyl ligand in the stereochemically favoured transition state.

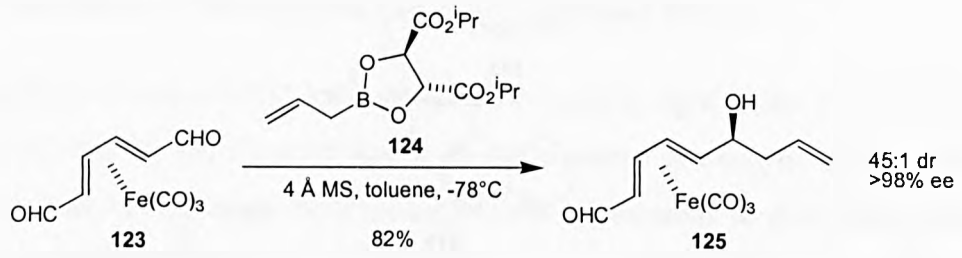

Scheme 1.45

Dialdehyde diene/$Fe(CO)_3$ complex **123** has also been employed as the substrate for the asymmetric addition of dialkyl zinc reagents catalysed by proline derivative **126**[83] (scheme 1.46). The high selectivity is again explained by dipole-dipole interactions, in this case between the metal carbonyl moiety and the dialkyl zinc species.

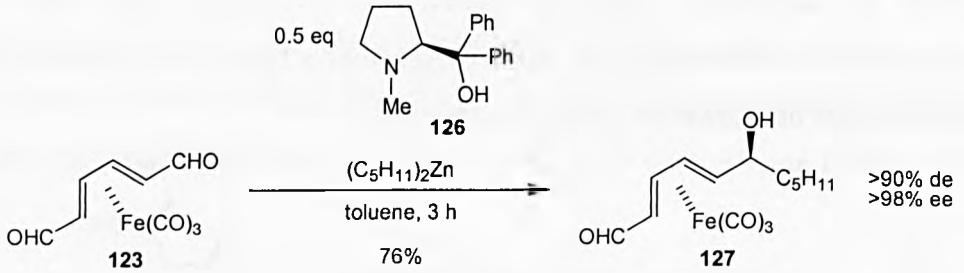

Scheme 1.46

The asymmetric Horner-Wadsworth-Emmons reaction can also be applied to the desymmetrisation of *meso* dialdehydes. Using chiral phosphonate **129**, Rein has desymmetrised dialdehyde **128** with very good diastereoselectivity[84] (scheme 1.47). This selectivity was observed to increase even further by adjusting the reaction conditions to encourage the '*meso* trick', and α,β-unsaturated ester **130** was obtained in a 97:3 diastereomeric ratio and 36% yield.

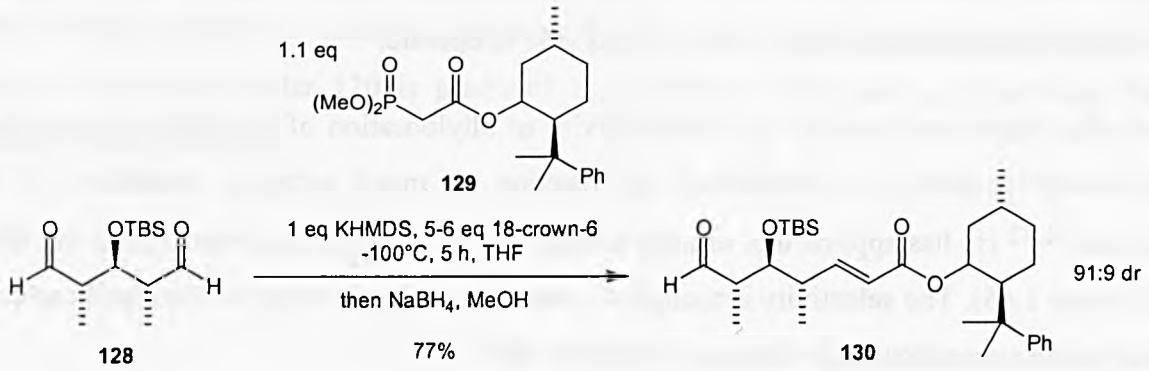

Scheme 1.47

Oppolzer used his asymmetric aldol methodology to desymmetrise *meso* dialdehyde **128** en route to (-)-denticulatins A and B.[85] The aldol product spontaneously cyclised to give hemiacetal **132**, which revealed that the aldol reaction had proceeded with a diastereomeric ratio of greater than 92:8 (scheme 1.48).

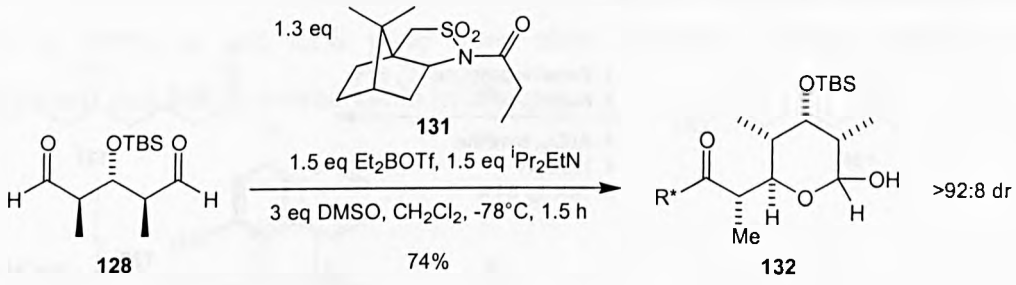

Scheme 1.48

Carboxylic acid substrates

Desymmetrisation of these substrates mainly relies on the selective attack of enantiotopic carbonyl groups, but has also been achieved by the enantioselective protonation of dicarboxylates and via second order asymmetric transformations.

Achiral and *meso* diacids can be desymmetrised by the double addition of a homochiral nucleophile, followed by a diastereoselective reaction of the nonsymmetrical product[86] (scheme 1.49). (-)-Dimenthyl succinate **134** can be deprotonated with lithium 2,2,6,6-tetramethylpiperidine to give a dianion, which reacts with bromochloromethane in a diastereoselective fashion to give cyclopropane **135** in excellent de.

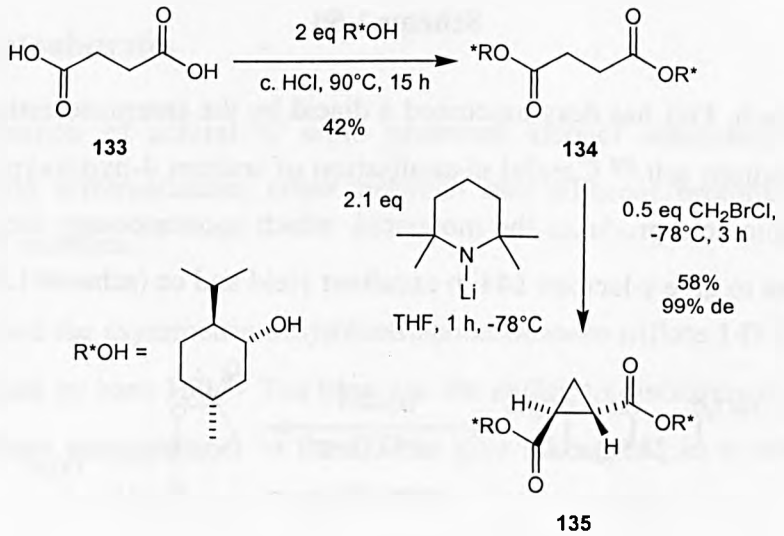

Scheme 1.49

Oda and co-workers have used C_2-symmetric diamine **138** to discriminate between enantiotopic carbonyl groups remote from a prochiral centre, albeit in a slightly lengthy procedure[87,88] (scheme 1.50). Cyclic alcohol **139** underwent a diastereoselective lactonisation to give lactone **140** in excellent yield and ee. This compound was transformed into lactone **142** by further reduction and lactonisation.

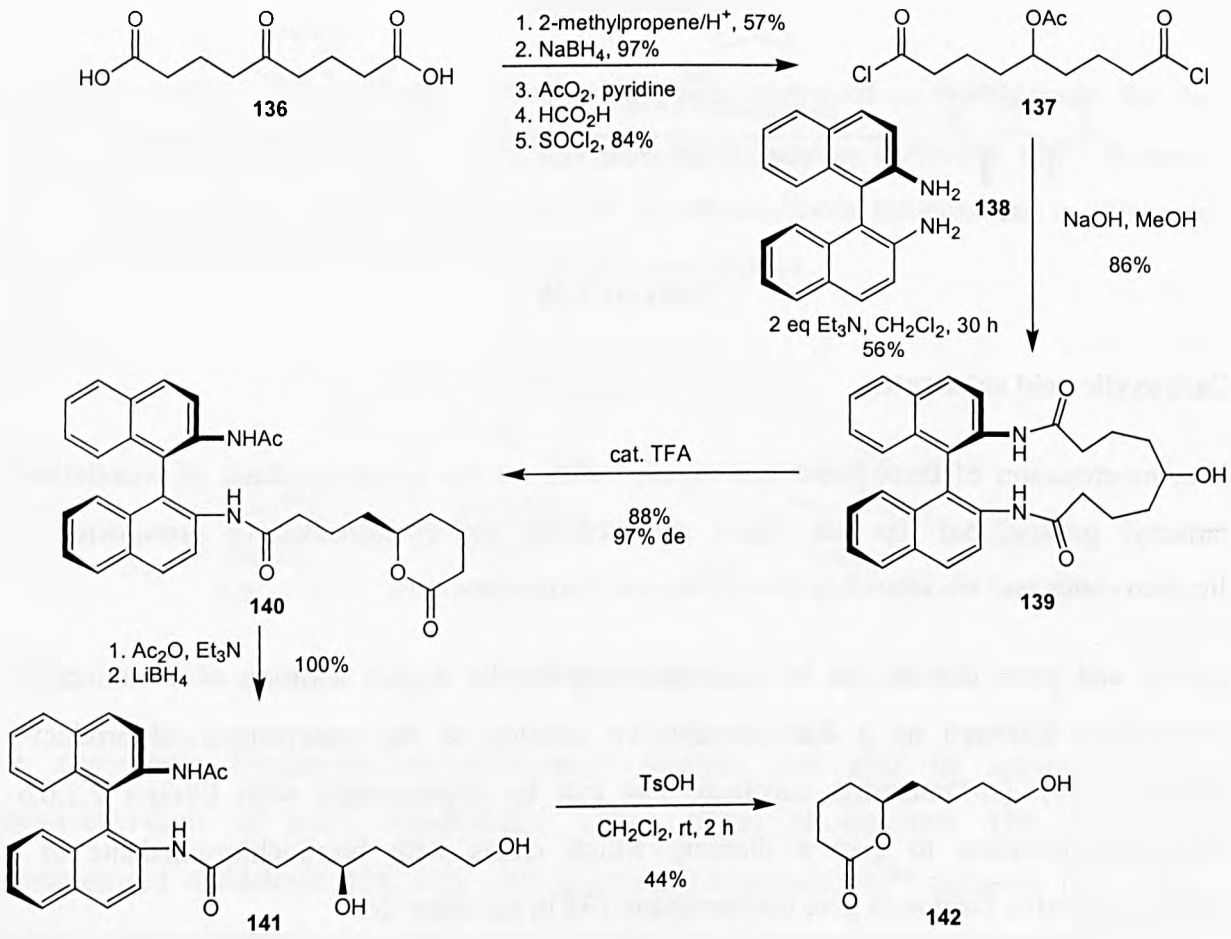

Scheme 1.50

In a unique approach, Fuji has desymmetrised a diacid by the enantioselective protonation of a dicarboxylate sodium salt.[89] Careful neutralisation of sodium 4-hydroxypimelate **143** with (+)-camphorsulfonic acid produces the monoacid, which spontaneously lactonises under the reaction conditions to give γ-lactone **144** in excellent yield and ee (scheme 1.51).

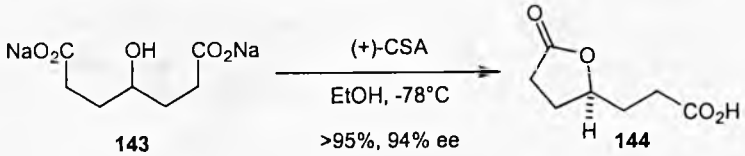

Scheme 1.51

Fukumoto has devised a method for the asymmetric synthesis of chiral propane-1,3-diols, involving a very interesting crystallisation induced asymmetric transformation[90] (scheme 1.52). Coupling of ethyl malonate **145** with menthol gives diastereomeric monoesters **146** and **147** in an 11:9 ratio. However, leaving this oily mixture for 5 days at room temperature induced a second order asymmetric transformation, and crystalline monoester **146** was obtained in >99% de and 82% yield from ethyl malonate. Further manipulation gave desymmetrised diol **148** in a remarkable >99% ee.

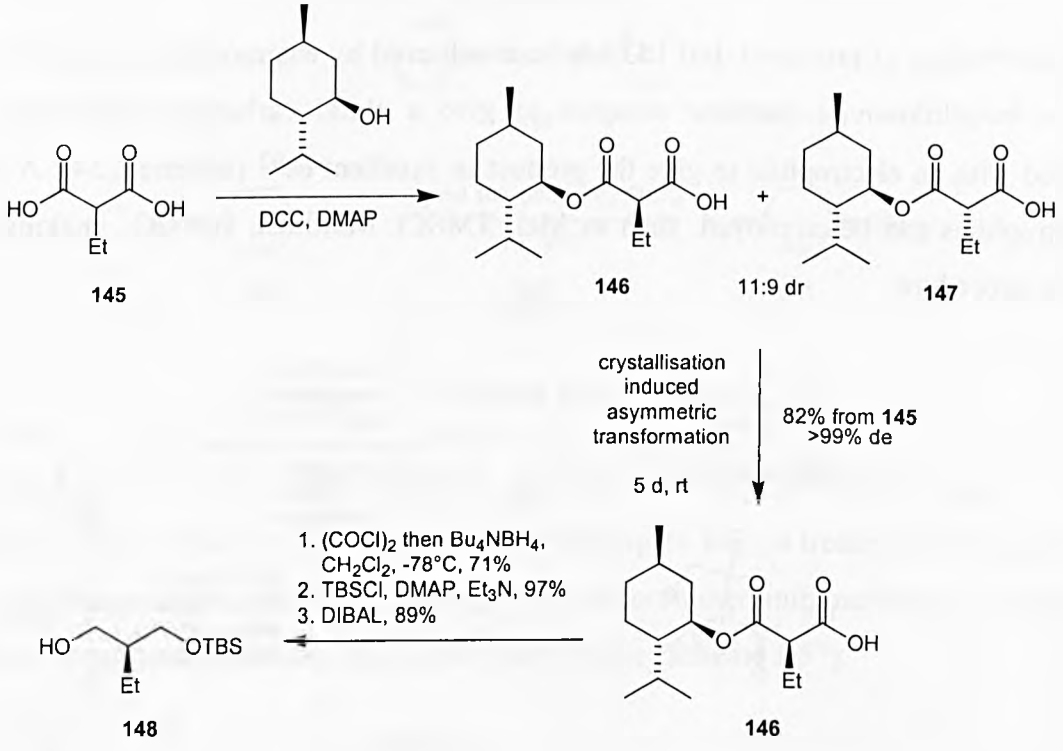

Scheme 1.52

Protected alcohol substrates

The desymmetrisation of achiral or *meso* protected alcohol substrates usually involves enantiotopic group differentiation, either between two adjacent protons or between two protected alcohol moieties.

Sakai has published the asymmetric desymmetrisation of *meso* triflate **149** by an asymmetric elimination induced by base **150**.[91] The base has the ability to discriminate between the two enantiotopic protons antiperiplanar to the OTf to give alkene **151** in a remarkable 99% ee (scheme 1.53).

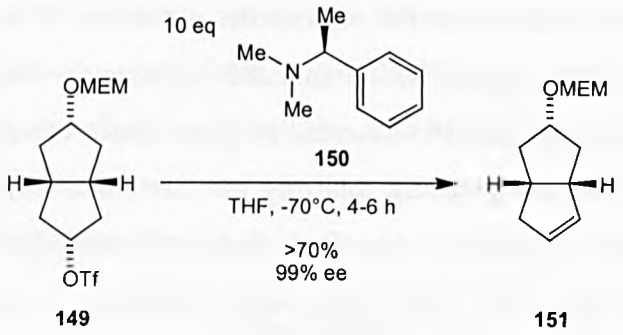

Scheme 1.53

Desymmetrisation of protected diol **153** has been achieved by enantioselective deprotonation with sec-butyllithium/(-)-sparteine complex to give a chiral carbanion, which was then quenched with an electrophile to give the product in excellent ee[92] (scheme 1.54). A variety of electrophiles can be employed, such as MeI, TMSCl, Me_3SnCl, and CO_2, making this a versatile procedure.

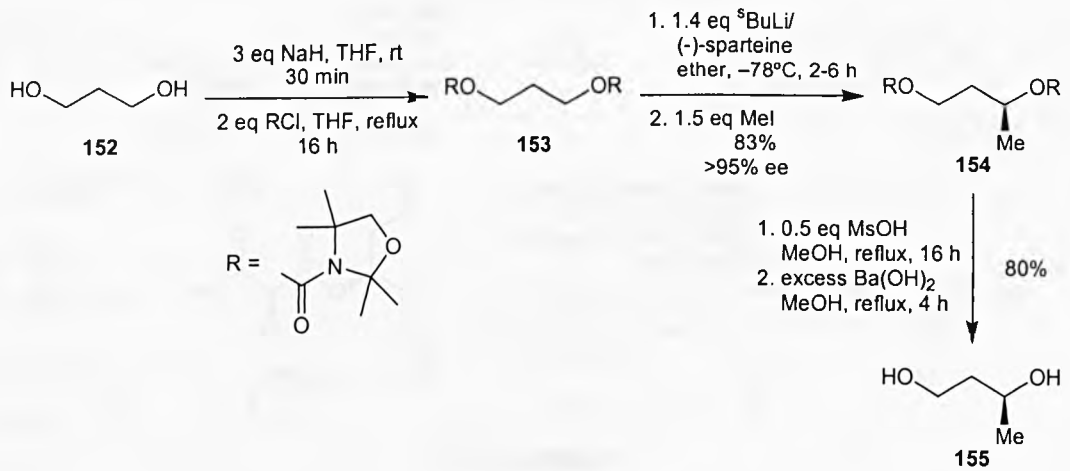

Scheme 1.54

Ogasawara has achieved the asymmetric isomerisation of di-TBS protected enediol **156** using a chiral Rh-BINAP reagent.[93] Cleavage of the intermediate silyl enol ether on acid workup gave silyloxy ketone **158** in excellent chemical and optical yield (scheme 1.55).

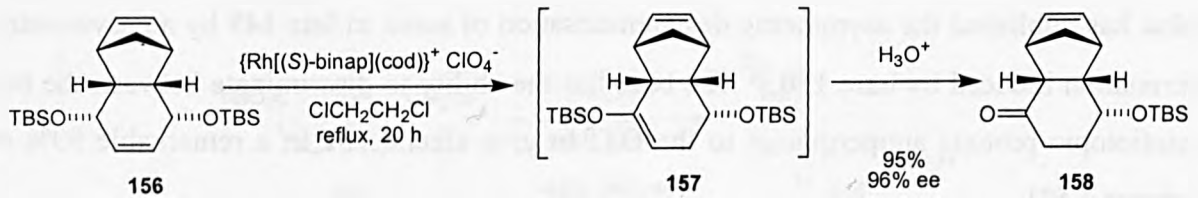

Scheme 1.55

Trost has developed an extremely efficient palladium catalysed desymmetrisation of di-benzoyl protected enediols and applied it to the total synthesis of (-)-epibatidine.[94] Protected diol **159** and $TMSN_3$ were treated with a catalyst derived from cyclohexyl ligand **160** and $(dba)_3Pd_2{\cdot}CHCl_3$ to give azide **161** in almost quantitative yield and excellent enantiomeric purity (scheme 1.56).

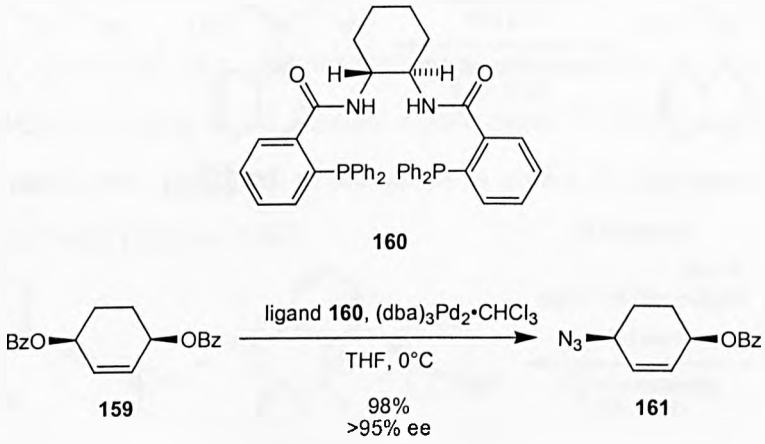

Scheme 1.56

Trost has recently adapted this chemistry to include the desymmetrisation of *meso-bis*-carbamates.[95] *Bis*-carbamate **162** forms π-allyl-Pd complex **163** on treatment with ligand **160** and a palladium catalyst, which then undergoes a base promoted intramolecular cyclisation to give bicyclic oxazolidinone **164** in excellent yield and ee (scheme 1.57).

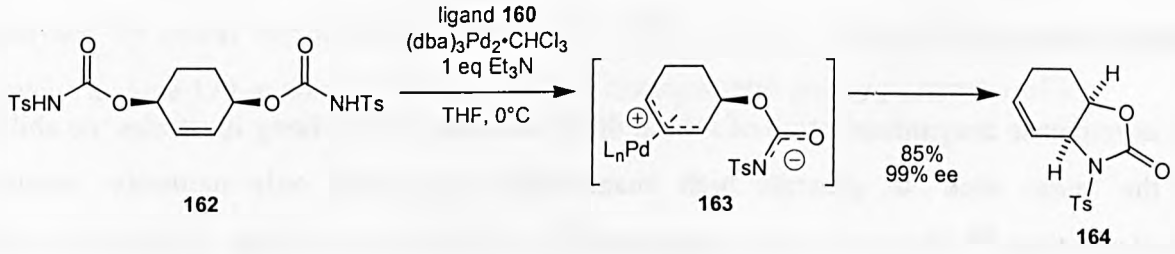

Scheme 1.57

Desymmetrisation of aryl triflates has been achieved by palladium catalysed cross-coupling. Ditriflate **165**, when treated with chiral phosphine-palladium catalyst **167** and phenylmagnesium bromide gives axially chiral biaryl **168**.[96] Even higher enantioselectivities were observed for the coupling of the ditriflate with triphenylsilylethynylmagnesium bromide[97] (scheme 1.58).

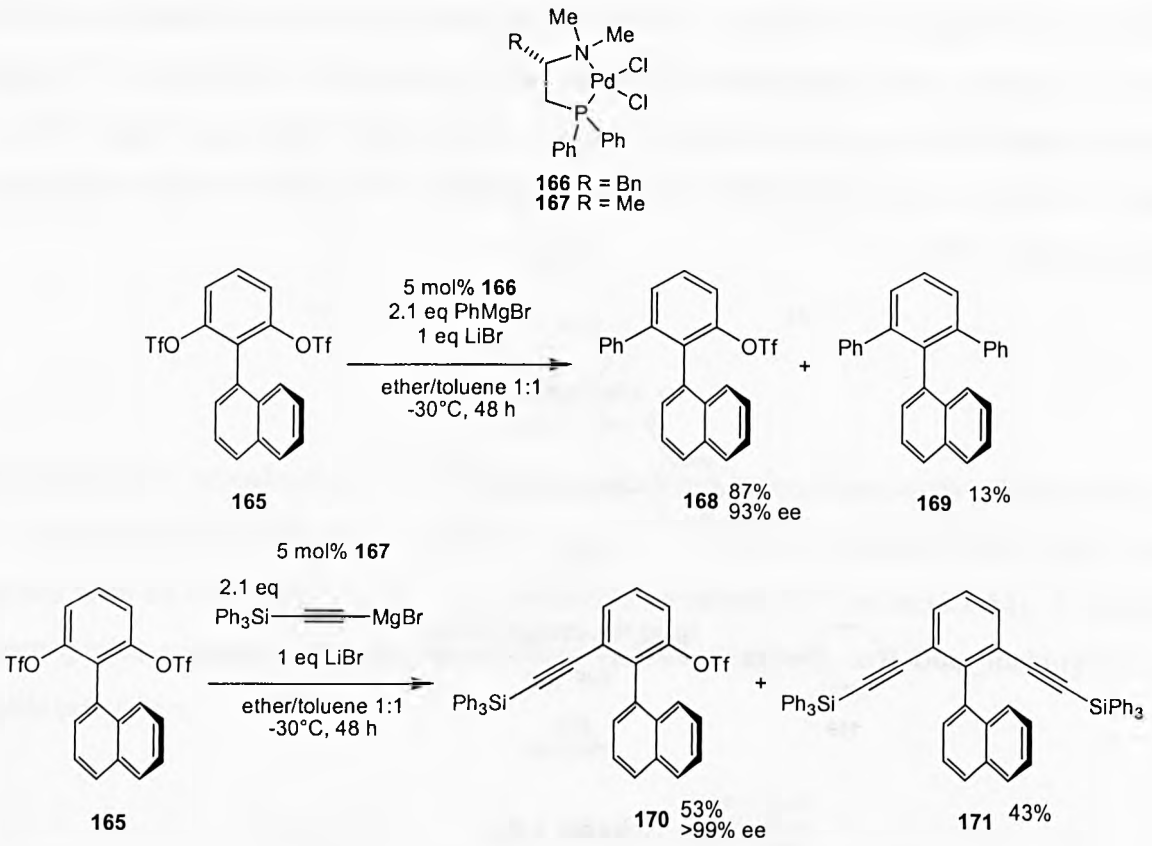

Scheme 1.58

In both cases the inherent selectivity of the cross-coupling was of the order of 85% ee but could be increased significantly by allowing the formation of the di-coupled products **169** and **171**, once again demonstrating the utility of the '*meso* trick'.

Miscellaneous substrates

An asymmetric desymmetrisation of achiral dihalides reported by Chong illustrates the ability of the '*meso* trick' to generate high enantioselectivities from only modestly selective transformations.[98] The enantiotopic group selective reduction of dihalide **172** proceeds with initially low ees but as the reaction progresses and more of the direduced compound **174** is produced, the enantioselectivity increases to such an extent as to become synthetically useful (scheme 1.59).

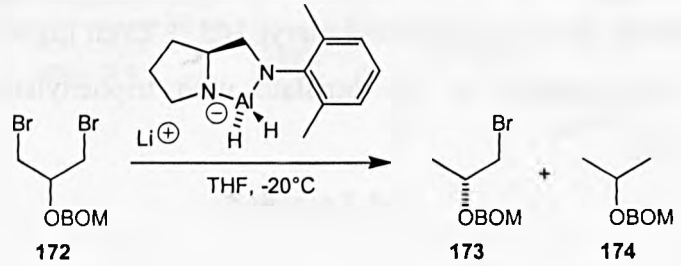

Reaction time (min)	Product distribution **172** : **173** : **174**	Yield of **173** (%)	%ee of **173**
30	29 : 69 : 2	55	25
50	10 : 86 : 4	69	42
60	3 : 91 : 6	74	53
90	- : 77 : 23	62	60
130	- : 60 : 40	48	74
240	- : 18 : 82	17	87

Scheme 1.59

Another example involving the desymmetrisation of halides is the enantioselective elimination of halide **175** using chiral lithium amide bases.[99] The chiral base discriminates between the two enantiotopic protons β to the halide to give α,β-unsaturated acid **176** in good chemical and optical yield (scheme 1.60).

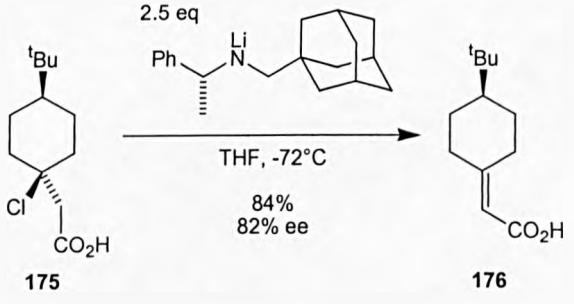

175 **176**

Scheme 1.60

Desymmetrisation by the catalytic asymmetric C-H insertion reaction of cyclohexyl diazoacetates has been reported.[100] Diazo decomposition of cyclohexyl diazoacetate **177** catalysed by chiral dirhodium(II)carboxamide **178** resulted in the formation of cis-fused bicyclic lactone **179** in good yield and excellent cis/trans ratio and ee (scheme 1.61).

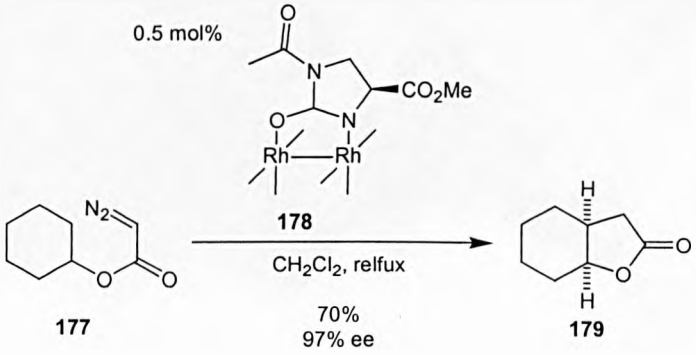

177 **179**

Scheme 1.61

Enantiotopic group selective C-H oxidation can be employed to desymmetrise prochiral cyclic ethers and amines. Mn-salen complex **180** catalyses the oxidation α to a heteroatom in *meso*

tetrahydrofuran and pyrrolidine derivatives in reasonable yield and very good ee[101,102] (scheme 1.62).

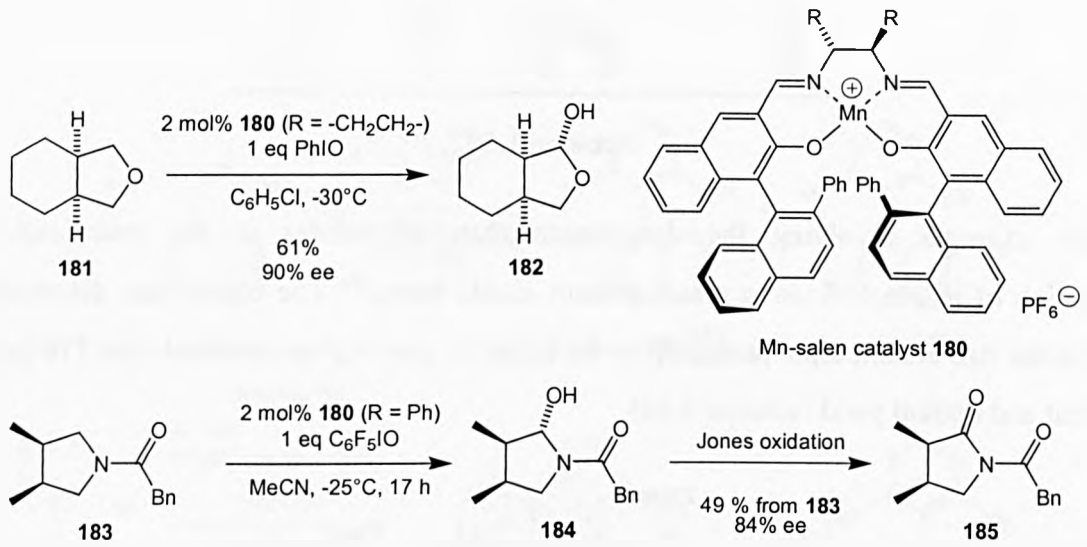

Scheme 1.62

Summary

To summarise then, it is clear to see from the examples presented above that asymmetric desymmetrisation is a powerful and versatile technique, encapsulating a vast array of reactions and substrates. When combined with the strategy of two-directional synthesis it allows for the efficient and highly selective asymmetric synthesis of a diverse range of synthetic targets, as confirmed by the numerous examples already published. In view of this proven track record, when considering the synthesis of natural products, we should all be challenged to identify elements of symmetry present in molecules to be able to apply this expedient technique.

Chapter 2: Asymmetric Desymmetrisation of 2-Pyridone [4 + 4]-Photodimers: 'Three-Dimensional' Desymmetrisation

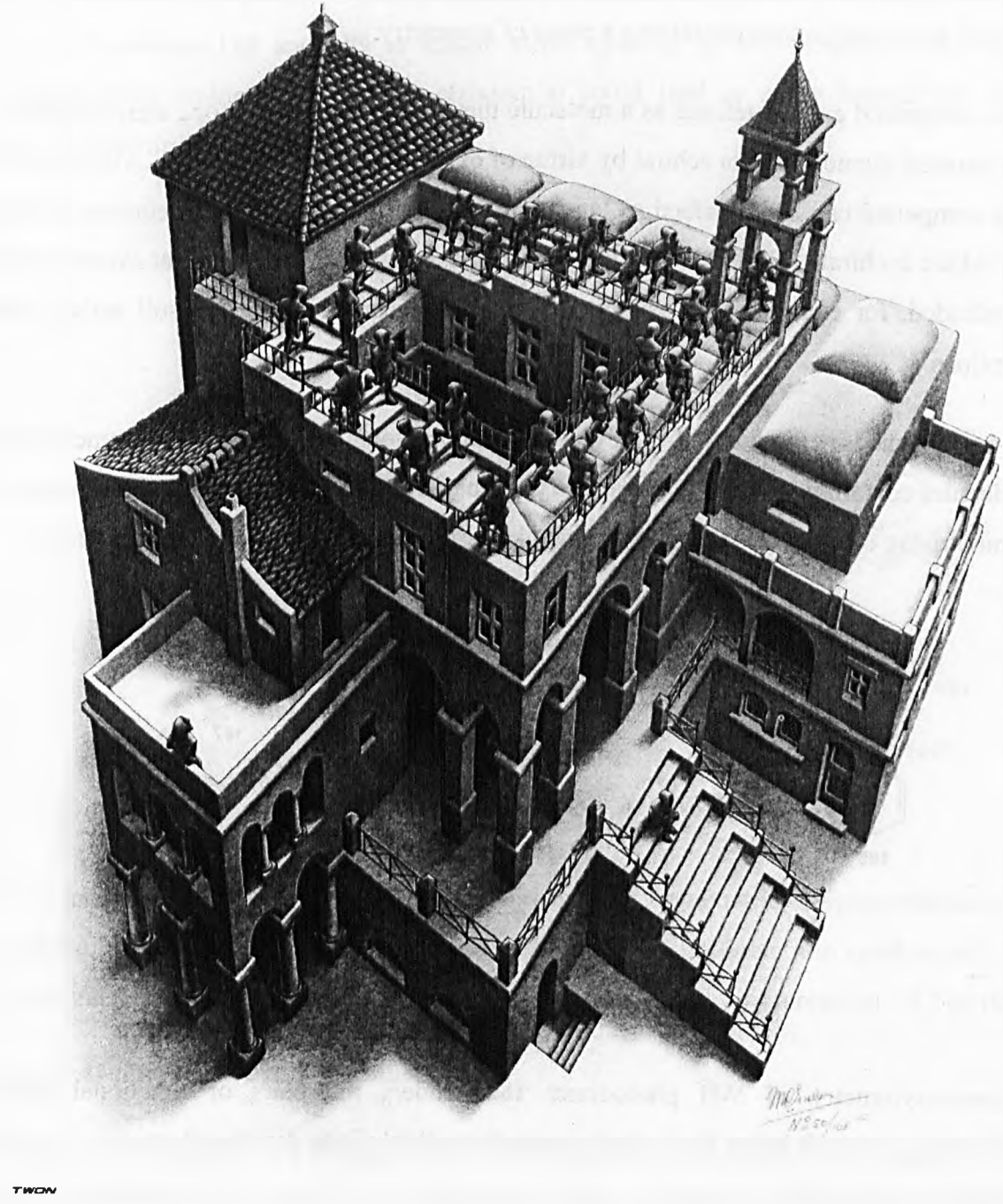

The perplexities of working in three dimensions.

Chapter 2: Asymmetric Desymmetrisation of 2-Pyridone [4+4]-Photodimers: 'Three-Dimensional' Desymmetrisation

The concept: 'three-dimensional' asymmetric desymmetrisation

The asymmetric desymmetrisation of *meso* intermediates is an attractive strategy in organic synthesis. However, to the best of our knowledge, this tactic has only been applied to 'classical' *meso* compounds containing a plane of symmetry.

A *meso* compound can be defined as a molecule that contains more than one stereocentre (or stereochemical element) but is achiral by virtue of overall molecular symmetry. Alternatively, a *meso* compound can be described as 'an achiral member of a set of diastereomers, at least one of which is chiral'. With either of these definitions other types of molecular symmetry are not precluded, for example centrosymmetric molecules can be *meso* and still satisfy both descriptions.

We were intrigued by the possibility of the 'three-dimensional' asymmetric desymmetrisation of molecules containing a centre of symmetry. Of particular interest to us was the prospect of desymmetrising centrosymmetric 2-pyridone [4+4]-photodimer derivatives (scheme 2.1).

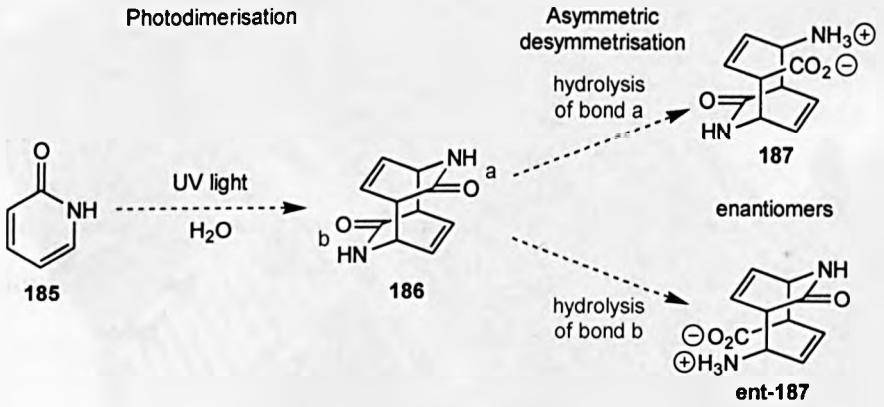

Scheme 2.1

The centrosymmetry of *N*-H photodimer **186** renders the pairs of functional groups enantiotopic, the result being that selective transformation of one functional group in a pair in preference to the other produces a single enantiomer in excess. For example, selective hydrolysis of bond a would give one enantiomer of amino-acid **187**, whereas exclusive hydrolysis of bond b would give the opposite enantiomer, **ent-187**.

The benefits of this strategy are obvious, four stereocentres are established and a high degree

of molecular complexity is attained in just two synthetic steps. Furthermore, as the photodimerisation is performed in aqueous solution using ultra-violet light and if enzymes are employed catalytically to perform the asymmetric desymmetrisation, the process has the potential to be highly environmentally benign.

Further elaboration

The desymmetrised product could conceivably be transformed into pseudoenantiomeric β-carboxyaspartates **188** and **189** in simple steps, opening up a conceptually new route to functionalised amino-acids. Further elaboration could lead to many homochiral building blocks (scheme 2.2).

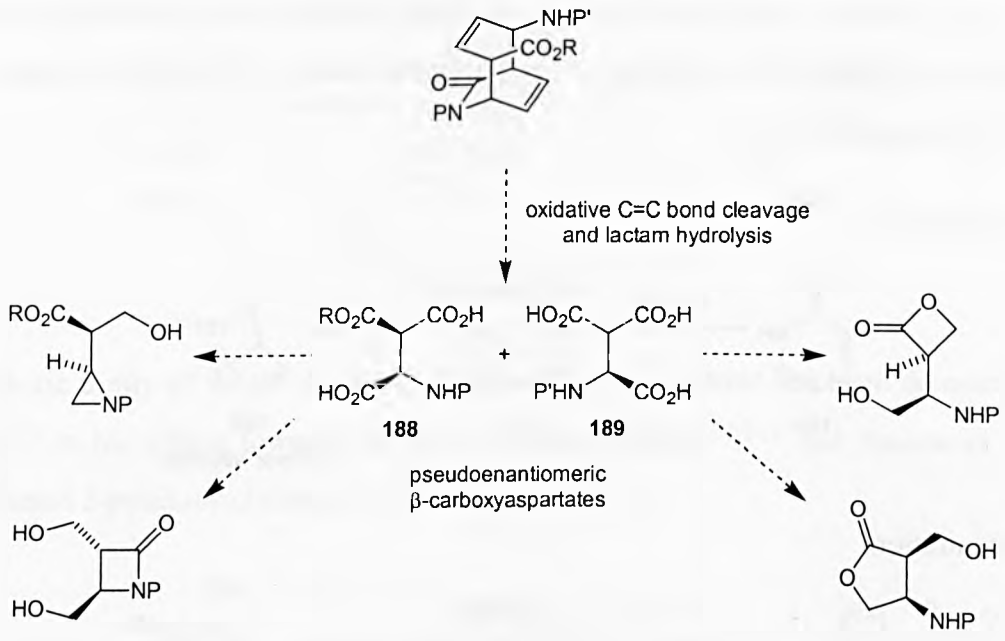

Scheme 2.2

This chapter details our efforts towards achieving the asymmetric desymmetrisation of 2-pyridone [4+4]-photodimer derivatives and elaborating the products into synthetically useful compounds, preceded by a brief introduction to the photodimerisation reaction of 2-pyridone.

The [4+4]-photodimer of 2-pyridone

The photodimerisation of 2-pyridone was first discovered in 1960 by Taylor and Paudler.[103] They observed that 2-pyridone, on irradiation with ultra-violet light in aqueous solution, gives a solid dimer to which they assigned structure **190**, the product of a [2+2]-photodimerisation. Shortly after, the structure of the photodimer was reassessed by De Mayo in the light of new

data, and the centrosymmetric [4+4]-cycloaddition product **186** was proposed (figure 2.1).[104-106]

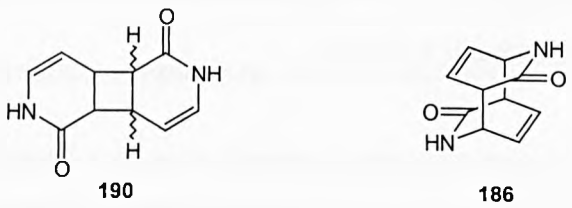

Figure 2.1

This compound is thought to be formed by a radical mechanism, whereby ultra-violet irradiation of 2-pyridone forms a 3,6-diradical **191**.[107] Depending on the concentration of 2-pyridone, this diradical can either undergo an intermolecular [4+4]-cycloaddition reaction with a second ground state molecule, or react intramolecularly to form its valence isomer **192**[108-110] (scheme 2.3).

Low concentration

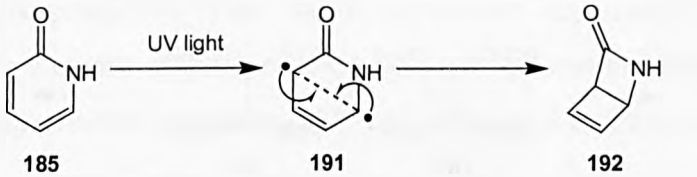

High concentration

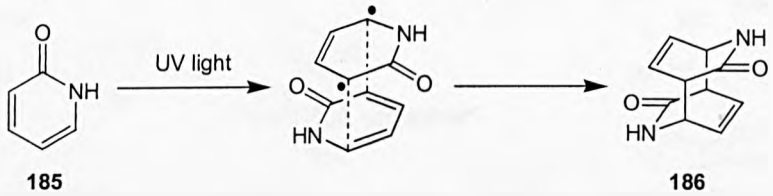

Scheme 2.3

Clearly the structure of the photodimer is dependent upon the relative orientation of the reacting 2-pyridone molecules, leading to a total of four possible regioisomers (figure 2.2). The *cis/trans* and *syn/anti* nomenclature refers to the relative orientations of the double bond and lactam functions respectively.[111]

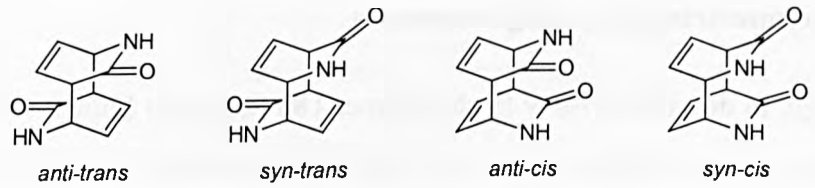

Figure 2.2

However, the photodimerisation of 2-pyridone in aqueous solution leads to predominantly the *anti-trans* product. This is thought to be the result of preorganisation of the 2-pyridone molecules by dipole-dipole interactions, resulting in the appropriate orientation to give the *anti-trans* product on irradiation[112] (scheme 2.4).

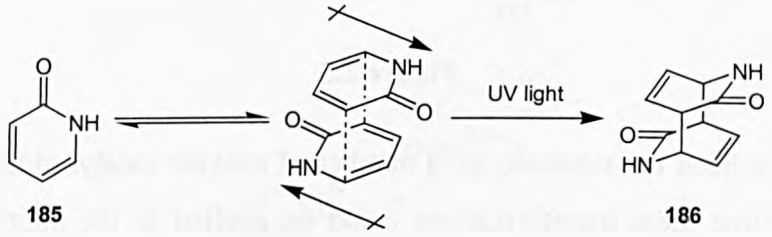

Scheme 2.4

The synthetic utility of the [4+4]-photodimerisation of 2-pyridone has been demonstrated by Sieburth[113] in his efforts towards the ring systems of taxol[114,115] and fusicoccin A[116-118] using tethered 2-pyridones (scheme 2.5).

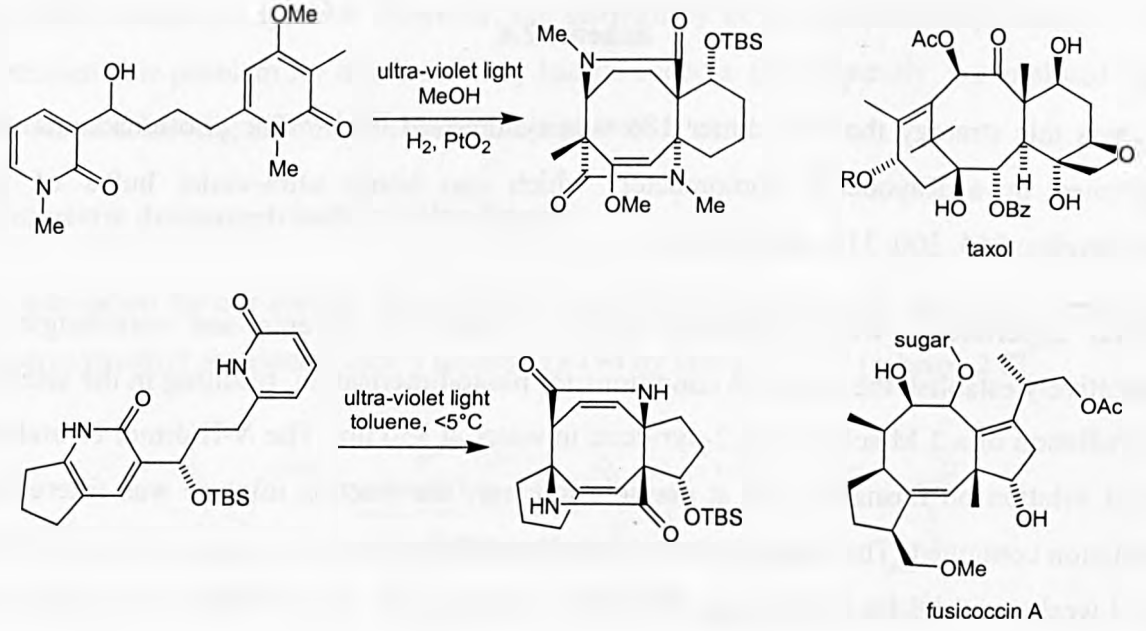

Scheme 2.5

Asymmetric desymmetrisation: using lactamases

Our initial strategy to desymmetrise *N*-H photodimer **186** (hereafter known simply as the *N*-H dimer) was to use lactamases to perform an asymmetric hydrolysis, as shown in scheme 2.1. One reason for chosing to investigate lactamases was that the photodimer exhibits a high degree of structural homology with bicyclic lactam **193**, known as Vince's lactam (figure 2.3). Each enantiomer of Vince's lactam is equivalent to one of the photodimer faces.

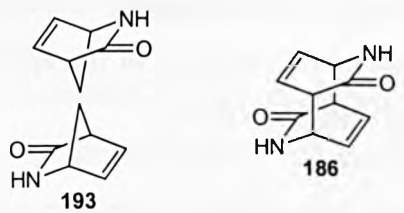

Figure 2.3

Vince's lactam has been the substrate for a number of enzyme catalysed kinetic resolutions, and we reasoned that these transformations could be applied to the photodimer system to achieve asymmetric desymmetrisation. In particular, kinetic resolution of racemic Vince's lactam **(±)-193** by Chiroscience using lactamases appeared interesting[119] (scheme 2.6).

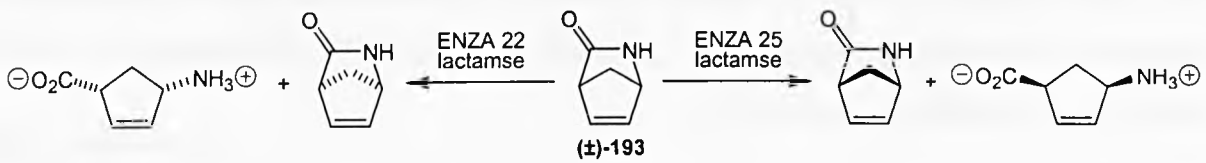

Scheme 2.6

Towards this strategy the *N*-H dimer **186** was synthesised.[107,120] The photoreactions were performed in a Rayonet™ photoreactor, which can house ultra-violet bulbs of four wavelengths: 254, 300, 310, and 350 nm.

Several experiments were performed with a variety of solvents and wavelengths to qualitatively establish the optimum conditions for photodimerisation, resulting in the selection of irradiation of a 3 M solution of 2-pyridone in water at 350 nm. The *N*-H dimer crystallised out of solution on formation and at periodic intervals the reaction mixture was filtered and irradiation continued. The reactions were typically performed on a 20 g scale over a period of 2 to 4 weeks, with yields in the range of 40-50% (scheme 2.7). The *N*-H dimer was isolated as a white crystalline solid, on recrystallisation from glacial acetic acid, and as a single *anti-trans* regioisomer.

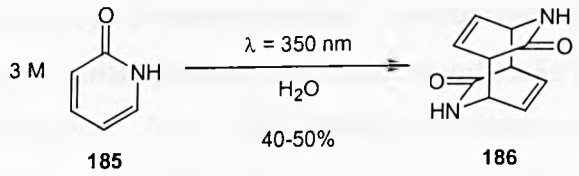

Scheme 2.7

It became apparent at this stage that the *N*-H dimer was insoluble in most solvents. The compound was only found to be soluble in deuterated trifluoroacetic acid (for the purposes of NMR), hot glacial acetic acid (for recrystallisation), and was sparingly soluble in warm water. This insolubility was presumably due to the formation of a hydrogen bonded array of photodimer molecules (figure 2.4).

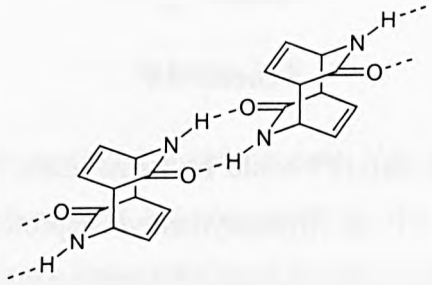

Figure 2.4

With the *N*-H dimer in hand we contacted Chiroscience in order to attempt the enzyme catalysed lactam cleavage. Two 1 g samples of the *N*-H dimer were sent in order for them to apply their lactamase systems. However, the insolubility of the photodimer proved to be an insurmountable problem for them, and they had no success. Consequently, we explored other methods of achieving asymmetric desymmetrisation.

Asymmetric desymmetrisation: using lipases

The inspiration for our second strategy arose from the lipase catalysed resolution of racemic *N*-hydroxymethyl protected Vince's lactam **(±)-194** by Hongo[121,122] (scheme 2.8).

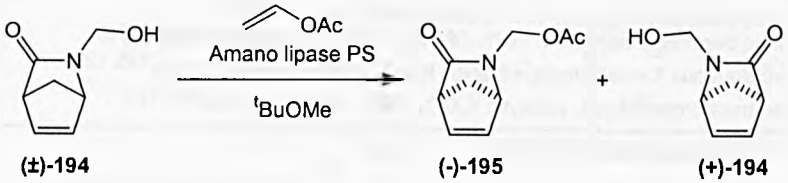

Scheme 2.8

We envisaged that the asymmetric desymmetrisation of *N*-hydroxymethyl and *N*-acetoxymethyl protected photodimers might be possible using lipases, by enantioselective acylation and hydrolysis respectively (scheme 2.9).

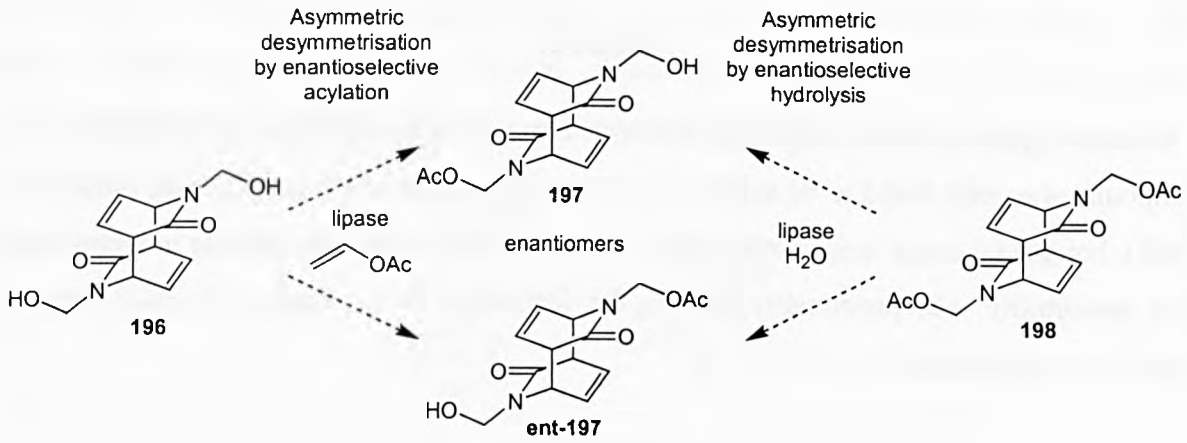

Scheme 2.9

Once desymmetrised, **197** and **ent-197** could be transformed into products resembling **187** and **ent-187** from scheme 2.1 by hydroxymethyl deprotection followed by selective hydrolysis of the primary amide in the presence of the secondary.

When synthesising *N*-protected photodimers, two options present themselves; direct protection of the *N*-H photodimer, or protection of 2-pyridone followed by photodimerisation. Direct *N*-hydroxymethyl protection of the *N*-H dimer by heating to 120°C with paraformaldehyde in a sealed container failed, so the *N*-hydroxymethyl protection of 2-pyridone was investigated (table 2.1).

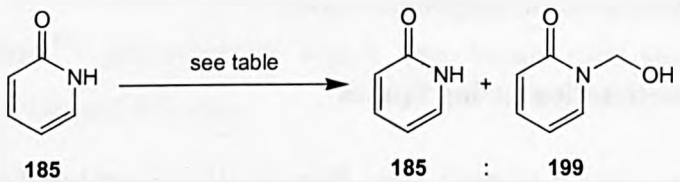

Entry	Conditions	Ratio[a] (%) 185 : 199
1	2 eq trioxane,[b] NaOH, EtOH, reflux, 3 h[123]	100 : 0
2	1.1 eq paraformaldehyde, 100°C, sealed container, 3 h[124]	80 : 20
3	1.2 eq paraformaldehyde, 5 mol% DMAP, 110°C, sealed container, 3.5 h	93 : 7
4	2 eq aqueous formaldehyde, catalytic K_2CO_3, MeOH, reflux , 2 days[125,126]	13 : 87
5	2 eq paraformaldehyde, catalytic K_2CO_3, H_2O, sonication, 24 h[121,125]	17 : 83

[a] by ^{1}H NMR; [b] a cyclic trimer of formaldehyde

Table 2.1

The sonication conditions (entry 5) were considered optimum as they consistently yielded the cleanest products. The hydroxymethyl group had a tendency to fall off on silica and to a lesser extent during recrystallisation from chloroform, however, despite this clean *N*-hydroxymethyl-2-pyridone was routinely isolated in yields of 47-58%.

Attempts to synthesise the *N*-acetoxymethyl dimer from *N*-acetoxymethyl-2-pyridone **200**[127] resulted in ester hydrolysis during the photodimerisation, giving the *N*-hydroxymethyl dimer **196** (scheme 2.10).

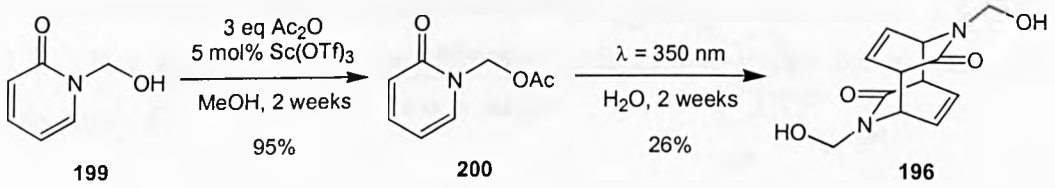

Scheme 2.10

Photodimerisation of *N*-hydroxymethyl-2-pyridone gave *N*-hydroxymethyl dimer **196**, albeit in low yield, and acylation furnished *N*-acetoxymethyl dimer **198** almost quantitatively, providing the two substrates for the lipase catalysed desymmetrisations (scheme 2.11).

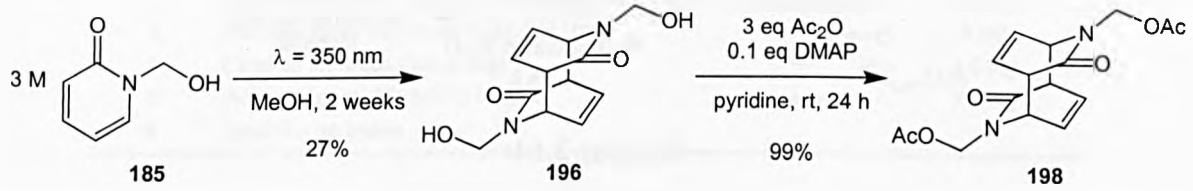

Scheme 2.11

Prior to performing the asymmetric desymmetrisations however, it was decided to characterise the expected desymmetrised product. Therefore, the partial hydrolysis of the *N*-acetoxymethyl dimer was performed with 1 equivalent of lithium hydroxide, to give the racemic *N*-acetoxymethyl/*N*-hydroxymethyl dimer **(±)-197** (scheme 2.12).

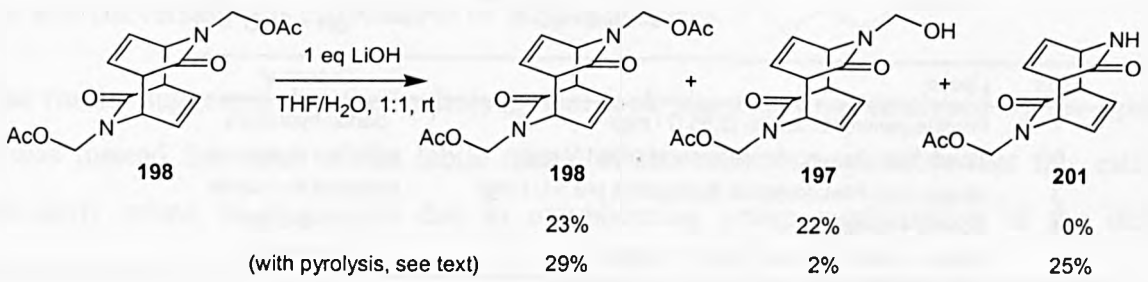

Scheme 2.12

It was found that heating the crude residue to 150°C under vacuum for 1 hour as part of the workup effected hydroxymethyl deprotection. This *in situ* deprotection differentiates more decisively between the two amides, paving the way to compounds like **187** and **ent-187** (scheme 2.1).

The asymmetric acylation of the *N*-hydroxymethyl dimer was attempted using Amano lipase PS and vinyl acetate in *tert*-butyl methyl ether.[121,128] However, no reaction was observed after 24 hours and starting material was recovered (scheme 2.13).

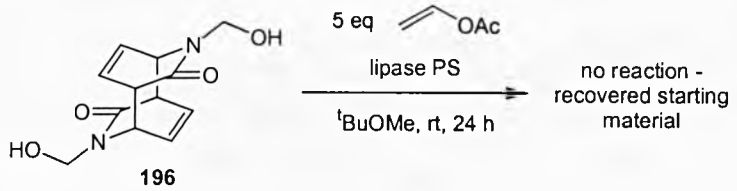

Scheme 2.13

Similarly, the asymmetric hydrolysis of the *N*-acetoxymethyl dimer was attempted using Amano lipase PS in diisopropyl ether (washed with aqueous sodium sulfite solution to remove peroxides) saturated with water. Once again, no reaction was observed (scheme 2.14).

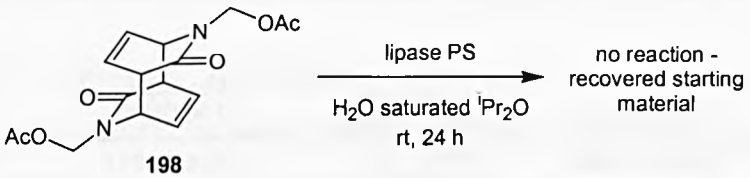

Scheme 2.14

At this point the activity of the enzymes was called into question. Therefore, a series of hydrolysis experiments was performed, with a variety of lipases and phenyl acetate as the substrate, to confirm the catalytic activity of the enzymes (table 2.2). Two control reactions were set up, one containing no lipase (entry 4), and the other containing no lipase and a drop of acetic acid (entry 5) to monitor the background rates of hydrolysis.

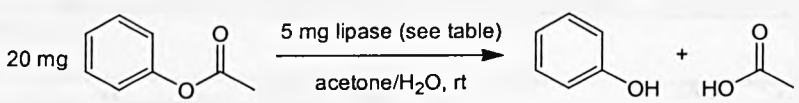

Entry	Lipase	Outcome[a]
1	Porcine pancreatic lipase (2.55 U / mg)	partial hydrolysis
2	Lipase from Pseudomonas cepacia (609 U / mg)	complete hydrolysis
3	Lipase from Pseudomonas fluorescens (42.5 U / mg)	complete hydrolysis
4	Control – no lipase	no hydrolysis
5	Control – no lipase and 1 drop of acetic acid	no hydrolysis

[a] by TLC after 1 h

Table 2.2

After a period of 1 hour, the reactions containing Pseudomonas cepacia and Pseudomonas fluorescens had gone to completion (entries 2 and 3), and the reaction containing Porcine pancreatic lipase showed evidence of reaction (entry 1). Both control reactions showed no reaction at all, indicating a relatively slow background hydrolysis rate, even in the presence of acetic acid (entries 4 and 5).

With the activity of the enzymes established, a more detailed study of the asymmetric hydrolysis of the *N*-acetoxymethyl dimer was undertaken. Six reactions were set up in a stem block, each containing 1 mg of the *N*-acetoxymethyl dimer in 0.05 M pH 7.2 buffer/acetone (table 2.3). Once again a control reaction was performed to gauge the uncatalysed rate of hydrolysis (entry 6).

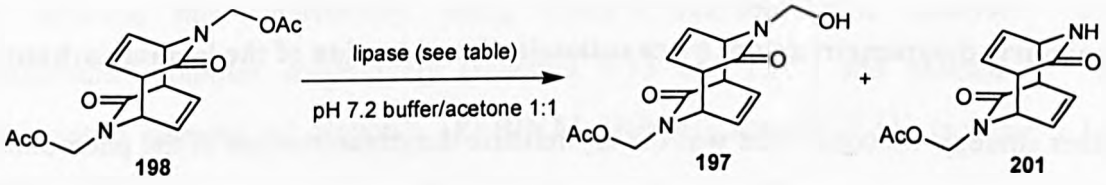

Entry	Lipase	Amount of lipase
1	Porcine liver esterase (PLE), suspension in 3.2 M $(NH_4)_2SO_4$ (19 mg protein / ml, 210 U / mg protein)	100 mg
2	Porcine pancreatic lipase (~23 mg protein, 61-200 U / mg protein)	8 mg
3	Pseudomonas fluorescens (31.5 U / mg)	6 mg
4	Candida antartica (3.3 U/ mg)	7.5 mg
5	'Amano' lipase PS (870 U / mg)	7.5 mg
6	Control – no lipase	-

Table 2.3

After stirring for 24 hours at room temperature very little reaction was observed, so the temperature was increased to 35°C and the stirring continued for another 4 days. Formation of the *N*-acetoxymethyl/*N*-hydroxymethyl dimer and small amounts of the *N*-acetoxymethyl/*N*-H dimer were observed by TLC, however, they were present in all reactions to an equal extent, including the control reaction containing no lipase. The reactions were stirred for a total of 8 days, and conversion was estimated to be 50% in all cases.

These results suggested that the hydrolysis that took place was not catalysed by the lipases, but was instead the result of the labile nature of the ester. It is possible that this ester is particularly prone to hydrolysis due to neighbouring group participation of the lactam nitrogen (scheme 2.15).

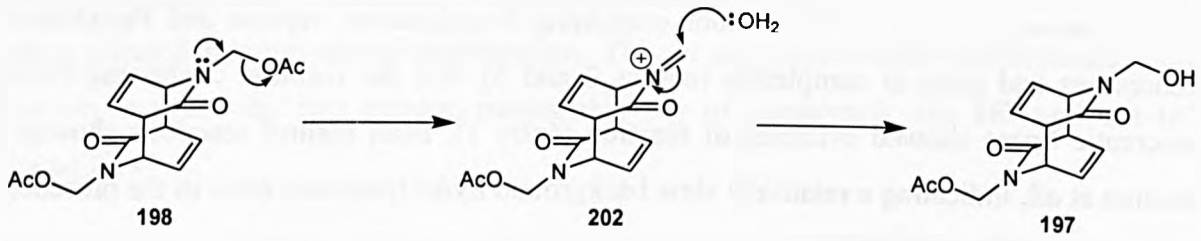

Scheme 2.15

It was apparent that the lipases were not participating in the reaction, perhaps indicating that the photodimer molecules are too big to fit into the active sites of these enzymes.

In the light of these complications and the success of other desymmetrisation strategies, we decided to focus our efforts elsewhere.

Asymmetric desymmetrisation: by enantioselective reduction of the lactam carbonyl

Another strategy we considered was the asymmetric desymmetrisation of the photodimers by enantioselective reduction.[129,130] A homochiral hydride reducing agent could potentially differentiate between the two enantiotopic carbonyl groups and give ring opened amino-aldehyde **203** or **ent-203** in excess (scheme 2.16).

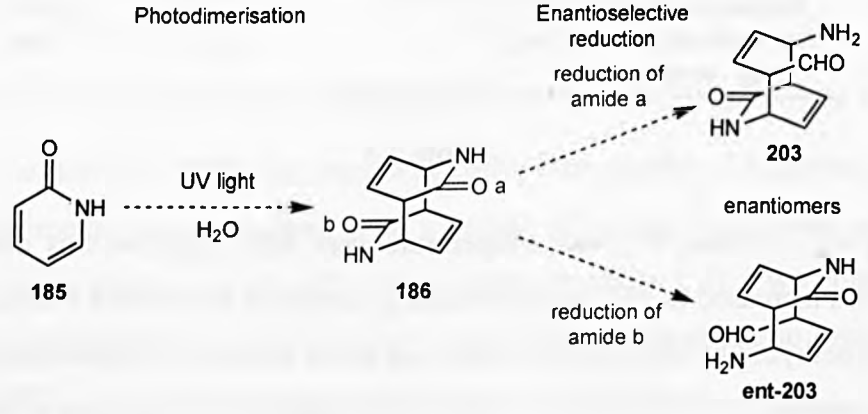

Scheme 2.16

The amino-aldehydes **203** and **ent-203** differ only in oxidation state to the compounds **187** and **ent-187** presented in the original concept (scheme 2.1).

Literature precedents

At the outset of our work, only one account existed in the literature pertaining to the hydride reduction of a photodimer system. Paquette has reported the reduction of a tetrahydro

derivative of an *N*-methyl protected photodimer with lithium aluminium hydride[107] (scheme 2.17). However, in our case, complete reduction of the carbonyl groups to methylenes is undesirable, as subsequent ring opening would become more problematic.

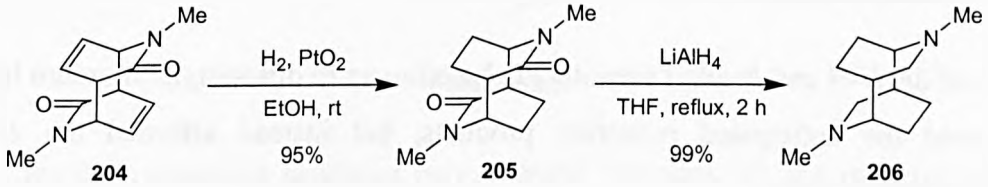

Scheme 2.17

Reports on the enantioselective hydride reduction of amidic compounds are limited to the asymmetric desymmetrisation of cyclic *meso* imides. Both Speckamp[17,18] and Kang[15,16] have achieved this catalytically, using Corey's oxazaborolidine catalyst[131] and a thiazincolidine complex respectively (schemes 1.13 and 1.12), and Matsuki[13,14] using stiochiometric amounts of Noyori's (*R*)-BINAL-H(ROH) reagent[132,133] (scheme 1.11) as reported in chapter 1.

N-Alkyl protection

Our initial investigations in this area involved the synthesis and reduction of various *N*-alkyl substituted photodimers. In all cases it was more efficient to alkylate 2-pyridone prior to photodimerisation than to directly alkylate the *N*-H dimer itself, as its insolubility proved problematic. In this way the known *N*-Me[103,104] and novel *N*-Bn photodimers were prepared (scheme 2.18), both of which were far more soluble in organic solvents than the *N*-H dimer. The *N*-Bn dimer offered the added advantage of being easier to deprotect than the *N*-Me dimer.

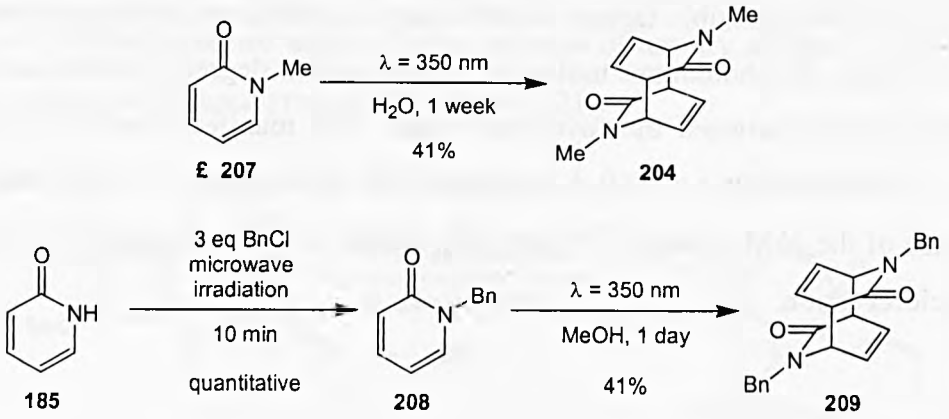

Scheme 2.18

A remarkable reaction was employed for the synthesis of *N*-Bn-2-pyridone **208** which used microwave irradiation. Depending on the benzyl halide, the N *versus* C alkylation selectivity can be completely reversed by simply changing the power of the microwave irradiation or by using conventional heating.[134,135]

Subjection of the *N*-H and *N*-alkyl substituted photodimers to diisobutylaluminium hydride[136] did not yield the anticipated reduction products, but instead afforded the 2-pyridone 'monomers' (scheme 2.19).

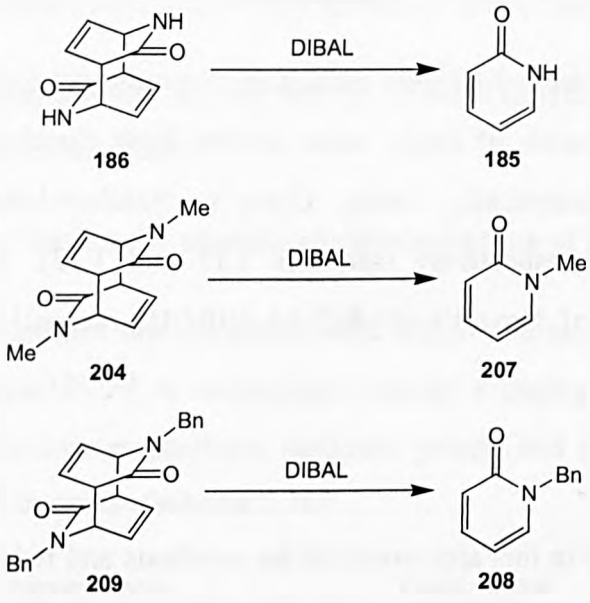

Scheme 2.19

Similarly, treatment of the *N*-H dimer with 3 equivalents of lithium aluminium hydride in refluxing tetrahydrofuran for 5 hours gave a small amount of 2-pyridone with mainly starting material.

There appear to be two possible factors contributing to the tendency of these photodimers to cyclorevert. Firstly, the photodimer molecules have a certain degree of strain brought about by the close contacts between the 'pyridone' rings. This manifests itself in a long 'inter monomer' C-C bond length, i.e. 1.60 Å compared with the average C-C bond length of 1.54 Å (in the case of the *N*-Me dimer,[137] figure 2.5). Relief of this strain may be a contributing factor to cycloreversion.

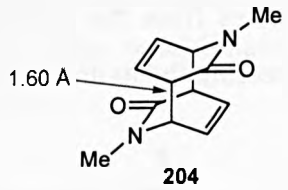

204

Figure 2.5

Secondly, the cycloreversion produces two aromatic 'monomers', the two molecules of 2-pyridone. This gain in aromaticity may be a contributing factor to cycloreversion.

Furthermore, we speculated that the cycloreversion could be facilitated by the Lewis acidity of organoaluminium compounds (scheme 2.20).

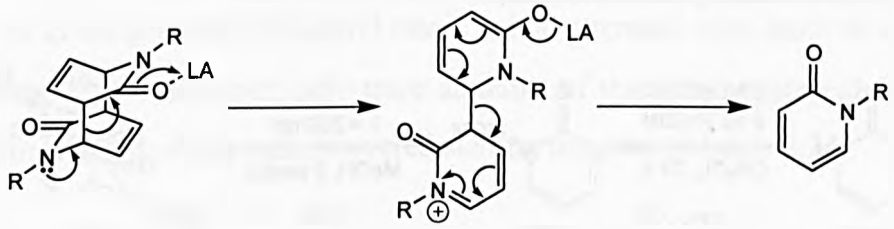

Scheme 2.20

It seems likely that Paquette chose to hydrogenate the photodimers prior to treatment with lithium aluminium hydride (scheme 2.17) in order to remove one of the driving forces for cycloreversion, namely the gain in aromaticity.

N-Methoxymethyl protection

In an effort to encourage lactam reduction in preference to cycloreversion, we investigated the reduction of *N*-MOM photodimer **211**. Mori and co-workers have reported the selective reduction of *N*-MOM protected amides in the presence of tertiary amides as the final step in their total synthesis of Pretomaymycin[138] (scheme 2.21).

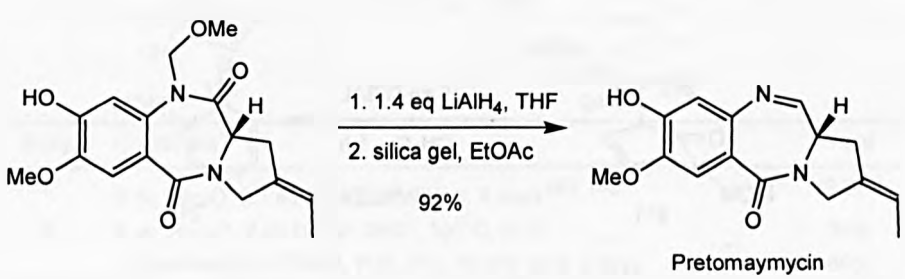

Pretomaymycin

Scheme 2.21

It is thought that this selectivity arises from the coordination of the reducing agent to the methoxymethyl substituent, thus directing the hydride on to the amide carbonyl (figure 2.6).

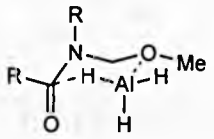

Figure 2.6

N-MOM protection of 2-pyridone by treatment with methoxymethyl chloride and Hünigs base afforded *N*-MOM-2-pyridone **210** in excellent yield,[138] which was then photodimerised to *N*-MOM dimer **211**. The *N*-MOM dimer was also synthesised by direct alkylation of the *N*-H dimer, but not as efficiently (scheme 2.22).

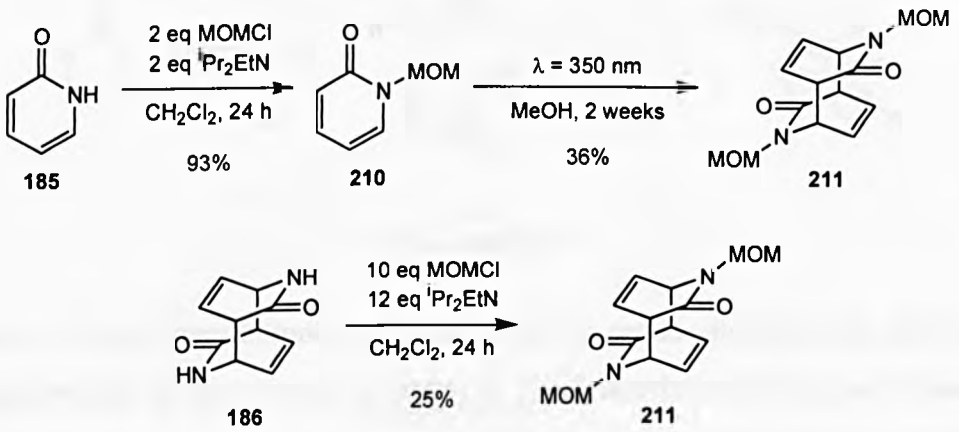

Scheme 2.22

Attempted reduction of the *N*-MOM dimer with 10 equivalents of sodium borohydride in ethanol/dichloromethane[138] resulted in no reaction, and the starting material was recovered in 94% yield. However, treatment of the *N*-MOM dimer with diisobutylaluminium hydride resulted in quantitative cycloreversion to *N*-MOM-2-pyridone, an analogous result to the other *N*-alkyl substituted photodimers (scheme 2.23).

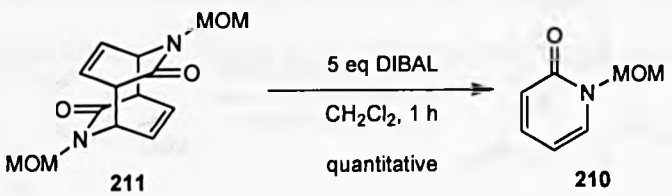

Scheme 2.23

It became clear at this point that more would have to be done to activate the photodimers towards reduction, and protecting groups would have to be selected that increase the electrophilicity of the lactam carbonyls.

Lactam activation: by *N*-protection

The electrophilicity of an amide carbonyl is compromised by conjugation of the adjacent nitrogen lone pair. It therefore follows that the presence of electronegative or conjugating groups on nitrogen increase the electrophilicity of the carbonyl by drawing electron density away from it. Examples of protecting groups that perform this function are nitroso, carbamate, sulfonyl, and phosphinyl, amongst others.

As *N*-nitroso lactams have recently been shown to be highly activated towards hydride reduction, even in the presence of methyl esters, initial attempts were made to synthesise the *N*-nitroso dimer.[139-141] However, only trace amounts of the mono protected *N*-nitroso/*N*-H dimer **212** were isolated, along with recovered starting material (scheme 2.24).

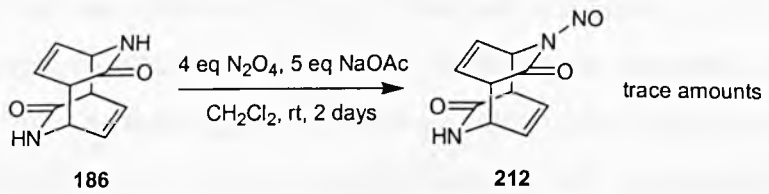

186 **212**

Scheme 2.24

In view of this, and the hazardous nature of *N*-nitroso compounds, it was decided to pursue other options.

The next protecting group attempted was the *tert*-butoxycarbonyl (Boc) group. Efforts to synthesise the *N*-Boc dimer **213** were hindered by the low solubility of the *N*-H dimer. Extensive experimentation revealed three sets of conditions for *N*-Boc protection (table 2.4).

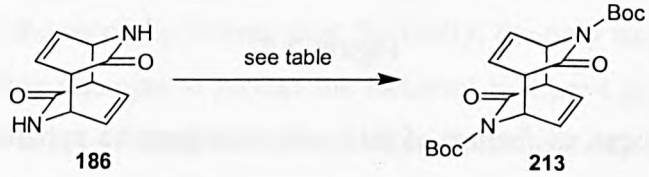

186 **213**

Entry	Conditions	Yield
1	6 eq Boc_2O, 2.1 eq DMAP, MeCN, rt, 4 days[142,143]	19-91%
2	4 eq, Boc_2O, 2 eq DMAP, NMP, 100°C, 24 h	35%
3	2.5 eq Boc_2O, 2.2 ^nBuLi, THF, 0°C, 30 min to rt, 2 days	80%

Table 2.4

Treatment of the *N*-H dimer with Boc_2O and stoichiometric DMAP in acetonitrile afforded *N*-Boc dimer **213** (entry 1), however, the initially high yields fell significantly when the reaction was scaled up. Alternative conditions employed *N*-methyl pyrrolidinone (NMP) as a solvent, with heating to 100°C to encourage the *N*-H dimer into solution. Unfortunately, the removal of the NMP proved problematic, involving multiple washes with water and recrystallisations, leading to a low isolated yield of the *N*-Boc dimer (entry 2). The eventual conditions elaborated involved treatment of a suspension of the *N*-H dimer in THF with ^{n}BuLi, followed by the addition of Boc_2O. This procedure routinely gave the *N*-Boc dimer in high yields, even on scale-up, and used less equivalents of the expensive Boc_2O reagent than the previous methods (entry 3).

As anticipated, the two Boc groups rendered the *N*-Boc photodimer more soluble in organic solvents than the *N*-H dimer, making it much easier to work with.

Reduction of the *N*-Boc dimer

With the *N*-Boc dimer synthesised, the next step was to attempt the hydride reduction.[144] Promisingly, initial attempts using DIBAL yielded small amounts of mono and di reduced products **(±)-214** and **215** along with recovered starting material, with no evidence of cycloreversion. Interestingly, the isolated reduction products were not the expected ring opened amino-aldehydes (as in scheme 2.16) but instead the ring closed lactamols* (figure 2.7).This is perhaps due to the rigid nature of the cage like photodimer structure, holding the lactamol ring closed.

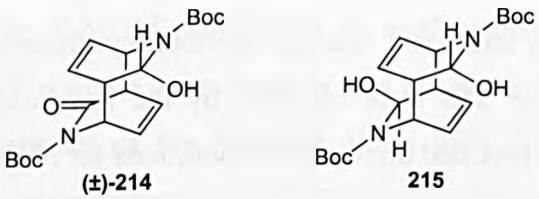

Figure 2.7

An interesting stereochemical feature of this reduction became apparent at this point. Only one face of each carbonyl group is available for nucleophilic attack, the other face is obscured by the alkene moiety of the opposite 'pyridone' ring (figure 2.8).

* We prefer the term lactamol[144] in preference to cyclic hemi-aminal, by analogy with lactone → lactol, lactam → lactamol.

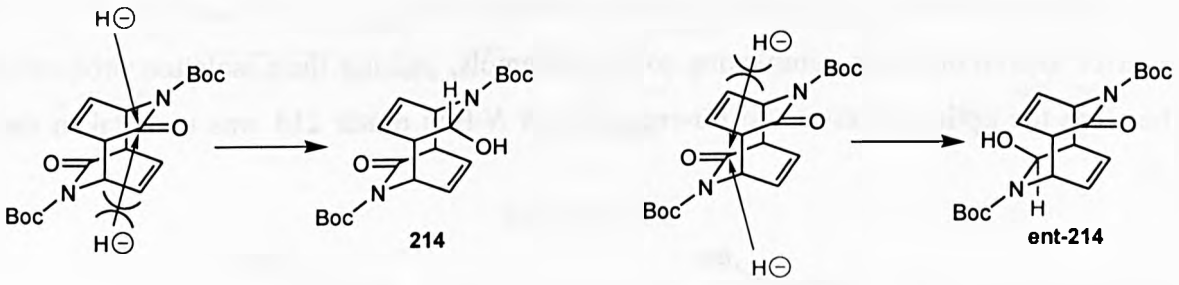

Figure 2.8

The result of this is that only 'axial' attack of hydride takes place, giving rise to products with an axial hydrogen, as depicted in figure 2.7. No other epimers of mono or di lactamols were observed by ^{1}H NMR, and x-ray crystal structures of other reduced photodimer derivatives also showed only axial* epimers (for example, see figures 2.11, 2.14 and 2.20).

However, it could be argued that the conformation of the lactamol centre can interconvert via *N*-acyl iminium ion **216** (scheme 2.25), and we are simply observing the thermodynamic product.

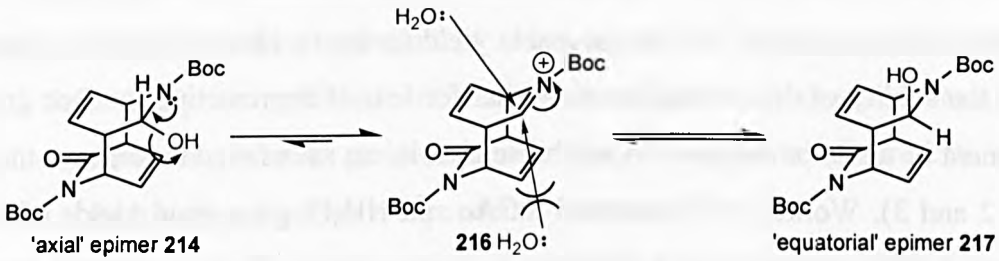

Scheme 2.25

This is not thought to be the case for two reasons. Firstly, if the equilibrium exists as depicted in scheme 2.25 then one would predict that the major isomer would be the equatorial epimer **217**. This is because the equatorial attack of H_2O to give axial epimer **214** is unfeasible due to the steric hindrance of the second pyridone ring. Secondly, the only time an equatorial epimer was observed was during attempts to protect the lactamol hydroxyl group of a monoreduced photodimer derivative as a (+)-camphorsulfonyl ester (scheme 2.41). This suggests that the equilibrium depicted in scheme 2.25 is not in operation unless the lactamol hydroxyl function is made into a better leaving group.

* With respect to hydrogen.

The yields and recovery of the initial reduction attempts were low. This was thought to be the result of aluminium salts complexing to the lactamols, making their isolation problematic. Therefore the optimisation of the *bis*-reduction of *N*-Boc dimer **213** was undertaken (table 2.5).

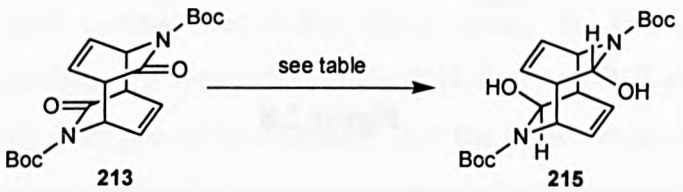

213 **215**

Entry	Conditions[a]	Workup	Yield **215**
1	5 eq DIBAL, 1 h	0.2 M HCl	64%
2	2 eq DIBAL, 5 min	Rochelle's salt[b][145]	43%
3	2 eq DIBAL, 5 min	saturated KF then 10% NaOH[146]	58%
4	2 eq DIBAL, 1 h	saturated KOAc and NH_4Cl[144]	71%
5	2.5 eq DIBAL, 10 min	10% citric acid	73%

[a] All reactions were performed in CH_2Cl_2 at rt. [b] Rochelles salt = sodium potassium tartrate.

Table 2.5

Exposure of the *N*-Boc dimer to 5 equivalents of DIBAL followed by workup with 0.2 M HCl furnished *N*-Boc dilactamol **215** in reasonable yield (entry 1). However, we were reluctant to increase the acidity of the workup much further for fear of deprotecting the Boc groups. The employment of workups designed to solubilise aluminium salts failed to improve the situation (entries 2 and 3). Workup with saturated KOAc and NH_4Cl gave good yields of the *N*-Boc dilactamol, but the procedure was laborious and messy (entry 4). The optimum procedure in terms of yield and practicability involved workup with 10 % citric acid solution, affording *N*-Boc dilactamol **215** in 73% yield.

Interestingly, and subsequent to our studies, Sieburth published the hydride reduction of the *N*-Boc protected lactam of photodimer system **218**[147] (scheme 2.26). Lactamol **219** was isolated, but the stereochemistry of the lactamol centre was not established (by analogy with our work, the lactamol hydroxyl is probably oriented equatorially). Furthermore, he found that refluxing the lactamol with excess reducing agent afforded ring-opened amino-alcohol **220**, a transformation that could be of use to us when further elaborating the desymmetrised products.

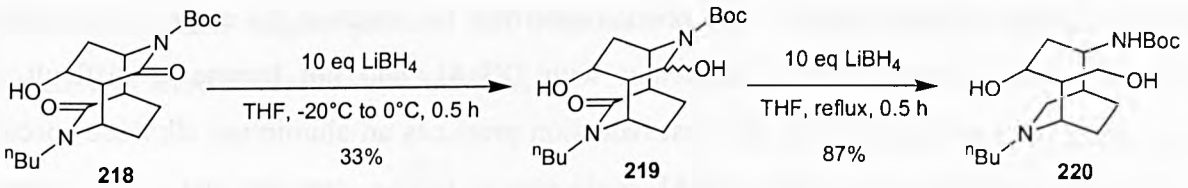

Scheme 2.26

With the reduction procedure optimised, another reduction was performed using 1 equivalent of DIBAL in order to isolate and characterise the racemic *N*-Boc monolactamol **(±)-214** (scheme 2.27).

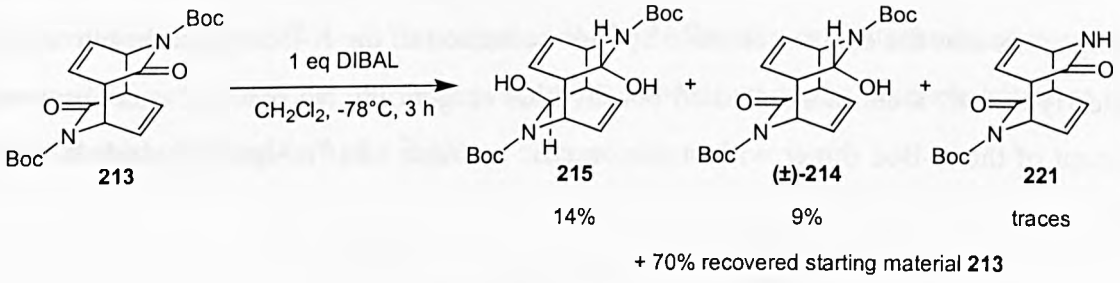

Scheme 2.27

Surprisingly, *N*-Boc monolactamol **(±)-214** was isolated in smaller quantities than the dilactamol. Statistically, on treatment with 1 equivalent of reducing agent one would expect the monolactamol to be present in greater amounts than the dilactamol (figure 2.9), assuming that reaction at each carbonyl occurs independently.

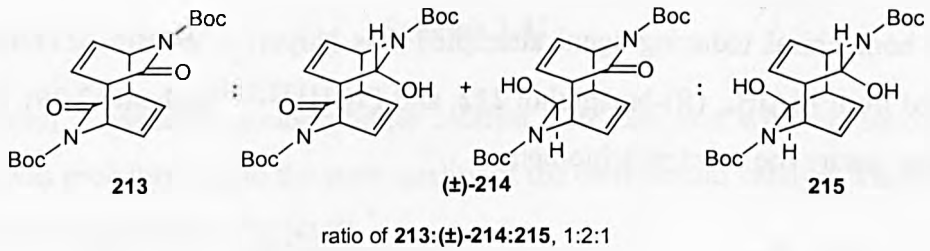

Figure 2.9

This result suggests that there are co-operative effects in operation, i.e. that the reactivity of one carbonyl is increased on reaction of the other. Co-operative effects were also observed during the DIBAL reduction of other photodimer derivatives (scheme 2.35, and 2.83). We initially speculated that this was probably the result of subtle conformation changes of the photodimer induced by the first reduction. However, this theory was later disproved when the borane reduction of a photodimer derivative gave the monolactamol as the major product

(table 2.6, entry 1), indicating that this phenomenon was the result of the reagent and not the substrate. This co-operativity of reduction with DIBAL and not borane is difficult to rationalise, but we speculate that the first reduction produces an aluminium alkoxide species which then aggregates with other DIBAL molecules to form a complex that allows 'quasi-intramolecular' reduction of the second carbonyl.

In preparation for the asymmetric reduction, a chiral HPLC assay was developed and the two enantiomers of the racemic *N*-Boc lactamol were baseline resolved.

Asymmetric reduction of the *N*-Boc dimer

Investigations into the enantioselective hydride reduction of the *N*-Boc dimer began with (*R*)-Alpine Hydride®, a chiral substituted borohydride reagent.[148] No reaction was observed on treatment of the *N*-Boc dimer with stoichiometric amounts of (*R*)-Alpine Hydride® (scheme 2.28).

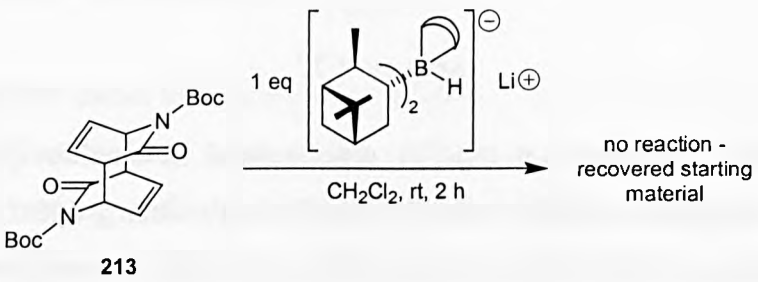

213

Scheme 2.28

The second homochiral reducing agent attempted was Noyori's (*R*)-BINAL(EtOH) reagent **223**, prepared from $LiAlH_4$, (*R*)-binaphthol **222**, and EtOH[132,133] (scheme 2.29). The $LiAlH_4$ was titrated to ensure the exact stoichiometry.

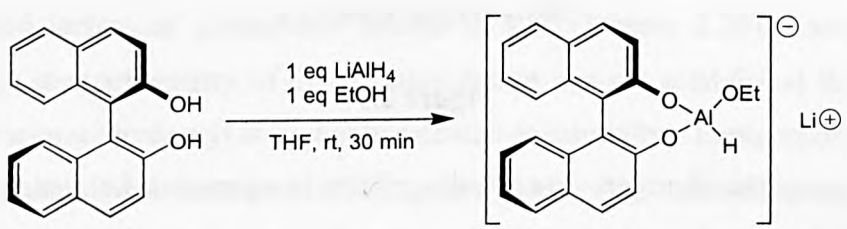

222 223

Scheme 2.29

However, no reaction was observed on exposure of the *N*-Boc dimer to 2.5 equivalents of the

(*R*)-BINAL(EtOH) reagent (scheme 2.30), the same conditions employed by Matsuki for his reduction of *meso* imides[13,14] (scheme 1.11).

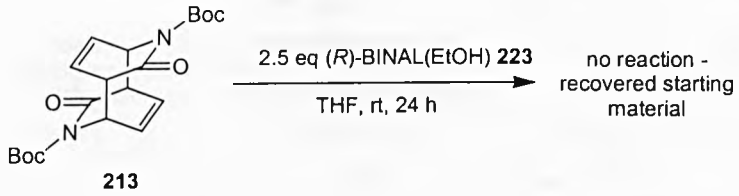

Scheme 2.30

Speckamp's conditions for the reduction of *meso* imides[17,18] (scheme 1.13) using Corey's oxazaborolidine catalyst[131] were then applied to the *N*-Boc dimer. Catecholborane was used as the stoichiometric hydride source to prevent hydroboration of the alkenes, but once again no reaction was observed (scheme 2.31).

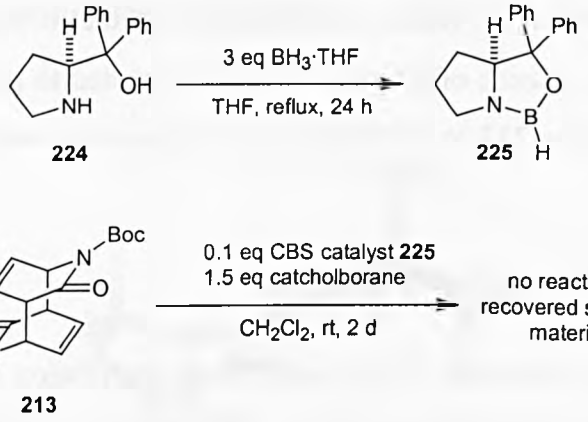

Scheme 2.31

Reduction with *B*-methyl oxazaborolidine catalyst **226** also met with no success (scheme 2.32). This was probably due to the poor quality of the commercial catalyst which was shown to be both wet and impure by ^{1}H NMR.*

* Indeed, in a test reaction, the commercial catalyst completely failed to reduce acetophenone. Conditions: 0.1 eq catalyst, 0.6 eq BH_3·THF, THF, rt, 24 h.[149]

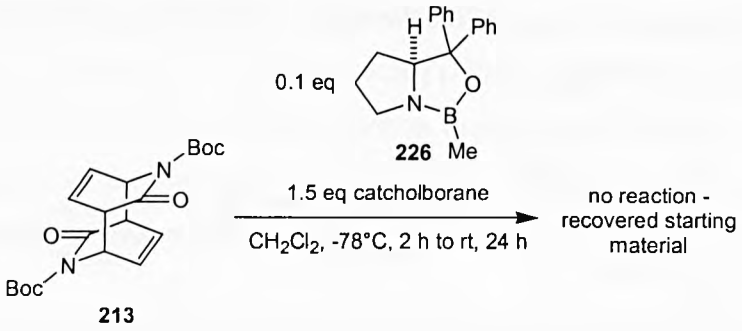

Scheme 2.32

The poor reactivity of the *N*-Boc dimer towards these homochiral reducing agents was puzzling, especially in the light of the successful DIBAL reductions. So, it was decided to select an asymmetric reduction system and investigate it in more depth. We chose Corey's oxazaborolidine system as it was catalytic and had the most potential for optimisation, for example by variation of the substituent on boron, the geminal aryl groups, and the stoichiometric hydride source. A recent review has shown that it is possible to perform the CBS* reduction in the prescence of alkenes,[131] but we decided to perform the optimisations on *N*-Boc tetrahydro dimer **227** to eliminate any complications associated with competing alkene hydroboration.

Preparation of the *N*-Boc tetrahydro dimer

According to Paquette's procedure,[107] the catalytic hydrogenation of the *N*-H dimer using Adam's catalyst yielded *N*-H tetrahydro dimer **228**, but the insolubility of the *N*-H dimer made it very difficult to drive the reaction to completion. Boc protection of the products showed an approximately 5:1 ratio of *N*-Boc tetrahydro dimer **227** to *N*-Boc dimer **213**, which were difficult to separate by chromatography (scheme 2.33).

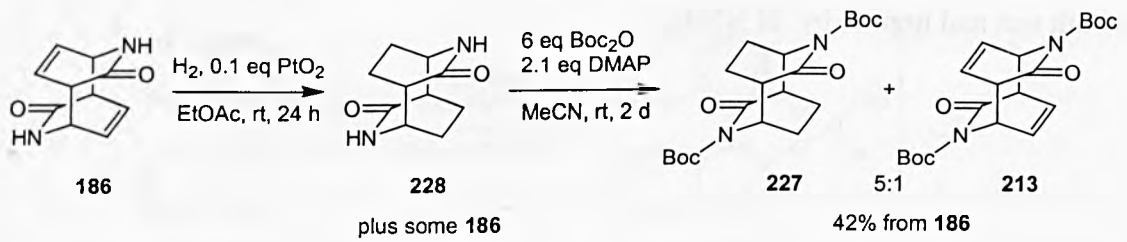

Scheme 2.33

* CBS = Corey-Bakshi-Shibata.

However, hydrogenation of the more soluble *N*-Boc dimer gave *N*-Boc tetrahydro dimer **227** almost quantitatively (scheme 2.34).

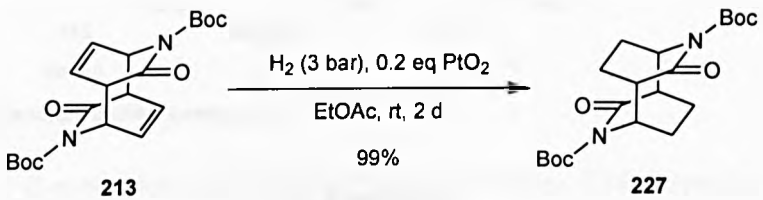

Scheme 2.34

An x-ray crystal structure of *N*-Boc tetrahydro dimer **227** clearly showed the centrosymmetry of the molecule and the *anti-trans* orientation of the 'pyridone' rings relative to one another. Also, the carbonyls of the Boc groups are co-planar with the lactam carbonyl groups, which can be interpreted as evidence of the Boc groups withdrawing electron density from the lactam carbonyls and increasing their electrophilicity, providing a similar conformation exists in solution (figure 2.10).

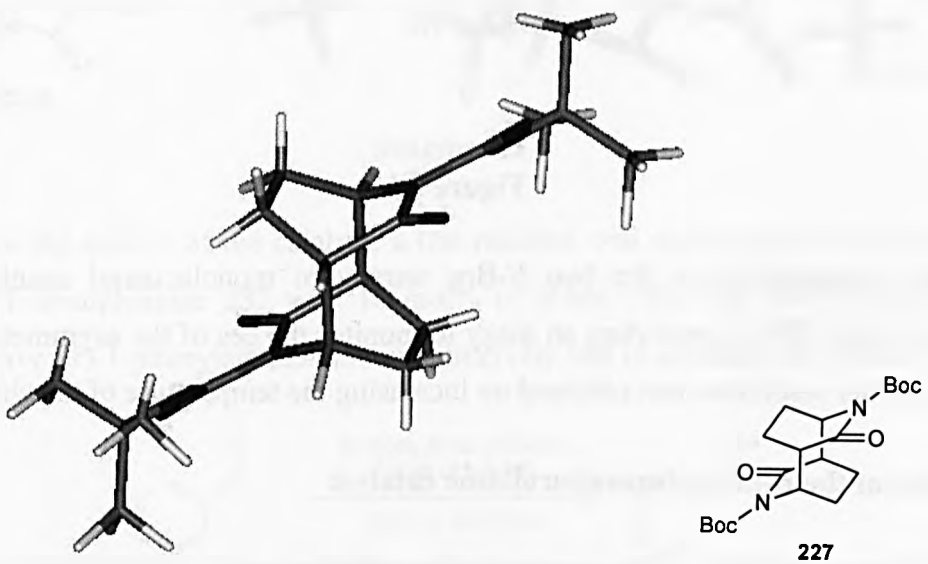

Figure 2.10

As before, the *N*-Boc tetrahydro dimer was subjected to DIBAL in order to isolate and characterise the reduction products. Treatment with 2 equivalents of DIBAL yielded both the *N*-Boc tetrahydro di and monolactamols **230** and **(±)-229**, recovered starting material **227**, and also trace amounts of two over-reduction products **231** and **232** formed by reduction of the Boc carbonyl (scheme 2.35).

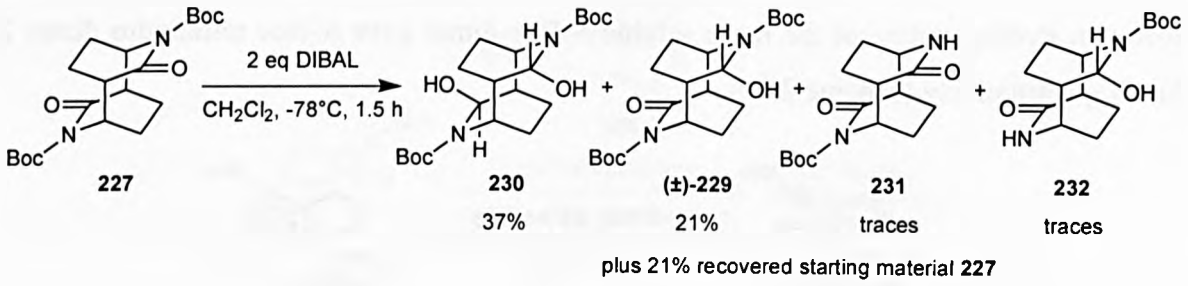

Scheme 2.35

An x-ray crystal structure of racemic *N*-Boc tetrahydro monolactamol **(±)-229** was obtained, which clearly showed the hydrogen of the lactamol centre to be axial, thereby confirming the stereochemistry of reduction (figure 2.11).

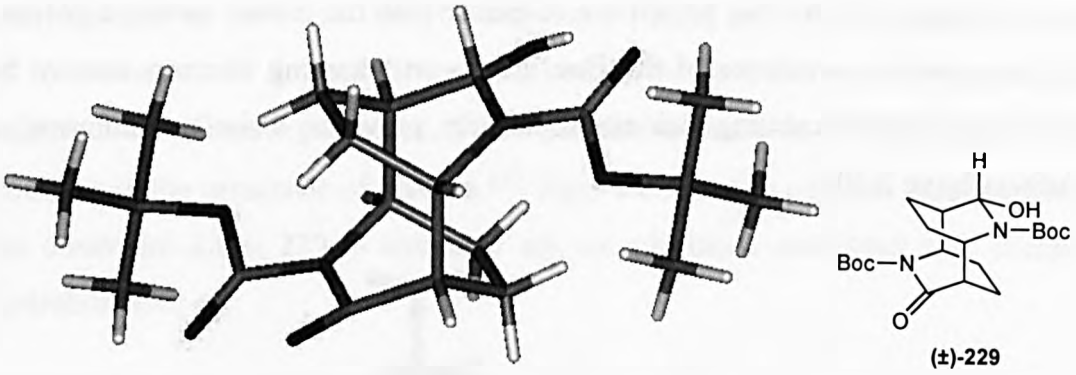

Figure 2.11

The peaks corresponding to the two *N*-Boc tetrahydro monolactamol enantiomers were resolved by chiral HPLC, providing an assay to monitor the ees of the asymmetric reduction. Unusually, better resolution was obtained on increasing the temperature of the chiral column.

Preparation of the *B*-methyloxazaborolidine catalyst

In view of the poor quality of the commercially available catalyst, we chose to synthesise the *B*-methyloxazaborolidine/borane complex **236** according to the procedure of Mathre,[150] as it is known that the borane complex of the catalyst is both easier to handle and less air and moisture sensitive than the free catalyst. Also, as commercial (*S*)-diphenylprolinol is expensive we chose to synthesise the catalyst from (*S*)-proline (scheme 2.36). Proline was reacted with phosgene followed by Et_3N to give the *N*-carboxyanhydride **234**. Treatment of this compound with excess phenylmagnesium chloride followed by an acidic workup gave (*S*)-diphenylprolinol sulfate, which was neutralised with NaOH to give (*S*)-diphenylprolinol **224**.

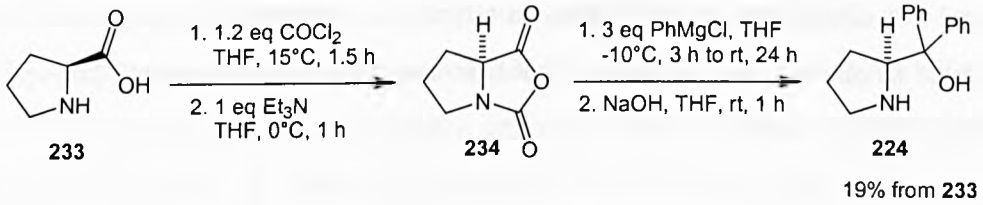

Scheme 2.36

The preparation of *B*-methyloxazaborolidine/borane complex **236** (hereafter known as *B*-Me CBS·BH_3) involved the exposure of (*S*)-diphenylprolinol **224** to trimethyl boroxine followed by borane/dimethylsulfide (BH_3·DMS). The *B*-Me CBS·BH_3 catalyst was crystallised on addition of hexane to give a white, free flowing solid which is stable at 4°C under nitrogen for extended periods (scheme 2.36).

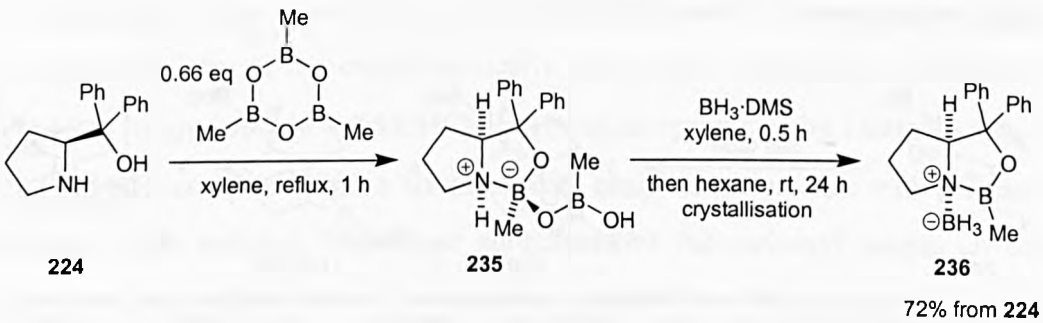

Scheme 2.37

To determine the quality of the catalyst, a test reaction was performed on acetophenone.[149] Treatment of acetophenone **237** with 10 mol% of *B*-Me CBS·BH_3 and 0.6 equivalents of BH_3·DMS gave (*R*)-1-phenylethanol **238** quantitatively and in excellent ee (scheme 2.38).

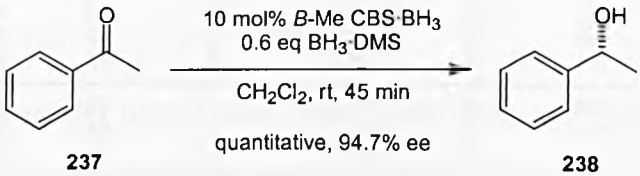

Scheme 2.38

Asymmetric reduction of the *N*-Boc tetrahydro dimer

With the CBS catalyst in hand and its quality established, our attention turned towards the asymmetric reduction of the *N*-Boc tetrahydro dimer. The first reaction conditions attempted involved the treatment of the *N*-Boc tetrahydro dimer with 10 mol% of *B*-Me CBS·BH_3

complex and 0.6 equivalents of BH_3·DMS in CH_2Cl_2 at room temperature for 26 hours. We were delighted to observe the formation of *N*-Boc tetrahydro monolactamol **229** in 23% yield and 62.2% ee (scheme 2.39).

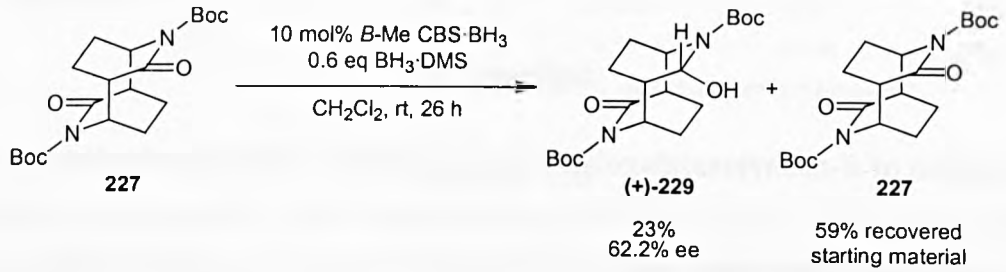

Scheme 2.39

A systematic investigation of the asymmetric reduction was then undertaken, with a view to determining the optimum conditions (table 2.6).

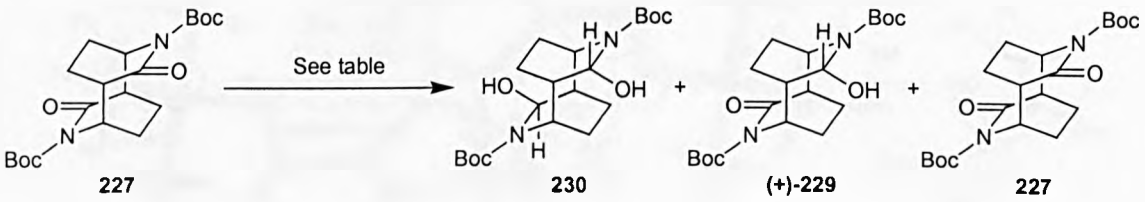

Entry[a]	Equivalents of *B*-Me CBS·BH_3	Equivalents of BH_3·DMS	Time (h)	Solvent (mL)	Dilactamol **230**	Monolactamol **(+)-229**		Starting material **227**
					Yield[b] (%)	Yield[b] (%)	Ee[c] (%)	Yield[b] (%)
1	0	1.2	22	CH_2Cl_2 (10)	0	16	0	75
2[d]	0.1	0.6	26	CH_2Cl_2 (10)	1	23	62.2	59
3	0.2	1.2	22	CH_2Cl_2 (10)	2	34	66.2	42
4	0.2	1.2	6	CH_2Cl_2 (10)	0	16	64.1	65
5	1	2	6	CH_2Cl_2 (10)	4	41	86.0	22
6	1	1	14	CH_2Cl_2 (10)	6	57	93.6	19
7	1	1	14	$CHCl_3$ (5)	7	63	96.0	7
8	0.5	0.5	14	$CHCl_3$ (2)	1	49	≥97	20
9	0.5	0.5	22	$CHCl_3$ (1)	9	76	≥97	6
10[d]	0.5	0.5	22	$CHCl_3$ (2)	5	42	95.2	18
11	0.5	0.4	22	$CHCl_3$ (1)	3	57	96.3	14
12	0.2	0.4	22	$CHCl_3$ (1)	1	43	94.1	42
13	0.2	0.4	44	$CHCl_3$ (1)	3	58	92.4	28
14	0.2	0.4	66	$CHCl_3$ (1)	4	55	91.3	29

[a] All reactions performed on a 100 mg scale unless otherwise noted. In all cases, small amounts (~6%) of a mixture of *N*-Boc/*N*-H tetrahydro dimer **231** and *N*-Boc/*N*-H tetrahydro monolactamol **232** were isolated. [b] Isolated yields after column chromatography. [c] Determined by chiral HPLC [Column: Chiralcel OD (25 × 0.46 cm), eluting with 99.2:0.8 hexane ^{i}PrOH, 1.0 mL min^{-1}, 40°C, UV detection at 225 nm]. [d] Performed on a 200 mg scale.

Table 2.6

The uncatalysed reduction with BH_3·DMS was found to be slow but significant, yielding 16% of the *N*-Boc tetrahydro monolactamol after 22 hours (entry 1). Initial reactions employing catalytic amounts of *B*-Me CBS·BH_3 and excess BH_3·DMS gave moderate ees and low

conversions, thought to be the due to competing reduction by BH_3·DMS and low catalyst loading respectively (entries 2-4). The use of stoichiometric amounts of *B*-Me CBS·BH_3 and fewer equivalents of BH_3·DMS significantly improved both the yields and ees (entries 5-7). Performing the reactions at higher concentration in $CHCl_3$ permitted the use of sub-stoichiometric amounts of the catalyst (entries 8-11), and gave the *N*-Boc tetrahydro monolactamol **(+)-229** in 76% yield and an excellent ≥97% enantiomeric excess (entry 9). Further investigations revealed that catalytic amounts of *B*-Me CBS·BH_3 could in fact be employed to give very good ees and reasonable yields, when the amount of BH_3·DMS was lowered (compare entries 12-14 with 2-4). The presence of the dilactamol in most of the reactions suggests that the '*meso* trick' may be operation, but this possibility was not further investigated.

With the asymmetric desymmetrisation successfully achieved, it remained to establish the absolute stereochemistry of the enantiomerically pure *N*-Boc tetrahydro monolactamol **(+)-229** {$[\alpha]_D$ +8.0, $[\alpha]_{365}$ +90.2 (c = 0.5 $CHCl_3$)}. The model proposed by Liotta[151] suggests that the *B*-Me CBS·BH_3 complex forms a six-membered chair transition state with the carbonyl of the compound to be reduced. The larger substituent of the carbonyl adopts an equatorial position to avoid an unfavourable 1,3-diaxial or *syn*-pentane interaction with the *B*-methyl group of the catalyst (figure 2.12).

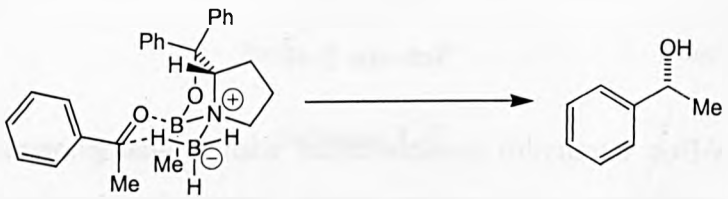

Figure 2.12

Speckamp applies this model to his *meso* imide substrates, and suggests that the *N*-alkyl substituent is the larger group that adopts the equatorial position[17,18] (figure 2.12).

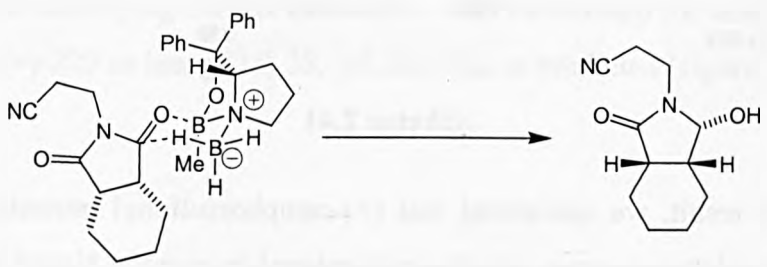

Figure 2.12

Based on these models, we predicted that reduction would take place at the carbonyl with the *Re*-face exposed, with the larger *N*-Boc substituent orientated equatorially (figure 2.13).

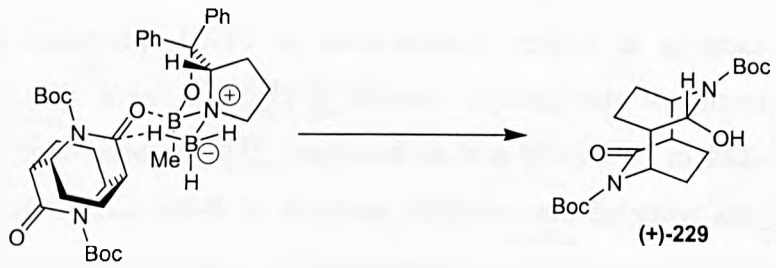

Figure 2.13

To confirm this prediction and determine the absolute configuration of the homochiral *N*-Boc tetrahydro monolactamol, several attempts were made to protect the lactamol hydroxyl group with chiral auxiliaries and obtain an x-ray crystal structure. Attempts to form the Mosher ester[152,153] of the monolactamol resulted in no reaction and recovered starting material (scheme 2.40).

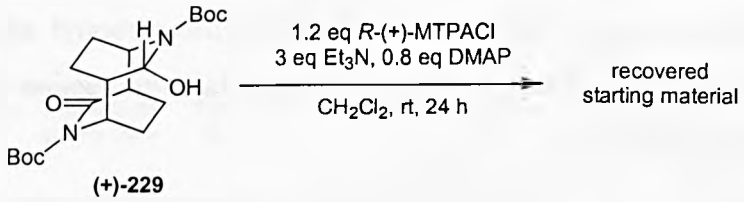

Scheme 2.40

Treatment of the *N*-Boc tetrahydro monolactamol with (+)-camphorsulfonyl chloride and DMAP in refluxing MeCN gave a product which appeared to be that resulting from the epimerisation of the lactamol centre (scheme 2.41).

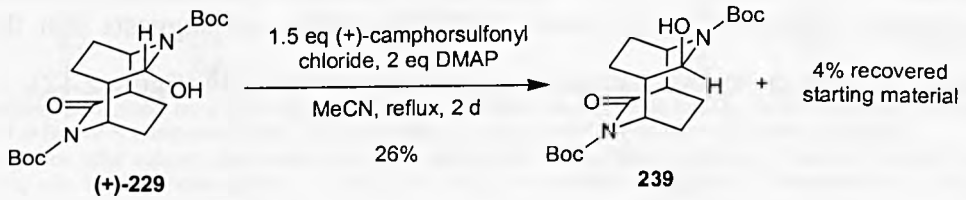

Scheme 2.41

To rationalise this result, we speculated that (+)-camphorsulfonyl protection converted the lactamol into a good leaving group, which was displaced to give the *N*-acyl iminium ion. This was then attacked by H_2O to give the *N*-Boc tetrahydro monolactamol epimer **239** (scheme

2.42).

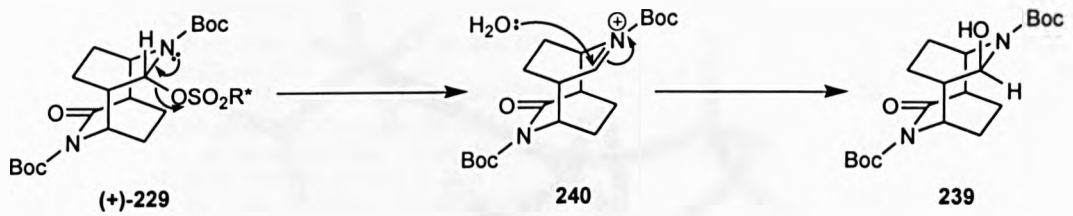

Scheme 2.42

Attempts to protect the lactamol with *R*-methyl chloroformate resulted in protection of the hydroxy group, followed by ring-opening and proton loss to give the enol carbonates **241** and **242** as a 1:1 mixture of isomers (scheme 2.43).

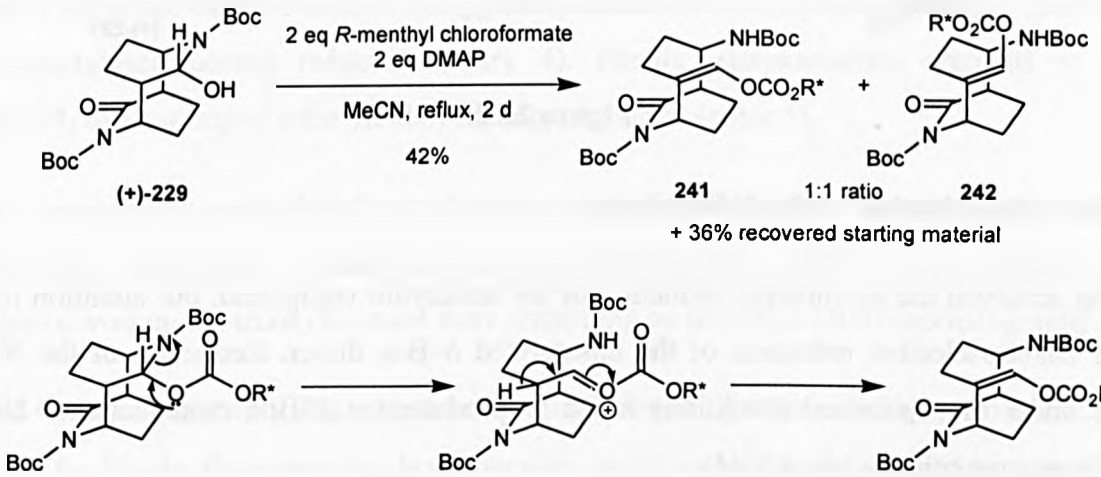

Scheme 2.43

Unfortunately, these derivatives were not crystalline and consequently an x-ray crystal structure could not be obtained.

However, eventually we were able to grow x-ray quality crystals of the underivatised *N*-Boc tetrahydro monolactamol and performed a single crystal x-ray structure determination using the Bijvoet method employing Cu-Kα irradiation. This established the absolute configuration of monolactamol **(+)-229** as being (1*S*, 2*S*, 3*R*, 5*R*, 6*R*), as predicted (figure 2.14).

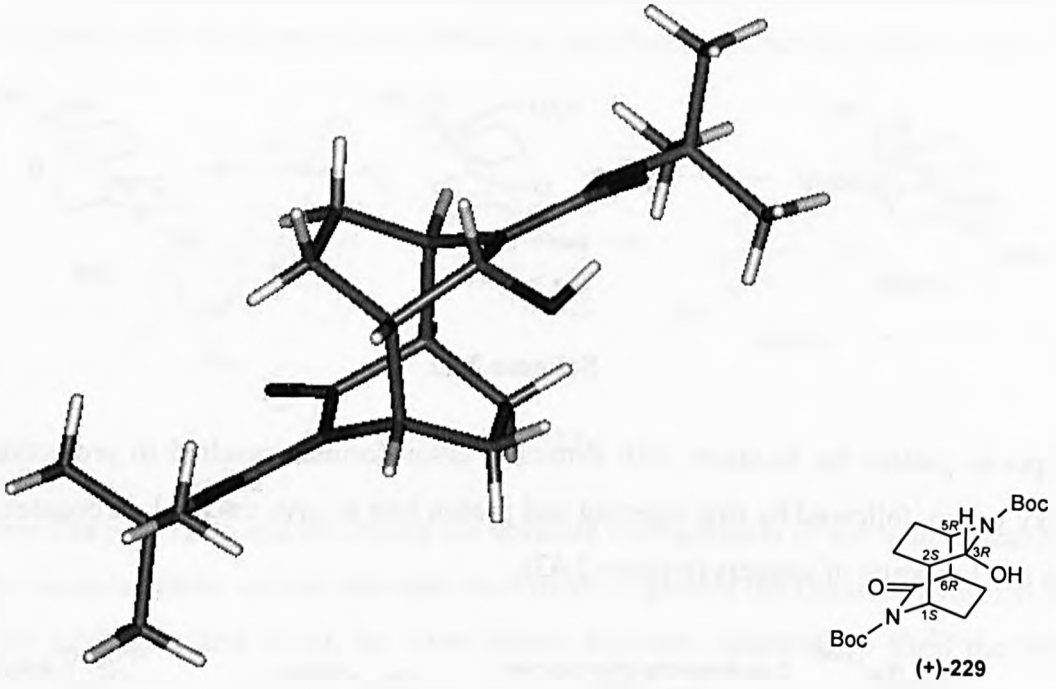

Figure 2.14

Asymmetric reduction of the *N*-Boc dimer

Having achieved the asymmetric reduction of the tetrahydro compound, our attention turned to the enantioselective reduction of the unsaturated *N*-Boc dimer. Reduction of the *N*-Boc dimer under the optimised conditions failed to produce the *N*-Boc monolactamol **214** in significant quantities (scheme 2.44).

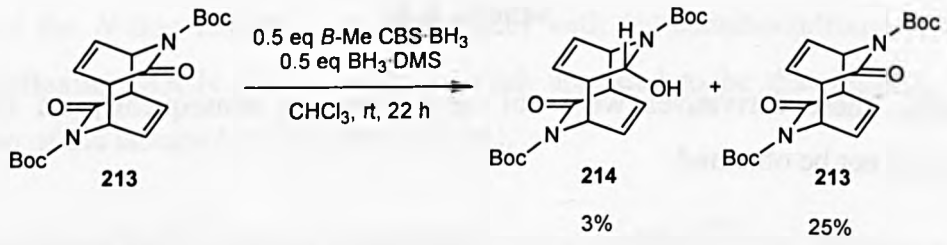

Scheme 2.44

A variety of conditions were then investigated in an attempt to increase the yield of the *N*-Boc monolactamol (table 2.7).

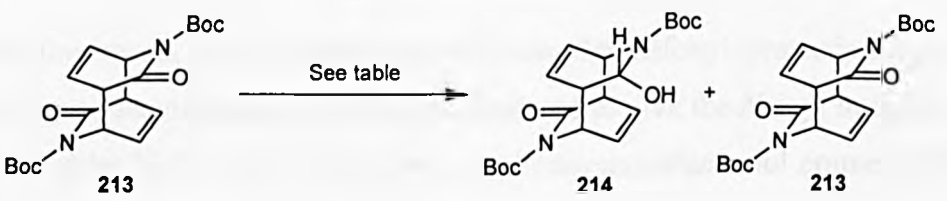

Entry	Conditions	Monolactamol **214**		Starting material **213**
		Yield (%)	Ee (%)	Yield (%)
1	0.2 eq *B*-Me CBS·BH_3, 1.2 eq BH_3·DMS, CH_2Cl_2, rt, 26 h	3	49.9	12
2	0.2 eq *B*-Me CBS·BH_3, 1.2 eq BH_3·THF, CH_2Cl_2, rt, 26 h	2	≥97	64
3	0.2 eq *B*-Me CBS·BH_3, 1.2 eq BH_3·DMS, 0.19 eq DIBAL, CH_2Cl_2, rt, 26 h[154]	1	-	33
4	0.2 eq *B*-Me CBS·BH_3, 1.2 eq BH_3·THF, 0.19 eq $Yb(OTf)_3$, CH_2Cl_2, rt, 26 h	9	6.7	42
5	1 eq *B*-Me CBS·BH_3, 1.2 eq BH_3·THF, CH_2Cl_2, rt, 26 h	-	-	63

Table 2.7

Reactions employing catalytic amounts of *B*-Me CBS·BH_3 gave small amounts of the monolactamol and in varying ee (entries 1 and 2). The addition of an organoaluminium promoter failed to improve the situation (entry 3), and the use of $Yb(OTf)_3$ increased the yield slightly but at the expense of the ee, suggesting that the Lewis acid promoter was accelerating the uncatalysed borane reduction (entry 4). Finally, stoichiometric amounts of *B*-Me CBS·BH_3 did not improve the yield of the monolactamol (entry 5).

It was interesting to note that the total recovery of material in these reactions was quite low. This could be the result of competing alkene hydroboration, and that in the absence of an oxidative workup the trialkylboranes were remaining on the silica after chromatography.

Faced with the possibility that hydroboration was competing with reduction, two options were open to us. Firstly, the competing hydroboration could potentially be reduced by employing a less reactive stoichiometric borane source. Secondly, the electrophilicity of the lactam carbonyl could be increased further by employing different protecting groups on nitrogen.

Catecholborane can be used as the stoichiometric reductant in the CBS system,[155] and it known to be much less reactive towards alkene hydroboration than borane. In preparation for using catecholborane in the asymmetric reduction of the photodimers, we performed a test reaction on acetophenone (scheme 2.45).

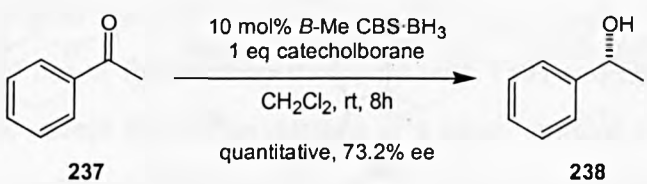

Scheme 2.45

While the reaction was observed to proceed quantitatively, the ee was inferior to those obtained with BH_3·DMS (scheme 2.38). Substitution of BH_3·DMS for catecholborane in the reduction of the *N*-Boc tetrahydro dimer gave *N*-Boc tetrahydro monolactamol **(±)-229** in lower yield and ee than the procedures employing borane (table 2.6). Also, significantly more over-reduction products were observed (scheme 2.46).

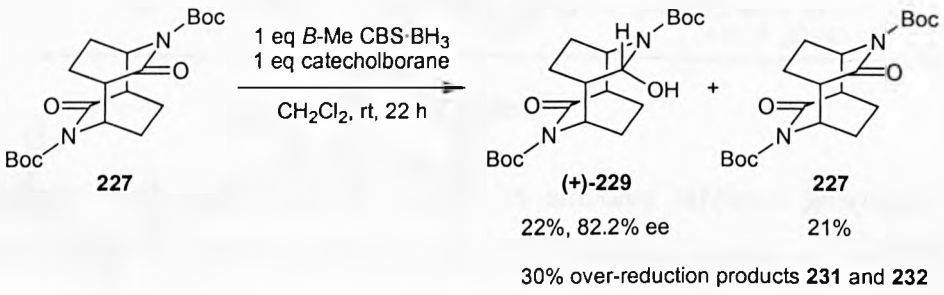

Scheme 2.46

In the light of these compromised yields and ees, we decided to focus our efforts on alternative nitrogen protecting groups that would increase the reactivity of the lactam carbonyl towards reduction.

Lactam activation: by *N*-sulfonyl protection

We envisaged that a sulfonyl protecting group would increase the electrophilicity of the lactam carbonyl to a greater extent than a Boc group. A sulfonyl group is more efficient at drawing electron density away from an amide nitrogen as sulfur is more electronegative than nitrogen, and the sulfur-oxygen double bonds can conjugate with the nitrogen lone pair.

Many reports of *N*-tosyl lactam formation exist in the literature. Of particular interest to us was an account published by Weinreb in which *N*-tosyl lactam **243** is synthesised and reduced by DIBAL as part of a synthetic strategy towards the marine alkaloid sarain A[156] (scheme 2.47).

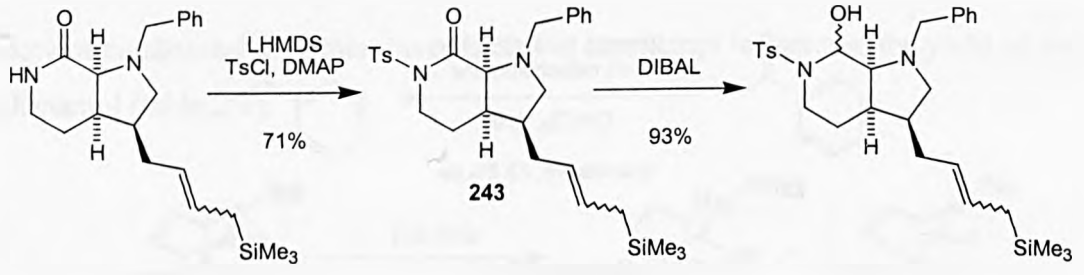

Scheme 2.47

Another interesting report was the *N*-tosyl protection of Vince's lactam[157] (scheme 2.48), particularly relevant to our efforts in view of its structural similarity to the *N*-H photodimer (figure 2.3).

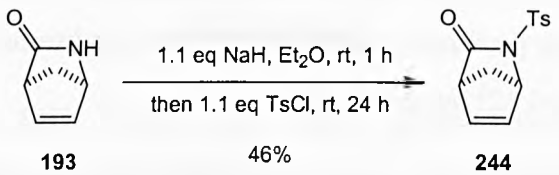

193 **244**

Scheme 2.48

With this literature precedent we were optimistic about synthesising *N*-Ts dimer **246**, and investigations were carried out to delineate conditions for direct protection of the *N*-H dimer (table 2.8).

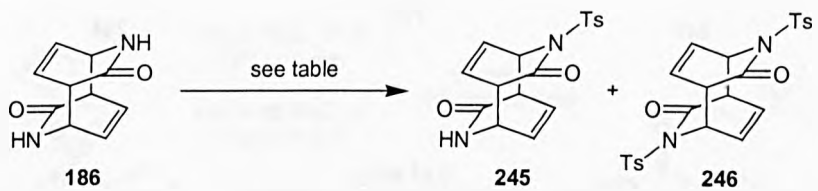

186 **245** **246**

Entry	Conditions	Result
1	3 eq NaH, 3 eq TsCl, 0.5 eq DMAP, THF, rt, 24 h[157]	3% *N*-Ts/*N*-H dimer
2	4 eq NaH, 4 eq TsCl, 2.5 eq DMAP, 0.2 eq ^{t}BuOK, THF, reflux, 24 h[157]	no reaction
3	3 eq ^{n}BuLi, THF, -78°C, 15 min, then 4 eq TsCl, 0.5 eq DMAP, rt, 24 h[158]	no reaction
4	4 eq KH, 4 eq TsCl, Et_2O, rt, 24 h	no reaction
5	2.2 eq TsCl, 30% aq NaOH, 0.1 eq $BnEt_3NCl$, CH_2Cl_2, rt, 24 h[159]	no reaction
6	3 eq TsCl, 2.5 eq Cs_2CO_3, 2.5 eq AgCN, H_2O:acetone, 1:1, rt, 24 h	no reaction
7	4 eq TsCl, 30% aq NaOH, H_2O, Et_2O, rt, 24 h[160]	traces of *O*-Ts-2-pyridone
8	6 eq TsCl, 2.1 eq DMAP, MeCN, rt, 3 d	no reaction
9	5 eq TsCl, 3 eq LHMDS, DMF:HMPA 1:1, 150°C, 2 h to 100°C, 24 h[156,158]	29% *O*-Ts-2-pyridone
10	5 eq TsCl, 3 eq LHMDS, DMF, 100°C, 10 min to rt, 24 h[156,158]	Me_2NTs plus 2-pyridone derivatives
11	5 eq TsCl, 140°C, 24 h	no reaction
12	4 eq NaH, 8 eq TsCl, 140°C, 24 h	traces of 2-pyridone derivatives

Table 2.8

Initial experiments involved the deprotonation of a suspension of the *N*-H dimer in ethereal solvents by a variety of bases, followed by treatment with TsCl and DMAP (entries 1-4). No reaction was observed, except for the production of a small amount of the *N*-Ts/*N*-H dimer **245** (entry 1). To overcome solubility problems, a number of biphasic experiments were performed using aqueous base as the *N*-H dimer is sparingly soluble in water (entries 5-7). No reaction was observed on employing a phase transfer catalyst (entry 5) or AgCN (entry 6), but

a small amount of *O*-Ts-2-pyridone was isolated in entry 7. To encourage the *N*-H dimer into solution, a series of reactions involving heat and/or polar solvents were carried out (entries 8-10). However, only *O*-Ts-2-pyridone (from the heat induced cycloreversion of the *N*-H dimer, entry 9) and *N*-Ts-dimethylamine (from the decomposition of DMF, entry 10) were isolated. Finally, two reactions were performed under solvent free conditions in molten TsCl with and without base (entries 11 and 12) but to no avail.

At this point we suspected that TsCl might not be reactive enough to protect the photodimer, so the more reactive TsBr[161] **248** and TsI[162] **249** were synthesised from the sodium salt of *para*-toluenesulfinic acid **247** (scheme 2.49).

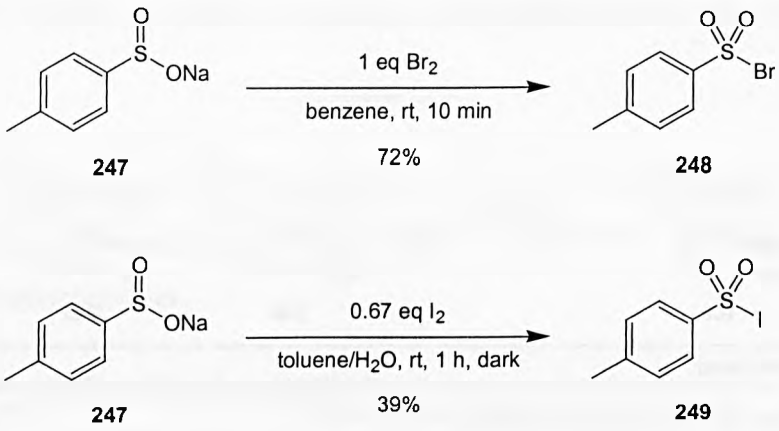

Scheme 2.49

However, both reagents failed to react with the *N*-H dimer (scheme 2.50).

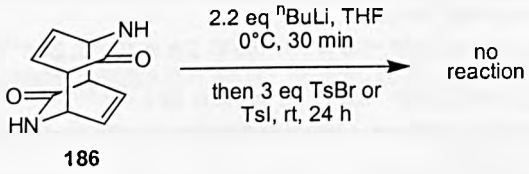

Scheme 2.50

Our next strategy was to synthesise and photodimerise *N*-Ts-2-pyridone.[158] Tosyl protection of 2-pyridone proceeded in good yield, but irradiation with ultra-violet light did not afford the expected *N*-Ts dimer but instead gave rearranged 5-Ts-2-pyridone (scheme 2.51).

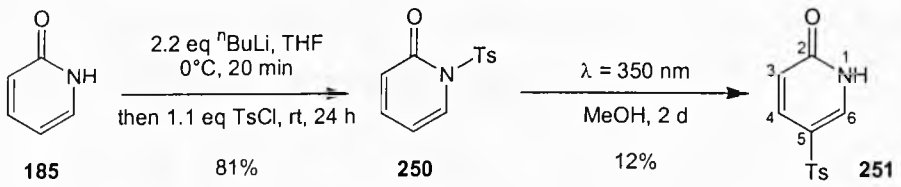

Scheme 2.51

The protection of the *N*-H dimer with other sulfonyl protecting groups such as methanesulfonyl and trifluoromethanesulfonyl was also investigated. Part of the reasoning behind the use of the Ms group was that it is well known that MsCl can undergo elimination to form a reactive sulfene, which is the active sulfonylating agent. This pathway is not believed to operate for TsCl. Two attempts to mesylate the *N*-H dimer were made, with MsCl and Ms_2O, and ^{n}BuLi, but both met with failure with butylmethylsulfone isolated on both occasions (scheme 2.52).

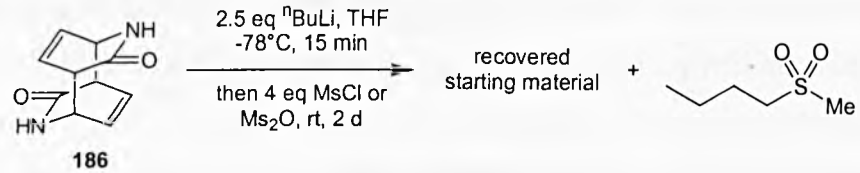

Scheme 2.52

Small amounts of the *N*-Tf/*N*-H dimer **252** was isolated on treatment of *N*-H dimer **186** with Tf_2O in pyridine (scheme 2.53).

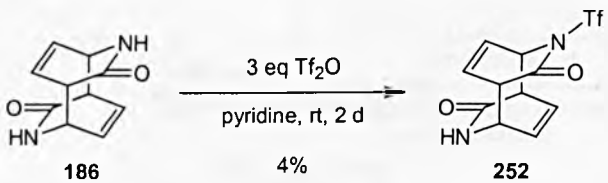

Scheme 2.53

_N_-Sulfonyl protection: oxidation strategy

With all attempts to directly sulfonyl protect the *N*-H dimer proving unsuccessful, an alternative route to *N*-sulfonyl lactams was considered, involving *N*-sulfinyl or *N*-sulfenyl[163,164] protection followed by oxidation with mCPBA or H_2O_2. Once again, many precedents for this strategy exist in the literature.

Our efforts began with the synthesis of *p*-toluenesulfinyl chloride **253** from *p*-toluenesulfinic acid **247**. However, attempted *N*-sulfinyl protection of the *N*-H dimer failed (scheme 2.54).

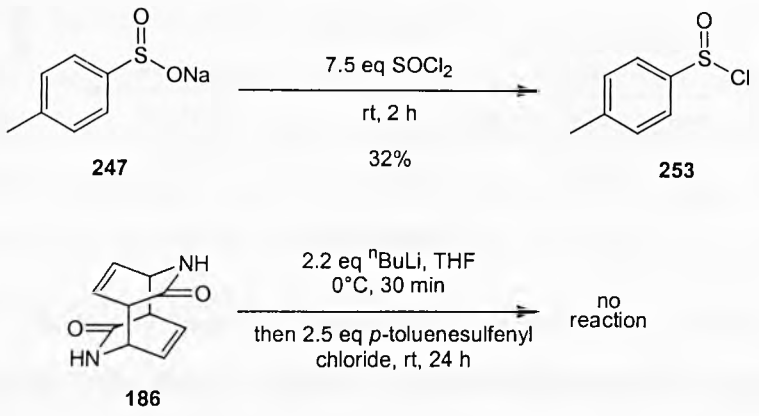

Scheme 2.54

The synthesis of *p*-toluenesulfenyl chloride **255** proceeded almost quantitatively by the treatment of *p*-thiocresol **254** with chlorine (scheme 2.55).

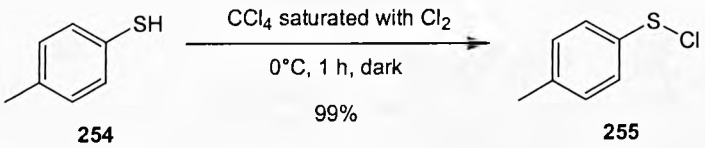

Scheme 2.55

Two attempts were made to *N*-sulfenyl protect[165] the *N*-H dimer. The first resulted in the formation of ^{n}BuLi/*p*-toluenesulfenyl chloride adduct **256**, and the second showed no reaction (scheme 2.56).

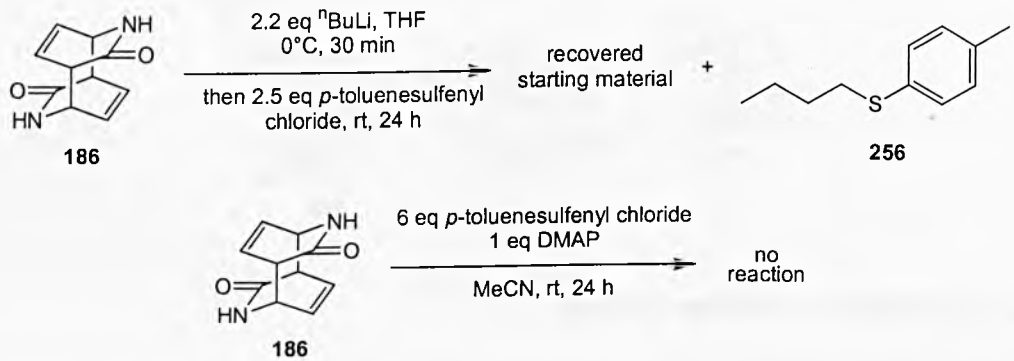

Scheme 2.56

We then planned to synthesise the *N*-sulfenyl dimer by the *N*-sulfenyl protection of 2-pyridone followed by photodimerisation. The first attempt at synthesising *N*-*p*-toluenesulfenyl-2-pyridone **258** using NaH gave 10% of 5-*p*-toluenesulfenyl-2-pyridone **257**. However, the second attempt using ^{n}BuLi gave very small amounts of the desired product, *N*-

p-toluenesulfenyl-2-pyridone, although photodimerisation of this compound led to decomposition and no *N*-sulfenyl dimer was formed (scheme 2.57).

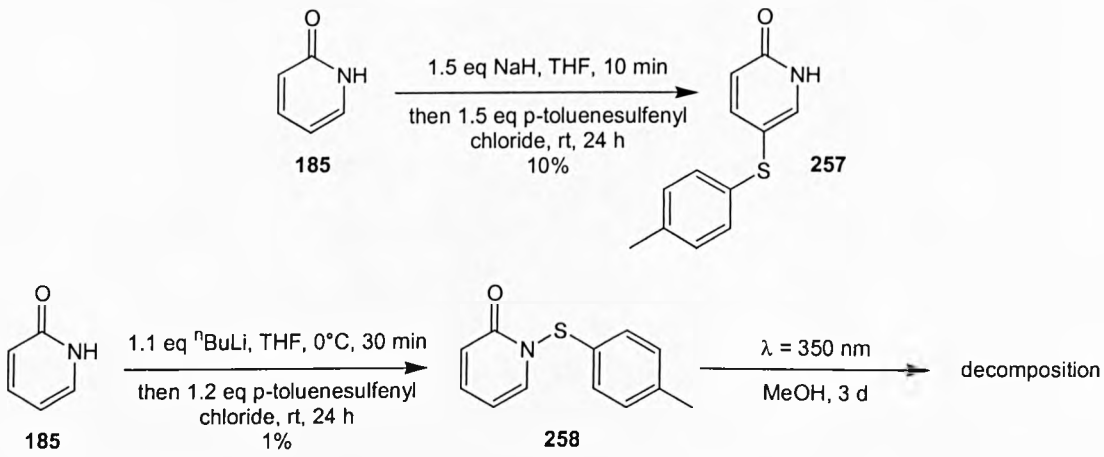

Scheme 2.57

Our final attempts to introduce a sulfonyl group to the *N*-H dimer relied on the reaction of lactam derived TMS lactim ethers with TsCl. A test reaction of 2-pyridone with trimethylsilyl trichloroacetate[166] gave 2-(trimethylsilyloxy)-pyridine in a 1:1.4 ratio with starting material. As the lactim ether was hydrolysed on silica, the crude mixture was used directly for the next reaction. However, treatment with CsF and TsCl gave no *N*-Ts-2-pyridone (scheme 2.58).

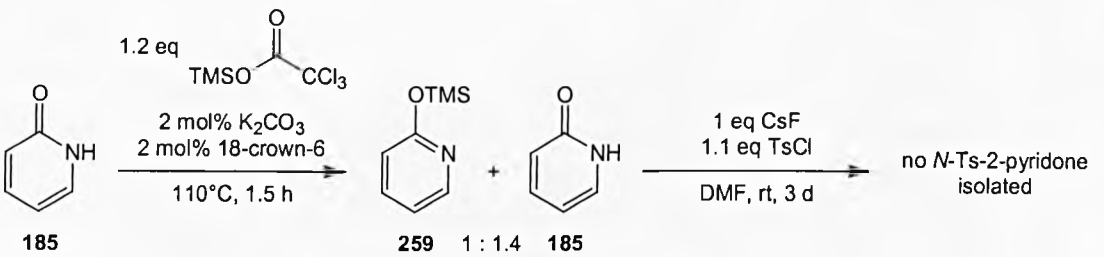

Scheme 2.58

Application of these conditions to the *N*-H dimer failed to give the TMS lactim ether (scheme 2.59).

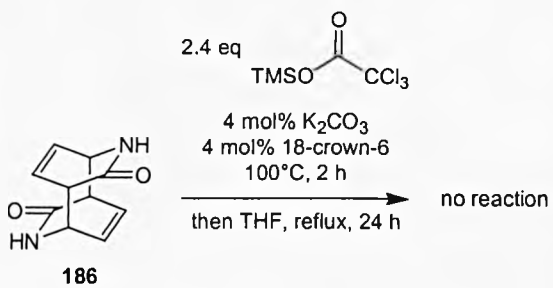

Scheme 2.59

At this stage we had exhausted most of the possibilities for *N*-sulfonyl protection of an amide, and the *N*-sulfonyl dimer still remained elusive. Consequently, we decided to move on to other amide protecting groups.

Lactam activation: by *N*-phosphinyl protection

The failure to *N*-sulfonyl protect the photodimers inspired attempts to protect the lactam nitrogen with other protecting groups in order to increase the electrophilicity of the lactam carbonyl.

We were interested in introducing the *N*-phosphinyl protecting group as it has been shown by Sweeney to be a powerful electron withdrawing group, for which nucleophilic attack at phosphorus is slow, and which can be deprotected with mild acid.[167,168] Treatment of the *N*-H dimer with ^{n}BuLi followed by diphenylphosphinyl chloride gave traces of the *N*-DPP dimer **260** and *N*-DPP/*N*-H dimer **261**, along with significant quantities of the unexpected DPP adducts **262** and **263** (scheme 2.60).

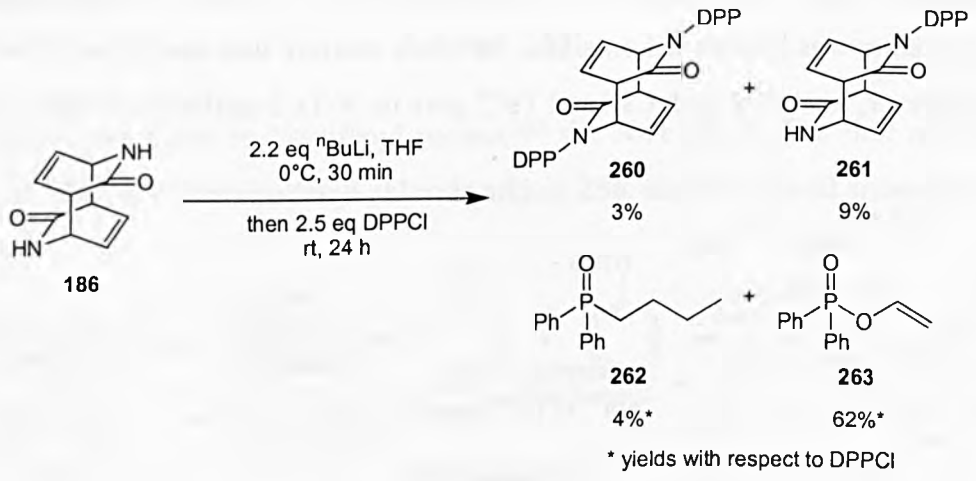

Scheme 2.60

Product **262** presumably arises from direct nucleophilic attack of ^{n}BuLi on DPPCl. We reasoned that product **263** was formed by base induced fragmentation of THF, followed by reaction of the resulting enolate with DPPCl (scheme 2.61).

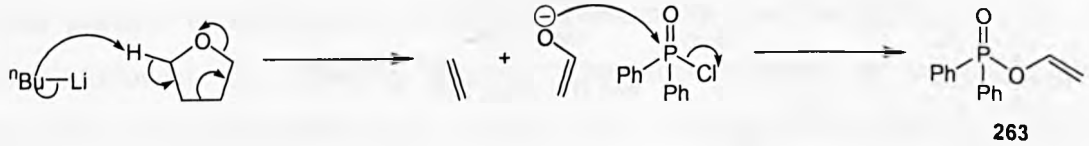

Scheme 2.61

Interestingly, database searches revealed that the DPP enol-ether is a novel compound which might find potential application as a dienophile in inverse electron demand Diels-Alder reactions.

Further investigation of this side reaction revealed that the formation of diphenylbutylphosphine oxide **262** *versus* DPP enol-ether **263** is dependent on the order of addition of the reagents (scheme 2.62).

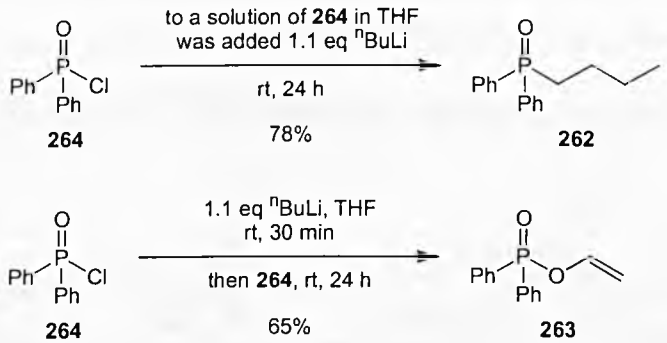

Scheme 2.62

When ^{n}BuLi is added directly to a solution of DPPCl in THF, only diphenylbutylphosphine oxide **262** is produced. Alternatively, when ^{n}BuLi is stirred in THF for 30 minutes prior to the addition of DPPCl, then DPP enol-ether **263** is formed exclusively, as the enolate will have had time to form. These observations suggest that the *N*-H dimer is very unreactive towards deprotonation, since during the 30 minutes prior to adding the DPPCl the ^{n}BuLi preferentially reacts with THF.

Attempts to increase the yield of the *N*-DPP dimer by employing ^{n}BuLi in DMF, dioxane and CH_2Cl_2, and by using NaH in DMF failed, with only the DPPCl adducts and no *N*-DPP dimer being formed.

Unfortunately, the yields of *N*-DPP dimer obtained were too low to be synthetically useful, and no attempts were made to reduce these dimers.

Lactam activation: by *N*-pivaloyl protection

A further strategy utilised the pivaloyl (*tert*-butylcarbonyl) group as an amide protecting group. We envisaged that this group would withdraw electron density to a greater extent than the Boc group due to the lack of a carbamate oxygen, and that reduction of the pivaloyl carbonyl in preference to the lactam carbonyl would be discouraged by the bulky *tert*-butyl group.

N-Pivaloyl protection of the *N*-H dimer proceeded in 56% yield under similar conditions to the Boc protection (scheme 2.63).

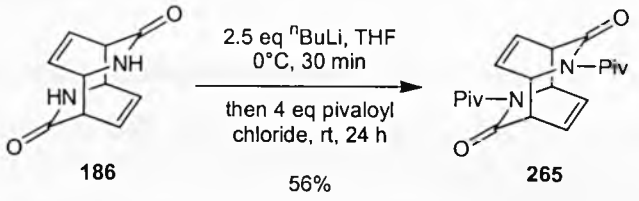

Scheme 2.63

Subsequently, the *N*-pivaloyl dimer **265** was treated with 3 equivalents of DIBAL (scheme 2.64).

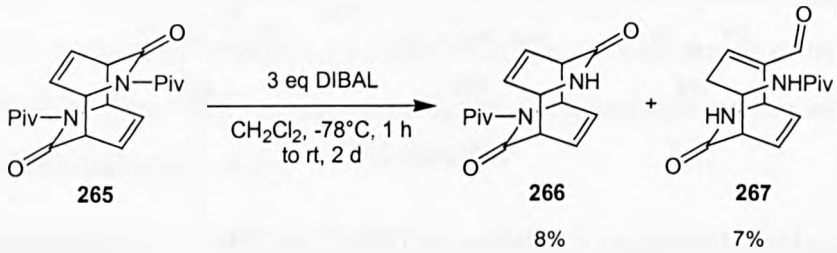

Scheme 2.64

However, no lactamols were isolated, and instead the *N*-pivaloyl/*N*-H dimer **266** and *N*-pivaloyl/*N*-H α,β-unsaturated amino-aldehyde **267** were observed. The formation of both of these products involves reduction of the pivaloyl carbonyl. Examination of molecular models revealed that it is not possible for the pivaloyl carbonyl and the lactam carbonyl to be co-planar without an unfavourable steric interaction of the *tert*-butyl group with either the lactam oxygen or the protons α to the carbonyl (figure 2.15).

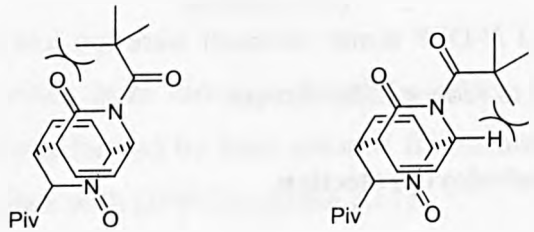

Figure 2.15

Therefore the pivaloyl group will adopt a conformation out of the plane of the lactam, and as a result renders the pivaloyl carbonyl more electrophilic and the lactam carbonyl less

electrophilic, due to the disruption of the conjugation between the two groups.

This explains the isolation of products with the pivaloyl group cleaved, and the isolation of a low amount of lactam reduction products. It may also explain the low mass recovery of the reaction as double pivaloyl cleavage would form the insoluble *N*-H dimer, and a precipitate was observed during the workup of this reaction.

The α,β-unsaturated amino-aldehyde **267** was presumably formed as the result of ring opening and double bond tautomerism of the *N*-pivaloyl/*N*-H monolactamol **268**, probably during the mildly acidic workup (scheme 2.65).

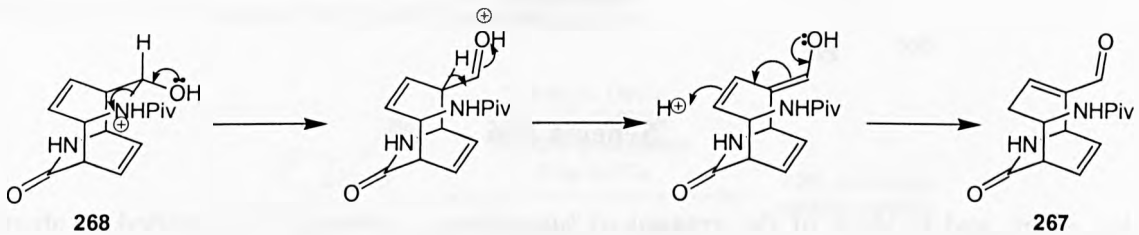

Scheme 2.65

In the light of these results, it was clear that the pivaloyl group was unsuitable for our purposes.

Summary of *N*-protection

The upshot of all the aforementioned *N*-protection studies was that we had successfully achieved the carbamate (Boc) and amide (pivaloyl) protection of the *N*-H dimer, but had been unable to achieve analogous sulfonamide (Ts, Ms) or phosphinamide (DPP) protection.

The most important difference between these groups is the geometry of the atom by which they are attached to the lactam nitrogen, sp^2 hybridised carbon (trigonal planar) *versus* sp^3 hybridised sulfur or phosphorus (tetrahedral) (figure 2.16).

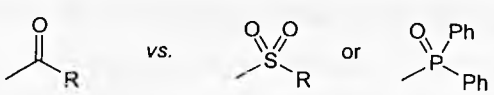

Figure 2.16

Not only is the tetrahedral geometry more sterically demanding, but sulfur and phosphorus are significantly larger than carbon. This would explain the failure to achieve *N*-sulfonyl and *N*-phosphinyl protection.

Furthermore, these effects would be exaggerated in the photodimer system, where the rigid structure will not permit the relief of steric interactions by undergoing conformational change.

Lactam activation: by carbonyl thionation

In a final attempt to increase the electrophilicity of the lactam carbonyls of the photodimer, we tried the thionation of the *N*-Boc tetrahydro dimer using Lawesson's reagent[169] (scheme 2.66). Unfortunately, no reaction was observed in both refluxing benzene and CH_2Cl_2.

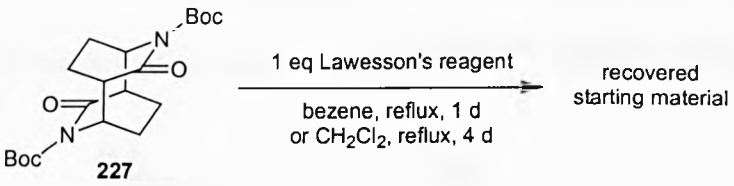

Scheme 2.66

At this point, and in view of the amount of time already invested, we decided to abandon attempts to increase the electrophilicity of the lactam carbonyl, and concentrate on other methods of minimising competing alkene hydroboration during the asymmetric reduction of the unsaturated *N*-Boc dimer.

Alkene protection

Another way to avoid competing hydroboration is to temporarily protect the alkenes. We considered the Diels-Alder reaction as a potential strategy because it is known to be reversible, but we anticipated that the size of commonly employed protecting groups (e.g. anthracene and its derivatives[170]) would probably be too sterically demanding and interfere with reduction.

Another option was to oxidise the alkenes, either to the diol or to the epoxide. These were attractive methods because we planned to oxidatively cleave the alkenes at a later stage, which can be achieved directly on diols and epoxides.

Literature precedents exist for the dihydroxylation of Vince's lactam derivatives. Generally, *cis*-dihydroxylation takes place exclusively from the less hindered *exo* face.[171] However, when the *exo* face is blocked, dihydroxylation can take place from the *endo* face,[172] a result that bodes well for the dihydroxylation of the photodimer systems (scheme 2.67).

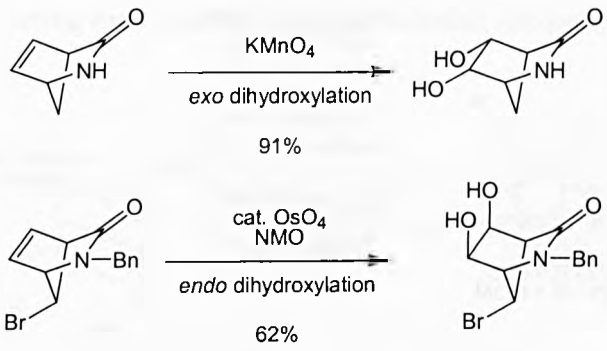

Scheme 2.67

However, when the *N*-Boc dimer was subjected to Warren's racemic dihydroxylation conditions[173] no reaction took place (scheme 2.68).

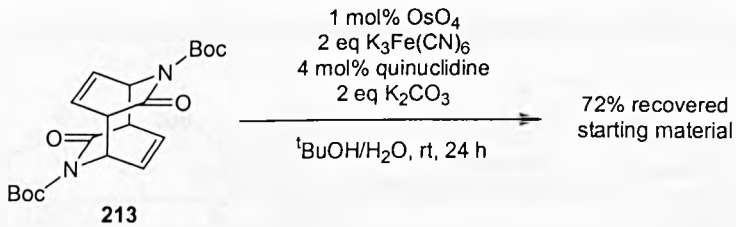

Scheme 2.68

Exposure of the *N*-Boc dimer to the Upjohn dihydroxylation conditions also gave recovered starting material (scheme 2.69).

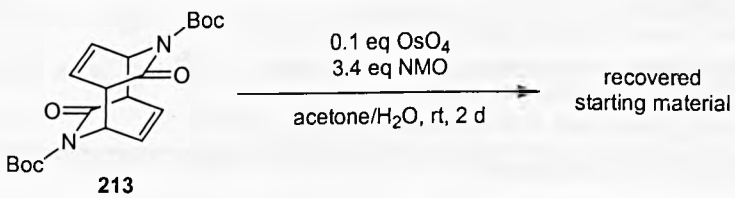

Scheme 2.69

We considered the possibility that any diols formed might be water soluble and thus be remaining in the aqueous phase. However, two reactions (on the *N*-Boc and *N*-MOM dimers) where the aqueous extracts were evaporated to dryness following workup and the residues treated with 2,2-dimethoxypropane and TsOH (acetonide protection) showed no sign of the desired products (scheme 2.70).

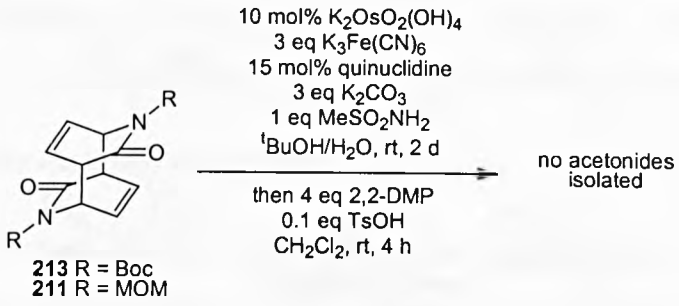

Scheme 2.70

This unreactivity was perplexing, especially considering the fact that the Vince's lactam and derivatives undergo dihydroxylation readily. As a result, we redirected our efforts towards epoxidation.

A variety of conditions was investigated to epoxidise the *N*-Boc dimer (table 2.8).

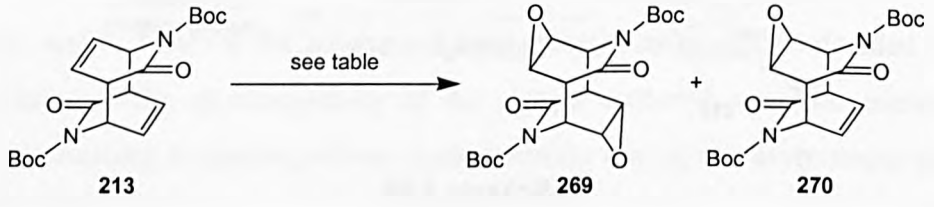

Entry	Conditions	Yield (%) diepoxide **269**	monoepoxide **270**	*N*-Boc dimer **213**
1	10 eq DDO, CH_2Cl_2, rt, 24 h[174]	traces	29	60
2	10 eq DDO, CH_2Cl_2, rt, 15 d[174]	10	42	44
3	2.5 eq mCPBA, CH_2Cl_2, reflux, 24 h	-	22	68
4	5 eq mCPBA, 5 mol%, radical inhibitor,[a] CH_2Cl_2, reflux, 6 d[175]	43	12	0
5	5 eq mCPBA, 5 mol%, radical inhibitor,[a] $ClCH_2CH_2Cl$, reflux, 3 d[175]	2	3	-
6	20 eq mCPBA, 20 eq Na_2HPO_4, CH_2Cl_2, H_2O, rt, 11 d	20	-	-
7	5 eq $(CF_3CO)_2O$, 20 eq UHP, 17.5 eq Na_2HPO_4, CH_2Cl_2, rt, 3 d[176]	-	19	79

[a] 5-*tert*-butyl-4-hydroxy-2-methylphenylsulfide

Table 2.8

Epoxidation with dimethyldioxirane failed to give substantial quantities of the diepoxide, even after extended reaction periods (entries 1 and 2). Epoxidation with mCPBA gave the best yield of the diepoxide, 43% with a radical inhibitor in refluxing CH_2Cl_2 for 6 days (entries 3 and 4), but increasing the temperature of the reflux by using 1,2-dichloroethane caused decomposition (entry 5). Finally, the use of trifluoroperacetic acid (entry 6) and mCPBA under biphasic conditions (entry 7) failed to improve on entry 5.

With the *N*-Boc dimer diepoxide in hand, the racemic and asymmetric reduction of this compound were explored. Treatment of this compound with 3 equivalents of DIBAL resulted

in the consumption of starting material into uncharacterisable products, and no lactamols were detected (scheme 2.71).

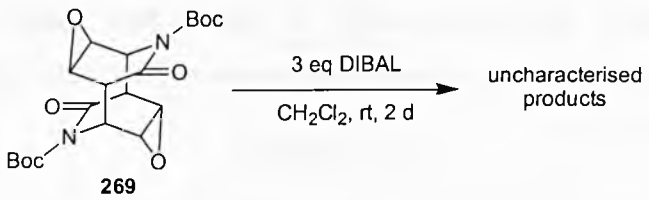

269

Scheme 2.71

Nonetheless, we proceeded with investigations into the asymmetric reduction and the results are summarised in table 2.9.

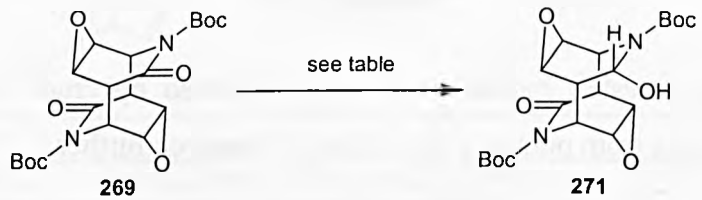

269 **271**

Entry	Conditions	Result
1	3 eq BH_3·DMS, CH_2Cl_2, rt, 4 d	recovered starting material
2	0.5 eq *B*-Me CBS·BH_3, 0.5 eq BH_3·DMS, CH_2Cl_2, rt, 22 h	recovered starting material
3	2 eq *B*-Me CBS·BH_3, 2 eq BH_3·DMS, CH_2Cl_2, rt, 5 d	recovered starting material

Table 2.9

Borane alone was not reactive enough to reduce the *N*-Boc dimer diepoxide (entry 1) and starting material was recovered. Both catalytic and stoichiometric amounts of *B*-Me CBS·BH_3 resulted in no reaction at all, and no lactamols were observed (entries 2 and 3).

We speculated that the failure of the diepoxide to be reduced was the result of the epoxide blocking the trajectory of hydride attack (figure 2.17). The epoxide group, though small, could impede the Burgi-Dunitz trajectory of the nucleophile[177] by a steric interaction, or by an electrostatic repulsion of the negatively charged nucleophile by the epoxide oxygen lone pairs.

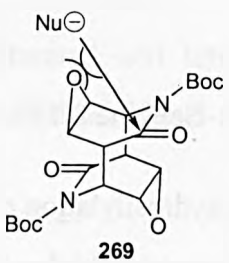

269

Figure 2.17

Asymmetric desymmetrisation: by alkene oxidation

Given the success of the epoxidation of the *N*-Boc dimer, we couldn't resist the opportunity to attempt the asymmetric desymmetrisation of the *N*-Boc dimer by enantioselective epoxidation. The *N*-Boc dimer was submitted to Jacobsen's catalytic asymmetric epoxidation conditions[178] (scheme 2.72).

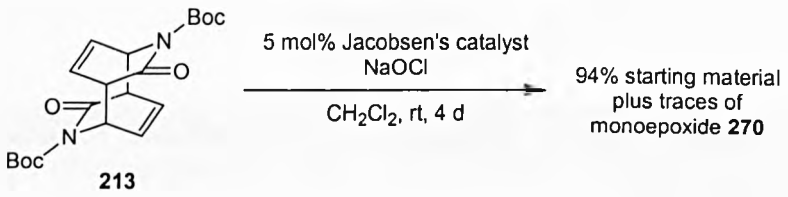

213

Scheme 2.72

Unfortunately, only traces of monoepoxide were observed by crude ^{1}H NMR, and time constraints prevented us from pursuing this avenue of research further.

Asymmetric hydrosilylation

As part of the investigations into achieving the asymmetric reduction of the *N*-Boc dimer, we considered the possibility of asymmetric hydrosilylation of the lactam carbonyls. This has the advantage that, on workup, the same lactamols are produced as are observed on hydride reduction. Once again, the possibility exists of competing reaction of the alkenes, but there are numerous examples in the literature of carbonyl hydrosilylation in the presence of alkenes.

To investigate this chemistry, the C_2 symmetric Pybox-$RhCl_3$ catalyst **273** was synthesised[179] (scheme 2.73).

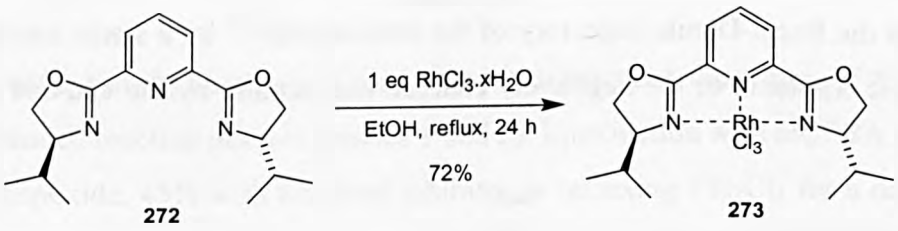

272 273

Scheme 2.73

With catalyst in hand, the asymmetric hydrosilylation of acetophenone was carried out to test the procedure (scheme 2.74). The ee was not as high as that reported in the literature[179] (94% ee), perhaps due to the quality of the extremely air and moisture sensitive reagents.

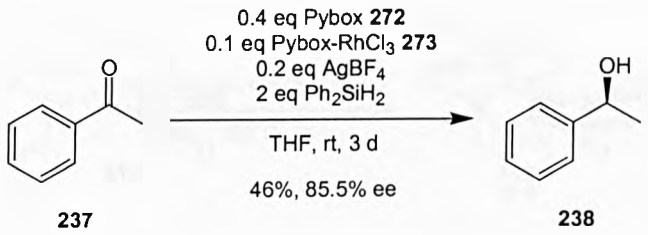

Scheme 2.74

The asymmetric hydrosilylation was attempted first on the *N*-Boc tetrahydro dimer, under a variety of conditions (table 2.10).

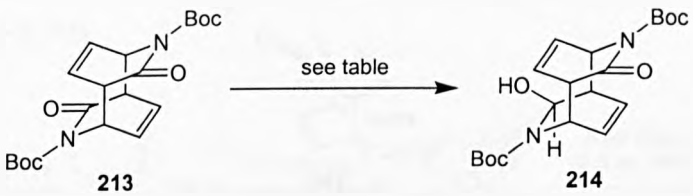

Entry	Conditions	Result
1	4 mol% Pybox, 1 mol% Pybox-$RhCl_3$, 2 mol% $AgBF_4$, 1.6 eq Ph_2SiH_2, CH_2Cl_2, rt, 2 d	starting material
2	0.4 eq Pybox, 0.1 eq Pybox-$RhCl_3$, 0.2 eq $AgBF_4$, 2 eq Ph_2SiH_2, CH_2Cl_2, rt, 5 d	starting material
3	0.4 eq Pybox, 0.1 eq Pybox-$RhCl_3$, 0.2 eq $AgBF_4$, 2 eq Ph_2SiH_2, THF, rt, 3 d	starting material

Table 2.10

No reaction was observed on any of the attempts, indicating that asymmetric hydrosilylation is not a reactive enough method to reduce the *N*-Boc tetrahydro dimer, and therefore almost certainly not reactive enough to reduce the unsaturated *N*-Boc dimer. In view of this, asymmetric hydrosilylation was pursued no further.

α-Methyl substituted photodimer systems

Another avenue of research that we pursued involved the synthesis and reduction of substituted photodimer systems. The [4+4]-photodimerisation of 2-pyridones is tolerant of a wide variety of substituents on the pyridone ring, allowing access to functionalised photodimers.

We decided to investigate the unsaturated and tetrahydro α-methyl *N*-Boc photodimer systems **274** and **275** (figure 2.18), synthesised from 3-methyl-2-pyridone.

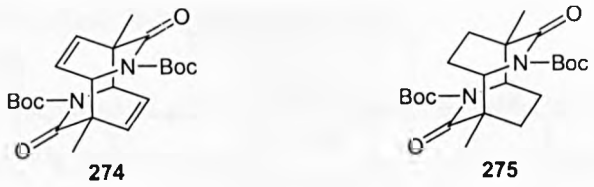

Figure 2.18

Substitution α to the carbonyl offers several advantages over the unfunctionalised photodimer systems. Firstly, it opens up a route to more highly functionalised amino-acids possessing an extra substituent at the β position (scheme 2.75).

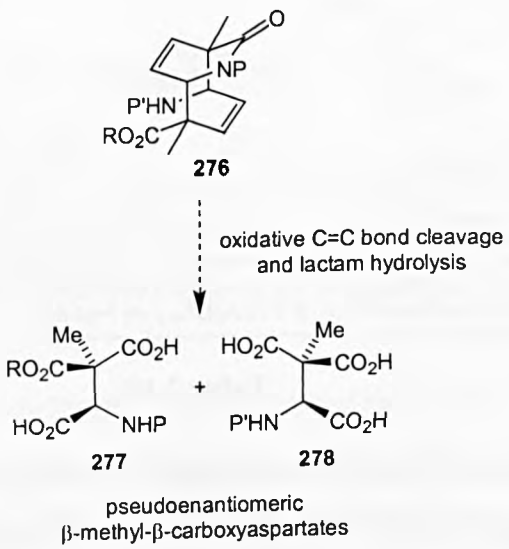

Scheme 2.75

Secondly, there is a significant possibility of epimerisation at the β-position of the amino-acids presented in scheme 2.2, due to the acidity of the β-proton. Substitution at this position would prevent epimeristion, and therefore preserve the stereochemical integrity of the amino-acids.

Finally, this strategy represents a method of synthesising quaternary chiral centres, which remains a difficult task in organic chemistry. A variety of substituents could be introduced α to the carbonyl in the photodimer systems by photodimerising the appropriate 3-substituted-2-pyridones, synthesised from the palladium catalysed cross-coupling of 3-bromo-2-pyridone. This has been demonstrated by Iain Lingard, an MChem project student in our group, who achieved the Stille coupling of 3-bromo-2-pyridone and tetramethyl stannane, illustrating the potential of this route (scheme 2.76).

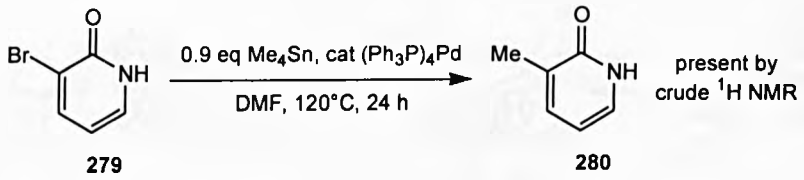

279 280

Scheme 2.76

However, for initial studies the α-methyl *N*-Boc dimer **274** was synthesised by the diazotisation of commercially available 2-amino-3-methylpyridine **281**,[120] followed by the photodimerisation of 3-methyl-2-pyridone **280**[120] and Boc protection of α-methyl *N*-H dimer **282** in NMP (scheme 2.77).

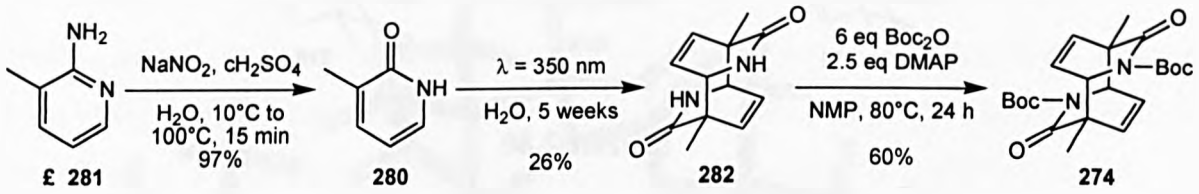

£ 281 280 282 274

Scheme 2.77

Once again, in preparation for the asymmetric reduction, the achiral reduction of the α-methyl *N*-Boc dimer with DIBAL was performed, and the mono and dilactamols **(±)-283** and **284** isolated (scheme 2.78).

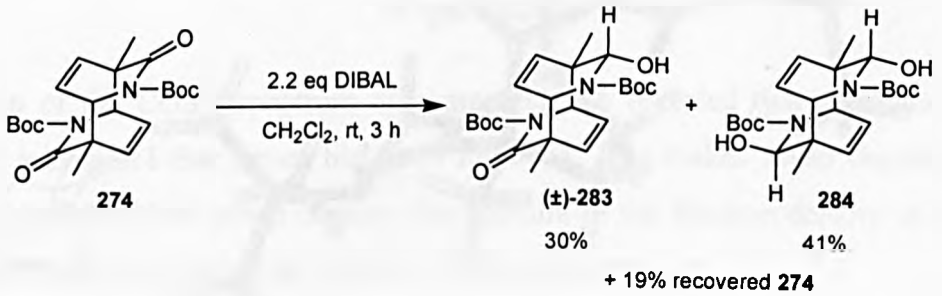

274 (±)-283 30% 284 41%

+ 19% recovered **274**

Scheme 2.78

Interestingly, a small amount of 3-methylpyridine was observed in the crude ^{1}H NMR, probably the result of the reductive cleavage of the dilactamol Boc groups, followed by elimination of H_2O and cycloreversion (scheme 2.79).

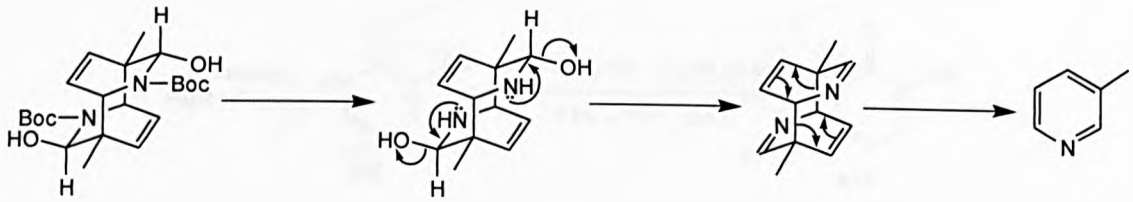

Scheme 2.79

Furthermore, the α-methyl *N*-Boc tetrahydro dimer was prepared by catalytic hydrogenation, which proceeded almost quantitatively (scheme 2.80).

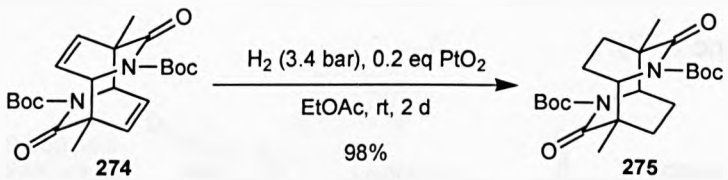

Scheme 2.80

The x-ray crystal structure of this compound was obtained, which clearly showed the quaternary methyl groups α to the carbonyls (figure 2.19).

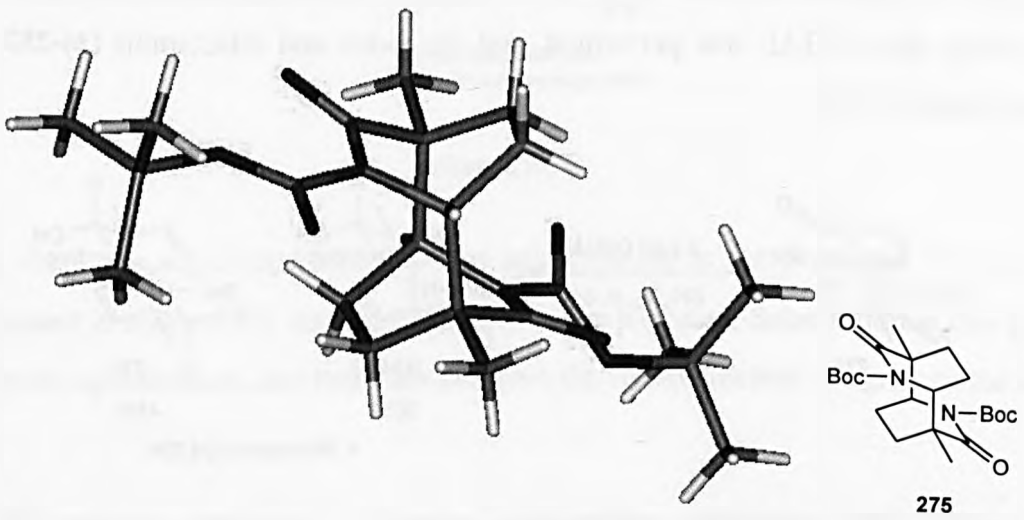

Figure 2.19

Reduction of the α-methyl *N*-Boc tetrahydro dimer with 5 equivalents of DIBAL gave dilactamol **285**, along with a substantial quantity of α-methyl *N*-Boc/*N*-H tetrahydro monolactamol **286**, the product of reductive cleavage of a Boc group (scheme 2.81).

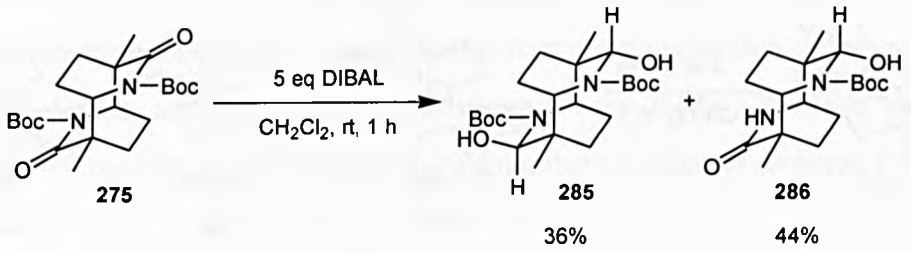

Scheme 2.81

An x-ray crystal structure of dilactamol **285** was obtained, and the 'axial' epimer at each lactamol centre was observed, once again confirming the axial attack of hydride (figure 2.20).

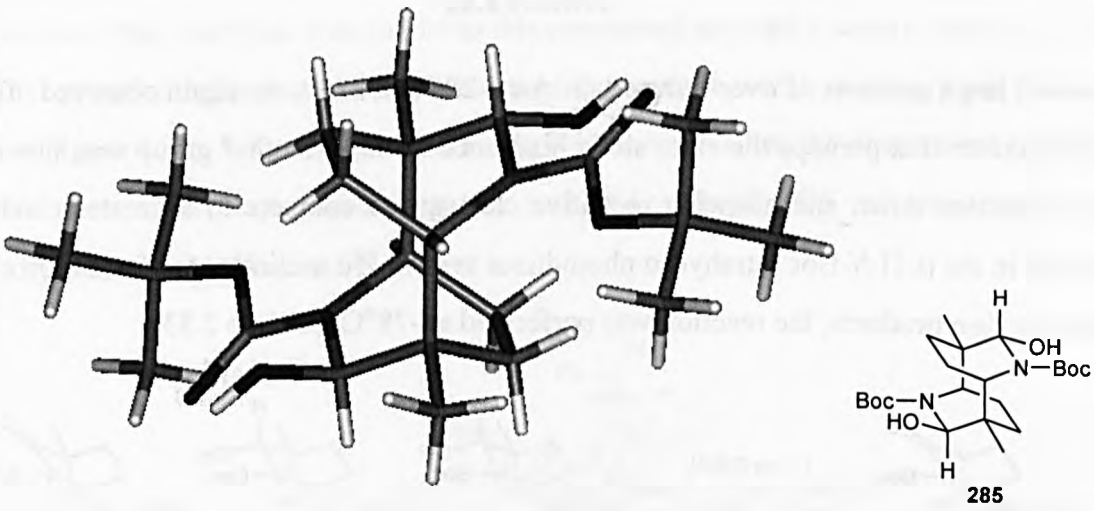

Figure 2.20

Examination of the COSY spectrum of compound **286** revealed that a lactam Boc group rather than a lactamol Boc group had been removed. This makes sense chemically, as the carbonyl of a lactam Boc group is more electrophilic as the electron density of the nitrogen lone pair is withdrawn to a certain extent by the lactam carbonyl.

We reasoned that the large excess of reducing agent was the cause of the over-reduction, and so performed a reaction employing only 2 equivalents of DIBAL (scheme 2.82).

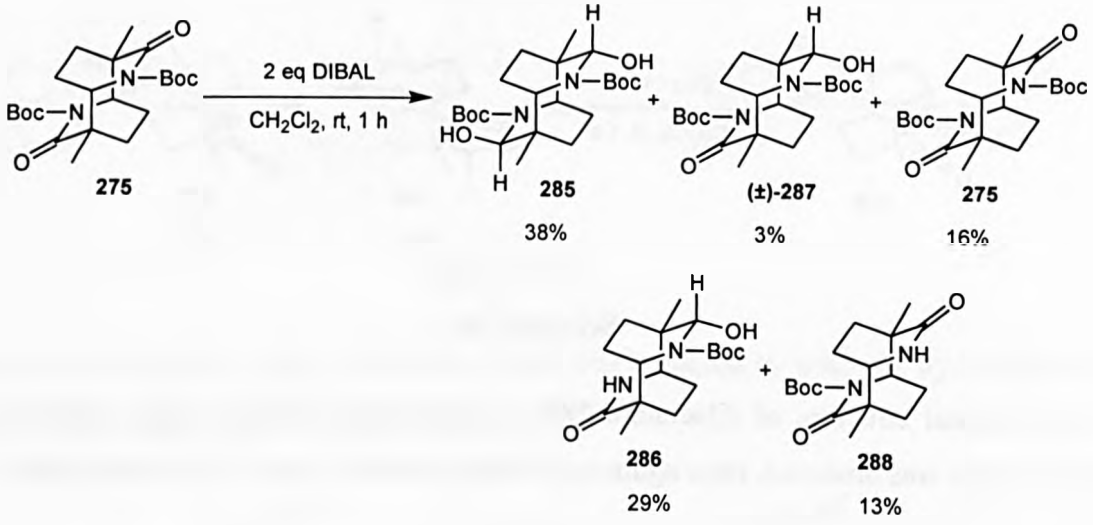

Scheme 2.82

However, large amounts of over-reduced products **286** and **288** were again observed. This led us to speculate that perhaps the extra steric hindrance of the α-methyl group was slowing the rate of reaction down and allowing reductive cleavage to compete to a greater extent than observed in the α-H *N*-Boc tetrahydro photodimer system. To minimise the formation of these over-reduction products, the reaction was performed at -78°C (scheme 2.83).

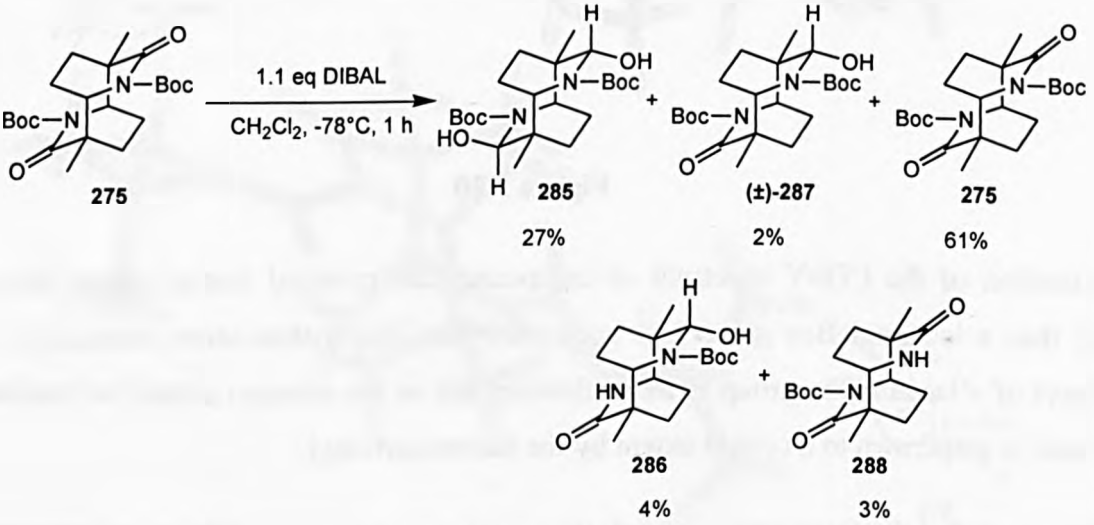

Scheme 2.83

The lower temperature significantly reduced the amount of Boc cleavage during the reaction. What became apparent at this point was the large amount of dilactamol **285** relative to monolactamol **(±)-287**, indicating co-operativity of reduction again, and to a greater extent than that observed for the *N*-Boc dimer (scheme 2.27). The reason behind this could be that, with a slower rate of reduction, the subtle co-operative effects become more significant and have a greater bearing on the selectivity.

With the reduction products of the unsaturated and tetrahydro α-methyl *N*-Boc dimers isolated and characterised, work proceeded on the asymmetric reduction of these compounds. The α-methyl *N*-Boc tetrahydro dimer was treated with *B*-Me CBS·BH_3 complex and BH_3·DMS, but no reaction was observed despite a number of attempts (scheme 2.84).

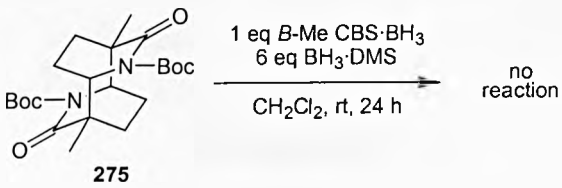

Scheme 2.84

Application of the transition state model to this compound revealed a severe steric clash of the α-methyl group with the *B*-methyl substituent of the catalyst, which could explain the lack of reaction (figure 2.21). Subsequent to this work, Knochel published the observation that ketone subtrates containg tertiary centres α to the carbonyl undergo CBS reduction with greatly reduced yields and selectivities.[180]

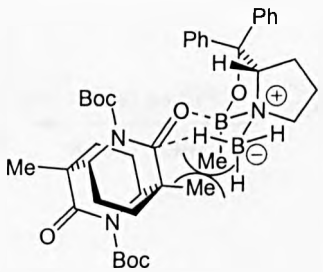

Figure 2.21

In the light of this, work on the α-methyl photodimer systems ceased, as the potential advantages of the α-methyl group were far outweighed by its interference in the crucial asymmetric desymmetrisation step.

Further elaboration of the desymmetrised products

In parallel with the asymmetric desymmetrisation studies, we investigated the further elaboration of the desymmetrised lactamols, and explored their chemistry.

Attempts were made to further reduce the lactamols using $NaBH_3CN$, which is known to ne able to reduce *N*-Boc lactamols and not *N*-Boc lactams.[181] Treatment of *N*-Boc dilactamol **215** with $NaBH_3CN$ and AcOH afforded a product which seemed to correspond to *N*-Boc

diamine **289**, but the analytical data was inconclusive and the compound remained uncharacterised (scheme 2.85).

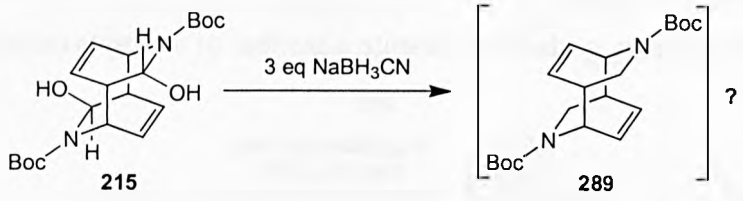

Scheme 2.85

One of the most useful reactions we wanted to achieve was the acid catalysed lactamol opening to give the ring opened amino-aldehydes. Initial attempts involved the treatment of the di and mono lactamols **215** and **(±)-214** with TsOH (scheme 2.86).

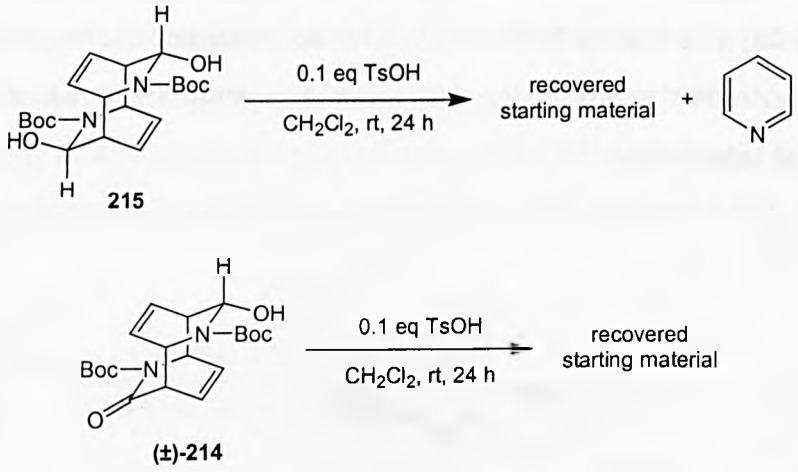

Scheme 2.86

Both compounds were resistant to lactamol opening, with a small amount of pyridine produced in the case of the dilactamol, the result of acid catalysed Boc removal, elimination of H_2O and cycloreversion (scheme 2.87).

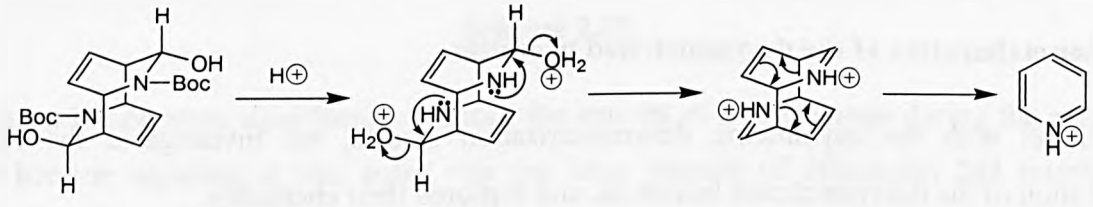

Scheme 2.87

It was thought that the resistance to lactamol opening of these compounds was due to the rigid

'cage-like' photodimer structure holding the lactmols closed, and the stabilisation of the lactamols by hydrogen bonding to the Boc carbonyl (figure 2.22). The signals corresponding to the hydroxyl groups in the IR spectra of these lactamols are broadened, which can be interpreted as evidence for hydrogen bonding. Furthermore, all of the x-ray crystal structures obtained for *N*-Boc lactamol photodimer derivatives show the hydrogen of the lactamol hydroxyl group oriented towards the Boc carbonyl, providing additional evidence for hydrogen bonding (figures 2.11, 2.14, and 2.20).

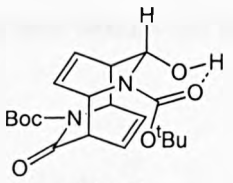

(±)-214

Figure 2.22

To disrupt this hydrogen bonding, we attempted the simultaneous Boc deprotection and lactamol opening with TFA (scheme 2.88).

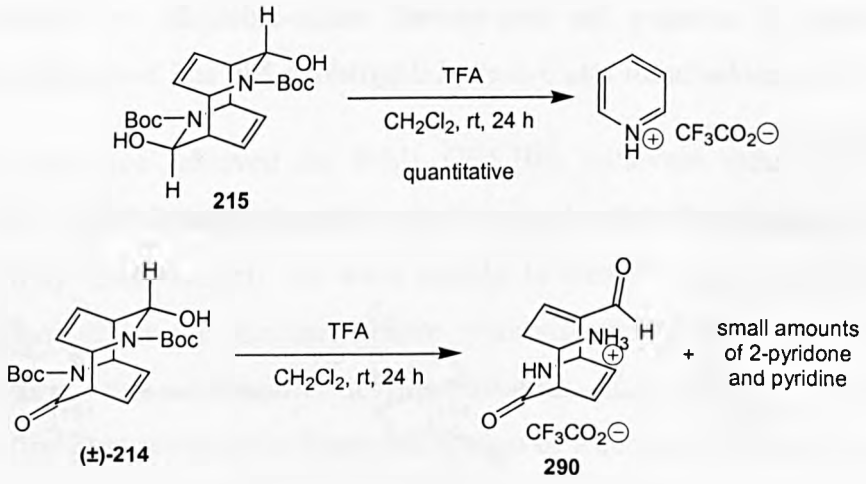

Scheme 2.88

Treatment of the dilactamol with TFA resulted in Boc deprotection, H_2O elimination, and cycloreversion to give pyridinium trifluoroacetate in a similar manner to that proposed in scheme 2.87. However, the monolactamol underwent Boc deprotection and lactamol opening, followed by an acid catalysed double bond isomerisation to give α,β-unsaturated amino-aldehyde **290** (scheme 2.89). The fact that small amounts of 2-pyridone and pyridine were observed illustrated that it also possible for the monolactamol to cyclorevert.

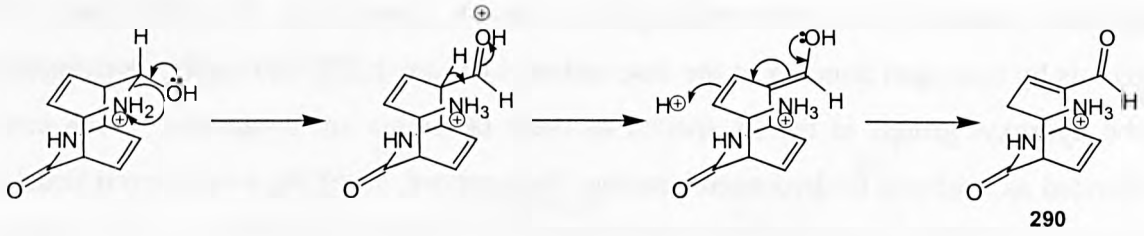

Scheme 2.89

We reasoned that the methyl group of the α-methyl *N*-Boc monolactamol **(±)-283** would prevent the double bond shift and yield the amino-aldehyde, and so treated monolactamol **(±)-283** with TFA (scheme 2.90).

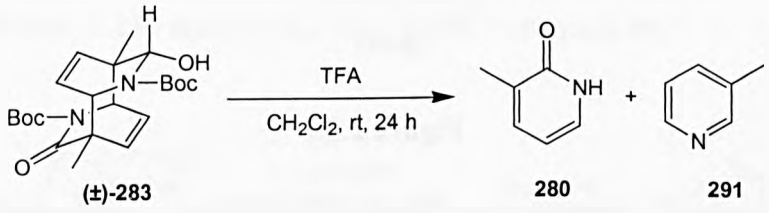

Scheme 2.90

However, instead of isolating the ring-opened amino-aldehyde, we observed complete conversion of the monolactamol into 3-methyl-2-pyridone **280** and 3-methylpyridine **291**, the products of cycloreversion.

These results suggest that the following equilibrium exists (scheme 2.91).

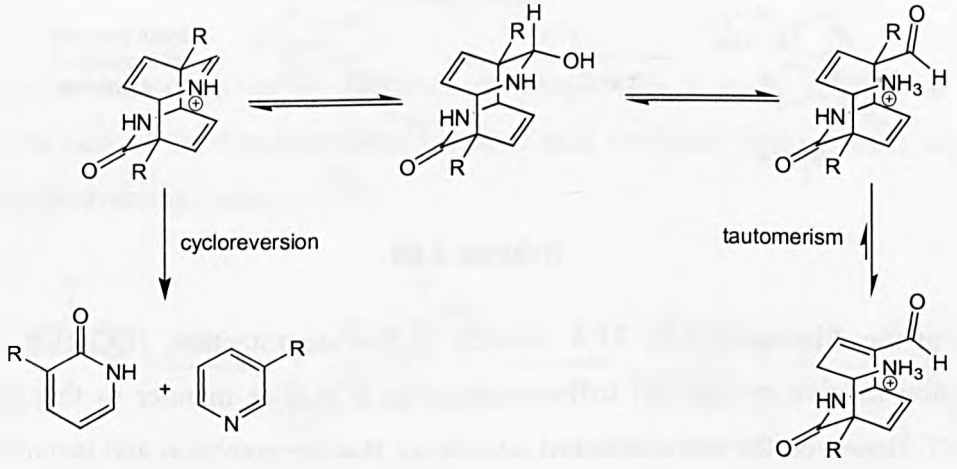

Scheme 2.91

When R = methyl, double bond tautomerism cannot take place and the equilibrium proceeds

to the left hand side, resulting in irreversible cycloreversion. When R = H however, double bond tautomerism can occur and the α,β-unsaturated amino-aldehyde product is favoured. The observation that the amounts of 2-pyridone and pyridine increase with time during the reaction of *N*-Boc monolactamol **(±)-214** with TFA, suggests all of the α,β-unsaturated amino-aldehyde will eventually cyclorevert given sufficient time.

Finally, an attempt to open the lactamols by trapping the amino-aldehyde with a Horner-Wadsworth-Emmons reaction was made by treating α-methyl *N*-Boc tetrahydro dilactamol **285** with trimethylphosphonoacetate and NaH, but only starting material was recovered (scheme 2.92).

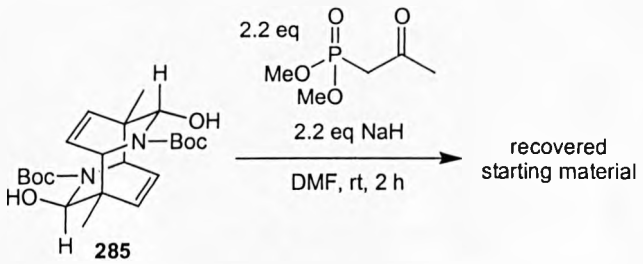

Scheme 2.92

Conclusion

In conclusion, we have achieved the *B*-Me CBS·BH_3 catalysed reduction of the *N*-Boc tetrahydro dimer with virtually complete enantiotopic group selectivity (≥97% ee) and in good yield (76%). Unfortunately we were unable to transfer these conditions on to the unsaturated *N*-Boc dimer and therefore unable synthesise the functionalised amino-acids as planned. However, the asymmetric desymmetrisation of the *N*-Boc tetrahydro dimer represents the first ever asymmetric desymmetrisation of a centrosymmetric *meso* compound, and establishes five stereocentres in a single step. It is also the first example of an asymmetric reduction of a *meso* diamide, and as such represents a significant extension of the scope and versatility of the CBS reduction process.

Future work

A number of options for future work are open.

The lactamase catalysed enantioselective lactam hydrolysis of the *N*-H dimer should be reinvestigated. Chiroscience encountered solubility problems with the *N*-H dimer, however it

is sparingly soluble in warm water and therefore, with optimisation, asymmetric desymmetrisation using lactamases may be possible.

Potential still exists for asymmetric desymmetrisation using lipases. The *N*-hydroxyethyl dimer **292** (figure 2.23) is known,[107] and it may be possible to achieve the enantioselective acylation of this compound using lipases. Longer alkyl chains may permit access of the hydroxyethyl groups to the enzyme active site, and precedent does exist for lipase catalysed acylations of alcohols remote from prochiral centres with excellent selectivity.

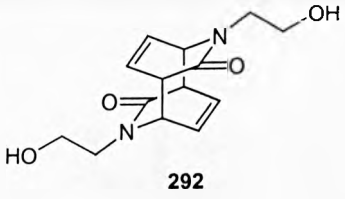

292

Figure 2.23

It has recently been shown that a 2:1 complex of DMAP-OsO_4 is an effective reagent for the dihydroxylation of sterically hindered alkenes.[182] This reagent may be reactive enough to effect dihydroxylation of a photodimer system, and the use of chiral DMAP derivatives may permit oxidative asymmetric desymmetrisation.

Finally, the formation of a small amount of monoepoxide during the enantioselective epoxidation of the *N*-Boc dimer with Jacobsen's catalyst (scheme 2.73) provides hope for the epoxidative asymmetric desymmetrisation strategy. Further optimisation and the use of more active catalysts may prove successful, and may yet provide a route to functionalised amino-acids.

Chapter 3: Asymmetric Desymmetrisation of Meso Decalin Diallylic Alcohols: Towards the Synthesis of Celastraceae Sesqiterpenoids

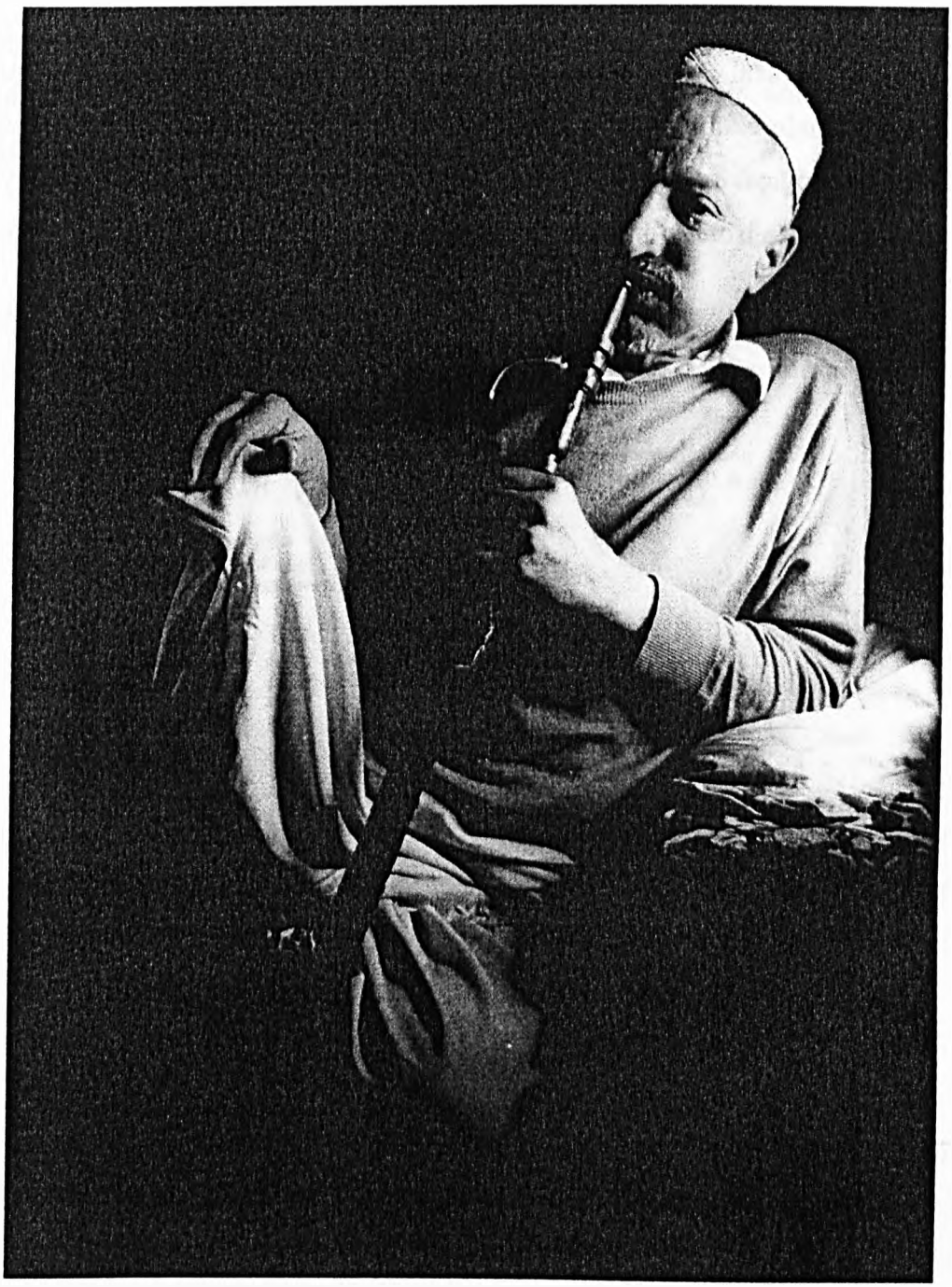

A gentleman chewing 'khat', a natural product of the *Celastraceae.*

Chapter 3: Asymmetric Desymmetrisation of Meso Decalin Diallylic Alcohols: Towards the Synthesis of Celastraceae Sesqiterpenoids

Natural products of the *Celastraceae*

The *Celastraceae* family consists of approximately 55 genera and 850 species of plant, indigenous to the tropical and sub-tropical regions of the world, namely Africa, Asia, and South America. Crude extracts of the *Celastraceae* have been valued since antiquity for a wide variety of biological activity, and a diverse array of natural products from many classes of compound have been isolated from these plants[183] (figure 3.1).

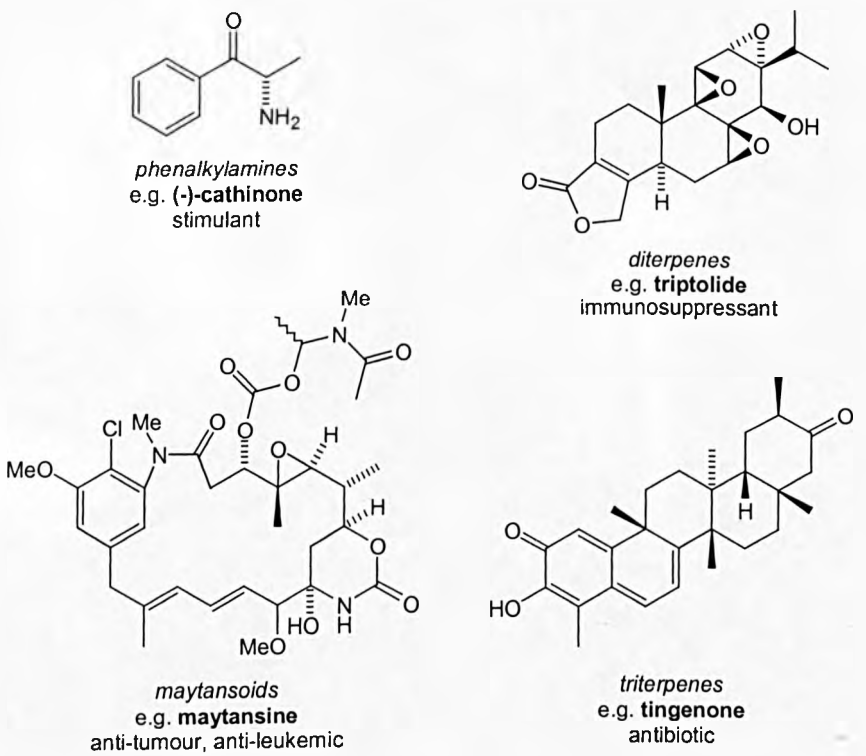

Figure 3.1

Of significant social importance in north eastern parts of Africa such as Ethiopia and the Yemen, is the addiction known as 'khatism'. The leaves of the *Catha edulis* ('khat') plant are chewed for their stimulant and appetite-suppressive effects, thought to be caused by (-)-cathinone,[184] which has a similar structure to (+)-amphetamine (figure 3.2). This addiction is becoming increasingly widespread and is blamed for many of the region's social and economic problems.

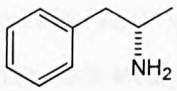

(+)-amphetamine

Figure 3.2

However, other natural products of the *Celastraceae* are of considerably more benefit to mankind, exhibiting immunosuppressant, anti-tumour, anti-leukemic, antibiotic, anti-arthritic, insect repellent, and memory restorative effects.[183]

***Celastraceae* sesquiterpenoids**

Prevalent amongst the natural products of the *Celastraceae* is a large family of polyhydroxylated sesquiterpene esters containing a dihydro-β-agarofuran skeleton (figure 3.3).

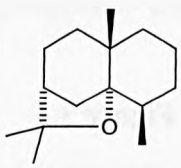

dihydro-β-agarofuran

Figure 3.3

Many members of this family, particularly esters of three polyhydroxylated agarofurans: euonyminol, 4β-hydroxyalatol, and 14-deoxyalatol, exhibit significant biological activity[185-188] (figure 3.4).

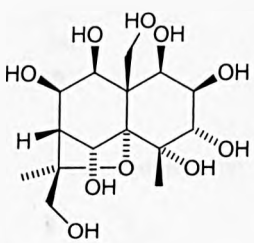

euonyminol

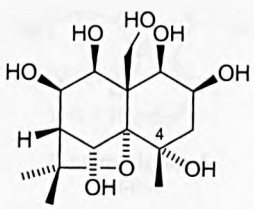

4β-hydroxyalatol

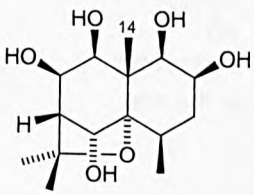

14-deoxyalatol

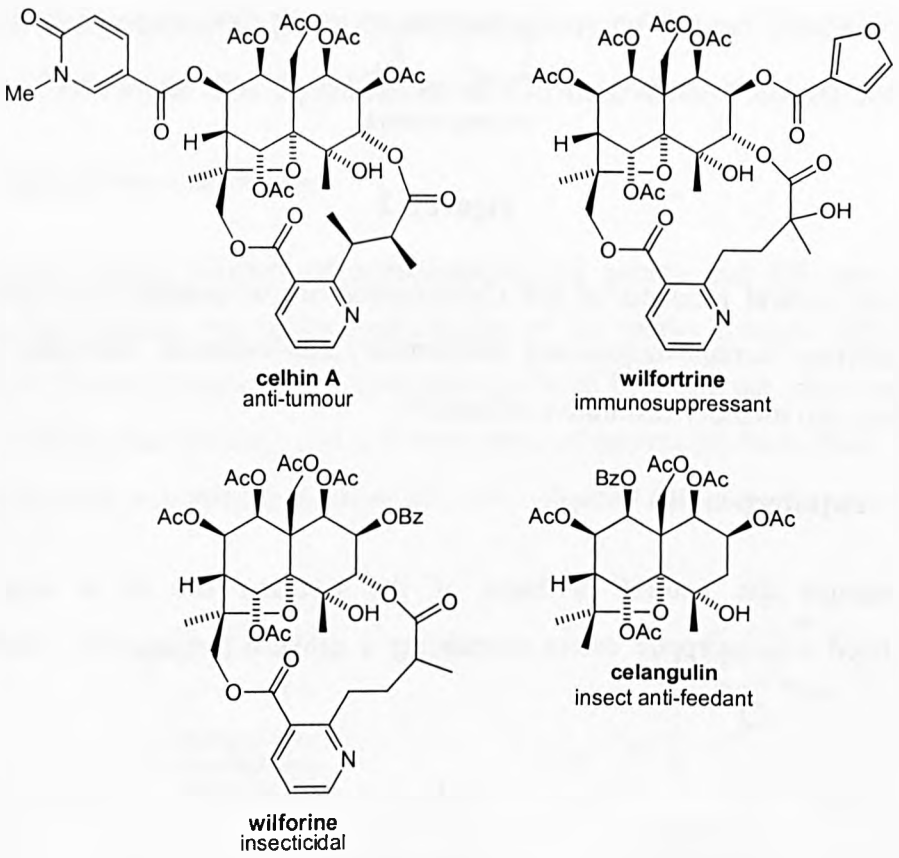

Figure 3.4

In particular, hypogluanine B and related macrocyclic lactone derivatives of euonyminol have recently been shown to display significant anti-HIV activity[189,190] (figure 3.5).

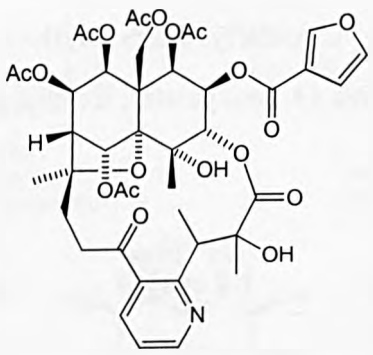

Figure 3.5

Synthetic strategy

A striking feature of the three core structures common to these natural products is the symmetric array of hydroxyl groups on the top face of the 'northern hemisphere' of these molecules. The synthetic strategy devised by our group planned to exploit this symmetry to

facilitate the synthesis of these compounds. Epoxy-alcohol **I** was identified as a pivotal intermediate for the preparation of all three core structures, and it was envisaged that the two-directional synthesis of *meso* diallylic alcohol **II**, followed by epoxidative asymmetric desymmetrisation would provide an efficient, stereoselective route to this intermediate (scheme 3.1).

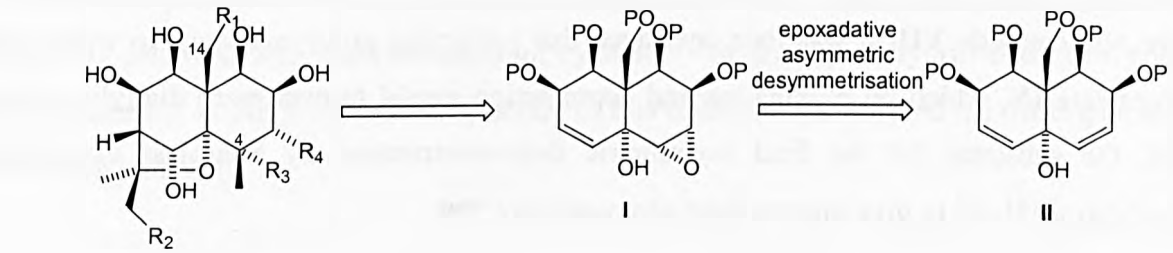

euonyminol: R_1, R_2, R_3, R_4 = OH
4β-hydroxyalatol: R_1, R_3 = OH, R_2, R_4 = H
14-deoxyalatol: R_1, R_2, R_3, R_4 = H

Scheme 3.1

The two-directional synthesis of epoxy-alcohol intermediate **293** was designed as follows (scheme 3.2).

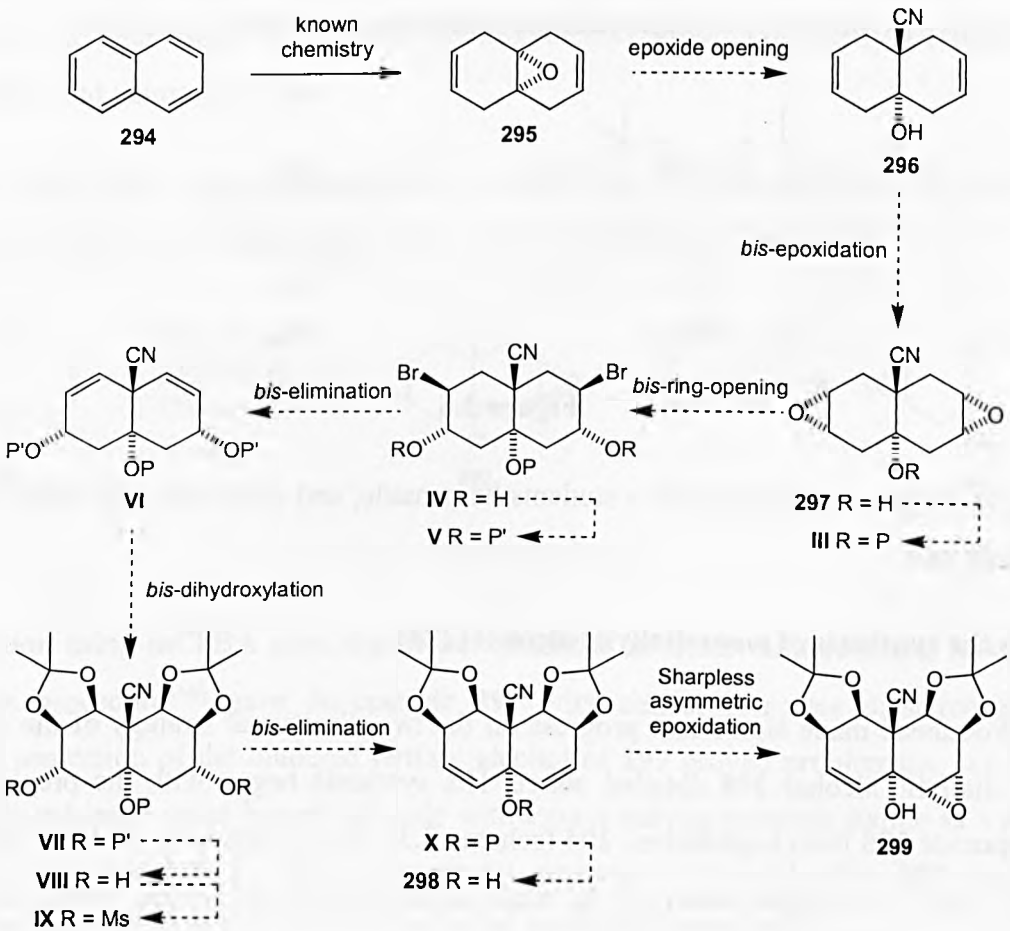

Scheme 3.2

Known epoxide **295**, synthesised from naphthalene **294**, could undergo ring-opening with cyanide to give cyanohydrin **296**, with the nitrile acting as a masked hydroxymethyl group. *Bis*-epoxidation of diene **296** directed on to the bottom face by the tertiary alcohol, followed by *trans* diaxial epoxide ring-opening of protected *bis*-epoxide **III** was expected to give dibromide **V** on protection of the two hydroxyl groups. *Bis*-elimination of this compound and subsequent diastereoselective *bis*-dihydroxylation and acetonide protection was expected to give *bis*-acetonide **VII**. It was then envisaged that protecting group exchange to would give dimesylate **IX**, which on elimination and deprotection would furnish *meso* diallylic alcohol **298**, the substrate for the final asymmetric desymmetrisation by Sharpless asymmetric epoxidation[191,192] to give intermediate epoxy-alcohol **299**.

Previous work

Our group has been working towards the total synthesis of *Celastraceae* sesquiterpenoids since 1995. Work was initiated by Steven Woodhead during his PhD, who made substantial progress towards the synthesis of *meso* diallylic alcohol **298**. Another student, Matthew Weston, currently entering the final year of his PhD, has successfully achieved the synthesis and epoxidative asymmetric desymmetrisation of model system **300** (figure 3.6).

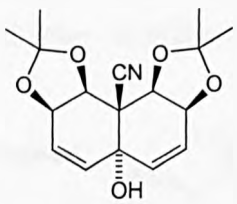

298

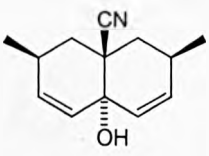

300

Figure 3.6

This section details the progress these students have made, and establishes the context for my work in this area.

Towards the synthesis of *meso* diallylic alcohol (298)

Steven Woodhead made significant progress on the two-directional strategy of the synthesis of *meso* diallylic alcohol **298** detailed above. His synthesis began with the preparation of known epoxide **295** from naphthalene **294** (scheme 3.3). Birch reduction of naphthalene gave isotetralin **301**,[193] and epoxidation of the most electron rich double bond furnished epoxide **295** in good yield.[194]

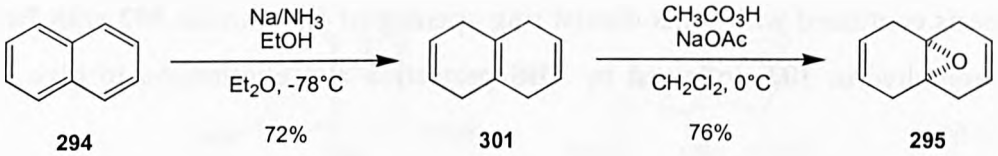

Scheme 3.3

This epoxide proved resistant to nucleophilic opening with a variety of reagents, but was eventually achieved with diethylaluminium cyanide[195] to give cyanohydrin **296** in excellent yield (scheme 3.4). An x-ray crystal structure of this compound confirmed the *trans* geometry of the ring junction.

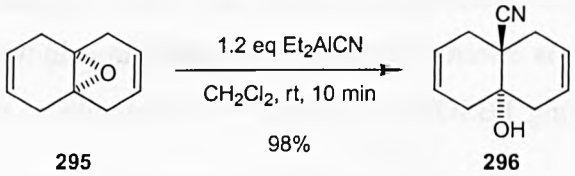

Scheme 3.4

The nitrile was considered to be a useful 'masking group' which could be hydrolysed and reduced at a later stage to give the hydroxymethyl group commonly observed in the sesquiterpenoid natural products.

The next step involved diastereoselective epoxidation of the bottom face of the two alkenes directed by the hydroxy group, followed by benzyl protection (scheme 3.5).

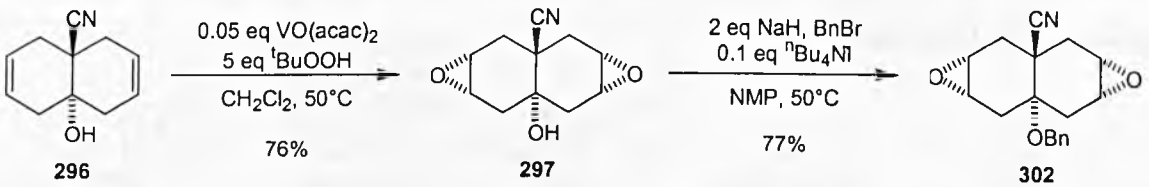

Scheme 3.5

Epoxidation using mCPBA gave significant quantities of other diastereomers, however, the Sharpless procedure[196] gave *bis*-epoxide **297** with almost complete diastereoselectivity. Initially, protection of the hindered tertiary alcohol of **297** proved problematic, but this was eventually achieved using benzyl bromide with tetra-*n*-butylammonium iodide as a promoter in *N*-methyl pyrrolidinone. The x-ray crystal structure of benzyl ether **302** showed the stereochemistry of the two epoxides to be *syn* to the benzyl ether group.

His synthesis continued with *trans*-diaxial ring opening of *bis*-epoxide **302** with Br_2/PPh_3[197] to give bromohydrin **303**, followed by TBS protection and elimination to give diene **305** (scheme 3.6).

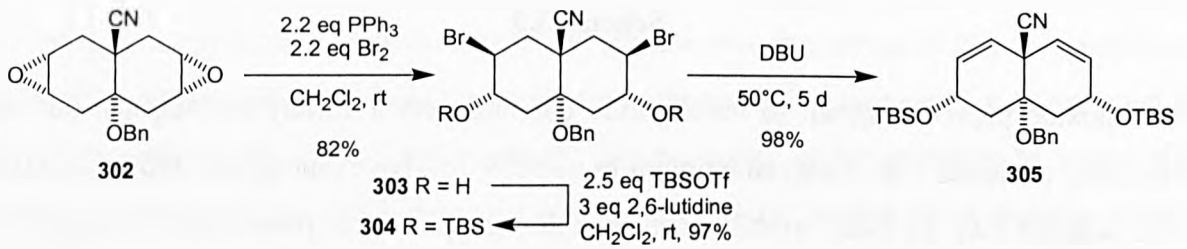

Scheme 3.6

Although this sequence was efficient, attempts were made to achieve the same transformation in a one-pot procedure using TBSOTf and DBU,[198-200] but with no success.

With diene **305** synthesised, his efforts turned to establishing the symmetrical hydroxyl array on the 'northern hemisphere' of the molecule. According to Kishi's empirical rule, dihydroxylation of diene **305** was expected to occur from the top face (i.e. anti to the TBS ether C-O bonds),[201] and this diastereoselectivity was expected to be reinforced by the steric bulk of the TBS groups blocking the bottom face.

Attempted *bis*-dihydroxylation using the Upjohn conditions[202,203] only gave the diol **306**, which was protected with 2,2-dimethoxypropane to give acetonide **307** (scheme 3.7). This termination of the *bis*-dihydroxylation of dialkene substrates after only one oxidation is often observed in the literature.[204]

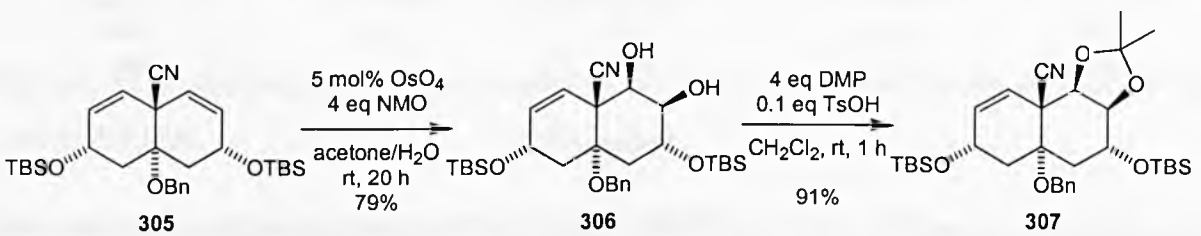

Scheme 3.7

Interestingly, he observed that if the dihydroxylation reaction was prolonged, imidolactone **308** was also isolated, the result of attack of the γ-hydroxyl on the nitrile (figure 3.7). Attempted dihydroxylation of diene **305** under the more basic Warren dihydroxylation conditions[173] resulted in quantitative conversion to this imidolactone.

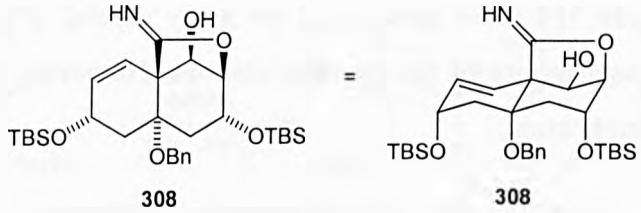

Figure 3.7

He found that this imidolactone could be hydrolysed to the lactone and reduced to give the hydroxymethyl compound, a potentially useful sequence for 'unmasking' the nitrile.

Attempted dihydroxylation of the second alkene of mono acetonide **307** under the Upjohn conditions failed, and treatment with the Warren conditions was expected to deliver the imidolactone/acetonide **309** (figure 3.8).

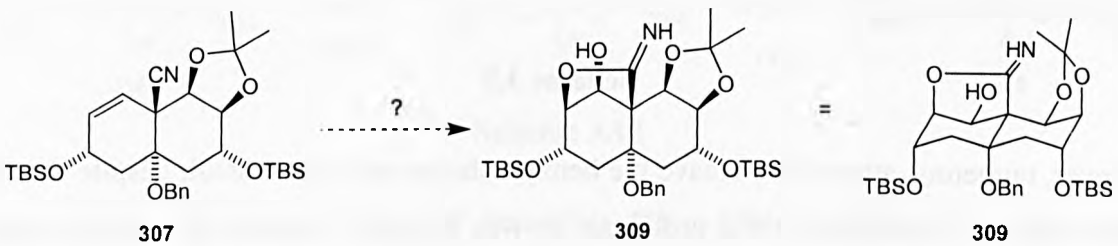

Figure 3.8

However, to his surprise he isolated diol/acetonide **310** in 69% yield, with imidolactone/acetonide **309** present in only 7% yield. The diol/acteonide was protected with 2,2-dimethoxypropane to give symmetrical *bis*-acetonide **311** (scheme 3.8).

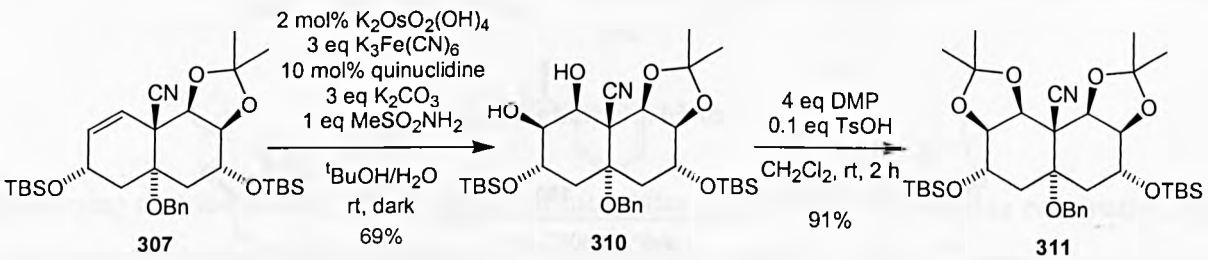

Scheme 3.8

This reduced inclination to form the imidolactone on the second dihydroxylation compared with the first is possibly the result of increased rigidity of the decalin system induced by the acetonide ring. It is also possible that a conformational change has taken place such that the γ-hydroxyl group is further removed from the nitrile, thus reducing the propensity to form the imidolactone.

Crystals of bis-acetonide **311** were grown and an x-ray crystal structure obtained which confirmed the diastereoselectivity of the dihydroxylations. However, the quality of the data was not sufficient for publication.

The synthesis was continued with the silyl deprotection, mesylation and elimination of *bis*-acetonide **311** (scheme 3.9), which proceeded to give benzyl protected diallylic alcohol **314** in good yield, although the elimination was slow.

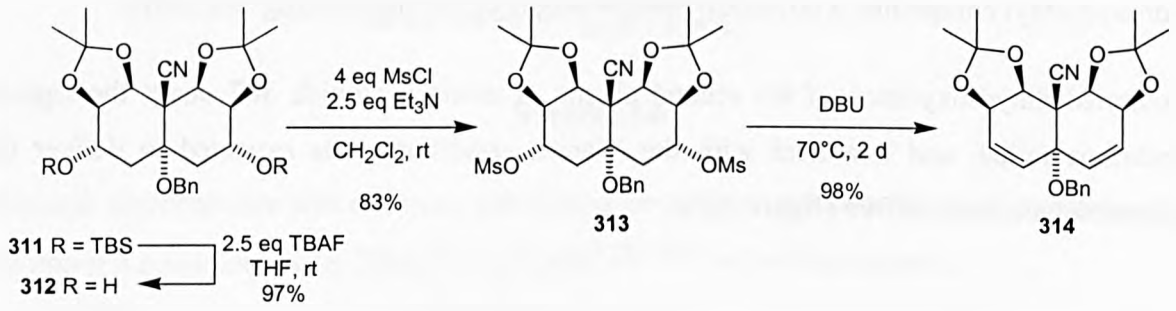

Scheme 3.9

However, numerous attempts to cleave the benzyl ether were unsuccessful, despite extensive experimentation. Faced with these problems, he was forced to consider alternative routes to diallylic alcohol **298**, as well as alternative methods of asymmetric desymmetrisation.

Cogniscent of the work of Sakai on the asymmetric desymmetrisation of *meso* triflates by enantioselective deprotonation using chiral bases[91] (see chapter 1, scheme 1.53), he attempted the asymmetric desymmetrisation of dimesylate **313** (scheme 3.10). Unfortunately, the mono eliminated products was obtained as a racemate.

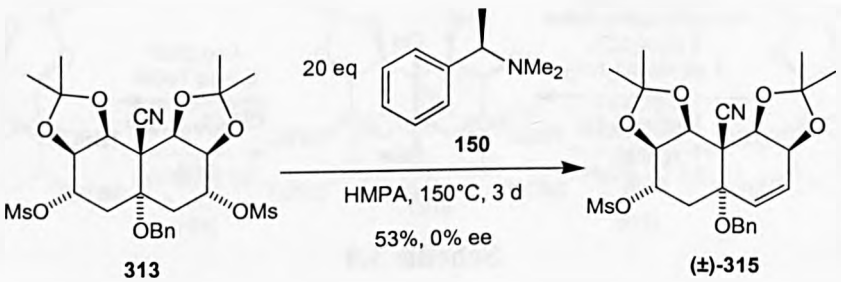

Scheme 3.10

As a result, efforts were redirected into the synthesis of diallylic alcohol **298**. Attempts to deprotect the benzyl ether prior to elimination eventually succeeded. The treatment of protected triol **311** with dissolving metal reduction conditions gave a mixture of diol **316** and triol **317** (scheme 3.11).

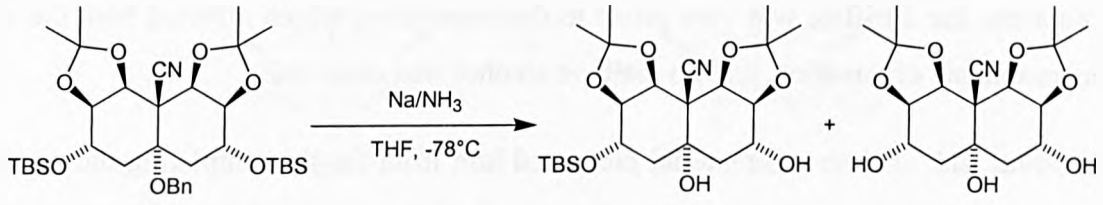

Scheme 3.11

The remaining TBS group was deprotected with TBAF and the secondary alcohols of triol **317** selectively mesylated (scheme 3.12).

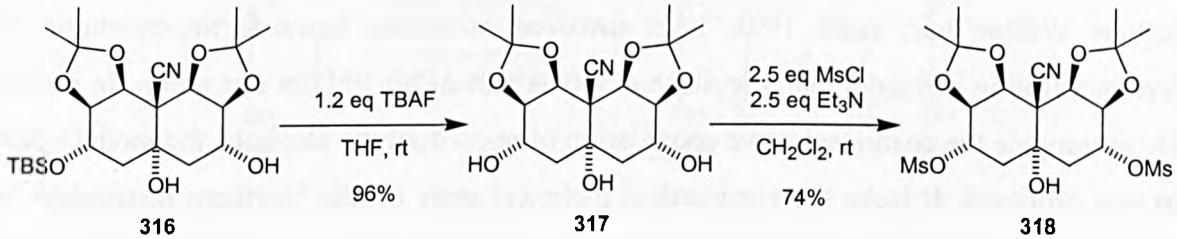

Scheme 3.12

He then investigated the elimination of dimesylate **318** in DBU (scheme 3.13). The reaction proceeded very slowly as in previous attempts, but even with heating to 70°C only the mono eliminated product **319** was obtained.

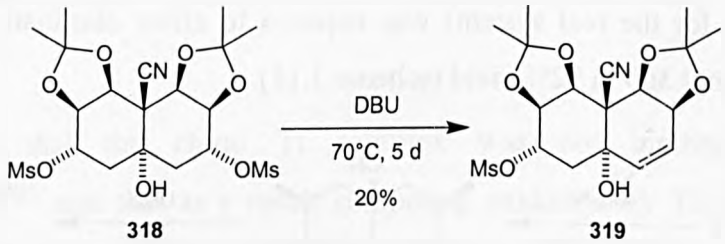

Scheme 3.13

Reasoning that the leaving group ability of mesylates was insufficient for this elimination, he attempted the synthesis and elimination of ditriflate **320** (scheme 3.14).

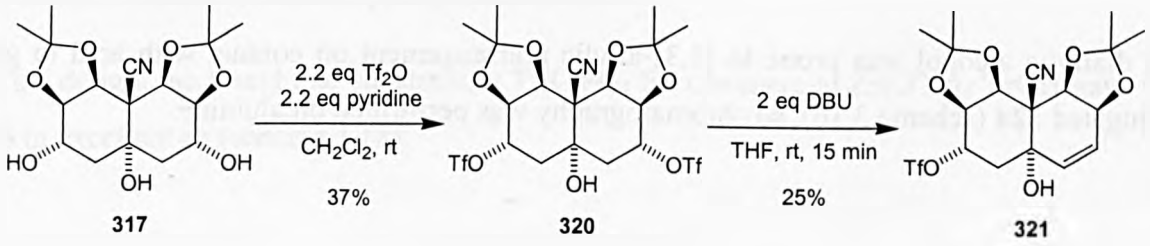

Scheme 3.14

Unfortunately, the ditriflate was very prone to decomposition, which affected both the yields of preparation and elimination, and no diallylic alcohol was observed.

At this point, lack of time and material prevented him from finally completing the synthesis, and his studies came to a close with the diallylic alcohol just out of sight. However, he did succeed in establishing the majority of the groundwork required for the synthesis of this compound, and passed the baton on to Matthew Weston and myself to achieve the synthesis of the elusive diallylic alcohol **298** and its asymmetric desymmetrisation.

Synthesis and epoxidative asymmetric desymmetrisation of model system (300)

Matthew Weston has, since 1998, been involved in studies towards the synthesis and desymmetrisation of model diallylic alochol **300** as part of his PhD in our group. In order to fully investigate the enantioselective epoxidation of *meso* diallylic alcohols, the model system **300** was proposed. It lacks the symmetrical hydroxyl array on the 'northern hemisphere' of the real system and is therefore easier to synthesise, furthermore the 'southern hemisphere' is identical.

His synthesis of model diallylic alcohol **300** began from *bis*-epoxide **297**. *Trans*-diaxial opening of the epoxide functions with trimethylaluminium gave triol **322**, which was selectively mesylated to give dimesylate **323**. Exposure to neat DBU and heating at 100°C (compared to 70°C for the real system) was required to effect elimination and furnish the model diallylic alcohol **300** in 92% yield (scheme 3.15).

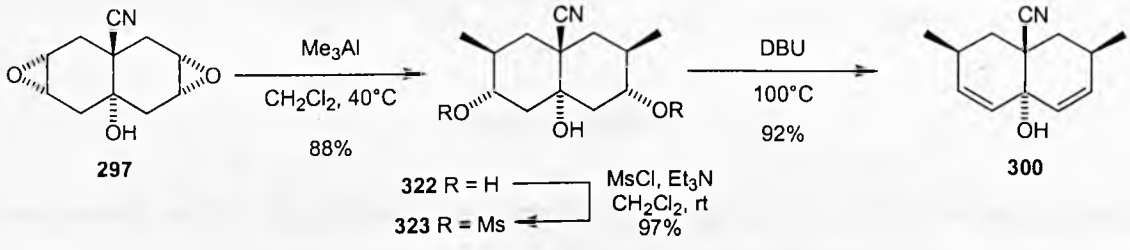

Scheme 3.15

The diallylic alcohol was prone to [1,3]-allylic rearrangement on contact with acid to give conjugated **324** (scheme 3.16), so chromatography was performed on alumina.

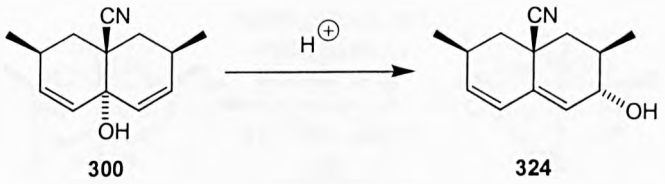

300 **324**

Scheme 3.16

In preparation for the enantioselective epoxidation, he performed the catalytic epoxidation of the diallylic alcohol and isolated and characterised racemic epoxy-alcohol **(±)-325** and *meso bis*-epoxide **326** (scheme 3.17).

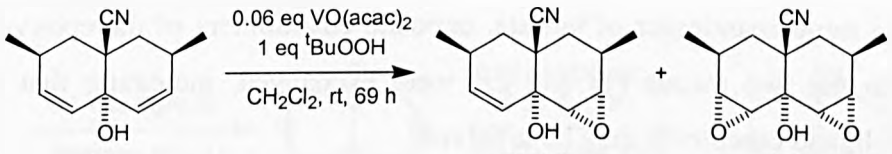

300 **(±)-325** **326**

34% 16%

Scheme 3.17

Sharpless asymmetric epoxidation[191,192,205] using either catalytic of stoichiometric amounts of $Ti(O^iPr)_4$/D(-)-DIPT gave epoxy-alcohol **(-)-325** in yields of up to 70%, but despite extensive experimentation the ee never exceeded 17%. Known variations employing other tartrate or tartramide ligands[206] and promoters such as CaH_2 and silica[207] failed to improve the situation.

It was believed that the chiral Ti complex was not binding to the tertiary alcohol,[191,192,208,209] and that as a result competing oxidation by $Ti(O^iPr)_4$ and ^tBuOOH without the chiral ligand was lowering the ees. In order to circumvent this problem, the use of Zr in place of Ti was explored, the reasoning being that the increased bond length of Zr-O compared with Ti-O would facilitate complex formation.[210,211] Indeed, stoichiometric $Zr(O^nPr)_4$/ dicyclohexyltartramide has been shown to effect the asymmetric epoxidation of homoallylic alcohols, albeit in poor yields and ee.[210]

To his delight, he found that substituting $Ti(O^iPr)_4$ for commercial $Zr(O^iPr)_4 \cdot {}^iPrOH$ gave **(+)-325** in excellent ee (scheme 3.18).

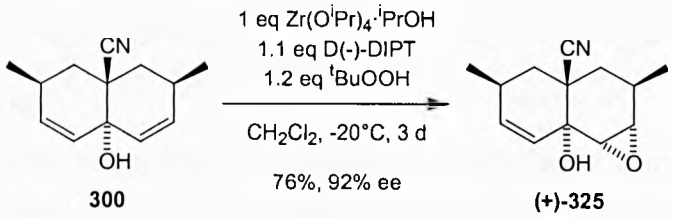

300 (+)-325

Scheme 3.18

The use of the opposite enantiomer of the ligand, L(+)-DIPT, gave epoxy alcohol **(-)-325** in 90% yield and 92% ee. Unfortunately, attempts to employ sub-stoichiometric amounts of $Zr(O^iPr)_4$ have so far been unsuccessful. An interesting observation during these studies was that, using the same enantiomer of tartrate, opposite enantiomers of the epoxy-alcohol were obtained when the two metals (Ti and Zr) were exchanged, indicating that topologically distinct metal-ligand complexes may be involved.

At this juncture, Matthew Weston's studies took him in the direction of establishing the 'southern hemisphere' functionality present in euonyminol using the model system, leaving the epoxidative asymmetric desymmetrisation of the real system for me to achieve.

Aims

My aims then, at the outset of this work, were to achieve the following:

- Obtain an x-ray quality crystal of *bis*-acetonide **311** in order to confirm the relative stereochemistry established in the sequential dihydroxylation sequence.
- Overcome the problematic elimination step and synthesise diallylic alcohol **298** of the real system.
- Apply the Zr based enantioselective epoxidation to the real system and achieve the asymmetric desymmetrisation of *meso* diallylic alcohol **298**.
- Adapt and optimise the synthetic procedure of diallylic alcohol **298** for large scale synthesis, as a number of reactions had proved difficult to scale-up.

Synthesis of *meso* diene (305)

The synthesis began with the Birch reduction of naphthalene which was performed on a 48 g scale, according to the literature procedure, giving isotetralin **301** in a 74% recrystallised yield. Epoxidation of isotetralin proceeded to give epoxide **295** in a significantly improved yield to the original procedure (scheme 3.19).

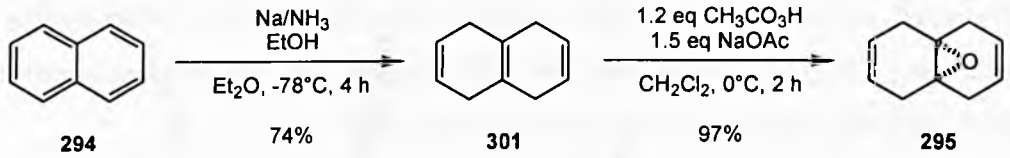

Scheme 3.19

Epoxide opening with diethylaluminium cyanide, followed by *bis*-epoxidation and benzyl protection proceeded smoothly (scheme 3.20). The yield of benzyl ether **302** was improved by rigorously drying the apparatus and reagents, and by monitoring hydrogen evolution to ensure complete deprotonation of alcohol **297**.

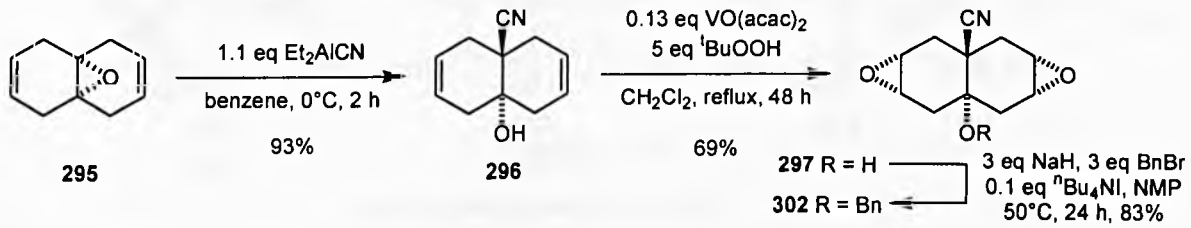

Scheme 3.20

The subsequent epoxide opening and TBS protection sequence had proven difficult to scale-up. Steven Woodhead performed the reactions on 2.77 g of benzyl ether **302**, isolating bromohydrin **303** in 82% yield, which on TBS protection afforded only 31% of the required di-TBS ether **304** and 47% of what was thought to be di-TBS ether **327**, the result of benzyl ether cleavage and TBS group migration (scheme 3.21).

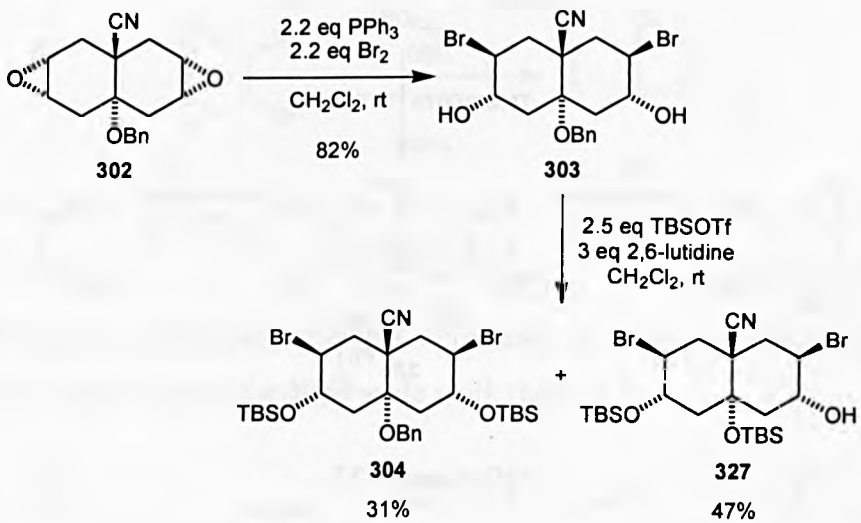

Scheme 3.21

Similarly, when I performed the above sequence on a larger scale, bromohydrin **303** was produced in only 43% yield, and subsequent TBS protection led to a mixture of products, with the required di-TBS ether in very low yield (scheme 3.22).

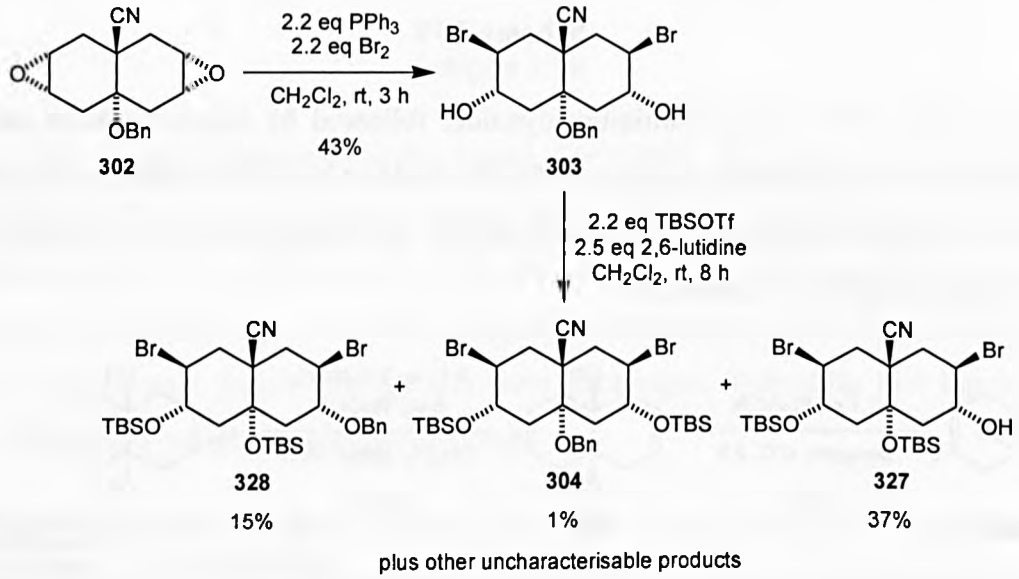

Scheme 3.22

Compounds **327** and **328** were believed to have been formed by intra and intermolecular nucleophilic attack on oxonium ion **329** by the pendant hydroxyl group and triflate anion respectively (scheme 3.23).

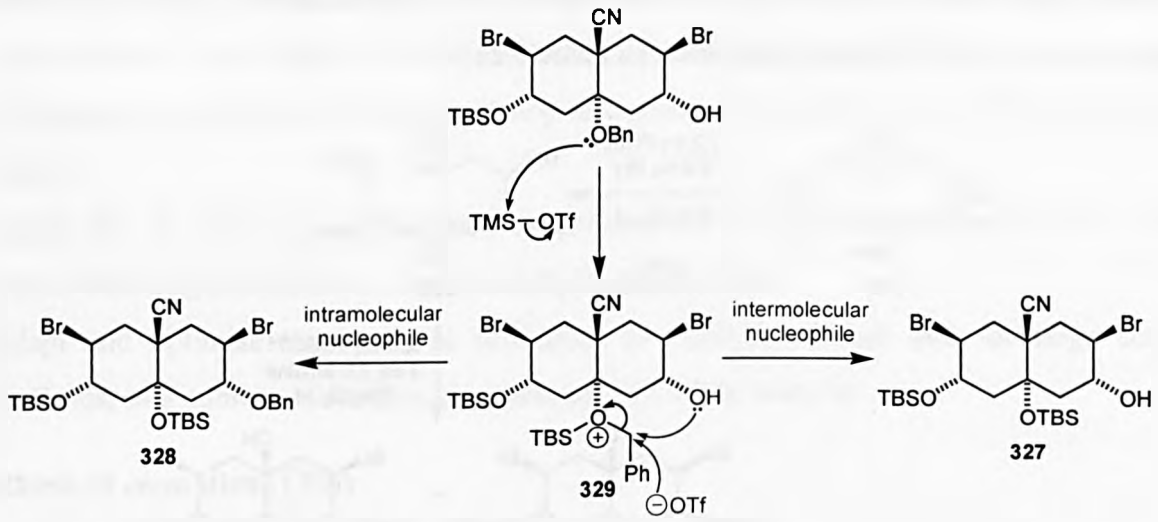

Scheme 3.23

Subsequently however, the structure of compound **327** was revised on obtaining an x-ray crystal structure, and shown to be cyclic ether **330** (figure 3.9).

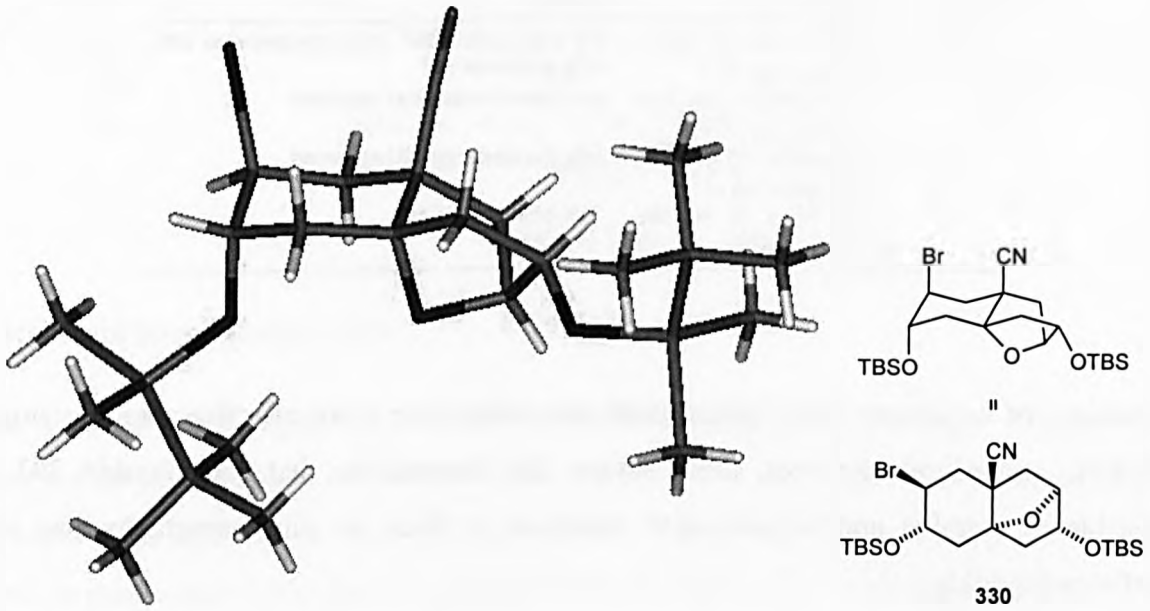

Figure 3.9

This compound may not be a synthetic 'dead end' however, as the potential exists for tetrahydrofuran ring to be opened with nucleophilic bromide to restore the symmetrical decalin system.

Steven Woodhead isolated a similar cyclic ether during studies towards an alternative route to diallylic alcohol **298**. Dibromide **331** was treated with DBU to effect double elimination, but intramolecular ether formation occurred preferentially to give cyclic ether **332** (scheme 3.24), the structure of which was confirmed by x-ray crystallography.

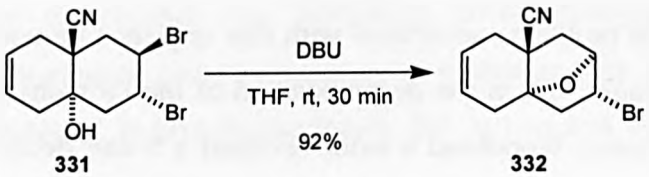

Scheme 3.24

In the light of these complications, attempts were made to determine conditions for epoxide opening that were more suitable for large scale work (table 3.1).

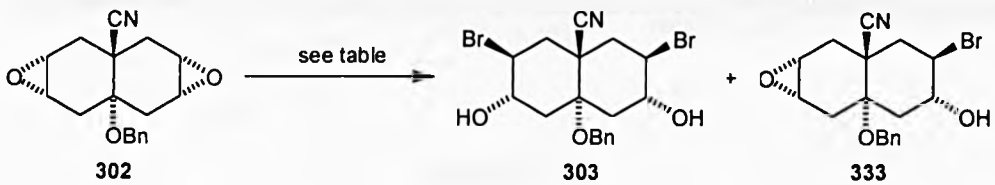

Entry	Conditions	Results
1	3 eq LiBr, 6 eq AcOH, THF, reflux, 24 h[212]	9% bromohydrin **303**, 46% monobromide **333**, 39% diepoxide **302**
2	3.2 eq $CuBr_2$, 6.4 eq LiBr, THF, reflux, 72 h[213]	only monobromide **333** observed
3	6 eq Bu_4NBr, 0.6 eq CAN, MeCN, reflux, 48 h[214]	only monobromide **333** observed
4	3 eq PPh_3, 3 eq Br_2, CH_2Cl_2, rt, 3 h[197]	71% bromohydrin **303**

Table 3.1

A variety of conditions were investigated, but none were more effective than the original Br_2/PPh_3 procedure. However, these studies did demonstrate that bromohydrin **303** was unstable to alumina and to prolonged exposure to silica, so chromatography had to be performed quickly.

Also, the oily foam of the bromohydrin was observed to decompose on standing at room temperature for a few days, and an odour of benzyl bromide was detected. This gave us clues as to the mechanism of formation of bridged ether compound **330** (scheme 3.25).

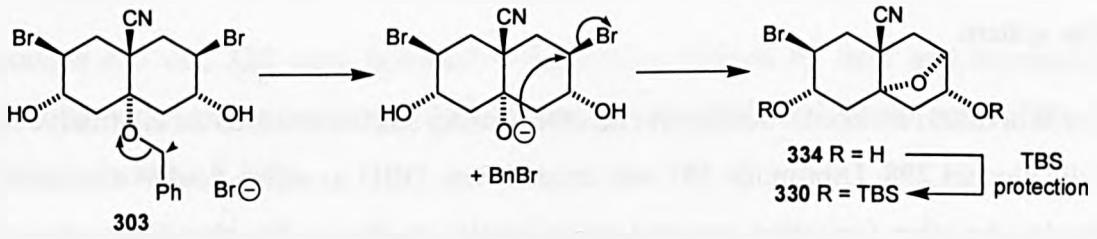

Scheme 3.25

This indicated that the problems associated with this sequence lie not in the TBS protection step as originally thought, but in the decomposition of the bromohydrin prior to protection. Re-examination of Steven Woodhead's work revealed a 5 day delay between bromohydrin formation and TBS protection, explaining his reduced yield of di-TBS ether (scheme 3.21).

It was found that formation of the bromohydrin by the Br_2/PPh_3 procedure with rapid columning on silica and storage in the freezer, followed by immediate TBS protection gave di-TBS ether **304** in excellent yield, even on a 10 g scale (scheme 3.26). Subsequent elimination of dibromide **304** proceeded slowly, but in good yield to give diene **305**.

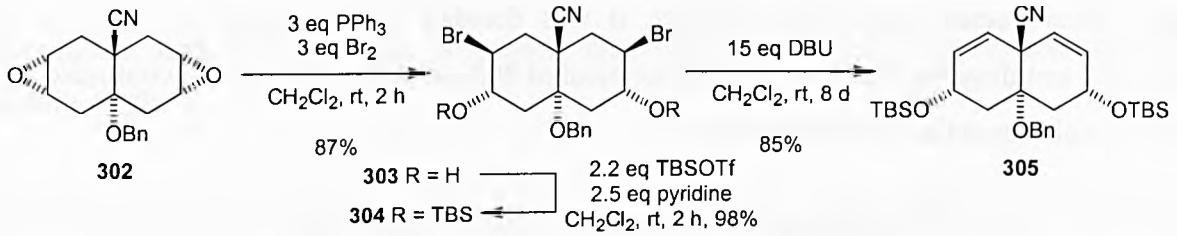

Scheme 3.26

Synthesis of *bis*-acetonide (311)

With diene **305** synthesised, our attention turned to the dihydroxylation steps. We wanted to effect the dihydroxylations in a simultaneous fashion rather than sequentially, and envisaged Narasaka's modification of the Upjohn procedure to be a potential solution as it has been shown to permit the simultaneous dihydroxylation of polyenes[215,216] (scheme 3.27).

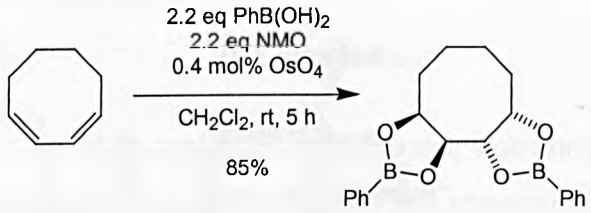

Scheme 3.27

The reaction is performed under anhydrous conditions and phenylboronic acid replaces H_2O as the agent that releases OsO_4 from the diol. Also, reaction times are decreased compared with the standard Upjohn procedure. We reasoned that, on application of these conditions to diene **305**, the *in situ* boronate ester protection would prevent the first diol from interfering with the formation of the second, thus facilitating *bis*-dihydroxylation. Potentially, the boronate esters could be cleaved using peroxide or by exchange with excess diol,[217,218] and the tetrol acetonide protected to give *bis*-acetonide **311** in two less synthetic steps than the sequential procedure.

However, treatment of the diene under the Narasaka conditions gave only recovered starting material and phenol, the product of oxidative cleavage of phenylboronic acid (scheme 3.28).

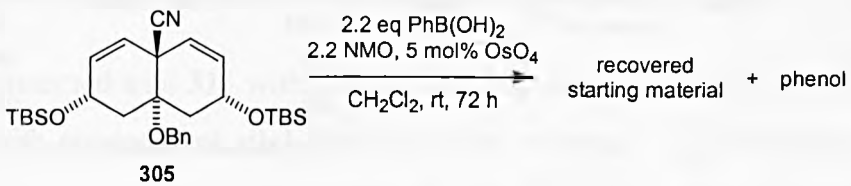

Scheme 3.28

Rather than pursue this strategy further, it was decided that the priority should be the synthesis and desymmetrisation of diallylic alcohol **298**, so the synthesis was continued with the original sequential oxidation steps.

The first dihydroxylation using the Upjohn procedure gave diol **306** in reasonable yield, along with a small amount of imidolactone **308**, suggesting that the reaction should have been worked up sooner (scheme 3.29).

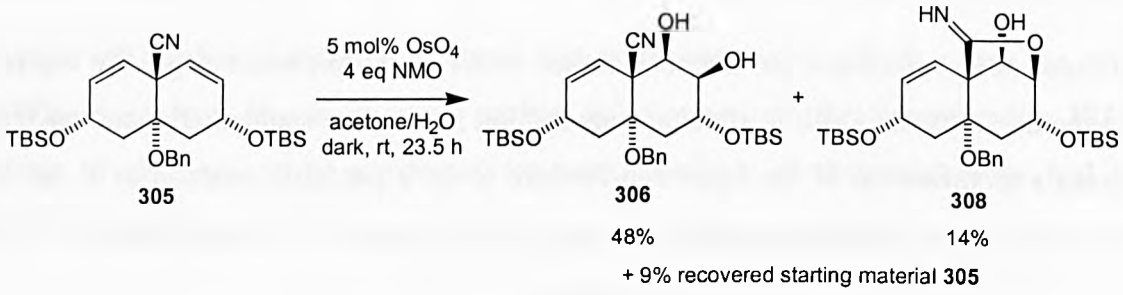

305 → **306** 48% + **308** 14%

+ 9% recovered starting material **305**

Scheme 3.29

Subsequent acetonide protection proceeded in excellent yield to give mono-acetonide **307** (scheme 3.30). Anhydrous reagents and solvents proved crucial for attaining high yields.

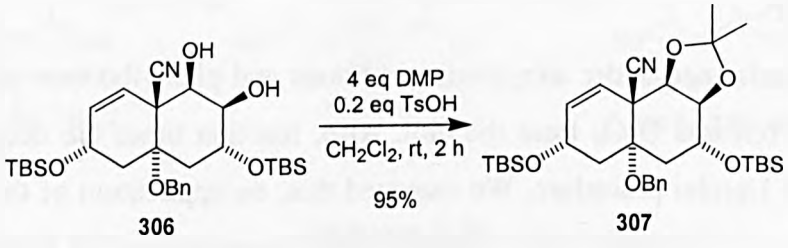

306 → **307**

Scheme 3.30

The second dihydroxylation using the Warren procedure gave diol/acetonide **310** in good yield, with only a small amount of imidolactone/acetonide **309** (scheme 3.31).

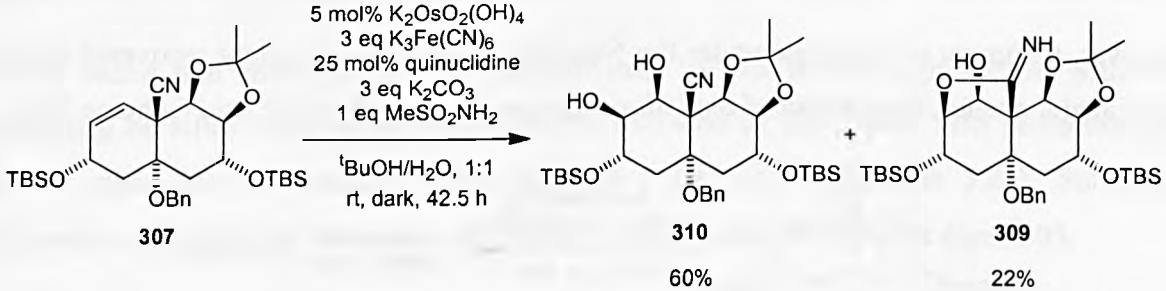

307 → **310** 60% + **309** 22%

+ 16% recovered starting material **307**

Scheme 3.31

Once again, acetonide protection proceeded almost quantitatively to give *bis*-acetonide **311** (scheme 3.32).

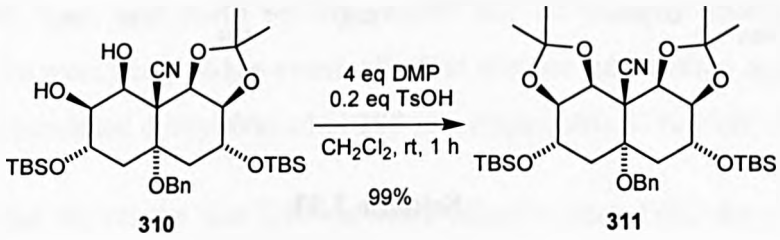

Scheme 3.32

Good quality crystals of *bis*-acetonide **311** were grown, and an x-ray structure was obtained, thereby confirming the diastereofacial selectivity of the dihydroxylation steps (figure 3.10).

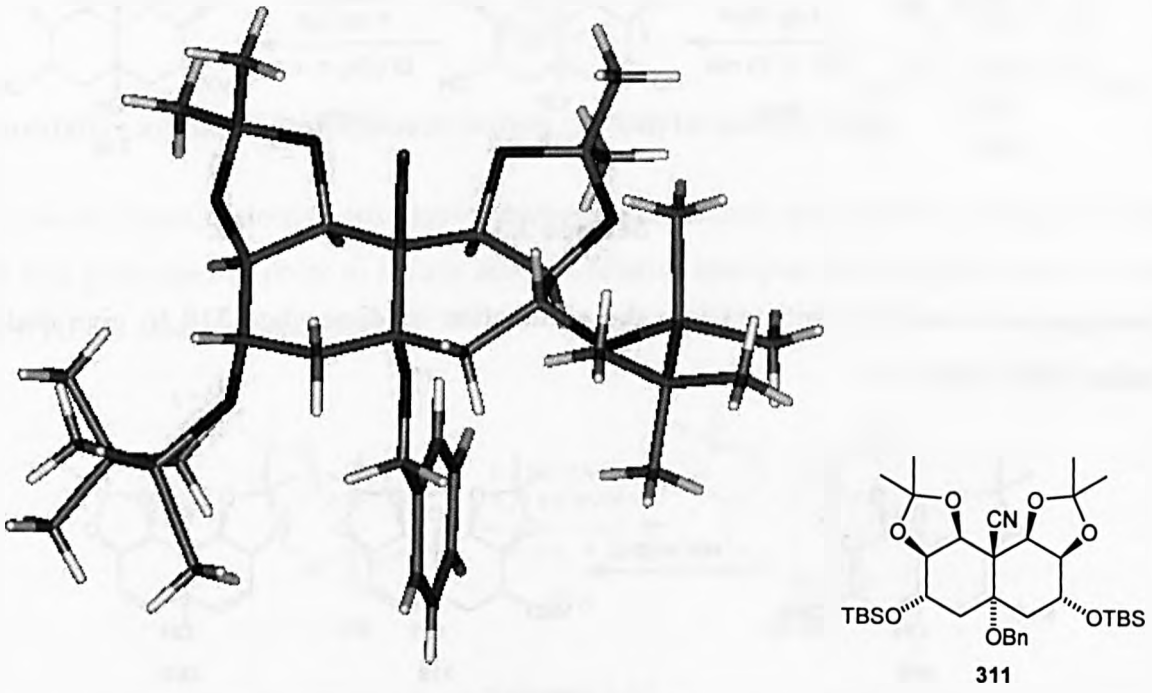

Figure 3.10

Synthesis of *meso* diallylic alcohol (298)

With the synthesis of *bis*-acetonide **311** accomplished, it remained to tackle the problematic final elimination step and complete the synthesis of diallylic alcohol **298**.

Treatment of protected triol **311** with sodium in liquid ammonia effected deprotection of the benzyl ether with concomitant silyl ether cleavage (scheme 3.33). Prolonging the reaction time was found to increase the proportion of triol **317** but to the detriment of the total recovery.

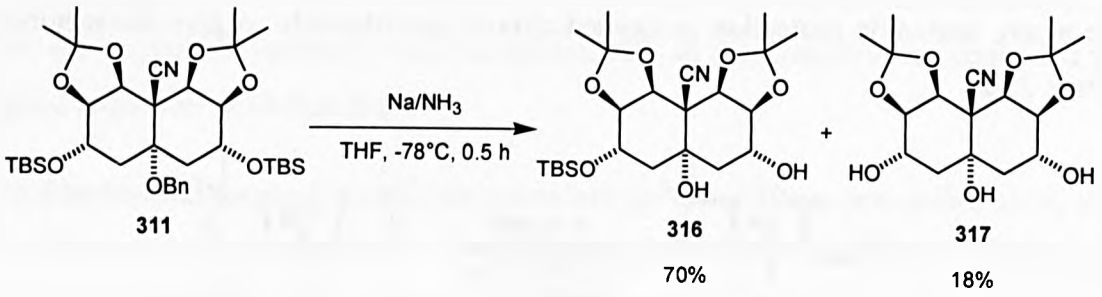

Scheme 3.33

Subsequent deprotection of silyl ether **316** with TBAF and *bis*-mesylation proceeded in excellent yield, significantly improving on the original mesylation yield (scheme 3.34).

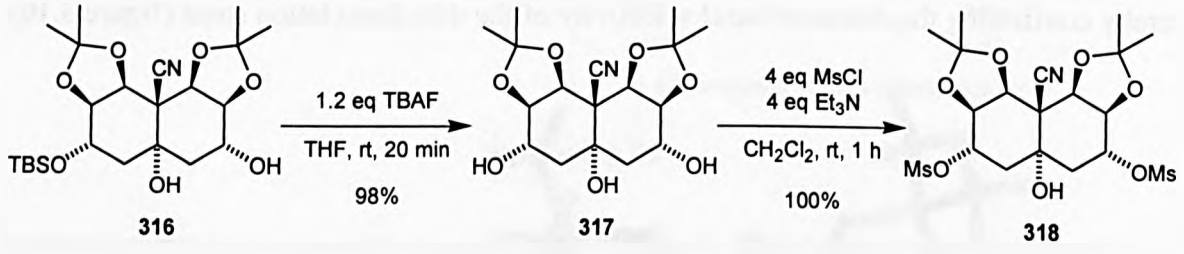

Scheme 3.34

Investigations were then initiated into the elimination of dimesylate **318** to give diallylic alcohol **298** (table 3.2).

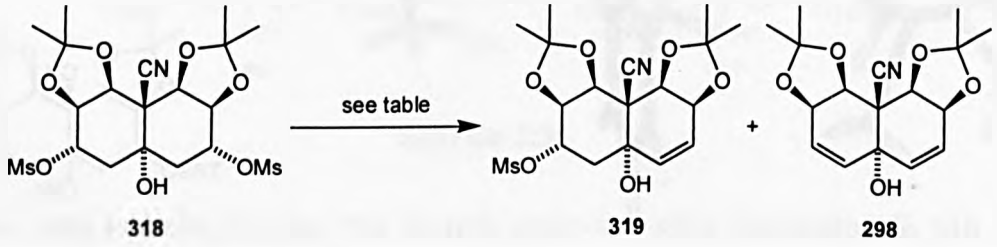

Entry	Conditions	Results
1[a]	neat DBU, 120°C, 20 h	15% diallylic alcohol **298**
2[b]	neat DBU, 100°C, 10 h	15% mono monomesylate **319**, 14% diallylic alcohol **298**
3	20 eq DBU, CH_2Cl_2, reflux, 48 h	no reaction
4	20 eq DBU, THF, reflux, 48 h	1:1 ratio of dimesylate **318** to monomesylate **319**
5	20 eq DBU, toluene, reflux, 48 h	1:1 ratio of dimesylate **318** to monomesylate **319**
6[b]	20 eq DBN, toluene, reflux, 20 h	67% diallylic alcohol **298**

[a] chromatography performed on alumina, [b] chromatography performed on silica

Table 3.2

Elimination in neat DBU at higher temperatures than those attempted by Steven Woodhead gave small amounts of the monomesylate **319** and diallylic alcohol **298** (entries 1 and 2). Unfortunately the total recovery of material was low, mainly due to difficulties associated

with removing the excess DBU. However, diallylic alcohol **298** was less prone to [1,3]-allylic rearrangement than the model diallylic alcohol **300**, and chromatography could be performed on silica. Subsequently, a series of reactions were performed with 20 equivalents of DBU in refluxing solvents with increasing boiling points, but no diallylic alcohol was observed (entries 3 to 5). We were delighted to eventually find that the substitution of DBU for DBN in refluxing toluene furnished diallylic alcohol **298** in a respectable 67% yield (entry 6).

We rationalised that the reason that DBN is more effective than DBU for this elimination is because it is smaller (figure 3.11), a crucial factor in this sterically demanding elimination.

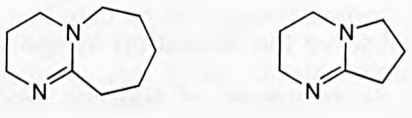

Figure 3.11

Epoxidative asymmetric desymmetrisation of diallylic alcohol (298)

Prior to any enantioselective epxodation attempts, the racemic epoxidation of diallylic alcohol **298** was performed in order to isolate and characterise epoxy-alcohol **(±)-299** and develop a chiral HPLC assay (scheme 3.35).

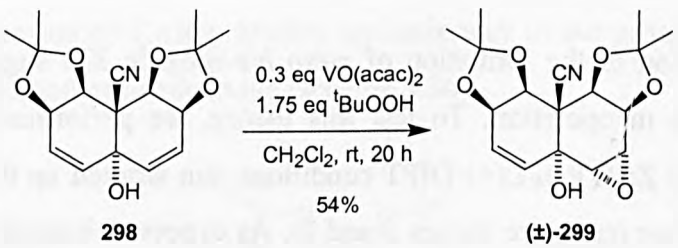

Scheme 3.35

Efforts then turned to the Zr-based enantioselective epoxidation of diallylic alcohol **298** (table 3.3).

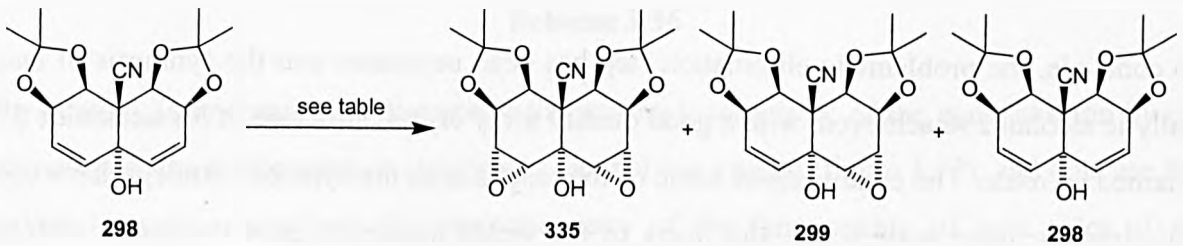

Entry	Conditions	*meso bis*-epoxide **335**	epoxy-alcohol **299**		starting material **298**
		Yield (%)	Yield (%)	Ee (%)	Yield (%)
1[a]	3 eq $Zr(O^iPr)_4$, 3.15 eq L(+)-DIPT, 3.3 eq ^{t}BuOOH, 4 Å MS, CH_2Cl_2, -20 °C, 74 h	10	42	(-) ≥95	20
2[b]	3 eq $Zr(O^iPr)_4$, 3.3 eq L(+)-DIPT, 3.4 eq ^{t}BuOOH, 4 Å MS, CH_2Cl_2, -20 °C, 69 h	19	54	(-) ≥95[d]	24
3[b]	3 eq $Zr(O^iPr)_4$, 3.3 eq D(-)-DIPT, 3.4 eq ^{t}BuOOH, 4 Å MS, CH_2Cl_2, -20 °C, 69 h	21	44	(+) ≥95[e]	20
4[a]	3 eq $Ti(O^iPr)_4$, 3.3 eq L(+)-DIPT, 3.4 eq ^{t}BuOOH, 4 Å MS, CH_2Cl_2, -20 °C, 71 h	7	40	(+) 13.8	40
5[c]	3 eq $Zr(O^iPr)_4$, 3.3 eq L(+)-DIPT, 3.4 eq ^{t}BuOOH, 4 Å MS, CH_2Cl_2, -20 °C, 24 h	8	37	(-) 81.3	26

[a] 10 mg scale, [b] 30 mg scale, [c] 19 mg scale, [d] $[\alpha]_D$ = -26.9°, [e] $[\alpha]_D$ = +30.5°

Table 3.3

We were extremely pleased to observe the formation of epoxy-alcohol **(-)-299** in 54% yield and excellent enantioselectivity on treatment of diallylic alcohol **298** with $Zr(O^iPr)_4$, L(+)-DIPT and ^{t}BuOOH (entry 2). An analogous reaction using D(-)-DIPT produced the opposite enantiomer, epoxy-alcohol **(+)-299**, in 44% yield and excellent ee (entry 3).

Epoxidation using standard Sharpless asymmetric epoxidation conditions with $Ti(O^iPr)_4$ and L(+)-DIPT, gave epoxy-alcohol **(+)-299** in only 13.8% ee (entry 4), illustrating the importance of employing Zr in place of Ti for this type of substrate. It was also interesting to note the reversal in the sense of asymmetric induction on exchanging Zr for Ti, with L(+)-DIPT as the chiral ligand in both cases (compare entries 2 and 4), as for the model system.

Finally, the observation of the formation of *meso bis*-epoxide **335** suggested that the *meso* trick may have been in operation. To test this theory, we performed an enantioselective epoxidation under the $Zr(O^iPr)_4$/L(+)-DIPT conditions, but worked up the reaction after only one day instead of three (compare entries 5 and 2). As expected, both the proportion of *meso bis*-epoxide **335** and the ee of epoxy-alcohol **(-)-299** were lower than that observed on prolonging the reaction time, indicating that the *meso* trick, the enhancement of ee as a function of time, was indeed in operation.

Conclusions

To conclude, the problematic elimination step has been overcome and the synthesis of *meso* diallylic alcohol **298** achieved, with a good quality x-ray crystal structure of *bis*-acetonide **311** obtained en route. The conditions of some of the reactions in the synthetic strategy have been optimised for large scale work, and many of the yields improved upon compared with the original procedure.

Most importantly, the asymmetric desymmetrisation of *meso* diallylic alcohol **298** has been achieved in good yield using a new Zr modified Sharpless asymmetric epoxidation procedure, establishing eight contiguous stereocentres with ≥95% ee in a single step. This represents an almost completely enantioselective synthesis of epoxy-alcohol **(-)-299**, a key intermediate in a potentially expedient synthesis of core structures of bioactive *Celastraceae* sequiterpenoids.

Future work

The absolute configuration of epoxy-alcohol **(-)-299** should be established to determine which enantiomer of DIPT is to be employed in the asymmetric epoxidation to give the correct enantiomer of (-)-euonyminol, and also to aid rationalisation of the stereochemical induction of the Zr/DIPT epoxidation system. An x-ray crystal structure of epoxy-alcohol **(-)-299** should be obtained, either with a chiral auxiliary attached, or using the Bijvoet method to obtain the absolute configuration directly.

That Zr is effective for the asymmetric epoxidation of tertiary allylic alcohols is a potentially very important finding, and it will be interesting to delineate the scope of this modified Sharpless asymmetric epoxidation procedure by screening a number of tertiary allylic alcohols to further demonstrate the synthetic utility of this reaction.

The next step towards the synthesis of *Celastraceae* sesquiterpene cores involves establishing the dimethyltetrahydrofuranyl C-ring. Studies are underway in our group to achieve this by a [1,3]-dipolar cycloaddition of nitrile oxide (scheme 3.36).

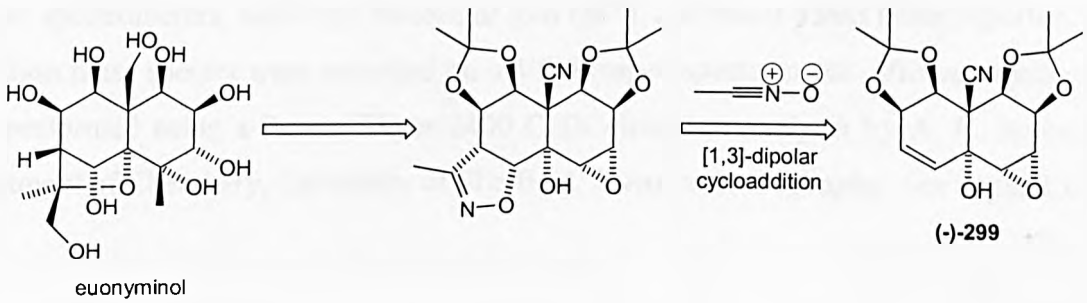

Scheme 3.36

The strategy is to control the diastereofacial and regioselectivity of the cycloaddition by co-ordination of the nitrile oxide to the tertiary alcohol via a metal (figure 3.12), and thus use this hydroxyl group to establish the stereochemistry of the functionality of both sides of the 'southern hemisphere'.

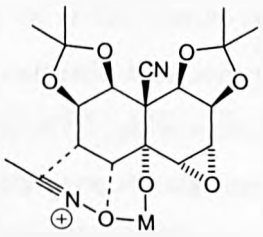

Figure 3.12

Obviously, once this is achieved, the goal should be to further elaborate the 'southern hemisphere' of this system in order to synthesise (-)-euonyminol, and eventually hypoglaunine B.

Chapter 4: Experimental

General Directions

Solvents and reagents: See appendices 1 and 2. ***Chromatography:*** Flash chromatography was performed on silica gel (Merck Kieselgel 60 F_{254} 230-400 mesh) according to the method of W. C. Still.[219] TLC was performed on aluminium backed plates pre-coated with silica (0.2 mm, 60 F_{254}) which were developed using standard visualising agents: UV fluorescence (254 and 366 nm), iodine, bromocresol green with heating, molybdic acid with heating, anisaldehyde with heating and $KMnO_4$ with heating. ***Melting points:*** These were determined on a Khofler hot stage. ***Optical rotations:*** These were recorded on a Perkin-Elmer 241 polarimeter at 589 nm (Na D-line), and with a path length of 0.1 dm. Concentrations (c) are quoted in g/100 ml. ***Infra red spectra:*** These were recorded as thin films, KBr disks, or as solutions in CH_2Cl_2 or $CHCl_3$, on a Perkin-Elmer Paragon 1000 fourier transform spectrometer. Only selected absorbances (υ_{max}) are reported. ***^{1}H NMR spectra:*** These were recorded at either 250 or 400 MHz on Bruker AC-250, or Bruker AM-400 instruments respectively. Chemical shifts (δ) are quoted in parts per million (ppm), referenced to the appropriate residual solvent peak. Coupling constants (*J*) are reported to the nearest 0.1 Hz. ***^{13}C NMR spectra:*** These were recorded at either 63 or 100 MHz on Bruker AC-250 or Bruker AM-400 instruments respectively. Chemical shifts (δ) are quoted in ppm, referenced to the appropriate solvent peak. Degenerate peaks are suffixed by the number of carbons. ***Mass spectra:*** Low-resolution mass spectra (*m/z*) were recorded on either a VG platform or VG prospec spectrometers, with only molecular ions (M^+), and major peaks being reported. High-resolution mass spectra were recorded on a VG Prospec spectrometer. ***Microanalysis:*** These were performed using a Perkin Elmer 2400 CHN elemental analyser by A. H. Jones at the Department of Chemistry, University of Sheffield. ***X-ray crystallography***: See appendix 3.

Experimental for Chapter 2

Trans-3,7-diazatricyclo[4.2.2.2^{2,5}]dodeca-9,11-diene-4,8-dione (186).[103]

185 186

A solution of 2-pyridone **185** (28.5 g, 3 M) in degassed water (100 mL) in a Pyrex reaction vessel was irradiated with ultra-violet light (350 nm) over a period of 2 weeks, whereupon the *N*-H dimer **186** separated out of solution. The reaction mixture was periodically filtered and irradiation continued. The *N*-H dimer was recrystallised from glacial AcOH to give 14.94 g (52%) of white 'needle-like' crystals: mp 222.0–222.6°C (*cf.* literature mp 225.5–227.5°C[103]); ^{1}H NMR (CF_3CO_2D, 400 MHz) δ 7.25 (ddd, *J* 8.0, 6.5, 1.5 Hz, 2 H), 6.68 (ddd, *J* 8.0, 6.5, 1.5 Hz, 2 H), 4.88 (ddd, *J* 10.0, 6.5, 1.5 Hz, 2 H), 4.26 (ddd, *J* 10.0, 6.5, 1.5 Hz, 2 H), NH protons absent; ^{13}C NMR (CF_3CO_2D, 100 MHz) δ 185.4 (2 C), 136.3 (2 C), 132.7 (2 C), 53.3 (2 C), 52.4 (2 C); IR (nujol mull) 1667 cm^{-1}; MS (CI+) *m/z* 191 M^+, 130, 113, 96; HRMS (CI+) calculated for $C_{10}H_{11}N_2O_2$ $(M + H)^+$ 191.0821, found 191.0821; Elemental analysis, calculated for $C_{10}H_{10}N_2O_2$: C, 63.15; H, 5.25; N, 14.66%. Found C, 62.87; H, 5.30; N, 14.73%.

1-Hydroxymethyl-1H-pyridin-2-one (199).[124]

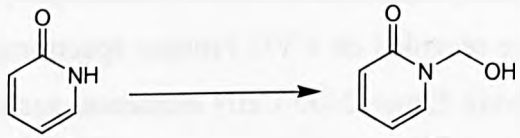

185 199

A solution of 2-pyridone **185** (2 g, 21 mmol), paraformaldehyde (1.26 g, 42 mmol), and K_2CO_3 (100 mg, 0.72 mmol) in distilled H_2O (10 mL) was sonicated and stirred under nitrogen. After 24 h the reaction mixture was concentrated *in vacuo* and the solid recrystalised from $CHCl_3$, affording *N*-CH_2OH-2-pyridone **199** as a cream coloured solid (2.19 g, 83%): ^{1}H NMR ($CDCl_3$, 250 MHz) δ 7.43 (ddd, *J* = 6.7, 2.1, 0.6 Hz, 1 H), 7.35 (ddd, *J* = 9.2, 6.7, 2.1 Hz, 1 H), 6.51 (ddd, *J* = 9.2, 1.2, 0.6 Hz, 1 H), 6.20 (ddd, *J* = 6.7, 6.7, 1.2 Hz, 1 H), 5.68 (s, 2 H), OH proton absent; ^{13}C NMR ($CDCl_3$, 63 MHz) δ 163.3, 140.9, 136.9, 120.8, 106.7,

74.1; MS (CI+) *m/z* 126 $(M + H)^+$, 113, 96, 67.

***1-Acetoxymethyl-1H-pyridin-2-one* (200).**

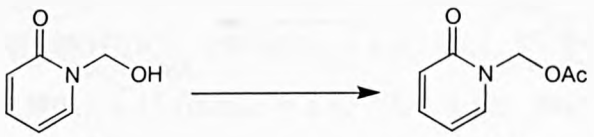

199 200

To a solution of *N*-CH_2OH-2-pyridone **199** (0.93 g, 9.7 mmol) and $Sc(OTf)_3$ (240 mg, 0.49 mmol) in MeCN (25 mL) was added Ac_2O (2.76 mL, 29.2 mmol), and the reaction stirred overnight at room temperature under nitrogen. The reaction mixture was evaporated to dryness, 0.1 M HCl (50 mL) added, and the aqueous phase extracted with CH_2Cl_2 (2 × 50 mL). The organic fractions were combined, washed with 0.1 M HCl (20 mL), dried ($MgSO_4$), and evaporated to dryness to afford *N*-CH_2OAc-2-pyridone **200** as a peach coloured oil (1.71 g, 95%) after flash chromatography (petrol/EtOAc 1:3): R_f = 0.76 (MeCN): ^1H NMR ($CDCl_3$, 250 MHz) δ 7.49 (ddd, *J* = 6.9, 2.1, 0.7 Hz, 1 H), 7.33 (ddd, *J* = 9.2, 6.7, 2.1 Hz, 1 H), 6.58 (ddd, *J* = 9.2, 1.5, 0.7 Hz, 1 H), 6.15 (ddd, *J* = 6.9, 6.7, 1.5 Hz, 1 H), 5.85 (s, 2 H), 2.12 (s, 3 H); ^{13}C NMR ($CDCl_3$, 63 MHz) δ 170.8, 162.5, 140.7, 138.1, 121.5, 106.1, 70.5, 20.7; IR ($CHCl_3$) 3009, 1745, 1670, 1604, 1543, 1368, 1245, 1179, 1151, 1028 cm^{-1}; MS (EI+) *m/z* 167 M^+, 137, 124, 108, 95; HRMS (EI+) calculated for $C_8H_9N_1O_3$ M^+ 167.0582, found 167.0579.

***3,7-Bis-hydroxymethyl-trans-3,7-diaza-tricyclo[4.2.2.2^{2,5}]dodeca-9,11-diene-4,8-dione* (196).**

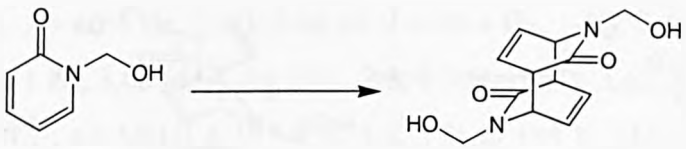

199 196

A solution of *N*-CH_2OH-2-pyridone **199** (9.2 g, 2.45 M) in MeOH (30 mL) in a Pyrex reaction vessel was irradiated with ultra-violet light (350 nm) over a period of 1 week, whereupon the *N*-CH_2OH photodimer **196** separated out of solution. The reaction mixture was periodically filtered and irradiation continued. The *N*-CH_2OH dimer was washed with MeOH and dried *in vacuo* to give a white solid (2.43 g, 27%): Elemental analysis, calculated for $C_{12}H_{14}N_2O_4$: C, 57.59; H, 5.64; N, 11.19%. Found C, 57.79; H, 5.56; N, 11.46%.

3,7-Bis-acetoxymethyl-trans-3,7-diaza-tricyclo[4.2.2.2^{2,5}]dodeca-9,11-diene-4,8-dione **(198).**

To a suspension of *N*-CH_2OH dimer **196** (500 mg, 2 mmol) and DMAP (24 mg, 0.2 mmol) in pyridine (10 mL) was added Ac_2O (0.57 mL, 6 mmol) and the reaction stirred overnight at room temperature under nitrogen. The pyridine was removed *in vacuo*, water added (20 mL), and the aqueous phase extracted with CH_2Cl_2 (5 × 20 mL). The organic fractions were combined, dried ($MgSO_4$), and evaporated to dryness to give clean *N*-CH_2OAc dimer **198** as a white solid (664 mg, 99%): ^1H NMR ($CDCl_3$, 250 MHz) δ 6.63 (ddd, *J* = 8.2, 6.7, 1.5 Hz, 2 H), 6.02 (ddd, *J* = 8.2, 7.0, 1.3 Hz, 2 H), 5.24 (d, *J* = 10.4 Hz, 2 H), 5.08 (d, *J* = 10.4 Hz, 2 H), 4.53 (ddd, *J* = 10.4, 6.7, 1.3 Hz, 2 H), 3.68 (ddd, *J* = 10.4, 7.0, 1.5 Hz, 2 H), 2.07 (s, 6 H); ^{13}C NMR ($CDCl_3$, 63 MHz) δ 174.9 (2 C), 171.2 (2 C), 134.6 (2 C), 130.6 (2 C), 70.4 (2 C), 57.1 (2 C), 50.1 (2 C), 20.8 (2 C); IR ($CHCl_3$) 1739, 1677, 1240, 1209, 1193, 1017 cm^{-1}; MS (CI+) *m/z* 335 $(M + H)^+$, 292, 275, 185, 168; HRMS (CI+) calculated for $C_{16}H_{19}N_2O_6$ $(M + H)^+$ 335.1243, found 335.1227; Elemental analysis, calculated for $C_{16}H_{18}N_2O_6$: C, 57.48; H, 5.43; N, 8.38%. Found C, 57.64; H, 5.48; N, 8.45%.

3-Acetoxymethyl-7-hydroxymethyl-trans-3,7-diaza-tricyclo[4.2.2.2^{2,5}]dodeca-9,11-diene-4,8-dione **(±)-(197) and** ***3-acetoxymethyl-trans-3,7-diaza-tricyclo[4.2.2.2^{2,5}]dodeca-9,11-diene-4,8-dione*** **(201).**

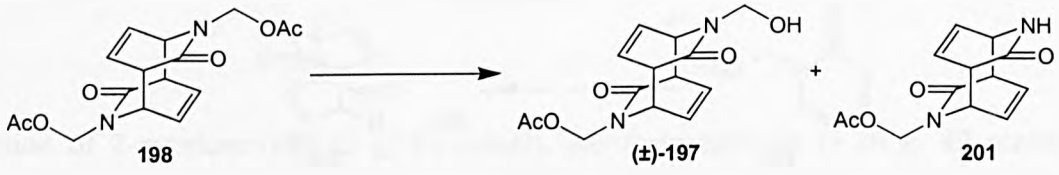

To a solution of *N*-CH_2OAc dimer **198** (100 mg, 0.3 mmol) in H_2O/THF (4 mL, 1:1) was added LiOH (13 mg, 0.3 mmol) and the reaction left to stir for 1 hour. The reaction mixture was then evaporated to dryness, water added (10 mL), and the aqueous phase extracted with CH_2Cl_2 (5 × 20 mL). The combined organic fractions were dried ($MgSO_4$) and evaporated to dryness. Flash chromatography, eluting with CH_2Cl_2/MeOH, 49:1 gave:

N-CH_2OAc dimer **198** as a white amorphous solid (23 mg, 23%): R_f = 0.61 (5% MeOH/EtOAc); analytical data as reported above.

N-CH_2OAc/*N*-CH_2OH dimer **(±)-197** as a white amorphous solid (19 mg, 22%): R_f = 0.25 (5% MeOH/EtOAc); ^{1}H NMR ($CDCl_3$, 250 MHz) δ 6.67 (ddd, *J* = 8.4, 6.6, 1.5 Hz, 1 H), 6.59 (ddd, *J* = 8.4, 6.9, 1.8 Hz, 1 H), 6.15 (ddd, *J* = 8.4, 7.3, 1.5 Hz, 1 H), 6.04 (ddd, *J* = 8.4, 6.9, 1.5 Hz, 1 H), 5.25 (d, *J* = 10.4 Hz, 1 H), 5.08 (d, *J* = 10.4 Hz, 1 H), 4.76 (d, *J* = 10.6 Hz, 1 H), 4.65 (d, *J* = 10.6, 1 H), 4.53 (ddd, *J* = 10.2, 7.0, 1.5 Hz, 1 H), 4.34 (ddd, *J* = 10.2, 6.9, 1.5 Hz, 1 H), 3.68 (ddd, *J* = 10.2, 6.9, 1.5 Hz, 1 H), 3.61 (ddd, *J* = 10.2, 6.9, 1.8 Hz, 1 H), 2.08 (s, 3 H), OH not present; ^{13}C NMR ($CDCl_3$, 63 MHz) δ 175.0, 171.1, 134.6, 133.8, 131.1, 130.6, 71.1, 70.2, 57.1, 55.8, 50.1, 49.9, 20.7; MS (CI+) *m/z* 293 $(M + H)^+$, 277, 203, 168, 96; HRMS (CI+) calculated for $C_{14}H_{17}N_2O_5$ $(M + H)^+$ 293.1137, found 293.1144.

The reaction was also performed with an alternative workup on a 51 mg scale. After stirring for 1 hour the solvents were evaporated off and the residue heated at 150°C under vacuum for 1 hour. Flash chromatography, eluting with a gradient of 1% to 7% MeOH/EtOAc gave:

N-CH_2OAc dimer **198** as a white amorphous solid (15 mg, 29%): R_f = 0.61 (5% MeOH/EtOAc); analytical data as reported above.

N-CH_2OAc/*N*-CH_2OH dimer **(±)-197** as a white amorphous solid (1 mg, 2%): R_f = 0.25 (5% MeOH/EtOAc); analytical data as reported above.

N-CH_2OAc/*N*-H dimer **201** as a white amorphous solid (10 mg, 25%): R_f = 0.17 (5% MeOH/EtOAc); ^{1}H NMR ($CDCl_3$, 250 MHz) δ 6.74 (ddd, *J* = 8.2, 6.7, 1.5 Hz, 1 H), 6.68-6.60 (m, 1 H), 6.37 (br d, 1 H), 6.13 (ddd, *J* = 8.6, 7.3, 1.5 Hz, 1 H), 6.05 (ddd, *J* = 8.2, 7.0, 1.2 Hz, 1 H), 5.26 (d, *J* = 10.4 Hz, 1 H), 5.08 (d, *J* = 10.4 Hz, 1 H), 4.51 (ddd, *J* = 10.1, 6.7, 1.5 Hz, 1 H), 4.24 (m, 1 H), 3.65 (ddd, *J* = 10.1, 7.0, 1.5 Hz, 1 H), 3.62-3.52 (m, 1 H), 2.07 (s, 3 H); ^{13}C NMR ($CDCl_3$, 63 MHz) δ 177.4, 175.5, 171.2, 135.7, 134.4, 130.9, 130.5, 70.4, 57.6, 51.6, 50.9, 50.4, 20.8; MS (ES+) *m/z* 285 $(M + Na)^+$; HRMS (ES+) calculated for $C_{13}H_{14}N_2O_4Na$ $(M + Na)^+$ 285.0851, found 285.0854.

Enzymatic hydrolysis of phenyl acetate.

Five reactions were performed, three containing lipases, one control containing no lipase, and one control containing no lipase with a drop of AcOH. To solutions of phenyl acetate (20 mg) in acetone/water (1:1, 1mL) were added lipase and the reactions stirred at room temperature for one hour. The reactions were monitored by TLC by comparison with an authentic sample of phenol. The products were not isolated due to their volatility.

Reaction	Lipase	Amount	Outcome
1	Porcine pancreatic lipase (2.55 U / mg)	5 mg	partial hydrolysis
2	Lipase from Pseudomonas cepacia (609 U / mg)	5 mg	complete hydrolysis
3	Lipase from Pseudomonas fluorescens (42.5 U / mg)	5 mg	complete hydrolysis
4	Control – no lipase	-	no hydrolysis
5	Control – no lipase and 1 drop of acetic acid	-	no hydrolysis

Enzymatic hydrolysis of *3,7-bis-acetoxymethyl-trans-3,7-diaza-tricyclo[4.2.2.2^{2,5}]dodeca-9,11-diene-4,8-dione* (198).

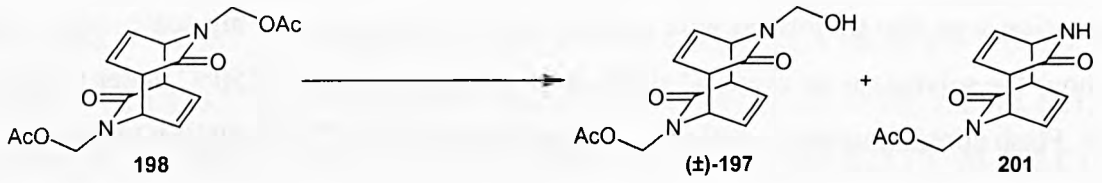

Six reactions were performed in a stem block, five containing lipases and one control reaction without lipase. To solutions of *N*-CH_2OAc dimer **198** in buffer (pH 7.2, 0.05 M)/acetone (1:1, 1mL) were added lipase and the reactions stirred for 1 day at room temperature. No reaction was observed by TLC so the reactions were heated to 35°C and stirred for a further 4 days. At this point, formation of the *N*-CH_2OAc/*N*-CH_2OH dimer **(±)-197** and *N*-CH_2OAc/*N*-H dimer **201** were observed in all six reactions, including the control, to equal extents (an estimated 50%).

Reaction	Lipase	Amount
1	Porcine liver esterase (PLE), suspension in 3.2 M $(NH_4)_2SO_4$ (19 mg protein / ml, 210 U / mg protein)	100 mg
2	Porcine pancreatic lipase (~23 mg protein, 61-200 U / mg protein)	8 mg
3	Pseudomonas fluorescens (31.5 U / mg)	6 mg
4	Candida antartica (3.3 U/ mg)	7.5 mg
5	'Amano' lipase PS (870 U / mg)	7.5 mg
6	Control – no lipase	-

***3,7-Dimethyl-trans-3,7-diazatricyclo[4.2.2.2^{2,5}]dodeca-9,11-diene-4,8-dione* (204).**[103]

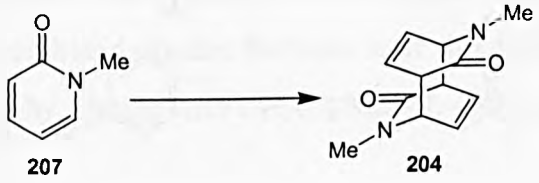

A solution of *N*-Me-2-pyridone **207** (28.5 g, 3 M) in degassed water (100 mL) in a Pyrex reaction vessel was irradiated with ultra-violet light (350 nm) for a period of 1 week. The solution was then extracted with $CHCl_3$ (3 × 100 mL), dried ($MgSO_4$), and evaporated to dryness. The crude product was recrystallised from EtOH/Et_2O to give *N*-Me dimer **204** as white 'needle-like' crystals (13.46 g, 41%): mp 221.1–222.4°C (*cf.* literature mp 222–222.5°C[103]); ^{1}H NMR ($CDCl_3$, 250 MHz) δ 6.61 (ddd, *J* 8.2, 6.7, 1.7 Hz, 2 H), 6.17 (ddd, *J* 8.2, 7.0, 1.3 Hz, 2 H), 3.96 (ddd, *J* 10.0, 6.7, 1.3 Hz, 2 H), 3.57 (ddd, *J* 10.0, 7.0, 1.7 Hz, 2 H), 2.78 (s, 6 H); ^{13}C NMR ($CDCl_3$, 63 MHz) δ 173.9 (2 C), 135.5 (2 C), 129.2 (2 C), 58.2 (2 C), 50.6 (2 C), 35.6 (2 C); IR ($CHCl_3$) 2990, 1661, 1650 cm^{-1}; MS (FAB+) *m/z* 437 $(2M + H)^+$, 391, 372, 328, 219 $(M + H)^+$.

***1-Benzyl-1H-pyridin-2-one* (208).[135]**

185 208

A mixture of 2-pyridone **185** (0.95 g, 10 mmol) and benzyl chloride (3.46 mL, 30 mmol) was subjected to microwave irradiation for 10 minutes, with the reaction mixture reaching a maximum temperature of 203°C. The excess benzyl chloride was evaporated off under the conditions of the reaction to give *N*-Bn-2-pyridone **208** as a yellow oil 1.85 g (100%): ^{1}H NMR ($CDCl_3$, 250 MHz) δ 7.35-7.22 (s, 7 H), 6.61 (ddd, *J* = 9.2, 1.2, 0.9 Hz, 1 H), 6.14 (ddd, *J* = 6.7, 6.7, 1.2 Hz, 1 H), 5.14 (s, 2 H); MS (FAB+) *m/z* 371 $(2M + H)^+$, 186 $(M + H)^+$.

***3,7-Dibenzyl-trans-3,7-diazatricyclo[4.2.2.2^{2,5}]dodeca-9,11-diene-4,8-dione* (209).**

208 209

A solution of *N*-Bn-2-pyridone **208** (771 mg) in MeOH (2.25 mL) in a Pyrex reaction vessel was irradiated with ultra-violet light (350 nm). After one day of irradiation, *N*-Bn photodimer **209** had separated out of solution as clear cubic crystals (344 mg, 43.4%): ^{1}H NMR ($CDCl_3$, 250 MHz) δ 7.30-7.22 (m, 6 H), 7.13-7.08 (m, 4 H), 6.51 (ddd, *J* = 8.2, 6.7, 1.5 Hz, 2 H), 6.02 (ddd, *J* = 8.2, 7.0, 1.2 Hz, 2 H), 5.08 (d, *J* = 15.0, 2 H), 3.99 (ddd, *J* = 10.1, 6.7, 1.2 Hz, 2 H),

3.57 (ddd, J = 10.1, 6.7, 1.5 Hz, 2 H), 3.56 (d, J = 15.0 Hz, 2 H); ^{13}C NMR ($CDCl_3$, 63 MHz) δ 173.9 (2 C), 136.0 (2 C), 135.0 (2 C), 130.3 (2 C), 128.8 (4 C), 128.0 (4 C), 127.7 (2 C), 55.1 (2 C), 50.6 (2 C), 50.3 (2 C); MS (FAB+) *m/z* 741 $(2M + H)^+$, 524, 460, 391, 371 $(M + H)^+$; HRMS (FAB+) calculated for $C_{24}H_{23}N_2O_2$ $(M + H)^+$ 371.1760, found 371.1757.

***1-Methoxymethyl-1H-pyridin-2-one* (210).**[220]

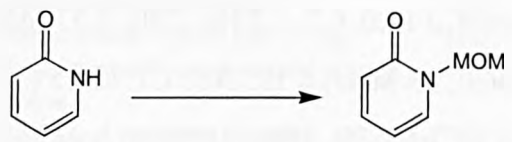

185 210

To a solution of 2-pyridone **185** (1 g, 10.5 mmol) in CH_2Cl_2 (50 mL) was added $^iPr_2EtN$ (1.83 mL, 21.1 mmol) followed by MOMCl (1.6 mL, 21.1 mmol) and stirred overnight, whereupon the solution turned from colourless to deep red/purple. The reaction mixture was evaporated to dryness, the residue partitioned between 0.2 M aqueous HCl (20 mL) and CH_2Cl_2 (30 mL), and the aqueous fraction extracted with CH_2Cl_2 (2 × 30 mL). The combined organic fractions were washed with 0.1 M HCl (20 mL), dried ($MgSO_4$) and concentrated *in vacuo* to give *N*-MOM-2-pyridone **210** as an orange/brown oil (1.37 g, 93%): R_f = 0.73 (10% H_2O/MeCN); ^{1}H NMR ($CDCl_3$, 250 MHz) δ 7.35 (ddd, J = 6.7, 2.1, 0.9 Hz, 1 H), 7.30 (ddd, J = 9.2, 6.7, 2.1 Hz, 1 H), 6.55 (ddd, J = 9.2, 1.2, 0.9 Hz, 1 H), 6.20 (ddd, J = 6.7, 6.7, 1.2 Hz, 1 H), 5.30 (s, 2 H), 3.35 (s, 3 H); MS (CI+) *m/z* 140 $(M + H)^+$, 124, 109, 96.

***3,7-Dimethoxymethyl-trans-3,7-diazatricyclo[4.2.2.2^{2,5}]dodeca-9,11-diene-4,8-dione* (211).**

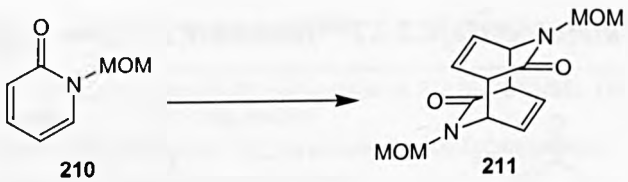

210 211

A solution of *N*-MOM-2-pyridone **210** (1.36 g, 9.75 mmol) in MeOH (2 mL) in a Pyrex reaction vessel was irradiated with ultra-violet light (350 nm) over a period of 2 weeks, whereupon the *N*-MOM dimer **211** separated out of solution. The reaction mixture was periodically filtered and irradiation continued. The *N*-MOM dimer was washed with MeOH and dried *in vacuo* to give white cubic crystals (482 mg, 36%): R_f = 0.47 (MeCN); ^{1}H NMR ($CDCl_3$, 250 MHz) δ 6.65 (ddd, J = 8.2, 6.7, 1.5 Hz, 2 H), 6.15 (ddd, J = 8.2, 7.0, 1.5 Hz, 2 H), 4.95 (d, J = 10.4 Hz, 2 H), 4.30 (ddd, J = 10.4, 6.7, 1.5 Hz, 2 H), 4.15 (d, J = 10.4 Hz, 2

H), 3.65 (ddd, J = 10.4, 7.0, 1.5 Hz, 2 H), 3.20 (s, 6 H); ^{13}C NMR ($CDCl_3$, 63 MHz) δ 175.0 (2 C), 134.3 (2 C), 130.9 (2 C), 77.3 (2 C), 56.3 (2 C), 54.1 (2 C), 50.1 (2 C); IR ($CHCl_3$) 3007, 1666, 1447, 1385, 1260, 1176, 1077 cm^{-1}; MS (CI+) *m/z* 279 $(M + H)^+$, 247, 140, 124, 109, 96; HRMS (CI+) calculated for $C_{14}H_{19}N_2O_4$ $(M + H)^+$ 279.1345, found 279.1335.

***3,7-Dimethoxymethyl-trans-3,7-diazatricyclo[4.2.2.2^{2,5}]dodeca-9,11-diene-4,8-dione* (211).**

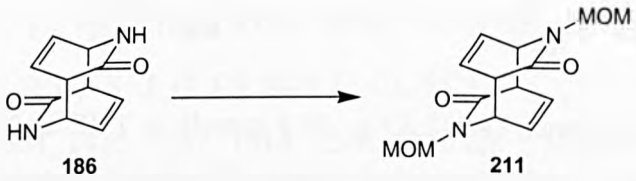

186 211

To a suspension of *N*-H dimer **186** (100 mg, 0.53 mmol) in CH_2Cl_2 (5 mL) was added $^iPr_2EtN$ (1.09 mL, 6.26 mmol) followed by MOMCl (0.42 mL, 5.47 mmol) and stirred overnight, whereupon the suspension turned from white to orange/brown. The reaction mixture was evaporated to dryness, the residue partitioned between 0.1 M aqueous HCl (20 mL) and $CHCl_3$ (30 mL), and the aqueous phase extracted with $CHCl_3$ (2 × 30 mL). The combined organic fractions were dried ($MgSO_4$) and concentrated *in vacuo* to yield *N*-MOM dimer **211** as white cubic crystals (36 mg, 25%): R_f = 0.47 (MeCN); analytical data as reported above.

DIBAL reduction of *3,7-dimethoxymethyl-trans-3,7-diazatricyclo[4.2.2.2^{2,5}]dodeca-9,11-diene-4,8-dione* (211).

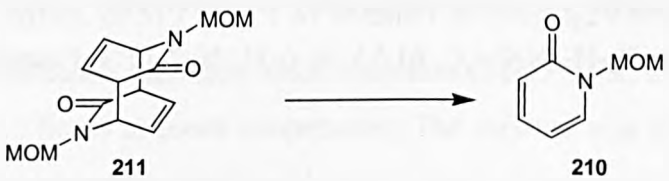

211 210

To a solution of *N*-MOM dimer **211** (100 mg, 0.36 mmol) in CH_2Cl_2 (5 mL) at room temperature under nitrogen was added DIBAL (1.8 mL, 1 M solution in toluene, 1.80 mmol) for 1 hour, during which the reaction turned from colourless to red. The reaction was quenched by adding saturated KOAc solution (3 mL) and saturated NH_4Cl/CH_2Cl_2 solution (1:3, 25 mL) and stirring for 30 minutes, whereupon the mixture was filtered through Celite and the aqueous phase extracted with CH_2Cl_2 (3 × 10 mL). The combined organic fractions were washed with saturated NH_4Cl solution (10 mL), dried ($MgSO_4$), and evaporated to dryness to give the red/brown oil of *N*-MOM-2-pyridone **210** (101 mg, 100%): R_f = 0.50

(MeCN); analytical data as reported above.

***3,7-Di-tert-butoxycarbonyl-trans-3,7-diazatricyclo[4.2.2.2^{2,5}]dodeca-9,11-diene-4,8-dione* (213).**

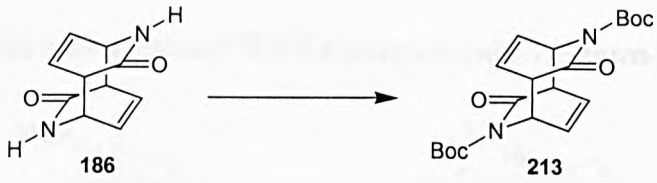

To a suspension of *N*-H dimer **186** (2.83 g, 14.9 mmol) in THF at 0°C under nitrogen was added ^{n}BuLi (13.11 mL, 2.5 M solution in hexanes, 32.8 mmol) and the reaction stirred for 30 minutes, whereupon Boc_2O (8.55 mL, 37.2 mmol) was added. The reaction was stirred for 2 days at room temperature, during which the white suspension turned to a peach colour. The solvent was evaporated off and the residue partitioned between CH_2Cl_2 (200 mL) and water (100 mL), and the aqueous phase extracted with CH_2Cl_2 (2 × 100 mL). The combined organic fractions were dried ($MgSO_4$) and evaporated to dryness to give an oily yellow solid which was recrystallised from ^{i}PrOH affording *N*-Boc dimer **213** as a white solid (4.60 g, 80%), R_f = 0.17 (petrol/EtOAc, 3:1): ^{1}H NMR ($CDCl_3$, 250 MHz) δ 6.55 (ddd, J = 8.2, 7.0, 1.5 Hz, 2 H), 6.10 (ddd, J = 8.2, 7.2, 1.5 Hz, 2 H), 4.95 (ddd, J = 10.4, 7.0, 1.5 Hz, 2 H), 3.75 (ddd, J = 10.4, 7.2, 1.5 Hz, 2 H), 1.45 (s, 18 H); ^{13}C NMR ($CDCl_3$, 63 MHz) δ 171.5 (2 C), 151.4 (2 C), 133.9 (2 C), 130.8 (2 C), 84.0 (2 C), 53.5 (2 C), 52.7 (2 C), 28.0 (6 C); IR ($CHCl_3$) 2984, 1773, 1720, 1389, 1371, 1297, 1245, 1149 cm^{-1}; MS (CI+) *m/z* 391 $(M + N)^+$, 314, 285, 276, 96; HRMS (CI+) calculated for $C_{20}H_{27}N_2O_6$ $(M + H)^+$ 391.1869, found 391.1858.; Elemental analysis, calculated for $C_{20}H_{26}N_2O_6$: C, 61.53; H, 6.71; N, 7.17%. Found C, 61.42; H, 6.75; N, 7.11%.

***3,7-Di-tert-butoxycarbonyl-4,8-dihydroxy-trans-3,7-diazatricyclo[4.2.2.2^{2,5}]dodeca-9,11-diene* (215).**

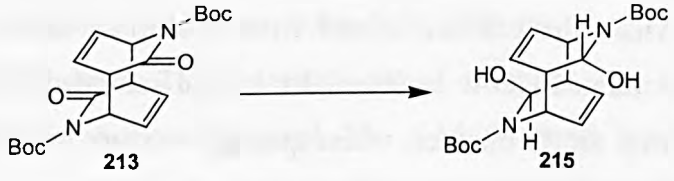

To a solution of *N*-Boc dimer **213** (300 mg, 0.77 mmol) in CH_2Cl_2 (10 mL) at room temperature under nitrogen was added DIBAL (1.92 mL, 1 M solution in CH_2Cl_2, 1.92

mmol). The reaction was stirred for 10 minutes before 10% aqueous citric acid solution (10 mL) was added. The aqueous phase was extracted with CH_2Cl_2 (3 × 20 mL), and the combined organic fractions dried ($MgSO_4$) and evaporated to dryness to give *N*-Boc dilactamol **215** as a white solid (222 mg, 73%), %), R_f = 0.75 (petrol/EtOAc, 3:1): ^{1}H NMR ($CDCl_3$, 250 MHz) δ 6.55 (ddd, *J* = 8.6, 7.3, 1.2 Hz, 2 H), 5.90 (dd, *J* = 8.6, 8.2 Hz, 2 H), 5.55 (d, *J* = 1.8 Hz, 2 H), 5.30 (dd, *J* = 3.7, 1.8 Hz, 2 H), 4.8 (dd, *J* = 9.8, 7.3 Hz, 2 H), 3.10 (dddd, *J* = 9.8, 8.2, 3.7, 1.2 Hz, 2 H), 1.45 (s, 18 H); ^{13}C NMR ($CDCl_3$, 63 MHz) δ 155.2 (2 C), 135.8 (2 C), 126.8 (2 C), 81.8 (2 C), 80.6 (2 C), 55.3 (2 C), 42.9 (2 C), 28.5 (6 C); IR ($CHCl_3$) 3429, 2980, 1661, 1415, 1337, 1314, 1240, 1170 cm^{-1}; MS (CI+, NH_3) *m/z* 412 $(M + NH_4)^+$, 395 $(M + H)^+$, 377, 356, 340; HRMS (CI+) calculated for $C_{20}H_{31}N_2O_6$ $(M + H)^+$ 395.2182, found 395.2194.

***3,7-Di-tert-butoxycarbonyl-4,8-dihydroxy-trans-3,7-diazatricyclo[4.2.2.2^{2,5}]dodeca-9,11-diene* (215), *3,7-di-tert-butoxycarbonyl-4-hydroxy-8-oxo-trans-3,7-diazatricyclo[4.2.2.2^{2,5}] dodeca-9,11-diene* (±)-(214), and *3-tert-butoxycarbonyl-3,7-diazatricyclo[4.2.2.2^{2,5}] dodeca-9,11-diene-4,8-dione* (221).**

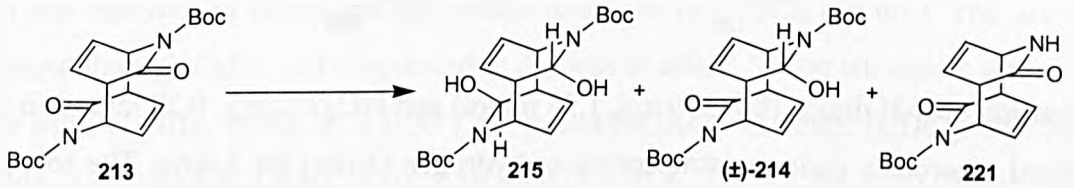

To a solution of *N*-Boc dimer **213** (200mg, 0.51 mmol) in CH_2Cl_2 (10 mL) at –78°C under nitrogen was added DIBAL (0.513 mL, 1 M solution in CH_2Cl_2, 0.51 mmol). The reaction stirred for 3 hours, whereupon saturated NH_4Cl solution/CH_2Cl_2 (1:2, 30 mL) was added and the mixture tirred for 3 hours at room temperature. The mixture was filtered through Celite and the aqueous phase extracted with CH_2Cl_2 (4 × 20 mL). The combined organic fractions were dried ($MgSO_4$) and evaporated to dryness to give 193 mg of crude residue. Flash chromatography, eluting with a gradient of 8:8:1 to 5:5:1 CH_2Cl_2/petrol/EtOAc then 10% MeOH/EtOAc gave:

N-Boc dilactamol **215** as a white solid (28 mg, 14%), R_f = 0.72 (petrol/EtOAc, 3:1): analytical data as reported above.

N-Boc monolactamol **(±)-214** as a white solid (17 mg, 9%), R_f = 0.33 (petrol/EtOAc, 3:1): ^{1}H NMR ($CDCl_3$, 250 MHz) δ 6.69 (ddd, *J* = 6.9, 6.6, 1.8 Hz, 1 H), 6.40 (ddd, *J* = 8.8, 7.0, 1.5

Hz, 1 H), 6.04 (dd, J = 8.4, 8.0 Hz, 1 H), 5.90 (ddd, J = 8.0, 7.3, 1.1 Hz, 1 H), 5.66 (d, J = 1.5 Hz, 1 H), 5.25 (dd, J = 3.7, 1.5 Hz, 1 H), 4.88 (dd, J = 9.9, 7.3 Hz, 1 H), 3.61 (ddd, J = 10.2, 7.3, 1.8 Hz, 1 H), 3.36 (dddd, J = 10.0, 8.0, 3.7, 1.1 Hz, 1 H), 1.51 (s, 9 H), 1.45 (s, 9 H), OH proton absent; ^{13}C NMR ($CDCl_3$, 63 MHz) δ 173.0, 151.3 (2 C), 136.8, 132.8, 130.1, 126.1, 83.0, 81.3, 79.9, 56.2, 54.1, 53.3, 43.7, 28.2 (3 C), 27.9 (3 C); IR ($CHCl_3$) 3436, 2982, 2249, 1770, 1711, 1667, 1370, 1252, 1154 cm^{-1}; MS (CI+, NH_3) *m/z* 393 $(M + H)^+$, 377, 354, 293, 180, 96; HRMS (CI+) calculated for $C_{20}H_{29}N_2O_6$ $(M + H)^+$ 393.2026, found 393.2014.

N-Boc dimer **213** as a white solid (139 mg, 70%), R_f = 0.22 (petrol/EtOAc, 3:1): analytical data as reported above.

N-Boc/*N*-H dimer **221** as a white solid (traces), R_f = 0.05 (petrol/EtOAc, 3:1): analytical data as reported above.

***Trans-3,7-diazatricyclo[4.2.2.2^{2,5}]dodeca-4,8-dione* (228).[103]**

A suspension of *N*-H dimer **186** (300 mg, 1.58 mmol) and PtO_2 (72 mg, 0.32 mmol) in EtOAc was stirred vigorously under an atmosphere of hydrogen (3 bar) for 2 days. The solvent was evaporated off affording 359 mg of crude solid which was recrystallised from glacial AcOH to give 128 mg of a 5:1 mixture of *N*-H tetrahydro dimer **228** and *N*-H dimer **186**.

N-H dimer **186**, R_f = 0.37 (10% H_2O/MeCN): analytical data as reported above.

N-H tetrahydro dimer **228**, R_f = 0.24 (10% H_2O/MeCN): ^{1}H NMR ($CDCl_3$, 250 MHz) δ 3.86 (dd, J = 11.3, 6.2 Hz, 2 H), 2.71 (ddd, J = 11.0, 5.5, 1.5 Hz, 2 H), 1.55-2.08 (m, 8 H).

***3,7-Di-tert-butoxycarbonyl-trans-3,7-diazatricyclo[4.2.2.2^{2,5}]dodeca-4,8-dione* (227).**

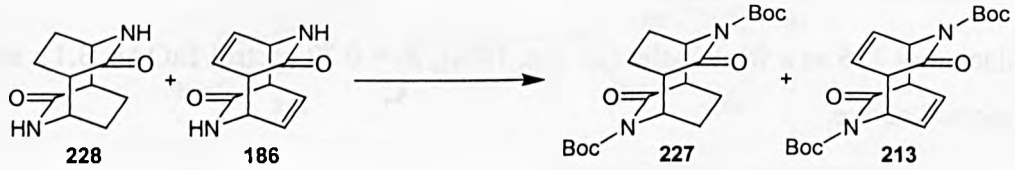

A suspension of crude *N*-H tetrahydro dimer **228** (300 mg, 1.55 mmol) containing a small

amount of *N*-H dimer **186** in MeCN (15 mL) at room temperature under nitrogen was treated with DMAP (396 mg, 3.25 mmol), followed by three portions of Boc_2O (2.13 mL, 9.28 mmol) at periodic intervals (3 eq at 0 h, 1.5 eq at 8 h, and 1.5 eq 24 h) with rapid stirring. After 2 days the solvent was evaporated off and the residue partitioned between $CHCl_3$ (20 mL) and 0.1 M aqueous HCl (20 mL). The aqueous phase was extracted with $CHCl_3$ (3 × 20 mL) and the combined organic fractions dried ($MgSO_4$) and evaporated to dryness, to give a light red solid which was washed with MeOH and dried *in vacuo* to yield 264 mg of a 3:1 mixture of *N*-Boc tetrahydro dimer **227** and *N*-Boc dimer **213**.

***3,7-Di-tert-butoxycarbonyl-trans-3,7-diazatricyclo[4.2.2.2^{2,5}]dodeca -4,8-dione* (227).**

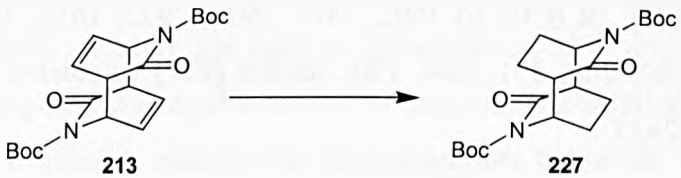

A vigorously stirred suspension of *N*-Boc dimer **213** (1 g, 2.56 mmol) and PtO_2 (116 mg, 0.51 mmol) in EtOAc (30 mL) was subjected to an atmosphere of hydrogen (3 bar) for 2 days. The solvent was removed *in vacuo* and the residue dissolved in CH_2Cl_2 (30 mL). The suspension was filtered through Celite and evaporated to dryness to afford *N*-Boc tetrahydro dimer **227** as a white solid (1.001g, 99%), R_f = 0.39 (2:1, petrol/EtOAc): ^{1}H NMR ($CDCl_3$, 250 MHz) δ 4.90 (ddd, *J* = 11.6, 5.2, 2.4 Hz, 2 H), 3.16 (ddd, *J* = 11.6, 3.7, 3.4 Hz, 2 H), 2.10-1.99 (m, 4 H), 1.94-1.83 (m, 4 H), 1.52 (s, 18 H); ^{13}C NMR ($CDCl_3$, 63 MHz) δ 173.1 (2 C), 152.0 (2 C), 84.0 (2 C), 51.9 (2 C), 47.9 (2 C), 28.0 (6 C), 24.1 (2 C), 19.9 (2 C); IR ($CHCl_3$) 2985, 1766, 1720, 1287, 1250, 1145 cm^{-1}; MS (CI+) *m/z* 395 $(M + H)^+$, 383, 366, 295, 279, 195; HRMS (CI+) calculated for $C_{20}H_{31}N_2O_6$ $(M + H)^+$ 395.2182, found 395.2173.

***3,7-Di-tert-butoxycarbonyl-4,8-dihydroxy-trans-3,7-diazatricyclo[4.2.2.2^{2,5}]dodecane* (230), *3,7-di-tert-butoxycarbonyl-4-hydroxy-trans-3,7-diazatricyclo[4.2.2.2^{2,5}]dodecane* (±)-(229), *3-tert-butoxycarbonyl-trans-3,7-diazatricyclo[4.2.2.2^{2,5}]dodeca-4,8-dione* (231), and *3-di-tert-butoxycarbonyl-4-hydroxy-trans-3,7-diazatricyclo[4.2.2.2^{2,5}]dodecane* (232).**

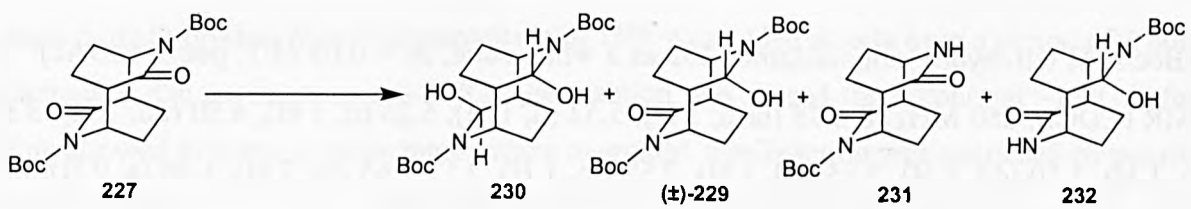

To a solution of *N*-Boc tetrahydro dimer **227** (200 mg, 0.51 mmol) in CH_2Cl_2 (10 mL) at –78°C under nitrogen was added DIBAL (1.015 mL, 1 M solution in CH_2Cl_2, 1.02 mmol). The reaction was stirred for 1.5 hours, whereupon saturated NH_4Cl solution/CH_2Cl_2 (1:2, 30 mL) was added and the mixture stirred for 1 hour at room temperature. The aqueous phase was extracted with CH_2Cl_2 (5 × 20 mL) and the combined organic fractions dried ($MgSO_4$) and evaporated to dryness to give 190 mg of crude products. Flash chromatography, eluting with 30:1 CH_2Cl_2/EtOAc, gave:

N-Boc tetrahydro dilactamol **230** as a white solid, R_f = 0.61 (4:1, petrol/EtOAc): ^{1}H NMR ($CDCl_3$, 250 MHz) δ 5.43 (d, *J* = 2.2 Hz, 2 H), 5.31 (dd, *J* = 3.3, 2.6 Hz, 2 H), 4.37 (ddd, *J* = 11.0, 5.5, 1.5 Hz, 2 H), 2.86-2.99 (m, 2 H), 2.41-2.52 (m, 2 H), 1.83-1.97 (m, 2 H), 1.52-1.67 (m, 4 H), 1.46 (s, 18 H); IR ($CHCl_3$) 3692, 3497, 2979, 2932, 1656, 1414, 1336 cm^{-1}; MS (EI+) *m/z* 398 M^+, 280, 268, 251, 224, 180; HRMS (EI+) calculated for $C_{20}H_{34}N_2O_6$ M^+ 398.2417, found 398.2423.

N-Boc tetrahydro monolactamol **(±)-229** as a white solid, R_f = 0.29 (4:1, petrol/EtOAc): ^{1}H NMR ($CDCl_3$, 250 MHz) δ 5.46 (d, *J* = 2.2 Hz, 1 H), 5.25 (dd, *J* = 2.9, 2.6 Hz, 1 H), 4.74-4.83 (m, 1 H), 4.47 (dd, *J* = 5.5, 11.0 Hz, 1 H), 2.98-3.19 (m, 2 H), 2.60-2.71 (m, 1 H), 1.63-2.01 (m, 7 H), 1.56 (s, 9 H), 1.53 (s, 9 H); ^{13}C NMR ($CDCl_3$, 63 MHz) δ 174.5, 156.6, 151.8, 83.0, 81.3, 80.8, 52.5, 50.5, 48.2, 37.4, 28.2 (3 C), 27.9 (3 C), 23.8, 23.0, 21.1, 20.4; IR ($CHCl_3$) 3690, 3506, 2981, 1764, 1712, 1665, 1294, 1149 cm^{-1}; MS (EI+) *m/z* 396 M^+, 296, 267, 196, 179, 151; HRMS (EI+) calculated for $C_{20}H_{32}N_2O_6$ M^+ 396.2260, found 396.2279. Elemental analysis, calculated for $C_{20}H_{32}N_2O_6$: C, 60.59; H, 8.13; N, 7.06%. Found C, 60.38; H, 8.07; N, 6.83%.

N-Boc tetrahydro dimer **227** as a white solid, R_f = 0.16 (4:1, petrol/EtOAc): analytical data as reported above.

N-Boc/*N*-H tetrahydro dimer **231** as a white solid, R_f = 0.05 (4:1, petrol/EtOAc): ^{1}H NMR ($CDCl_3$, 250 MHz) δ 6.40-6.50 (br d, *J* = 5.8 Hz, 1 H), 4.93 (dd, *J* = 11.3, 5.8 Hz, 1 H), 3.88-3.99 (m, 1 H), 2.98-3.12 (m, 2 H), 1.85-3.12 (m, 8 H), 1.55 (s, 9 H); MS (TSP+) *m/z* 295 $(M + H)^+$, 195; HRMS (ES+) calculated for $C_{15}H_{22}N_2O_4Na$ $(M + Na)^+$ 317.1477, found 317.1463.

N-Boc/*N*-H tetrahydro monolactamol **232** as a white solid, R_f = 0.05 (4:1, petrol/EtOAc): ^{1}H NMR ($CDCl_3$, 250 MHz) δ 6.75 (br d, 1 H), 5.52 (d, 1 H), 5.25 (d, 1 H), 4.50 (dd, 1 H), 3.82 (m, 1 H), 3.10 (dd, 1 H), 2.85 (dd, 1 H), 2.52 (m, 1 H), 2.13-1.65 (m, 7 H), 1.46 (s, 9 H); MS (TS+) *m/z* 297 $(M + H)^+$, 268, 254, 197.

***(S)-Proline-N-carboxyanhydride* (234).[150]**

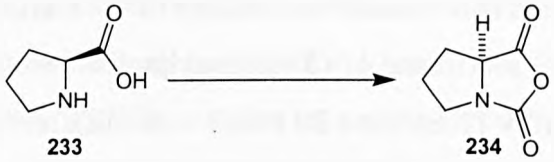

A three necked 500 mL round-bottomed flask was fitted with a nitrogen inlet tube, a thermometer, a pressure-equalising dropping funnel and a magnetic stirrer bar. The apparatus was flushed with nitrogen and charged with (*S*)-proline **233** (10 g, 86.9 mmol) and THF (100 mL) and the suspension cooled to 15°C. Phosgene (54 mL, 104.2 mmol) was added via the pressure equalising dropping funnel over a period of 20 minutes, maintaining the temperature below 20 °C. The reaction mixture was aged for 30 minutes at 35°C until the suspension went homogeneous, whereupon it was aged a further 30 minutes. The solution was concentrated to 13 mL under reduced pressure, maintaining the temperature below 20 °C, to remove excess phosgene and HCl. THF (100mL) was added and the solution cooled to 0°C. Et_3N (12.1 mL, 86.9 mmol) was added over a period of 20 minutes and the solution was aged for a further 30 minutes at 0-5°C whereupon a white precipitate of Et_3NCl was observed. The suspension was then filtered into a 250 mL pressure-equalising dropping funnel via a Schlenk funnel. The Et_3NCl cake was washed with THF (3 × 20 mL), and the filtrate and washes in the 250 mL pressure-equalising dropping funnel were used for the next step.

***Diphenylprolinol* (224).[150]**

A three-necked 500 mL round-bottomed flask was fitted with a nitrogen inlet tube, a thermometer, a magnetic stirrer bar, and a pressure-equalising dropping funnel containing (*S*)-proline-*N*-carboxyanhydride **234** in THF. The reaction vessel was flushed with nitrogen and charged with PhMgCl (133 mL, 2 M solution in THF, 266 mmol) and cooled to –10°C. The solution of (*S*)-proline-*N*-carboxyanhydride in THF was added slowly over a period of 1 hour, maintaining the temperature at –10°C. The reaction was stirred for 3 hours at –15°C before being allowed to warm to room temperature overnight. The reaction was quenched by pouring into 2 M H_2SO_4 (175 mL, 0.348 mmol) solution at 0°C over a period of 30 minutes. The

mixture was aged for 1 hour at 0-5°C whereupon a white precipitate of $MgSO_4$ was formed which was filtered off and the $MgSO_4$ cake washed with THF (3 × 85 mL). The filtrate and washings were combined and concentrated to a volume of ~166 mL and the mixture cooled to 0°C for 1 hour. The white precipitate of (*S*)-diphenylprolinol sulfate was then filtered off, washed with water at 5°C (2 × 17 mL) and EtOAc (3 × 30 mL), and dried *in vacuo*.

A two-necked 250 mL round-bottomed flask was fitted with a nitrogen inlet tube, a thermometer, and a magnetic stirrer bar. To the reaction vessel was added (*S*)-diphenylprolinol sulfate, THF (18.5 mL), and 2 M NaOH (18.5 mL) and the mixture was stirred at room temperature for 30 minutes until everything had dissolved. Then toluene (76 mL) was added and the mixture was aged for 30 minutes, whereupon the two-phase mixture was filtered through a sinter and partitioned. The organic phase was washed with water (10 mL) and evaporated to dryness to give an oil which crystallised on standing at room temperature to give diphenylprolinol **224** as light-tan crystals (5.08 g). Recrystallisation from a small volume of hexane afforded clean diphenylprolinol (4.17 g, 19% from (*S*)-proline **233**).

***3,3-Diphenyl-1-methyl-tetrahydro-pyrrolo[1,2-c][1,3,2]oxazaborole-borane complex* (236).**[150]

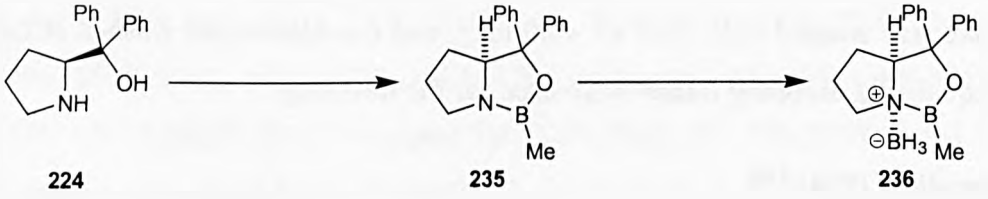

224 **235** **236**

A two-necked 100 mL round-bottomed flask was fitted with a nitrogen inlet tube with a teflon tap, a one-piece distillation head, and a magnetic stirrer bar. The flask was charged with (*S*)-diphenylprolinol **224** (3.513 g, 13.9 mmol) and xylene (17 mL). To the vigorously stirred solution at room temperature was added trimethylboroxine (1.494 mL, 10.7 mmol) in THF (1.5 mL) dropwise over a period of 10 minutes. At this point an exothermic reaction occurred and a precipitate of bismethylboronic acid was observed. The mixture was stirred for 30 minutes and heated and concentrated by distillation to a volume of ~8 mL. The mixture was cooled, xylenes added (17 mL) and removed by distillation once more to give an oil, which was heated to 170°C for 30 minutes then cooled to room temperature. The oil was diluted with xylenes (8 mL). At this point the distillation head was replaced with a sinter funnel, and a pressure-equalising dropping funnel was attached between the round-bottomed flask and the nitrogen inlet tube. To the stirred solution was added BH_3.DMS (1.397 mL, 14.7 mmol) over

a five minute period via syringe, and the mixture was stirred for 30 minutes. The mixture was slowly diluted with hexane and the reaction stirred at room temperature overnight, and the *B*-Me CBS·BH_3 complex **236** crystallised out of solution. The apparatus was inverted and the white precipitate filtered, washed with hexane (3 × 10 mL) and dried over a gentle flow of nitrogen to afford the *B*-Me CBS·BH_3 complex as a white crystalline solid (2.92 g, 72%): ^{1}H NMR ($CDCl_3$, 250 MHz) δ 7.50 (m, 2 H), 7.20-7.40 (m, 8 H), 4.60 (m, 1 H), 3.35 (m, 1 H), 3.20 (m, 1 H), 1.90 (m, 1 H), 1.60 (m, 1 H), 1.30 (m, 2 H), 0.70 (s, 3 H).

***(R)-1-Phenyl-ethanol* (238).[149]**

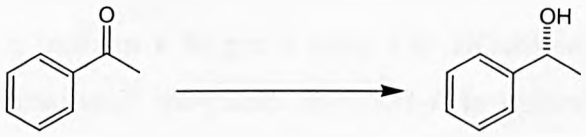

237 238

To a solution of *B*-Me CBS.BH_3 (12.5 mg, 0.04 mmol) and BH_3.DMS (0.024 mL, 0.26 mmol) in CH_2Cl_2 (5 mL) at room temperature under nitrogen was added acetophenone **237** (0.05 mL, 0.43 mmol). The reaction was stirred for 55 minutes before being quenched with MeOH (0.5 mL), stirred for 1.5 hours, and evaporated down. Flash chromatography, eluting with CH_2Cl_2, gave (*R*)-1-phenyl-ethanol **238** as a colourless oil (quantitative). ^{1}H NMR ($CDCl_3$, 250 MHz) δ 7.25-7.40 (m, 5 H), 4.90 (qd, J = 6.4, 1.8 Hz, 1 H), 1.99 (d, J = 1.8 Hz, 1 H), 1.49 (d, J = 6.4 Hz, 3 H); Chiral HPLC [Daicel Chiralcel OD (4.6 × 25 cm), eluting with 90:10 hexane/^{i}PrOH, 10°C, 0.5 mL min^{-1}, retention times of enantiomers: (a) 15.2 min, (b) 17.4 min] showed the alcohol to have a 94.7% ee of the (a) enantiomer.

Reduction of *N-Boc tetrahydro dimer* (227) with borane.

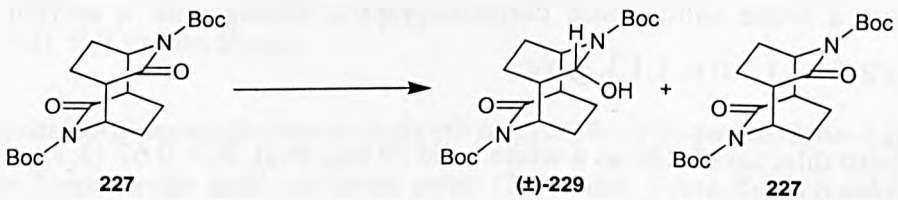

227 (±)-229 227

To a solution of *N*-Boc tetrahydro dimer **227** (100 mg, 0.25 mmol) in CH_2Cl_2 (10 mL) at room temperature under nitrogen was added BH_3·DMS (0.029 mL, 0.30 mmol) and the reaction stirred for 22 hours. The reaction was quenched by adding MeOH (0.5 mL) and stirring for 30 minutes. The solvents were removed *in vacuo*, MeOH (10 mL) added, and refluxed for 30 minutes. The solution was then evaporated to dryness to give a white solid.

Flash chromatography, eluting with a solvent gradient of CH_2Cl_2/petrol/EtOAc 1:1:0 to 5:5:2, gave:

N-Boc tetrahydro monolactamol **(±)-229** as a white solid (16 mg, 16%), R_f = 0.39 (3:1, petrol/EtOAc): analytical data as reported above. Chiral HPLC [Column: Chiralcel OD (25 × 0.46 cm), eluting with 99.2:0.8 hexane/^{i}PrOH, 1.0 mL min^{-1}, 40°C, UV detection at 225 nm] showed the monolactamol to be racemic.

N-Boc tetrahydro dimer **227** as a white solid (75 mg, 75%), R_f = 0.24 (3:1, petrol/EtOAc): analytical data as reported above.

Column flush with EtOAc/MeOH, 9:1 gave 6 mg of a mixture of *N*-Boc/*N*-H tetrahydro dimer **231** and a small amount of *N*-Boc/*N*-H tetrahydro monolactamol **232**, analytical data for both compounds as reported above.

Reduction of *N*-Boc tetrahydro dimer (227) with *B*-Me CBS·BH_3.

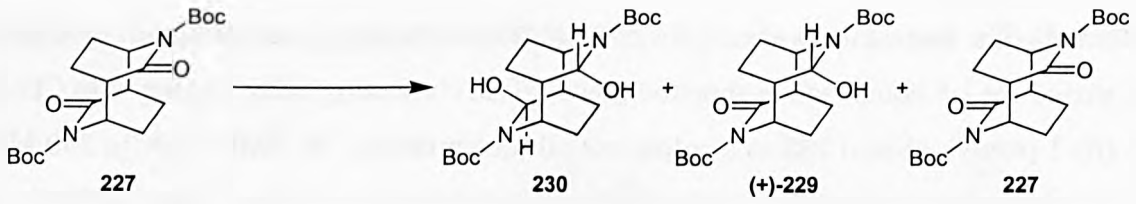

To a solution of *N*-Boc tetrahydro dimer **227** (100 mg, 0.25 mmol) and *B*-Me CBS·BH_3 (37 mg, 0.13 mmol) in CH_2Cl_2 (10 mL) at room temperature under nitrogen was added BH_3·DMS (0.012 mL, 0.13 mmol) and the reaction stirred for 22 hours. The reaction was quenched by adding MeOH (0.5 mL) and stirring for 30 minutes. The solvents were removed *in vacuo*, MeOH (10 mL) added, and refluxed for 30 minutes. The solution was then evaporated to dryness to give a white solid. Flash chromatography, eluting with a solvent gradient of CH_2Cl_2/petrol/EtOAc 1:1:0 to 1:1:1, gave:

N-Boc tetrahydro dilactamol **230** as a white solid (9 mg, 9%), R_f = 0.67 (3:1, petrol/EtOAc): analytical data as reported above.

N-Boc tetrahydro monolactamol **(+)-229** as a white solid (76 mg, 76%), R_f = 0.39 (3:1, petrol/EtOAc): Chiral HPLC [Column: Chiralcel OD (25 × 0.46 cm), eluting with 99.2:0.8 hexane ^{i}PrOH, 1.0 mL min^{-1}, 40°C, UV detection at 225 nm] showed the monolactamol to have an ee of ≥97%; $[\alpha]_D$ +8.0, $[\alpha]_{365}$ +90.2 (c = 0.5, $CHCl_3$); analytical data as reported

above.

N-Boc tetrahydro dimer **227** as a white solid (6 mg, 6%), R_f = 0.24 (3:1, petrol/EtOAc): analytical data as reported above.

Column flush with 10% MeOH/EtOAc gave 7 mg of a mixture of *N*-Boc/*N*-H tetrahydro dimer **231** and *N*-Boc/*N*-H tetrahydro monolactamol **232**, analytical data for both compounds as reported above.

(+)-Camphorsulfonyl protection of *N-Boc tetrahydro monolactamol* (+)-(229).

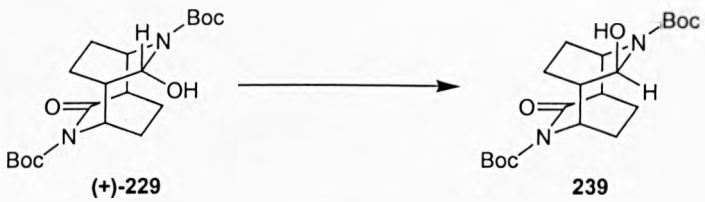

(+)-229 239

A solution of *N*-Boc tetrahydro monolactamol **(+)-229** (50 mg, 0.13 mmol), (+)-camphorsulfonyl chloride (48 mg, 0.19 mmol), and DMAP (31 mg, 0.25 mmol) in MeCN (10 mL) under nitrogen was refluxed for 2 days. The solvent was removed *in vacuo* to give a crude residue. Flash chromatography, eluting with a solvent gradient of CH_2Cl_2/EtOAc 19:1 to 5:1, gave:

N-Boc tetrahydro monolactamol **(+)-229** as a white solid (2 mg, 4%): R_f = 0.42 (CH_2Cl_2/EtOAc, 9:1); analytical data as previously reported.

N-Boc tetrahydro monolactamol epimer **239** as a white solid (13 mg, 26%): R_f = 0.15 (CH_2Cl_2/EtOAc, 9:1); ^{1}H NMR ($CDCl_3$, 250 MHz) δ 5.58-5.63 (br s, 1 H), 4.77-4.89 (m, 1 H), 4.31-4.40 (m, 1 H), 2.91-3.00 (m, 1 H), 2.62-2.72 (m, 1 H), 1.69-2.18 (m, 8 H), 1.52 (s, 9 H), 1.46 (s, 9 H), OH proton absent.

***2-tert-Butoxycarbonylamino-8-oxo-cis-5-menthyloxycarbonyloxymethylene-7-aza-bicyclo [4.2.2]decane-7-carboxylic acid tert-butyl ester* (241) and *2-tert-Butoxycarbonylamino-8-oxo-trans-5-menthyloxycarbonyloxymethylene-7-aza-bicyclo[4.2.2]decane-7-carboxylic acid tert-butyl ester* (242).**

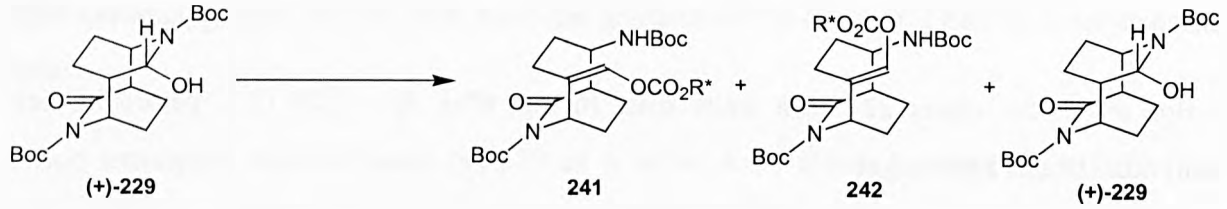

A solution of *N*-Boc tetrahydro monolactamol **(+)-229** (50 mg, 0.13 mmol), (*R*)-menthylchloroformate (0.054 mL, 0.25 mmol), and DMAP (31 mg, 0.25 mmol) in MeCN (2 mL) under nitrogen was refluxed for 2 days. The solvent was removed *in vacuo* to give a crude residue. Flash chromatography, eluting with a solvent gradient of CH_2Cl_2/EtOAc 20:1 to 5:1, gave:

N-Boc tetrahydro monolactamol **(+)-229** as a white solid (18 mg, 36%): R_f = 0.27 (CH_2Cl_2/EtOAc, 10:1); analytical data as previously reported.

Cis enol carbonate **241** as a glass (14 mg, 19%): R_f = 0.53 (CH_2Cl_2/EtOAc, 5:1); ^{1}H NMR ($CDCl_3$, 250 MHz) δ 6.99 (s, 1 H), 4.95 (br d, J = 5.5 Hz, 1 H), 4.57 (ddd, J = 4.3, 11.0 Hz, 1 H), 4.40-4.64 (br s, 1 H), 3.97-4.14 (br s, 1 H), 3.11-3.20 (br s, 1H), 2.79 (dd, J = 15.3, 8.9 Hz, 1 H), 1.35-2.32 (m, 14 H), 1.50 (s, 9 H), 1.44 (s, 9 H), 0.79-1.14 (m, 2 H), 0.91 (dd, J = 6.7, 2.4 Hz, 6 H), 0.78 (d, J = 7.02 Hz, 3 H); MS (CI+, NH_3) *m/z* 596 $(M + NH_4)^+$, 579 $(M + H)^+$, 496, 479, 423, 297; HRMS (CI+) calculated for $C_{31}H_{51}N_2O_8$ $(M + H)^+$ 579.3645, found 579.3632.

Trans enol carbonate **242** as a glass (17 mg, 23%): R_f = 0.45 (CH_2Cl_2/EtOAc, 5:1); 6.92 (s, 1 H), 5.42-5.35 (br dd, 1 H), 4.57 (ddd, J = 10.7, 10.7, 4.3 Hz, 1 H), 4.50-4.32 (br s, 1 H), 4.09-3.92 (br s, 1 H), 3.12 (ddd, J = 9.8, 2.8, 2.4 Hz, 1 H), 2.26-0.78 (m, 17 H), 1.47 (s, 9 H), 1.43 (s, 9 H), 0.91 (t, J = 6.4 Hz, 6 H), 0.75 (d, J = 7.0 Hz, 3 H).

Reduction of *N*-Boc dimer (213) with *B*-Me CBS·BH_3.

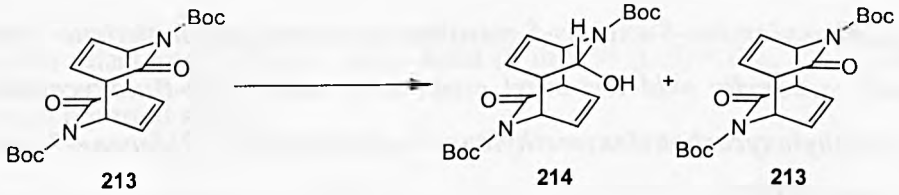

To a solution of *N*-Boc dimer **213** (200 mg, 0.51 mmol) and *B*-Me CBS·BH_3 (30 mg, 0.10 mmol) in CH_2Cl_2 (10 mL) at room temperature under nitrogen was added BH_3·THF (0.615 mL, 0.62 mmol) and the reaction stirred for 26 hours. The reaction was quenched by adding

MeOH (0.25 mL) and stirring for 20 minutes. The solution was then evaporated to dryness to give a white solid. Flash chromatography, eluting with a solvent gradient of CH_2Cl_2/petrol/EtOAc 1:1:0 to 1:1:1, gave:

N-Boc monolactamol **214** as a white solid (17 mg, 9%), R_f = 0.33 (petrol/EtOAc, 3:1 analytical data as reported above.

N-Boc dimer **213** as a white solid (139 mg, 70%), R_f = 0.22 (petrol/EtOAc, 3:1): analytical data as reported above.

***(R)-1-Phenyl-ethanol* (238).[155]**

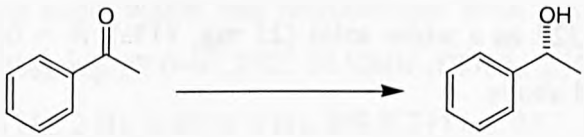

237 **238**

To a solution of *B*-Me CBS.BH_3 (25 mg, 0.09 mmol) and catecholborane (0.091 mL, 0.86 mmol) in CH_2Cl_2 (10 mL) at room temperature under nitrogen was added acetophenone **237** (0.1 mL, 0.86 mmol). The reaction was stirred for 8 hours before being quenched with MeOH (0.5 mL), stirred for 10 minutes, and the solvents removed *in vacuo*. The residue was dissolved in Et_2O (20 mL) and the organic phase washed with pH 13 buffer (1 M NaOH/saturated $NaHCO_3$, 2:1) until the aqueous washes were colourless. The aqueous fractions were extracted with Et_2O (2 × 10 mL) and the combined organic fractions washed with brine, dried ($MgSO_4$), and evaporated to dryness to give (*R*)-1-phenyl-ethanol **238** as a colourless oil (109 mg, 100%): R_f = 0.23 (petrol/EtOAc, 8:1); analytical data as reported above. Chiral HPLC [Daicel Chiralcel OD (4.6 × 25 cm), eluting with 90:10 hexane/^{i}PrOH, 10°C, 0.5 mL min^{-1}, retention times of enantiomers: (a) 15.2 min, (b) 17.4 min] showed the alcohol to have a 73.2% ee of the (a) enantiomer.

Reduction of *N*-Boc tetrahydro dimer (227) with *B*-Me CBS·BH_3 and catecholborane.

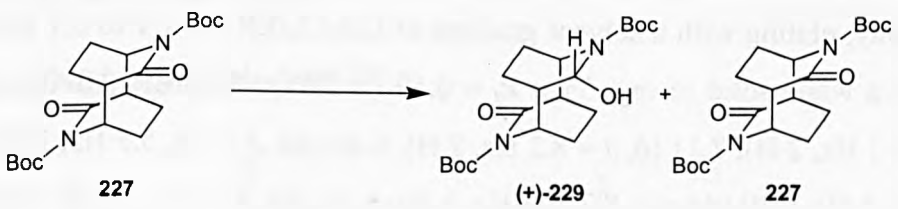

227 **(+)-229** **227**

To a solution of *N*-Boc tetrahydro dimer **227** (100 mg, 0.25 mmol) and *B*-Me CBS·BH_3 (74 mg, 0.25 mmol) in CH_2Cl_2 (10 mL) at room temperature under nitrogen was added

catecholborane (0.027 mL, 0.25 mmol) and the reaction stirred for 14 hours. The reaction was quenched by adding MeOH (0.5 mL) and stirring for 30 minutes. The solvents were removed *in vacuo*, MeOH (10 mL) added, and refluxed for 30 minutes. The solution was then evaporated to dryness to give a white solid which was dissolved in CH_2Cl_2 (20 mL). The organic phase was washed with pH 13 buffer (1 M NaOH/saturated $NaHCO_3$, 2:1). Flash chromatography, eluting with a solvent gradient of CH_2Cl_2/petrol/EtOAc 1:1:0 to 1:1:1, gave:

N-Boc tetrahydro monolactamol **(+)-229** as a white solid (22 mg, 22%), R_f = 0.40 (petrol/EtOAc, 3:1): analytical data as reported above. Chiral HPLC [Column: Chiralcel OD (25 × 0.46 cm), eluting with 99.2:0.8 hexane ^{i}PrOH, 1.0 mL min^{-1}, 40°C, UV detection at 225 nm] showed the monolactamol to have an ee of ≥82.2%.

N-Boc tetrahydro dimer **227** as a white solid (21 mg, 21%), R_f = 0.21 (petrol/EtOAc, 3:1): analytical data as reported above.

Column flush with 10% MeOH/EtOAc gave 22 mg of a mixture of *N*-Boc/*N*-H tetrahydro dimer **231** and *N*-Boc/*N*-H tetrahydro monolactamol **232**, analytical data for both compounds as reported above.

***3-(p-Toluenesulfonyl)-trans-3,7-diazatricyclo[4.2.2.2^{2,5}]dodeca-9,11-diene-4,8-dione* (245).**

186 **245**

To a suspension of NaH (60% dispersion in oil, 126 mg, 3.16 mmol) in THF (15 mL) at room temperature under nitrogen was added *N*-H dimer **186** (200 mg, 1.05 mmol) and the reaction stirred for 15 minutes. A suspension of TsCl (602 mg, 3.16 mmol) and DMAP (64 mg, 0.53 mmol) in THF (5 mL) was added and the reaction stirred for 24 hours. The solvent was evaporated off and, the residue partitioned between CH_2Cl_2 (100 mL) and aqueous 0.1 M HCl solution (100 mL) and the aqueous phase extracted with CH_2Cl_2 (2 × 50 mL). The combined organic fractions were dried ($MgSO_4$) and evaporated to dryness to give a crude residue. Flash chromatography, eluting with a solvent gradient of CH_2Cl_2/EtOAc 1:1 to 0:1 gave *N*-Ts/*N*-H dimer **245** as a white solid (6 mg, 3%): R_f = 0.19 (EtOAc); ^{1}H NMR ($CDCl_3$, 250 MHz) δ 7.83 (d, *J* = 8.2 Hz, 2 H), 7.31 (d, *J* = 8.2 Hz, 2 H), 6.80 (dd, *J* = 7.9, 5.5 Hz, 1 H), 6.63 (dd, *J* = 7.6, 6.7 Hz, 1 H), 6.19 (dd, *J* = 8.2, 8.2 Hz, 1 H), 6.12 (dd, *J* = 8.6, 7.9 Hz, 1 H), 5.77-5.84 (br s, 1 H), 5.33 (dd, *J* = 10.7, 7.3 Hz, 1 H), 4.10-4.24 (m, 1 H), 3.69-3.78 (m, 1 H), 3.54-3.64 (m, 1 H), 2.42 (s, 3 H); IR ($CHCl_3$) 3691, 2928, 1708, 1686, 1601, 1355, 1171 cm^{-1}.

***p-Toluenesulfonyl bromide* (248).**

247 248

To a vigorously stirred suspension of sodium *p*-toluenesulfinate **247** (5 g, 28.1 mmol) in benzene (15 mL) was slowly added bromine (1.45 mL, 28.1 mmol) until the bromine colour persisted. A further portion of sodium *p*-toluenesulfinate was added turning the suspension colourless. The mixture was filtered to remove precipitated NaBr and the filtrate evaporated to dryness to give a white solid, which was recrystallised from hexane to give TsBr **248** as white prisms (4.777 g, 72%): mp 97.0–97.3°C; ^{1}H NMR ($CDCl_3$, 250 MHz) δ 7.88 (d, J = 8.6 Hz, 2 H), 7.39 (d, J = 8.6 Hz, 2 H), 2.49 (s, 3 H); MS (CI+) *m/z* 237, 235 M^+, 157, 155, 139.

***p-Toluenesulfonyl iodide* (249).[162]**

247 249

A solution of iodine (4.77 g, 18.8 mmol) in toluene (50 mL) was added to a solution of sodium *p*-toluenesulfinate **247** (5 g, 28.1 mmol) in H_2O (60 mL), and the mixture stirred vigorously at room temperature in the dark for 1 hour. The organic phase was then separated, washed with water (2× 50 mL), and dried ($MgSO_4$). An equal volume of hexane was added (50 mL) and the solution stored overnight at –20°C, whereupon yellow crystals formed. The crystals were filtered off, washed with cold hexane and dried *in vacuo* to give TsI **249** as yellow prisms (3.053 g, 39%): mp 93.8-95.1°C (cf. literature 88-89°C[162]) ^{1}H NMR ($CDCl_3$, 250 MHz) δ 7.75 (d, J = 8.6 Hz, 2 H), 7.34 88 (d, J = 7.9 Hz, 2 H), 2.47 (s, 3 H); MS (CI+) *m/z* 283 $(M + H)^+$, 255, 185, 157, 139.

***1-p-Toluenesulfonyl-2-pyridone* (250).[221]**

185 250

To a solution of 2-pyridone **185** (1 g, 10.5 mmol) in THF (20 mL) at 0°C under nitrogen was added ^{n}BuLi (1.8 M solution in hexane, 5.58 mL, 11.6 mmol) and the reaction stirred for 20 minutes. A solution of TsCl (2.2 g, 11.6 mmol) in THF (10 mL) was added and the reaction stirred at room temperature for 24 hours. The reaction mixture was poured onto H_2O (50 mL) and the aqueous phase extracted with Et_2O (2 × 100 mL). The combined organic fractions were dried ($MgSO_4$) and evaporated to dryness to give *N*-Ts-2-pyridone **250** (2.132 g, 81%): R_f = 0.85 (EtOAc); ^{1}H NMR ($CDCl_3$, 250 MHz) δ 8.09 (ddd, *J* = 7.6, 1.8, 0.6 Hz, 1 H), 7.99 (d, *J* = 8.2 Hz, 2 H), 7.35 (d, *J* = 8.2 Hz, 2 H), 7.30 (ddd, *J* = 9.5, 6.4, 1.8 Hz, 1 H), 6.41 (ddd, *J* = 9.5, 1.2, 0.6 Hz, 1 H), 6.24 (ddd, *J* = 7.6, 6.4, 1.2 Hz, 1 H), 2.44 (s, 3 H); MS (CI+) *m/z* 250 $(M + H)^+$, 246, 185, 155, 108, 96.

***5-p-Toluenesulfonyl-2-pyridone* (251).**

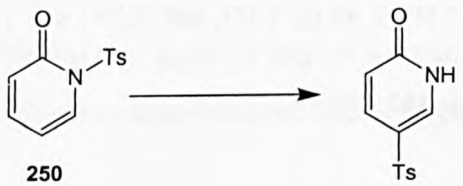

250 **251**

A solution of *N*-Ts-2-pyridone **250** (850 mg, 3.41 mmol) in MeOH (60 mL) in a Pyrex test tube was irradiated with ultra-violet light (λ = 350 nm) for 2 days. The solvent was removed *in vacuo* to give a yellow oil. Flash chromatography, eluting with CH_2Cl_2/EtOAc, 1:1 gave 5-Ts-2-pyridone **251** as a white solid: R_f = 0.58 (petrol/EtOAc, 1:1); ^{1}H NMR ($CDCl_3$, 250 MHz) δ 12.75-12.96 (br s, 1 H), 8.11 (dd, *J* = 2.8, 0.6 Hz, 1 H), 7.77 (d, *J* = 8.5 Hz, 2 H), 7.71 (dd, *J* = 9.8, 2.8 Hz, 1 H), 7.32 (d, *J* = 8.2 Hz, 2 H), 6.57 (dd, J = 9.8, 0.6 Hz, 1 H), 2.41 (s, 3 H); ^{13}C NMR ($CDCl_3$, 63 MHz) δ 164.2, 144.6, 138.2, 138.2, 137.8, 130.1 (2 C), 127.3 (2 C), 122.3, 120.9, 21.4; IR ($CHCl_3$) 2866 (br), 1681, 1659, 1615, 1324, 1161, 1115 cm^{-1}; MS (CI+) *m/z* 250 $(M + H)^+$, 189, 154, 108, 96; HRMS (CI+) calculated for $C_{12}H_{11}NO_3S$ M^+ 249.0460, found 249.0455.

***3-Trifluoromethanesulfonyl-3,7-diazatricyclo[4.2.2.2^{2,5}]dodeca-9,11-diene-4,8-dione* (252).**

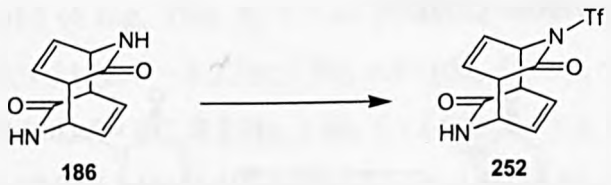

186 **252**

To a suspension of *N*-H dimer **186** (100 mg, 0.53 mmol) in pyridine (10 mL) at room temperature under nitrogen was added Tf_2O (0.266 mL, 1.58 mmol) and the reaction stirred for 24 hours. The solvent was removed *in vacuo* and the residue dissolved in CH_2Cl_2 (60 mL). The organic phase was washed with aqueous $CuSO_4$ solution (3 × 60 mL) and the aqueous fractions back extracted with CH_2Cl_2 (60 mL). The combined organic fractions were dried ($MgSO_4$) and evaporated to dryness to give a yellow/brown residue. Flash chromatography, eluting with EtOAc gave *N*-Tf/*N*-H dimer **252** as a white solid (7 mg, 4%): R_f = 0.40 (EtOAc): ^{1}H NMR ($CDCl_3$, 250 MHz) δ 6.76-6.84 (m, 2 H), 6.41-6.48 (br s, 1 H), 6.37 (ddd, J = 8.6, 7.0, 1.2 Hz, 1 H), 6.26 (ddd, J = 8.2, 7.3, 1.2 Hz, 1 H), 5.06 (dd, J = 9.8, 7.3 Hz, 1 H), 4.26-4.37 (m, 1 H), 3.85 (ddd, J = 10.1, 7.3, 1.5 Hz, 1 H), 3.71-3.80 (m, 1 H); ^{13}C NMR ($CDCl_3$, 63 MHz) δ 175.7, 170.6, 134.9, 133.8, 131.5, 131.4, 57.8, 53.0, 51.0, 50.3; IR ($CHCl_3$) 3425, 2928, 1746, 1689, 1411, 1229, 1140 cm^{-1}; MS (CI+, NH_3) *m/z* 340 $(M + NH_4)^+$, 323 $(M + H)^+$, 245, 228, 96; HRMS (CI+) calculated for $C_{11}H_{10}N_2O_4F_3S$ $(M + H)^+$ 323.0313, found 323.0299.

***p-Toluenesulfinyl chloride* (253).[222]**

247 **253**

To thionyl chloride (15.3 mL, 210.4 mmol) in a 50 mL round-bottomed flask at room temperature was added sodium *p*-toluenesulfinate **247** (5 g, 28.1 mmol) in portions over 15 minutes. A vigorous reaction occurred, with the evolution of a white gas, resulting in the formation of a white solid and a clear yellow liquid. The flask was protected from moisture by fitting a $CaCl_2$ drying tube and left to stand for 2 hours, during which time effervescence continued and the white solid disintegrated into a fine translucent deposit. The excess thionyl chloride was removed by distillation followed by co-evaporation with Et_2O (2 × 10 mL) to give a dark green/yellow oil and a white granular inorganic solid. The oil was dissolved in Et_2O, decanted away from the solid, and the solvent removed *in vacuo* to give a crude dark green/yellow oil, which was distilled to give *p*-toluenesulfinyl chloride **253** as a yellow oil (1.549 g, 32%): ^{1}H NMR ($CDCl_3$, 250 MHz) δ 7.78 (d, J = 8.6 Hz, 2 H), 7.40 (d, J = 7.9 Hz, 2 H), 2.47 (s, 3 H); MS (EI+) *m/z* 174 M^+, 155, 139, 91.

***p-Toluenesulfenyl chloride* (255).**[223]

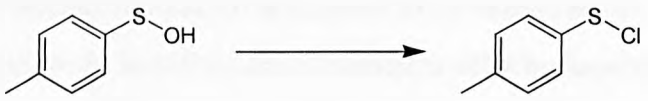

254 255

A two-necked 250 mL round-bottomed flask was fitted with a gas bubbler, a gas inlet tube and a magnetic stirrer bar. The flask was charged with CCl_4 (60 mL) and chlorine gas bubbled through until the CCl_4 was saturated (7.25 g of Cl_2, 1.25 hours), producing a yellow solution. The gas inlet tube was replaced with a septum, the reaction vessel protected from light with a towel and cooled to 0°C with an ice bath. A solution of *p*-toluenethiol **254** (4.4 g, 35.4 mmol) in CCl_4 (10 mL) was added slowly and the reaction stirred for 1 hour. A gas was evolved, and a slow flow of nitrogen was maintained trough the apparatus to prevent suck-back. The orange solution was transferred to a single-necked round-bottomed flask and the CCl_4 and Cl_2 removed *in vacuo* to give *p*-toluenesulfenyl chloride **255** as an orange oil (5.56 g, 99%): ^{1}H NMR ($CDCl_3$, 250 MHz) δ 7.62 (d, J = 8.2 Hz, 2 H), 7.23 (d, J = 7.9 Hz, 2 H), 2.40 (s, 3 H).

***5-p-Toluenesulfenyl-2-pyridone* (257).**

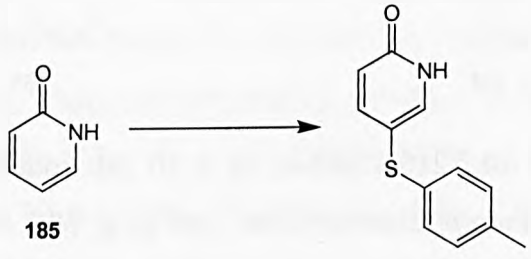

185 257

To a solution of NaH (0.38 g, 15.8 mmol) in THF (10 mL) at room temperature under nitrogen was added 2-pyridone **185** (1 g, 10.5 mmol) as a solution in THF (10 mL), and the volume of hydrogen evolved was measured (observed 225 mL evolved, expected 236 mL). After 10 minutes a solution of *p*-toluenesulfenyl chloride (2.5 g, 15.8 mmol) in THF (10 mL) was added and the reaction stirred for 24 hours. The solvent was removed *in vacuo* and the residue taken up into CH_2Cl_2 (40 mL) and H_2O (40 mL). The aqueous phase was extracted with CH_2Cl_2 (2 × 40 mL) and the combined organic fractions dried ($MgSO_4$) and evaporated to dryness to give a crude yellow oily solid. Flash chromatography, eluting with a solvent gradient of CH_2Cl_2/EtOAc 1:0 to 1:1 gave 5-*p*-toluenesulfenyl-2-pyridone **257** as a pale yellow solid (232 mg, 10%): R_f = 0.35 (CH_2Cl_2/EtOAc, 1:1): ^{1}H NMR ($CDCl_3$, 250 MHz) δ

7.58 (d, J = 2.1 Hz, 1 H), 7.50 (dd, J = 9.5, 2.7 Hz, 1 H), 7.06-7.17 (m, 4 H), 6.58 (dd, J = 9.5, 0.61 Hz, 1 H), 2.31 (s, 3 H), NH proton absent; ^{13}C NMR ($CDCl_3$, 63 MHz) δ 164.7, 147.1, 139.0, 136.9, 132.8, 130.0 (2 C), 129.1 (2 C), 121.0, 112.9, 21.0; MS (EI+) *m/z* 217 M^+, 190, 174, 129, 91; HRMS (EI+) calculated for $C_{12}H_{11}NOS$ M^+ 217.0561, found 217.0572.

***1-p-Toluenesulfenyl-2-pyridone* (258).**

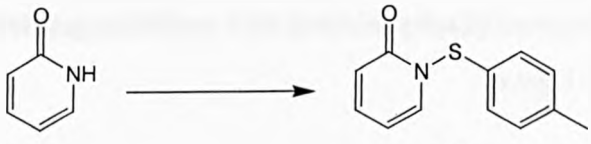

185 **258**

To a solution of 2-pyridone **185** (500 mg, 5.26 mmol) in THF (10 mL) at 0°C under nitrogen was added ^{n}BuLi (2.02 M solution in hexane, 2.86 mL, 5.78 mmol) and the reaction stirred for 30 minutes, whereupon a precipitate was observed. A solution of *p*-toluenesulfenyl chloride (1g, 6.31 mmol) in THF (10 mL) was added and the reaction stirred for 24 hours at room temperature. The solvent was removed *in vacuo* and the residue taken up into $CHCl_3$ (20 mL) and H_2O (20 mL). The aqueous phase was extracted with $CHCl_3$ (2 × 20 mL) and the combined organic fractions dried ($MgSO_4$) and evaporated to dryness to give a crude orange/brown solid. Flash chromatography, eluting with a solvent gradient of petrol/CH_2Cl_2 1:1 to CH_2Cl_2/EtOAc 3:1 gave *N-p*-toluenesulfenyl-2-pyridone **258** as a pale yellow solid (14 mg, 1%): R_f = 0.16 (petrol/EtOAc, 3:1): ^{1}H NMR ($CDCl_3$, 250 MHz) δ 7.44 (d, J = 7.9 Hz, 2 H), 7.26 (dd, J = 5.5, 1.8 Hz, 1 H), 7.23 (d, J = 8.5 Hz, 2 H), 6.82 (dd, J = 7.3, 1.8 Hz, 1 H), 6.16 (dd, J = 7.3, 6.7 Hz, 1 H), 2.38 (s, 3 H); MS (EI+) *m/z* 217 M^+, 200, 184, 167, 149, 94; HRMS (EI+) calculated for $C_{12}H_{11}NOS$ M^+ 217.0561, found 217.0565.

***Bis-(diphenylphosphinyl)-trans-3,7-diazatricyclo[4.2.2.2^{2,5}]dodeca-9,11-diene-4,8-dione* (260), *3-(diphenylphosphinyl)-trans-3,7-diazatricyclo[4.2.2.2^{2,5}]dodeca-9,11-diene-4,8-dione* (261), *1-(diphenylphosphinyl)-butane* (262), *and diphenyl-phosphinic acid vinyl ester* (263).**

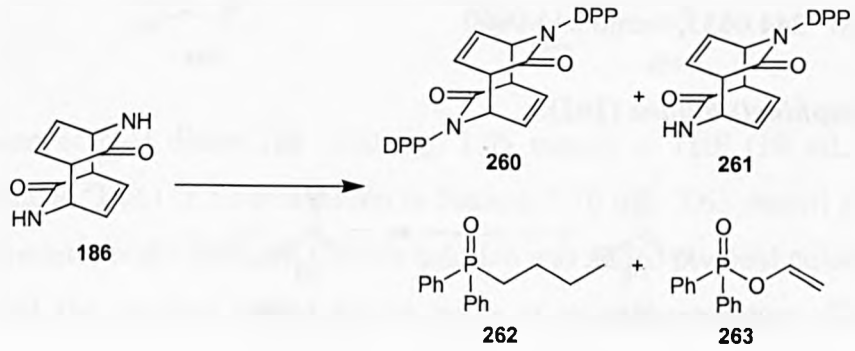

186 **260** **261** **262** **263**

To a suspension of *N*-H dimer **186** (200 mg, 1.05 mmol) in THF (20 mL) at room temperature under nitrogen was added ^{n}BuLi (2.07 M solution in hexane, 1.12 mL, 2.32 mmol) and the reaction stirred for 30 minutes, whereupon DPPCl (0.502 mL, 2.63 mmol) was added and the reaction stirred for 24 hours. The solvent was removed *in vacuo* and the residue taken up into CH_2Cl_2 (20 mL) and H_2O (20 mL). The aqueous phase was extracted with CH_2Cl_2 (2 × 20 mL) and the combined organic fractions dried ($MgSO_4$) and evaporated to dryness to give a crude yellow oil. Flash chromatography, eluting with a solvent gradient of CH_2Cl_2/EtOAc 1:0 to 1:1 to EtOAc/MeOH 9:1 gave:

N-DPP dimer **260** as a white solid (17 mg, 3%): R_f = 0.47 (EtOAc); ^{1}H NMR ($CDCl_3$, 250 MHz) δ 7.21-8.07 (m, 20 H), 6.45 (ddd, *J* = 7.9, 6.7, 1.2 Hz, 2 H), 5.81 (ddd, *J* = 7.9, 6.7, 1.2 Hz, 2 H), 5.23-5.35 (m, 2 H), 3.71 (dddd, *J* = 11.0, 6.1, 4.0, 1.2 Hz, 2 H); MS (CI+) *m/z* 591 $(M + H)^+$, 517, 497, 391, 333, 259; HRMS (CI+) calculated for $C_{34}H_{29}N_2O_4P_2$ $(M + H)^+$ 591.1603, found 591.1580.

N-DPP/*N*-H dimer **261** as a white solid (35 mg, 9%): R_f = 0.08 (EtOAc): ^{1}H NMR ($CDCl_3$, 250 MHz) δ 7.36 (m, 10 H), 6.93 (ddd, *J* = 7.9, 7.0, 0.9 Hz, 1 H), 6.22-6.32 (m, 3 H), 5.71 (ddd, *J* = 8.2, 7.0, 1.2 Hz, 1 H), 5.28-5.40 (m, 1 H), 4.04-4.15 (m, 1 H), 3.54-3.70 (m, 2 H); MS (CI+) *m/z* 391 $(M + H)^+$, 323, 296, 255, 232, 219.

Diphenylphosphinyl butane **262** as a pale yellow oil (15 mg, 4% wrt DPPCl): ^{1}H NMR ($CDCl_3$, 250 MHz) δ 7.42-7.78 (m, 10 H), 2.21-2.33 (m, 2 H), 1.52-1.69 (m, 2 H), 1.42 (tq, *J* = 7.3, 7.3 Hz, 2 H), 0.89 (t, *J* = 7.32 Hz, 3 H); MS (EI+) *m/z* 258 M^+, 229, 215, 201, 183, 155.

Diphenylphosphinyl enol ether **263** as a pale yellow oil (572 mg, 62% wrt DPPCl): R_f = 0.24 (CH_2Cl_2/EtOAc, 3:1): ^{1}H NMR ($CDCl_3$, 250 MHz) δ 7.76-7.89 (m, 4 H), 7.42-7.60 (m, 6 H), 6.67 (ddd, *J* = 13.7, 7.6, 5.8 Hz, 1 H), 4.98 (ddd, *J* = 13.7, 1.83, 1.53 Hz, 1 H), 4.59 (ddd, *J*= 5.8, 1.8, 0.6 Hz, 1 H); ^{13}C NMR ($CDCl_3$, 63 MHz) δ 141.1, 132.6 (2 C), 131.7 (4 C), 129.4, 128.7 (4 C), 100.7 (2 C); MS (EI+) *m/z* 244 M^+, 201, 183, 152, 104; HRMS (EI+) calculated for $C_{14}H_{13}O_2P$ M^+ 244.0653, found 244.0660.

***1-(Diphenylphosphinyl)-butane* (262).**

264 **262**

To a solution of DPPCl **264** (0.2 mL, 1.05 mmol) in THF (10 mL) at room temperature under nitrogen was added ^{n}BuLi (2.21 M solution in hexane, 0.522 mL, 1.15 mmol), and the solution turned orange from colourless. The reaction was stirred for 24 hours, whereupon a yellow solution and a white precipitate were formed. The solvent was removed *in vacuo* and the residue taken up into CH_2Cl_2 (10 mL) and H_2O (10 mL). The aqueous phase was extracted with CH_2Cl_2 (2 × 10 mL) and the combined organic fractions dried ($MgSO_4$) and evaporated to dryness to give DPP-butane **262** as a colourless oil (211 mg, 78%): analytical data as reported as above.

***Diphenyl-phosphinic acid vinyl ester* (263).**

264 **263**

To THF (10 mL) at room temperature under nitrogen was added ^{n}BuLi (2.21 M solution in hexane, 0.522 mL, 1.15 mmol) and the reaction stirred for 30 minutes. To this solution was added DPPCl **263** (0.2 mL, 1.05 mmol) and the reaction stirred for 24 hours. As the DPPCl was added the solution turned orange from colourless, but the colour disappeared almost immediately. After stirring overnight the reaction mixture was a pale yellow solution with a white suspension. The solvent was removed *in vacuo* and the residue taken up into CH_2Cl_2 (20 mL) and H_2O (10 mL). The aqueous phase was extracted with CH_2Cl_2 (2 × 20 mL) and the combined organic fractions dried ($MgSO_4$) and evaporated to dryness to give DPP-enol ether **264** as a yellow oil (167 mg, 65%): analytical data as reported as above.

***3,7-Bis-(2,2-dimethyl-propanoyl)-trans-3,7-diazatricyclo[4.2.2.2^{2,5}]dodeca-9,11-diene-4,8-dione* (265).**

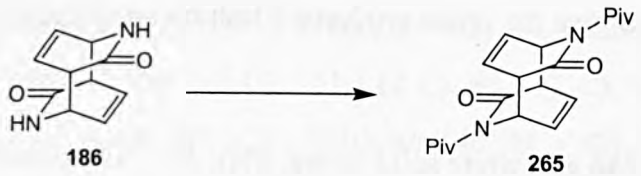

186 **265**

To a suspension of *N*-H dimer **186** (200 mg, 1.05 mmol) in THF (10 mL) at 0°C under nitrogen was added ^{n}BuLi (1.50 M solution in hexane, 1.76 mL, 2.63 mmol) and the solution stirred for 30 minutes under nitrogen. To this solution was added pivaloyl chloride (0.519 mL, 4.21 mmol) and the reaction stirred for 24 hours at room temperature. The solvent was

removed *in vacuo* and the residue taken up into CH_2Cl_2 (20 mL) and H_2O (20 mL). The aqueous phase was extracted with CH_2Cl_2 (2 × 20 mL) and the combined organic fractions dried ($MgSO_4$) and evaporated to dryness to give a crude oily yellow solid. Flash chromatography, eluting with petrol/CH_2Cl_2 1:3 gave *N*-pivaloyl dimer **265** as a white solid (209 mg, 56%): R_f = 0.28 (petrol/CH_2Cl_2, 1:3); ^{1}H NMR ($CDCl_3$, 250 MHz) δ 6.51 (ddd, *J* = 8.4, 7.0, 1.5 Hz, 2 H), 6.17 (ddd, *J* = 8.4, 7.0, 1.5 Hz, 2 H), 4.73 (ddd, *J* = 10.6, 7.3, 1.5 Hz, 2 H), 3.79 (ddd, *J* = 10.6, 7.0, 1.5 Hz, 2 H), 1.28 (s, 18 H); ^{13}C NMR ($CDCl_3$, 63 MHz) δ 185.8 (2 C), 172.1 (2 C), 134.1 (2 C), 131.0 (2 C), 53.9 (2 C), 52.7 (2 C), 42.9 (2 C), 26.7 (6 C); MS (CI+) *m/z* 359 $(M + H)^+$, 264, 208, 180, 96; HRMS (CI+) calculated for $C_{20}H_{27}N_2O_4$ $(M + H)^+$ 359.1971, found 359.1958.

***3-(2,2-dimethyl-propanoyl)-trans-3,7-diazatricyclo[4.2.2.2^{2,5}]dodeca-9,11-diene-4,8-dione* (266) and *N-(5-formyl-8-oxo-7-aza-bicyclo[4.2.2]deca-4,9-dien-2-yl)-2,2-dimethyl-propionamide* (267).**

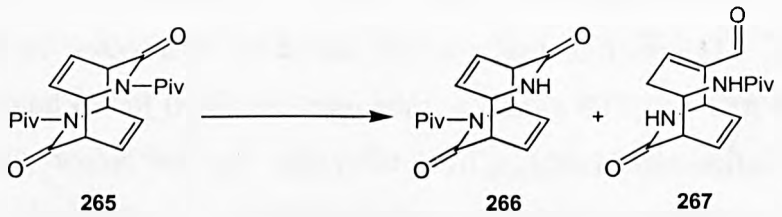

To a solution of *N*-pivaloyl dimer **265** (100 mg, 0.28 mmol) in CH_2Cl_2 (10 mL) at –78°C under nitrogen was added DIBAL (1 M solution in CH_2Cl_2, 0.279 mL, 0.28 mmol) and the reaction stirred for 1 hour at –78°C and 24 hours at room temperature. No reaction was observed by TLC so a further portion of DIBAL (0.559 mL, 0.56 mmol) was added and the reaction stirred for 24 hours. The reaction was quenched by adding CH_2Cl_2/saturated aqueous NH_4Cl (2:1, 30 mL) and stirring for 2 hours. H_2O (10 mL) was added and the aqueous phase extracted with CH_2Cl_2 (3 × 20 mL). The combined organic fractions were dried ($MgSO_4$) and evaporated to dryness to give the crude products. Flash chromatography, eluting with EtOAc gave:

N-Pivaolyl/*N*-H dimer **266** as a white solid (6 mg, 8%): R_f = 0.31 (EtOAc); ^{1}H NMR ($CDCl_3$, 250 MHz) δ 6.69 (ddd, *J* = 8.5, 7.0, 1.5 Hz, 1 H), 6.57 (ddd, *J* = 7.9, 7.0, 0.9 Hz, 1 H), 6.44-6.52 (br s, 1 H), 6.23 (ddd, *J* = 8.2, 7.0, 1.2 Hz, 1 H), 6.11 (ddd, *J* = 8.2, 7.0, 1.2 Hz, 1 H), 4.72 (ddd, *J* = 10.4, 7.0, 1.5 Hz, 1 H), 4.14-4.24 (m, 1 H), 3.62-3.72 (m, 2 H), 1.28 (s, 9 H); ^{13}C NMR ($CDCl_3$, 63 MHz) δ 185.7, 177.3, 172.5, 135.5, 134.1, 131.3, 130.1, 54.7, 53.5,

51.3, 50.0, 42.7, 26.6 (3 C); IR ($CHCl_3$) 3427, 2970, 1682, 1396, 1248, 1158 cm^{-1}; MS (CI+) *m/z* 275 $(M + H)^+$, 180, 96, 85, 67; HRMS (CI+) calculated for $C_{15}H_{19}N_2O_3$ $(M + H)^+$ 275.1396, found 275.1382.

N-Pivaloyl/*N*-H amino α,β-unsaturated aldehyde **267** as a white solid (5 mg, 7%): R_f = 0.31 (EtOAc); ^1H NMR ($CDCl_3$, 250 MHz) δ 9.33 (s, 1 H), 6.57 (dd, *J* = 7.3, 6.1 Hz, 1 H), 6.30 (dd, *J* = 9.2, 6.4 Hz, 1 H), 6.22-6.30 (br s, 1 H), 6.02 (dd, *J* = 8.9, 6.4 Hz, 1 H), 5.65-5.74 (br d, *J* = 8.55 Hz, 1 H), 5.09 (dd, *J* = 6.1, 5.2 Hz, 1 H), 4.61-4.73 (m, 1 H), 3.54-3.61 (m, 1 H), 3.02 (ddd, *J* = 16.2, 6.1, 3.4 Hz, 1 H), 2.84 (ddd, *J* = 16.2, 7.3, 7.0 Hz, 1 H), 1.17 (s, 9 H); ^{13}C NMR ($CDCl_3$, 63 MHz) δ 192.0, 177.4, 173.3, 148.5, 148.2, 128.9, 126.4, 49.7, 47.7, 47.3, 38.7, 32.0, 27.3 (3 C); MS (CI+, NH_3) *m/z* 294 $(M + NH_4)^+$, 277 $(M + H)^+$, 251, 175, 102, 96; HRMS (CI+) calculated for $C_{15}H_{21}N_2O_3$ $(M + H)^+$ 277.1552, found 277.1549.

Epoxidation of *N-Boc dimer* (213).

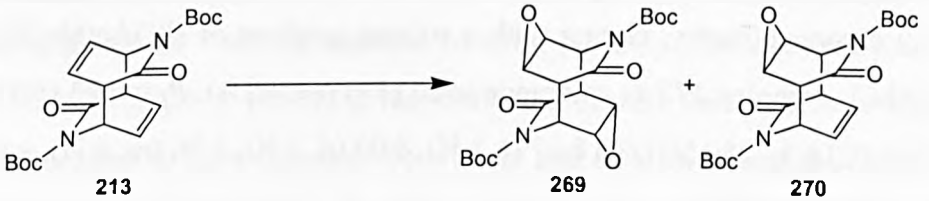

A solution of *N*-Boc dimer **213** (100 mg, 0.26 mmol), mCPBA (442 mg, 1.28 mmol), and 5-*tert*-butyl-4-hydroxy-2-methylphenylsulfide (5 mg, 0.014 mmol) in CH_2Cl_2 (10 mL) was refluxed for 6 days. The organic phase was washed with saturated aqueous $NaHCO_3$ solution (20 mL), dried ($MgSO_4$), and evaporated to dryness to give a crude solid. Flash chromatography, eluting with a solvent gradient of CH_2Cl_2/EtOAc 30:1 to 10:1 gave:

N-Boc diepoxide **269** as a white solid (46 mg, 43%): R_f = 0.53 (CH_2Cl_2/EtOAc, 8:1); ^1H NMR ($CDCl_3$, 250 MHz) δ 5.22 (ddd, *J* = 10.4, 4.3, 1.2 Hz, 2 H), 3.76 (ddd, *J* = 10.4, 4.3, 1.2 Hz, 2 H), 3.62 (ddd, *J* = 4.3, 4.0, 1.2 Hz, 2 H), 3.35 (ddd, *J* = 4.3, 4.3, 1.2 Hz, 2 H), 1.52 (s, 18 H); ^{13}C NMR ($CDCl_3$, 63 MHz) δ 166.1 (2 C), 151.1 (2 C), 85.1 (2 C), 49.7 (2 C), 49.6 (2 C), 48.8 (2 C), 47.8 (2 C), 28.0 (6 C); MS (CI+, NH_3) *m/z* 440 $(M + NH_4)^+$, 423 $(M + H)^+$, 367, 340, 323, 240; HRMS (CI+) calculated for $C_{20}H_{27}N_2O_8$ $(M + H)^+$ 423.1767, found 423.1750.

N-Boc monoepoxide **270** as a white solid (12 mg, 12%): R_f = 0.47 (CH_2Cl_2/EtOAc, 8:1); ^1H NMR ($CDCl_3$, 250 MHz) δ 6.51 (ddd, *J* = 8.5, 7.3, 1.5 Hz, 1 H), 6.08 (ddd, *J* = 8.2, 7.0, 0.9 Hz, 1 H), 5.20 (ddd, *J* = 10.7, 7.3, 1.2 Hz, 1 H), 5.08 (ddd, *J* = 10.4, 4.3, 1.5 Hz, 1 H), 3.83

(ddd, J = 10.4, 7.3, 1.5 Hz, 1 H), 3.70-3.78 (m, 2 H), 3.41 (ddd, J = 4.3, 4.3, 1.5 Hz, 1 H), 1.54 (s, 9 H), 1.51 (s, 9 H); ^{13}C NMR ($CDCl_3$, 63 MHz) δ 170.2, 167.0, 151.1, 151.0, 133.1, 130.1, 84.8, 84.3, 51.9, 51.7, 51.3, 51.1, 49.8, 49.5, 28.0 (3 C), 27.9 (3 C); MS (CI+, NH_3) *m/z* 424 $(M + NH_4)^+$, 407 $(M + H)^+$, 351, 324, 307, 224; HRMS (CI+) calculated for $C_{20}H_{27}N_2O_7$ $(M + H)^+$ 407.1818, found 407.1829.

***Pybox-RhCl$_3$* (273).[224]**

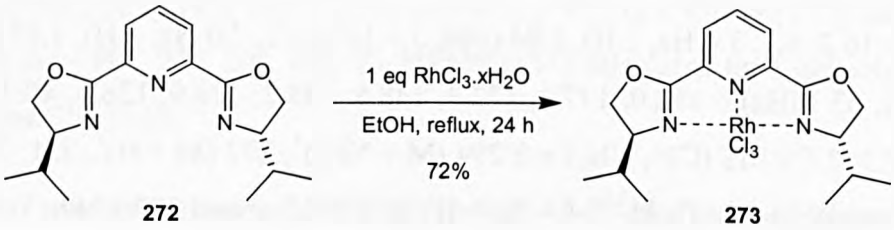

272 273

A solution of pybox **272** (400 mg, 1.3 mmol) and $RhCl_3$ (342 mg, 1.3 mmol) in EtOH (5 mL) under nitrogen was refluxed overnight. The solvent was removed *in vacuo* to give a brown residue. Flash chromatography, eluting with a solvent gradient of EtOAc/MeOH 1:0 to 9:1 gave pybox-$RhCl_3$ complex **273** as an orange solid (486 mg, 72%): R_f = 0.23 (EtOAc/MeOH, 19:1); ^{1}H NMR ($CDCl_3$, 250 MHz) δ 8.27 (t, 1 H), 8.00 (d, 2 H), 4.96 (m, 4 H), 4.64 (m, 2 H), 3.07 (m, 2 H), 1.00 (m, 12 H).

***(S)-1-Phenyl-ethanol* (238).[224]**

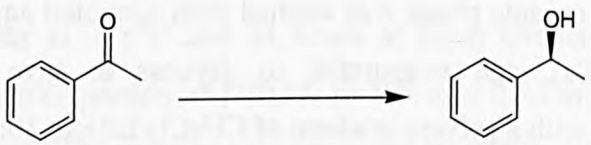

237 238

A solution of pybox (100 mg, 0.33 mmol), pybox-$RhCl_3$ (43 mg, 0.08 mmol), and $AgBF_4$ (32 mg, 0.17 mmol) in THF (5 mL) was stirred for 1 hour at room temperature under nitrogen. To this solution was added acetophenone **237** (0.097 mL, 0.83 mmol) and the reaction vessel was cooled to –15°C with an ethylene glycol/dry ice bath. Ph_2SiH_2 (0.309 mL, 1.66 mmol) was added and the reaction allowed to warm slowly to room temperature. No reaction was observed by TLC so the reaction was stirred for 3 days. The reaction was quenched with MeOH (0.5 mL) and stirred for 30 minutes before being poured onto 1 M aqueous HCl solution (10 mL) and stirred for 1 hour. The aqueous phase extracted with Et_2O (5 × 20 mL) and combined organic fractions were dried ($MgSO_4$) and evaporated to dryness to give a crude yellow/orange semisolid. Flash chromatography, eluting with petrol/EtOAc 8:1

gave (*S*)-1-phenyl-ethanol **238** as a colourless oil (47 mg, 46%): Rf = 0.18 (petrol/EtOAc, 8:1); analytical data as reported above. Chiral HPLC [Daicel Chiralcel OD (4.6 × 25 cm), eluting with 90:10 hexane/^{i}PrOH, 10°C, 0.5 mL min^{-1}, retention times of enantiomers: (a) 15.2 min, (b) 17.4 min] showed the alcohol to have a 85.5% ee of the (b) enantiomer.

***3-Methyl-1H-pyridin-2-one* (280).[120]**

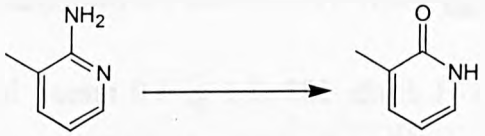

281 **280**

To a solution of 2-amino-3-methyl pyridine **281** (20 g, 185 mmol) was added concentrated H_2SO_4 (32 mL) and the resulting solution cooled to 15°C. Crushed ice (72 g) was added followed by a solution of $NaNO_2$ (14.8 g, 214 mmol) in H_2O (37 mL) which was added slowly to keep the reaction temperature below 10°C. After addition was complete the mixture was slowly heated to boiling in an oil bath and refluxed for 15 minutes. The pH of the cooled mixture was adjusted to 7 by the addition of solid Na_2CO_3. The aqueous phase was then extracted with $CHCl_3$ (10 × 100 mL), the combined organic fractions dried ($MgSO_4$), and evaporated to dryness to give 3-methyl-2-pyridone **280** as brown needles (19.7 g, 98%): mp 145.6-146.5°C; R_f = 0.23 (EtOAc); ^{1}H NMR ($CDCl_3$, 250 MHz) δ 13.12-13.30 (br s, 1 H), 7.28-7.35 (m, 2 H), 6.21 (dd, J = 6.7, 6.4 Hz, 1 H), 2.17 (s, 3 H); MS (EI+) *m/z* 109 M^+, 91, 80, 57, 53.

***1,5-Dimethyl-3,7-diaza-tricyclo[4.2.2.2^{2,5}]dodeca-9,11-diene-4,8-dione* (282).[120]**

280 **282**

A solution of 3-methyl-2-pyridone **280** (4.5 g) in H_2O (15 mL) was irradiated at 350 nm for 9 days. The α-methyl *N*-H dimer precipitated out of solution on formation and was periodically filtered off and irradiation continued. The solid was recrystallised from glacial AcOH to give the α-methyl *N*-H dimer **282** as colourless needles (2.95 g, 66%): ^{1}H NMR (CF_3CO_2D, 400 MHz) δ 6.67-6.63 (dd, *J* = 7, 9 Hz, 2 H), 5.84-5.81 (d, *J* = 9 Hz, 2 H), 3.75-3.73 (d, *J* = 7, 2 H), 1.41 (s, 6 H), NH protons absent; ^{13}C NMR (CF_3CO_2D, 100 MHz) δ 185.0 (2 C), 138.1 (2 C), 133.2 (2 C), 61.5 (2 C), 54.6 (2 C), 20.4 (2 C); MS (CI+) *m/z* 219 $(M + H)^+$, 110, 80, 53; HRMS (CI+) calculated for $C_{12}H_{15}N_2O_2$ $(M + H)^+$ 219.1134, found 219.1132.

***1,5-Dimethyl-4,8-dioxo-3,7-diaza-3,7-di-tert-butoxycarbonyl-tricyclo[4.2.2.2^{2,5}]dodeca-9,11-diene* (274).**

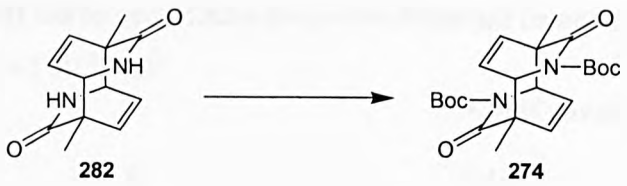

282 274

To a solution of α-methyl *N*-H dimer **282** (1,1 g, 5.0 mmol) in NMP (60 mL) was added DMAP (1.54 g, 12.6 mmol) and Boc_2O (6.95 mL, 30.2 mmol). The reaction mixture was stirred for 24 hours at 85°C under nitrogen before being diluted with CH_2Cl_2 (100 mL). The organic phase was washed with 0.1 M aqueous HCl solution (10 × 100 mL), dried ($MsSO_4$), and evaporated to dryness. Recrystallisation from EtOH yielded the α-methyl *N*-Boc dimer **274** as white cubes (1.27 g, 60%): R_f = 0.30 (petrol/EtOAc, 3:1); ^{1}H NMR ($CDCl_3$, 250 MHz) δ 6.50 (dd, *J* = 8.4, 7.3 Hz, 2 H), 5.81 (dd, *J* = 8.4, 1.5 Hz, 2 H), 4.48 (dd, *J* = 7.3, 1.5 Hz, 2 H), 1.62 (s, 6 H), 1.54 (s, 18 H); ^{13}C NMR ($CDCl_3$, 63 MHz) δ 173.7 (2 C), 152.5 (2 C), 137.2 (2 C), 132.3 (2 C), 83.9 (2 C), 62.4 (2 C), 54.8 (2 C), 28.1 (6 C), 23.0 (2 C); IR ($CHCl_3$) 2985, 2930, 1773, 1714, 1380, 1253 cm^{-1}; MS (CI+, NH_3) *m/z* 419 $(M + H)^+$, 380, 363, 319, 210, 110; HRMS (CI+) calculated for $C_{22}H_{31}N_2O_6$ $(M + H)^+$ 419.2182, found 419.2165; Elemental analysis, calculated for $C_{22}H_{30}N_2O_6$: C, 63.14; H, 7.23; N, 6.69%. Found C, 62.98; H, 7.12; N, 6.65%.

***1,5-Dimethyl-4,8-dioxo-3,7-diaza-3,7-di-tert-butoxycarbonyl-tricyclo[4.2.2.2^{2,5}]dodecane* (275).**

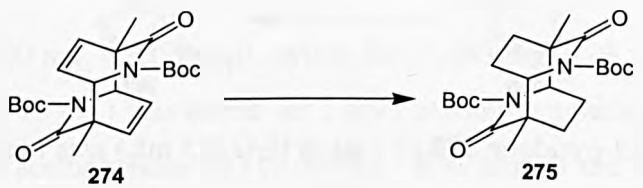

274 275

The α-methyl *N*-Boc tetrahydro dimer **274** (1 g, 2.39 mmol) was suspended in EtOAc (100 mL) and stirred vigorously for 2 days in an atmosphere of hydrogen (3.4 bar). The reaction mixture was evaporated off, the residue re-dissolved in $CHCl_3$ and decolourising charcoal added. The solution was then filtered through Celite and evaporated to dryness to give the α-methyl *N*-Boc tetrahydro dimer **275** as white cubes (989 mg, 98%): R_f = 0.23 (petrol/EtOAc, 3:1); ^{1}H NMR ($CDCl_3$, 250 MHz) δ 4.46 (dd, *J* = 5.1, 2.2 Hz, 2 H), 2.07-1.93 (m, 6 H), 1.65-

1.56 (m, 2 H), 1.56 (s, 18 H), 1.32 (s, 6 H); ^{13}C NMR ($CDCl_3$, 63 MHz) δ 175.1 (2 C), 152.8 (2 C), 83.9 (2 C), 59.9 (2 C), 49.1 (2 C), 28.8 (2 C), 28.0 (6 C), 26.6 (2 C), 23.4 (2 C); MS (CI+) *m/z* 423 $(M + H)^+$, 407, 395, 367, 323, 267, 222; HRMS (CI+) calculated for $C_{22}H_{35}N_2O_6$ $(M + H)^+$ 423.2495, found 423.2480; Elemental analysis, calculated for $C_{22}H_{34}N_2O_6$: C, 62.54; H, 8.11; N, 6.63%. Found C, 62.51; H, 8.14; N, 6.43%.

Reduction of *α-methyl N-Boc tetrahydro dimer* (275) with 5 eq DIBAL.

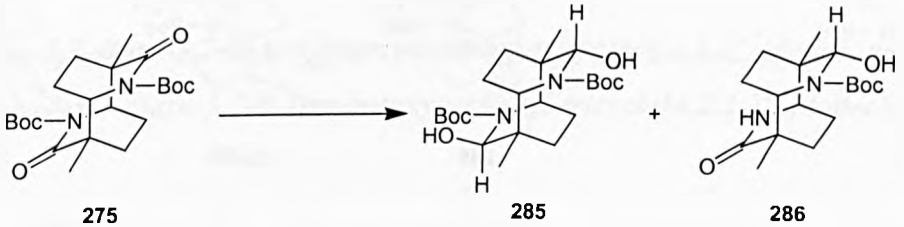

275 285 286

To a solution of α-methyl *N*-Boc tetrahydro dimer **275** (200 mg, 0.47 mmol) in CH_2Cl_2 (10 mL) at room temperature under nitrogen was added DIBAL (1 M solution in CH_2Cl_2, 2.37 mL, 2.37 mmol) and the reaction stirred for 1 hour. The reaction was quenched with CH_2Cl_2/saturated aqueous NH_4Cl solution (2:1, 30 mL), allowed to warm to room temperature, and stirred vigorously for 2 hours. The suspension was then filtered through Celite and the aqueous phase extracted with CH_2Cl_2 (2 × 20 mL). The combined organic fractions were dried ($MgSO_4$) and evaporated to dryness to give the crude products. Flash chromatography, eluting with CH_2Cl_2/EtOAc 29:1 gave:

α-Methyl *N*-Boc tetrahydro dilactamol **285** as clear prisms (73 mg, 36%): mp 213.4-214.0°C; R_f = 0.63 (petrol/EtOAc, 8:1): ^{1}H NMR ($CDCl_3$, 400 MHz) δ 5.37 (d, *J* = 2.2 Hz, 2 H), 5.00 (d, J = 2.6 Hz, 2 H), 3.98 (dd, *J* = 6.6, 1.8 Hz, 2 H), 3.00-2.86 (m, 2 H), 1.88 (ddd, *J* = 13.9, 11.3, 5.8 Hz, 2 H), 1.70-1.50 (m, 2 H), 1.51 (s, 18 H), 1.35-1.15 (m, 2 H), 1.15 (s, 6 H); ^{13}C NMR ($CDCl_3$, 63 MHz) δ 156.8 (2 C), 85.6 (2 C), 80.7 (2 C), 57.3 (2 C), 40.5 (2 C), 31.4 (2 C), 29.1 (2 C), 28.4 (6 C), 22.6 (2 C); IR ($CHCl_3$) 2979, 1655, 1415, 1368, 1149 cm^{-1}; MS (CI+) *m/z* 426 M^+, 408, 380, 308, 252, 224; HRMS (EI+) calculated for $C_{22}H_{38}N_2O_6$ M^+ 426.2730, found 426.2717.

α-Methyl *N*-Boc/*N*-H tetrahydro monolactamol **286** (67 mg, 44%): ^{1}H NMR ($CDCl_3$, 400 MHz) δ 6.66-6.61 (br d, *J* = 6.8 Hz, 1 H), 5.50 (d, *J* = 2.4 Hz, 1 H), 4.93 (d, *J* = 2.6 Hz, 1 H), 3.96 (dd, *J* = 6.5, 1.8 Hz, 1 H), 3.35 (ddd, *J* = 7.3, 7.3, 1.2 Hz, 1 H), 3.10 (ddd, *J* = 13.8, 10.9, 2.9 Hz, 1 H), 2.07-1.95 (m, 2 H), 1.88-1.65 (m, 3 H), 1.50 (s, 9 H), 1.48-1.40 (m, 1 H), 1.24-

1.14 (m, 1 H), 1.18 (s, 3 H), 1.13 (s, 3 H); ^{13}C NMR ($CDCl_3$, 63 MHz) δ 178.6, 156.8, 85.2, 81.3, 60.0, 56.9, 46.0, 42.0, 30.7, 30.6, 29.2, 28.3 (3 C), 25.6, 23.7, 22.8; IR ($CHCl_3$) 2979, 1660, 1468, 1406, 1344, 1155 cm^{-1}; MS (CI+) *m/z* 324 M^+, 306, 268, 224, 207; HRMS (EI+) calculated for $C_{17}H_{28}N_2O_4$ M^+ 324.2049, found 324.2046.

Reduction of *α-methyl N-Boc tetrahydro dimer* (275) with 2 eq DIBAL.

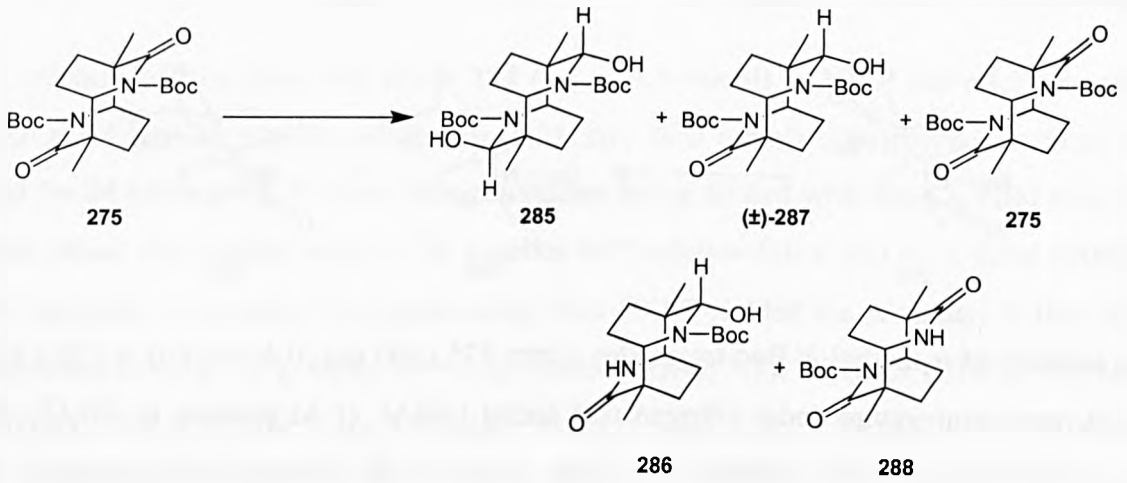

To a solution of α-methyl *N*-Boc tetrahydro dimer **275** (200 mg, 0.47 mmol) in CH_2Cl_2 (10 mL) at room temperature under nitrogen was added DIBAL (1 M solution in CH_2Cl_2, 0.95 mL, 0.95 mmol) and the reaction stirred for 1 hour. The reaction was quenched with CH_2Cl_2/saturated aqueous NH_4Cl solution (2:1, 30 mL), allowed to warm to room temperature, and stirred vigorously for 1 hour. The suspension was then filtered through Celite and the aqueous phase extracted with CH_2Cl_2 (2 × 20 mL). The combined organic fractions were dried ($MgSO_4$) and evaporated to dryness to give the crude products. Flash chromatography, eluting with CH_2Cl_2/EtOAc 29:1 gave:

α-Methyl *N*-Boc tetrahydro dilactamol **285** as a white amorphous solid (64 mg, 38%): R_f = 0.49 (petrol/EtOAc, 8:1): analytical data as reported previously.

α-Methyl *N*-Boc tetrahydro monolactamol **(±)-287** as a white amorphous solid (5 mg, 3%): R_f = 0.19 (petrol/EtOAc, 8:1); ^{1}H NMR ($CDCl_3$, 400 MHz) δ 5.37 (d, J = 2.4 Hz, 1 H), 4.93 (d, J = 2.6 Hz, 1 H), 4.45 (dd, J = 7.1, 1.8 Hz, 1 H), 3.99 (dd, J = 6.2, 2.6 Hz, 1 H), 3.14-3.06 (m, 1 H), 2.11-2.02 (m, 1 H), 1.83-1.68 (m, 4 H), 1.55 (s, 9 H), 1.53-1.45 (m, 1 H), 1.49 (s, 9 H), 1.26 (s, 3 H), 1.24-1.16 (m, 1 H), 1.22 (s, 3 H).

Recovered starting material α-methyl *N*-Boc tetrahydro dimer **275** as a white amorphous solid

(26 mg, 16%): R_f = 0.14 (petrol/EtOAc, 8:1); analytical data as previously reported.

α-Methyl *N*-Boc/*N*-H tetrahydro monolactamol **286** (45 mg, 29%): analytical data as previously reported.

α-Methyl *N*-Boc/*N*-H tetrahydro dimer **288** (20 mg, 13%): ^{1}H NMR ($CDCl_3$, 250 MHz) δ 6.84-6.77 (m, 1 H), 4.47-4.41 (m, 1 H), 3.42-3.31 (m, 1 H), 2.30-1.10 (m, 8 H), 1.55 (s, 9 H), 1.19 (s, 3 H), 1.13 (s, 3 H).

***4,8-Dihydroxy-3,7-diaza-3,7-di-tert-butoxycarbonyl-tricyclo[4.2.2.2^{2,5}]dodecane* (285) *and 8-hydroxy-4-oxo-3,7-diaza-3,7-di-tert-butoxycarbonyl-tricyclo[4.2.2.2^{2,5}]dodecane* (±)-(287).**

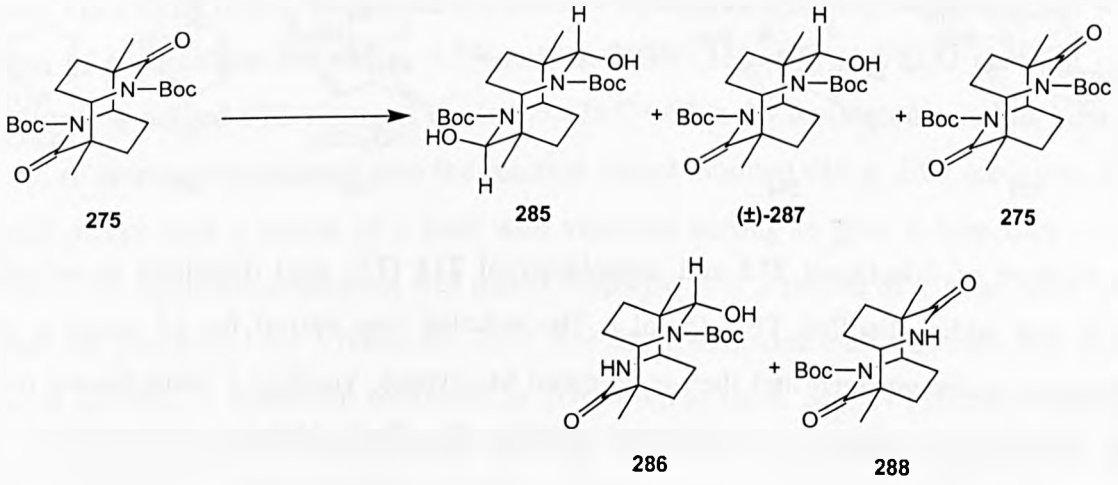

To a solution of α-methyl *N*-Boc tetrahydro dimer **275** (200 mg, 0.47 mmol) in dry CH_2Cl_2 (10 mL) at –78°C under nitrogen was added a 1 M solution of DIBAL in CH_2Cl_2 (0.521 mL, 0.52 mmol), and the reaction stirred for 1 hour. The reaction was quenched with CH_2Cl_2/saturated aqueous NH_4Cl solution (2:1, 30 mL), allowed to warm to room temperature, and stirred vigorously for 1 hour. The suspension was then filtered through Celite and the aqueous phase extracted with CH_2Cl_2 (2 × 20 mL). The combined organic fractions were dried ($MgSO_4$) and evaporated to dryness to give the crude products. Flash chromatography, eluting with CH_2Cl_2/EtOAc 29:1 gave:

α-Methyl *N*-Boc tetrahydro dilactamol **285** as a white amorphous solid (55 mg, 27%): R_f = 0.56 (petrol/EtOAc, 8:1); analytical data as previously reported.

α-Methyl *N*-Boc tetrahydro monolactamol **(±)-287** as a white amorphous solid (5 mg, 2%): R_f = 0.24 (petrol/EtOAc, 8:1); analytical data as previously reported.

Recovered starting material α-methyl *N*-Boc tetrahydro dimer **275** as a white amorphous solid (122 mg, 61%): R_f = 0.14 (petrol/EtOAc, 8:1); analytical data as previously reported.

α-Methyl *N*-Boc/*N*-H tetrahydro monolactamol **286** (6 mg, 4%): analytical data as previously reported.

α-Methyl *N*-Boc/*N*-H tetrahydro dimer **288** (5 mg, 3%): analytical data as previously reported.

5-Formyl-8-oxo-7-aza-bicyclo[4.2.2]deca-4,9-dien-2-yl-ammonium; trifluoro-acetate **(290).**

To a mixture of dilactamol **215** and monolactamol **214** (252 mg) dissolved in anhydrous CH_2Cl_2 was added distilled TFA (5 mL). The solution was stirred for 24 hours at room temperature under nitrogen and then evaporated to dryness, yielding a black/brown oil. ^{1}H NMR revealed the presence of protonated pyridine [δ_H (D_2O, 250MHz) 8.05 (2H, t), 8.59 (1H, m), 8.70 (2H, d)] which was removed by basification and extraction. To the black/brown oil was added 5 mL distilled H_2O and brought up to pH = 8 by the addition of aqueous NH_3 solution. The basified solution was then filtered through Celite and the pyridine removed by washing with CH_2Cl_2 (6 × 50 mL). The aqueous phase was then evaporated to dryness yielding a mixture of the amino aldehyde TFA salt **290** and 2-pyridone **185** as a brown amorphous solid.

α,β-unsaturated amino-aldehyde **290**: ^{1}H NMR (D_2O, 250 MHz) δ 9.25 (s, 1 H), 6.78 (dd, J = 7.6, 5.5 Hz, 1 H), 6.36 (dd, J = 8.9, 6.1 Hz, 1 H), 6.22 (dd, J = 8.9, 6.1 Hz, 1 H), 5.08 (d, J = 6.1 Hz, 1 H), 3.91 (ddd, J = 8.9, 4.0, 3.4 Hz, 1 H), 3.51 (dd, J = 6.1, 3.4 Hz, 1 H), 2.92 (dd, J = 7.6, 4.0 Hz, 1 H), 2.88 (dd, J = 8.9, 5.5 Hz, 1 H), NH protons absent; ^{13}C NMR (D_2O, 63 MHz) δ 195.4, 173.9, 162.8 (q, J = 0.56 ppm), 149.4, 146.4, 129.4, 124.4, 116.4 (q, J = 4.64 ppm), 53.2, 45.8, 45.7, 30.0; MS (CI+) *m/z* 193 M^+, 191, 113, 96; HRMS (CI+) calculated for $C_{10}H_{13}N_2O_2$ M^+ 193.0977, found 193.0972.

Experimental for Chapter 3

Isotetralin (301).[193]

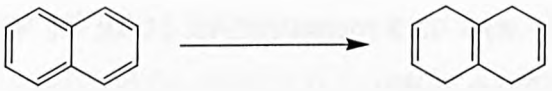

294 301

A five necked 2 L round bottomed flask was fitted with a mechanical stirrer, a 500 mL pressure equalising dropping funnel, a nitrogen line, a dry ice condenser, and a stopper (all glassware was oven dried prior to use). The dry ice condenser was connected to an ammonia cylinder via a KOH drying tower, and the pressure equalising dropping funnel charged with a solution of naphthalene **294** (48 g, 0.37 mol) in EtOH (150 mL) and Et_2O (190 mL). The apparatus was purged with nitrogen, cooled to –78 C with a dry ice/acetone cooling bath, and 750 mL of ammonia condensed into the reaction vessel. Sodium (48 g, 2.09 mol) was added in small pieces over a period of 1 hour with vigorous stirring to give a deep blue viscous solution. The naphthalene solution was added dropwise over a period of 1 hour, after which the reaction was stirred for 3 hours at –78 C. The dry ice/acetone bath was removed and the ammonia allowed to evaporate overnight to give a white solid. MeOH (50 mL) was added slowly to quench any unreacted sodium and the residue was partitioned between ice water (500 mL) and Et_2O (400 mL). The aqueous phase was extracted with Et_2O (400 mL) and the combined organic fractions dried with $MgSO_4$, filtered, and evaporated to dryness to give 47.98 g of crude isotetralin **301** (note: isotetralin has a low vapour pressure so high temperature and vacuum must be avoided to prevent loss of material). The crude material was recrystallised from MeOH, and the mother liquor evaporated to dryness. R_f = 0.54 (EtOAc); ^{1}H NMR ($CDCl_3$, 250 MHz) δ 5.73 (s, 4 H), 2.54 (s, 8 H).

Isotetralin epoxide (295).[194]

301 295

A two-necked 1 L round-bottomed flask was fitted with a pressure equalising dropping funnel, a nitrogen line, and a magnetic stirrer bar. The reaction vessel was charged with isotetralin **301** (26.13 g, 0.198 mol) and CH_2Cl_2 (250 mL), and cooled to 0°C. To this solution

was added NaOAc (24.36 g, 0.297 mol), followed by the dropwise addition of peracetic acid (50 mL, 4.75 M in AcOH, 0.238 mol). The reaction was stirred for 1 h 40 min before water was added (150 mL). The organic phase was washed with 5% aqueous NaOH solution (300 mL) and water (300 mL), dried ($MgSO_4$) and evaporated to dryness to give epoxide **295** as a white solid (28.55 g, 97%): R_f = 0.15 (petrol/EtOAc, 20:1); ^{1}H NMR ($CDCl_3$, 250 MHz) δ 5.49-5.45 (m, 4 H), 2.60-2.28 (m, 8 H).

***Cyanohydrin* (296).**

295 **296**

A two-necked 1 L round-bottomed flask was fitted with a pressure equalising dropping funnel, a nitrogen inlet tube, and a magnetic stirrer bar. The flask was charged with epoxide **295** (31.6 g, 0.21 mol) and benzene (300 mL), the dropping funnel charged with Et_2AlCN (244 mL, 1 M solution in toluene, 0.24 mol), and the apparatus cooled with an ice bath. The Et_2AlCN was added dropwise (caution: the addition was exothermic) and the reaction stirred for 2 hours at room temperature, whereupon a white precipitate was observed. At this point the reaction vessel was cooled with an ice bath and 5% aqueous NaOH solution (300 mL) added slowly. The aqueous phase was extracted with EtOAc (4 × 200 mL), basified with solid NaOH and further extracted with EtOAc (200 mL). The combined organic fractions were dried ($MgSO_4$) and evaporated to dryness to give cyanohydrin **296** as a white solid (34.9 g, 93%): R_f = 0.35 (petrol/EtOAc, 2:1); ^{1}H NMR ($CDCl_3$, 250 MHz) δ 5.74-5.69 (m, 4 H), 2.63-2.23 (m, 8 H), 1.99 (s, 1 H).

***Diepoxide* (297).**

296 **297**

A 1 L round-bottomed flask was fitted with a pressure-equalising dropping funnel and a magnetic stirrer bar. The reaction vessel was charged with diene **296** (27.02 g, 0.154 mol), $VO(acac)_2$ (4.09 g, 0.015 mol), and CH_2Cl_2 (200 mL), and the dropping funnel charged with

^{t}BuOOH (160 mL, 3.86 M solution in toluene, 0.618 mol). The apparatus was flushed with nitrogen and cooled with an ice bath, and the ^{t}BuOOH solution added dropwise, whereupon the solution turned from dark green to dark purple. The reaction was refluxed for 24 hours, and the colour changed to dark yellow/orange. TLC indicated that the reaction was not complete, so more ^{t}BuOOH (40 mL, 3.86 M solution in toluene, 0.154 mol) and $VO(acac)_2$ (1.02 g, 3.86 mmol) were added and the reaction refluxed for a further 24 hours. At this point the reaction was cooled with an ice bath and 10% aqueous sodium sulfate solution added slowly. All solids were crushed and dissolved and the biphasic system was stirred vigorously for 20 minutes. The aqueous phase was then extracted with CH_2Cl_2 (4 × 200 mL), and the combined organic fractions dried ($MgSO_4$) and evaporated to dryness to give an oily orange solid. The crude solid was washed with cold EtOAc and dried *in vacuo* to give clean diepoxide **297**. More product was obtained by evaporating the EtOAc washes down, dissolving the oil in a small amount of CH_2Cl_2, and precipitating with THF/petrol. Diepoxide **297** was isolated as a white solid (22.09 g, 69%): R_f = 0.15 (petrol/EtOAc, 1:1); ^{1}H NMR ($CDCl_3$, 250 MHz) δ 3.44 (s, 1 H), 3.38-3.29 (m, 4 H), 2.47-2.31 (m, 4 H), 2.19-2.00 (m, 4 H).

***Benzyl ether* (302).**

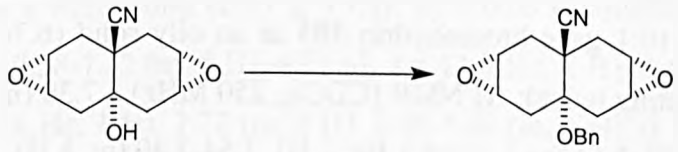

297 **302**

A 500 mL three-necked round-bottomed flask was fitted with a reflux condenser connected to a nitrogen line, a solids addition funnel, a teflon tap adapter leading to an inverted measuring cylinder filled with water, and a magnetic stirrer bar. The flask was charged with diepoxide **297** (19.54 g, 94.4 mmol) and NMP (200 mL), the solids addition funnel charged with NaH (6.8 g, 283.2 mmol), and the apparatus flushed with nitrogen. To the stirred suspension of the diepoxide in NMP was added NaH in portions, and effervescence was observed. The amount of hydrogen evolved was measured, expected 2.11 L and observed 2.93 L, indicating that complete deprotonation had occurred. The solids addition funnel was removed, Bu_4NI (3.49 g, 9.4 mmol) added quickly to prevent moisture from entering the apparatus, and the addition funnel was replaced with a teflon tap adapter with a septum. The flask was cooled with an ice bath and benzyl bromide (33.7 mL, 283.2 mmol) was added slowly. The reaction was heated to 50°C and stirred for 24 hours. Saturated aqueous NH_4Cl solution was added cautiously

and the mixture stirred for 30 minutes. CH_2Cl_2 (300 mL) was added and the organic phase was washed with H_2O (6 × 600 mL), dried ($MgSO_4$), and evaporated to dryness to give a crude orange solid. This was washed twice with ^{i}PrOH and dried *in vacuo* to give clean benzyl alcohol **302** as a white solid (23.25 g, 83%): R_f = 0.72 (petrol/EtOAc, 1:1); ^{1}H NMR ($CDCl_3$, 250 MHz) δ 7.46-7.19 (m, 5 H), 4.40 (s, 2 H), 3.28-3.22 (m, 4 H), 2.74 (d, J = 16.8 Hz, 2 H), 2.23-2.16 (m, 4 H), 2.89 (dd, J = 16.8, 2.4 Hz, 2 H).

***Bromohydrin* (303).**

302 **303**

To a solution of Ph_3P (13.25 g, 50.5 mmol) in CH_2Cl_2 (100 mL) at room temperature under nitrogen was added bromine to give a clear yellow solution. To this a solution of diepoxide **302** (5 g, 16.8 mmol) in CH_2Cl_2 (100 mL) was added and the reaction monitored by TLC. After 1 hour 50 minutes saturated aqueous $NaHCO_3$ (200 mL) solution was added and the aqueous phase was extracted with CH_2Cl_2 (2 × 200 mL). The combined organic fractions were dried ($MgSO_4$) and evaporated to give a crude foam. Column chromatography, eluting with CH_2Cl_2/EtOAc, 10:1 gave bromohydrin **303** as an oily solid (6.74 g, 87%): R_f = 0.31 (petrol/EtOAc, 2:1 eluting twice); ^{1}H NMR ($CDCl_3$, 250 MHz) δ 7.39 (m, 5 H), 4.61 (s, 2 H), 4.40-4.30 (m, 4 H), 3.21-3.14 (br d, J = 6.1 Hz, 2 H), 2.54-2.40 (m, 8 H).

***Di-TBS ether* (304).**

303 **304**

To a solution of diol **303** (11.24 g, 24.5 mmol) in CH_2Cl_2 (150 mL) at room temperature under nitrogen was added pyridine (4.95 mL, 61.2 mmol) followed by the dropwise addition of TBSOTf (12.37 mL, 53.9 mmol) and the reaction was monitored by TLC. After 1 hour and 40 minutes saturated aqueous citric acid solution (150 mL) was added and the mixture stirred for 10 minutes. The aqueous phase was extracted with CH_2Cl_2 (150 mL) and the combined organic fractions dried ($MgSO_4$) and evaporated to dryness to give di-TBS ether **304** as a

white solid (16.42 g, 98%): R_f = 0.64 (petrol/EtOAc, 4:1); ^{1}H NMR ($CDCl_3$, 250 MHz) δ ^{1}H NMR ($CDCl_3$, 250 MHz) δ 7.34-7.21 (m, 5 H), 4.58 (s, 2 H), 4.39 (dd, *J* = 10.7, 4.9 Hz, 2 H), 4.23 (dd, *J* = 11.6, 5.5 Hz, 2 H), 2.63 (dd, *J* = 15.0, 6.71 Hz, 2 H), 2.43 (dd, *J* = 14.7, 5.2 Hz, 2 H), 2.27 (d, *J* = 5.2 Hz, 4 H), 0.83 (s, 18 H), 0.05 (s, 6 H), 0.04 (s, 6 H).

(2R,3R,4aS,6S,7S,8aR)-2-Benzyloxy-3,6-dibromo-7,8a-bis-(tert-butyl-dimethyl-silanyloxy)-octahydro-naphthalene-4a-carbonitrile **(328) and** ***(1R,3S,4S,6S,8S,9R)-4-bromo-3,9-bis-(tert-butyl-dimethyl-silanyloxy)-11-oxa-tricyclo[6.2.1.0^{1,6}]undecane-6-carbonitrile*** **(330).**

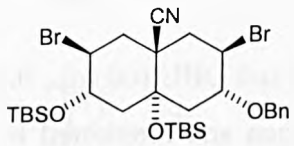

328

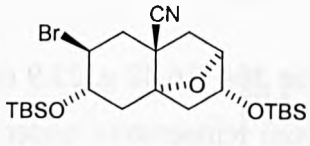

330

Bromohydrin **303** (11.45 g, 24.9 mmol) was synthesised from diepoxide **302** as previously described. The oily foam was then stored at room temperature for 8 days before being subjected to the TBS protection conditions detailed above. TLC revealed numerous products, and workup gave a crude oil. Column chromatography, eluting with a solvent gradient of petrol/CH_2Cl_2 4:1 to 1:1 gave:

Di-TBS ether **328** as a white solid (2.55 g, 15%): R_f = 0.68 (petrol/EtOAc, 4:1); ^{1}H NMR ($CDCl_3$, 250 MHz) δ 7.38-7.22 (m, 5 H), 4.71 (d, *J* = 11.0 Hz, 1 H), 4.40-4.09 (m, 4H), 3.85 (ddd, *J* = 13.1, 8.7, 4.6 Hz, 1 H), 2.72 (m, 2 H), 2.40-1.90 (m, 6 H), 0.88 (s, 9 H), 0.77 (s, 9 H), 0.16 (s, 3 H), 0.11 (s, 3 H), 0.01 (s, 3 H), -0.02 (s, 3 H); ^{13}C NMR ($CDCl_3$, 63 MHz) δ 137.7, 128.4 (2 C), 127.4, 126.6 (2 C), 122.3, 75.2, 72.8, 72.1, 63.1, 51.9, 49.4, 41.3, 40.4, 40.3, 35.0, 32.4, 25.9 (3 C), 25.8 (3 C), 18.3, 18.0, -4.3, -4.4, -4.8, -4.9; MS (CI+, NH_3) *m/z* 705 $(M + NH_4)^+$, 688 $(M + H)^+$, 630, 608, 518, 460; HRMS (CI+) calculated for $C_{30}H_{50}NO_3Si_2Br_2$ $(M + H)^+$ 686.1696, found 686.1713.

Di-TBS ether **304** as a white solid (0.15 g, 1%): R_f = 0.60 (petrol/EtOAc, 4:1); analytical data as previously reported.

Cyclic ether **330** as a white solid (5.45 g, 37%): R_f = 0.50 (petrol/EtOAc, 4:1); ^{1}H NMR ($CDCl_3$, 250 MHz) δ 4.26 (d, *J* = 5.2 Hz, 1 H), 4.16 (dd, *J* = 6.1, 3.1 Hz, 1 H), 4.05 (ddd, *J* = 6.4, 3.1, 1.2 Hz, 1 H), 3.98 (dd, *J* = 7.0, 2.7 Hz, 1 H), 2.67 (dd, *J* = 13.7, 7.0 Hz, 1 H), 2.58-2.05 (m, 4 H), 1.96-1.80 (m, 2 H), 1.44 (dd, *J* = 13.7, 2.1 Hz, 1 H), 0.87 (s, 18 H), 0.08 (s, 3 H), 0.06 (s, 6 H), 0.04 (s, 3 H); ^{13}C NMR ($CDCl_3$, 63 MHz) δ 123.8, 83.4, 82.8, 74.7,

69.7, 48.8, 47.1, 43.9, 37.6, 35.3, 30.4, 25.8 (3 C), 25.7 (3 C), 18.1, 18.0, -4.5, -4.6, -4.8, -5.0; MS (CI+, NH_3) *m/z* 535, 518, 460, 328, 301; HRMS (CI+) calculated for $C_{23}H_{43}NO_3Si_2Br_1$ $(M + H)^+$ 516.1965, found 516.1947.

***Diene* (305).**

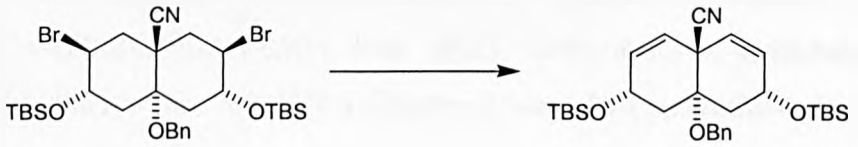

304 **305**

A solution of dibromide **304** (16.42 g, 23.9 mmol) and DBU (60 mL, 0.4 mol) in CH_2Cl_2 (60 mL) was stirred at room temperature under nitrogen and monitored by TLC. After 8 days CH_2Cl_2 (200 mL) was added and the organic phase washed with 1 M aqueous HCl solution (4 × 400 mL), dried ($MgSO_4$), and evaporated to dryness. Column chromatography, eluting with CH_2Cl_2/petrol 1:1 gave diene **305** as a white solid (11.8 g, 85%): R_f = 0.54 (CH_2Cl_2/petrol, 2:1): ^{1}H NMR ($CDCl_3$, 250 MHz) δ 7.29 (m, 5 H), 5.96 (ddd, J = 10.7, 3.4, 0.9 Hz, 2 H), 5.66 (dd, J = 9.8, 1.2 Hz, 2 H), 4.62, (s, 2 H), 4.46-4.39 (m, 2 H), 2.44-2.17 (m, 4 H), 0.81 (s, 18 H), 0.05 (s, 6 H), 0.02 (s, 6 H).

***Diol* (306).**

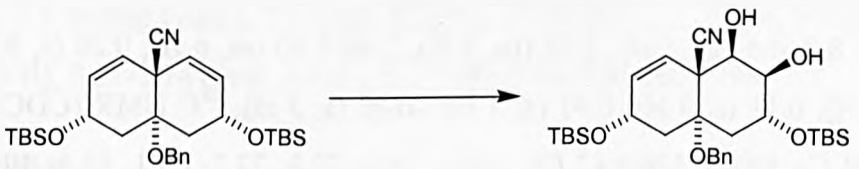

305 **306**

To a solution of diene **305** (5 g, 9.52 mmol) and NMO (4.46 g, 38.1 mmol) in acetone/H_2O (5:1, 120 mL) at room temperature under nitrogen was added OsO_4 (2.5% wt solution in ^{t}BuOH, 0.48 mmol) and the reaction stirred in the dark and monitored by TLC. After 23.5 hours the reaction mixture was added to CH_2Cl_2 (200 mL), saturated aqueous sodium metabisulfite solution (50 mL), and H_2O (50 mL) and stirred for 10 minutes. The aqueous phase was extracted with CH_2Cl_2 (2 × 100 mL) and the combined organic fractions dried ($MgSO_4$) and evaporated to dryness. Column chromatography of the crude material, eluting with a solvent gradient of CH_2Cl_2/EtOAc, 10:1 to 1:1 gave:

Diene **305** as a white solid (0.43 g, 9%): R_f = 0.73 (petrol/EtOAc, 2:1); analytical data as

previously reported.

Diol **306** as a white solid (2.54 g, 48%): R_f = 0.44 (petrol/EtOAc, 2:1); ^{1}H NMR ($CDCl_3$, 250 MHz) δ 7.36-7.15 (m, 5 H), 6.10 (dd, J = 9.8, 1.2 Hz, 1 H), 6.02 (dd, J = 10.1, 2.7 Hz, 1 H), 4.77 (d, J = 10.4 Hz, 1 H), 4.61 (d, J = 10.4 Hz, 1 H), 4.51-4.01 (m, 4 H), 2.50-2.09 (m, 4 H), 0.83 (s, 9 H), 0.78 (s, 9 H), 0.08 (s, 3 H), 0.06 (s, 3 H), 0.02 (s, 3 H), 0.00 (s, 3 H), OH protons absent.

***Acetonide* (307).**

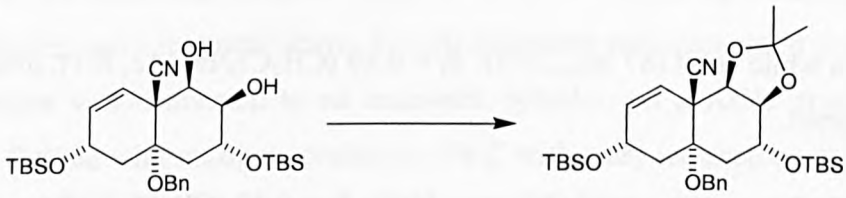

To a solution of diol **306** (2.54 g, 4.5 mmol) in CH_2Cl_2 (100 mL) at room temperature under nitrogen was added 2,2-dimethoxypropane (2.23 mL, 18.2 mmol) followed by TsOH (86 mg, 0.45 mmol) and the reaction stirred and monitored by TLC. TLC showed that starting material was still present after 1 hour so a further portion of TsOH (86 mg, 0.45 mmol) was added, and the reaction was complete after 1.5 hours. After 2 hours saturated aqueous $NaHCO_3$ solution (50 mL) and H_2O (50 mL) were added and the mixture stirred for 10 minutes. The aqueous phase was extracted with CH_2Cl_2 (2 × 100 mL) and the combined organic fractions dried ($MgSO_4$) and evaporated to dryness to give acetonide **307** as a white solid (2.58 g, 95%): R_f = 0.88 (CH_2Cl_2/EtOAc, 10:1); ^{1}H NMR ($CDCl_3$, 250 MHz) δ 7.34-7.16 (m, 5 H), 5.96 (ddd, J = 9.8, 3.7, 0.9 Hz, 1 H), 5.85 (dd, J = 9.8, 1.5 Hz, 1 H), 4.72 (d, J = 10.4 Hz, 1 H), 4.43 (d, J = 10.4 Hz, 1 H), 4.41-4.20 (m, 4 H), 2.42 (d, J = 15.9 Hz, 1 H), 2.22-2.10 (m, 3 H), 1.57 (s, 3 H), 1.30 (s, 3 H), 0.88 (s, 9 H), 0.80 (s, 9 H), 0.07 (s, 6 H), 0.04 (s, 3 H), 0.02 (s, 3 H).

***Diol/acetonide* (310).**

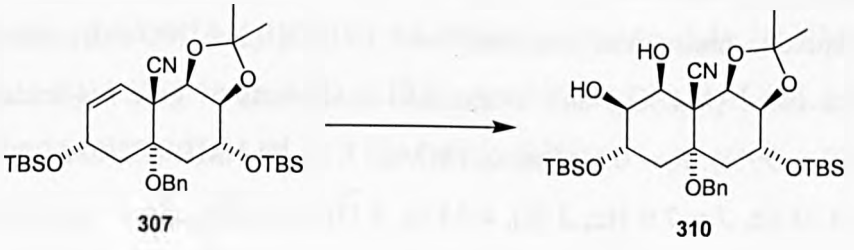

A 100 mL round-bottomed flask was charged with alkene **307** (0.32 g, 0.53 mmol),

$K_3Fe(CN)_6$ (0.53 g, 1.60 mmol), K_2CO_3 (0.22 g, 1.60 mmol), $K_2OsO_2(OH)_4$ (10 mg, 0.027 mmol), quinuclidine (15 mg, 0.13 mmol), $MeSO_2NH_2$ (51 mg, 0.53 mmol) and a magnetic stirrer bar. $^tBuOH/H_2O$ (1:1, 25 mL) was then added and the reaction stirred at room temperature under nitrogen in the dark and monitored by TLC. After 42.5 hours saturated aqueous sodium metabisulfite solution (25 mL), H_2O (25 mL), and CH_2Cl_2 (75 mL) were added and the mixture stirred vigorously for 10 minutes. The aqueous phase was extracted with CH_2Cl_2 (3 × 75 mL) and the combined organic fractions dried ($MgSO_4$) and evaporated to dryness to give a crude oil. Column chromatography, eluting with CH_2Cl_2/EtOAc, 6:1 gave:

Alkene **307** as a white solid (87 mg, 27%): R_f = 0.89 (CH_2Cl_2/EtOAc, 6:1); analytical data as previously reported.

Diol/acetonide **310** as a white solid (251 mg, 74%): R_f = 0.40 (CH_2Cl_2/EtOAc, 6:1); ^{1}H NMR ($CDCl_3$, 250 MHz) δ 7.33 (m, 5 H), 4.75-3.92 (m, 8 H), 3.27 (s, 1 H), 2.75 (s, 1 H), 2.34-2.00 (m, 4 H), 1.60 (s, 3 H), 1.33 (s, 3 H), 0.84 (s, 9 H), 0.78 (s, 9 H), 0.04 (s, 3 H), 0.02 (s, 6 H), 0.00 (s, 3 H).

Bis-acetonide **(311).**

310 **311**

To a solution of diol/acetonide **310** (1.61 g, 2.54 mmol) in CH_2Cl_2 (75 mL) at room temperature under nitrogen was added 2,2-dimethoxypropane (1.25 mL, 10.17 mmol) followed by TsOH (97 mg, 0.51 mmol) and the reaction stirred and monitored by TLC. TLC showed that the reaction was complete after 50 minutes. After 1 hour saturated aqueous $NaHCO_3$ solution (50 mL) and H_2O (50 mL) were added and the mixture stirred for 10 minutes. The aqueous phase was extracted with CH_2Cl_2 (2 × 100 mL) and the combined organic fractions dried ($MgSO_4$) and evaporated to dryness to give *bis*-acetonide **311** as a white solid (1.69 g, 99%): R_f = 0.60 (petrol/EtOAc, 3:1); ^{1}H NMR ($CDCl_3$, 250 MHz) δ 7.35-7.19 (m, 5 H), 4.58 (d, J = 7.0 Hz, 2 H), 4.53 (s, 2 H), 4.35 (dd, J = 11.6, 6.1 Hz, 2 H), 4.23 (dd, J = 7.0, 5.2 Hz, 2 H), 2.19 (d, J = 6.7 Hz, 4 H), 1.62 (s, 6 H), 1.37 (s, 6 H), 0.86 (s, 18 H),

0.06 (s, 12 H).

***Diol* (316) and *triol* (317).**

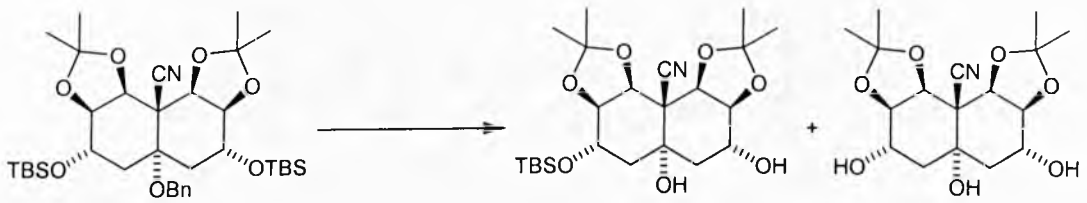

311 316 317

A three-necked 500 mL round-bottomed flask was fitted with a nitrogen inlet tube, a septum, a dry ice condenser, and a magnetic stirrer bar (all glassware was oven dried prior to use). The dry ice condenser was connected to an ammonia cylinder via a KOH drying tower. The apparatus was flushed with nitrogen, cooled to –78 C with a dry ice/acetone cooling bath, and ammonia (200 mL) condensed into the reaction vessel. Sodium (2 g, 87 mmol) was then added slowly with vigorous stirring to give a deep blue solution which was stirred for 30 minutes. A solution of protected triol **311** (1.69 g, 2.5 mmol) in THF (30 mL) was added and the reaction stirred for 30 minutes at –78 C. The reaction was quenched by the slow addition of MeOH (50 mL) until the blue colour disappeared and effervescence ceased. The mixture was stirred for 10 minutes and the dry ice bath was removed and the ammonia allowed to evaporate. The solvents were removed *in vacuo* and the residue taken up into CH_2Cl_2 (100 mL) and H_2O (100 mL). The aqueous phase was neutralised with citric acid and extracted with CH_2Cl_2 (3 × 100 mL). The combined organic fractions were dried ($MgSO_4$) and evaporated to dryness. Column chromatography of the crude material, eluting with a solvent gradient of CH_2Cl_2/EtOAc, 1:0 to 5:1 to 0:1 gave:

Diol **316** as a white solid (0.82 g, 70 %): R_f = 0.49 (petrol/EtOAc, 2:3); ^{1}H NMR ($CDCl_3$, 250 MHz) δ 5.47 (br d, J = 0.9 Hz, 1 H), 4.56-4.47 (m, 4 H), 4.34-4.23 (m, 2 H), 4.05 (d, J = 10.4 Hz, 1 H), 2.48-2.36 (m, 2 H), 1.93-1.79 (m, 2 H), 1.73 (d, J = 7.6 Hz, 6 H), 1.42 (s, 6 H), 0.89 (s, 9 H), 0.16 (s, 6 H).

Triol **317** as a white solid (0.16 g, 18%): R_f = 0.08 (petrol/EtOAc, 2:3); ^{1}H NMR ($CDCl_3$, 250 MHz) δ 5.05 (s, 1 H), 4.58-4.41 (m, 6 H), 3.39 (d, J = 7.0 Hz, 2 H), 2.45 (dd, J = 15.3, 4.6 Hz, 2 H), 1.96 (d, J = 15.6 Hz, 2 H), 1.74 (s, 6 H), 1.44 (s, 6 H).

***Triol* (317).**

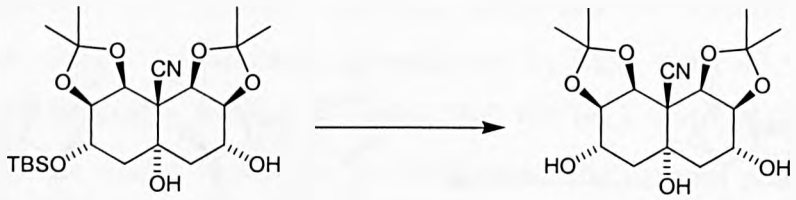

316 317

To a solution of TBS ether **316** (0.82 g, 1.75 mmol) in THF (50 mL) at room temperature under nitrogen was added TBAF (2.1 mL, 1 M solution in THF, 2.1 mmol) and the reaction monitored by TLC, which showed that the reaction was complete after 10 minutes. After 20 minutes the solvent was removed *in vacuo* to give a crude foam. Column chromatography, eluting with a solvent gradient of CH_2Cl_2/EtOAc, 1:1 to 0:1 gave triol **317** as a white solid (0.61 g, 98%): R_f = 0.22 (petrol/EtOAc, 1:4): analytical data as previously reported.

***Dimesylate* (318).**

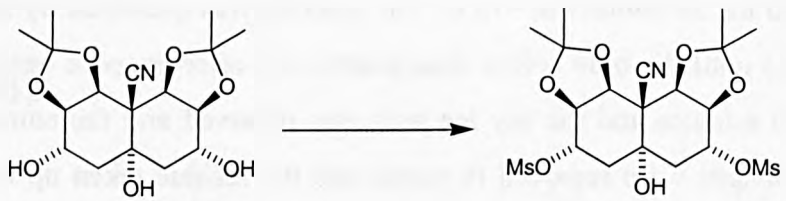

317 318

To a solution of triol **317** (0.77 g, 2.17 mmol) in CH_2Cl_2 (40 mL) at room temperature under nitrogen was added Et_3N (1.21 mL, 8.68 mmol) followed by MsCl (0.67 mL, 8.68 mmol) and the reaction monitored by TLC, which showed that the reaction was complete after 45 minutes. After 55 minutes the solvent was removed *in vacuo* to give a crude residue which was taken up into CH_2Cl_2 (30 mL) and H_2O (30 mL). The aqueous phase was extracted with CH_2Cl_2 (2 × 30 mL) and the combined organic fractions dried (hydrophobic frit) and evaporated to dryness to give a crude residue. Column chromatography, eluting with a solvent gradient of CH_2Cl_2/EtOAc, 1:1 to 0:1 gave dimesylate **318** as a white solid (1.11 g, 100%): R_f = 0.63 (EtOAc); ^{1}H NMR ($CDCl_3$, 250 MHz) δ 5.19-5.10 (m, 2 H), 4.61-4.50 (m, 4 H), 3.11 (s, 6 H), 2.90 (br s, 1 H), 2.64 (dd, J = 15.9, 7.0 Hz, 2 H), 2.21 (dd, J = 15.9, 5.2 Hz, 2 H), 1.67 (s, 6 H), 1.43 (s, 6 H).

***(3aS,7aR,10aS,10cR)-5a-Hydroxy-2,2,9,9-tetramethyl-3a,7a,10a,10c-tetrahydro-5aH-1,3,8,10-tetraoxa-dicyclopenta[a,h]naphthalene-10b-carbonitrile* (298).**

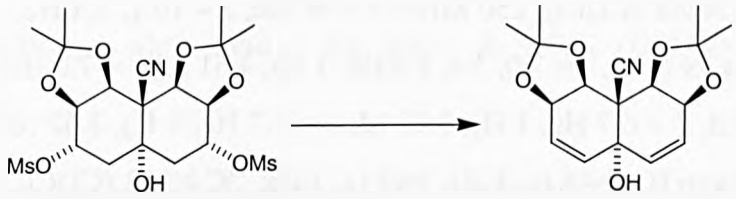

318 298

To a solution of dimesylate **318** (50 mg, 0.098 mmol) in toluene (5 mL) at room temperature under nitrogen was added DBN (0.242 mL, 1.96 mmol) and the reaction refluxed and followed by TLC. After 20 hours the solvent was removed *in vacuo* and the brown residue dissolved in CH_2Cl_2 (20 mL). The organic phase was washed 1 M aqueous citric acid solution (2 × 20 mL) and the aqueous phases back extracted with CH_2Cl_2 (10 mL). The combined organic fractions were dried (Na_2SO_4) and evaporated to dryness to give a light brown residue. Column chromatography on alumina, eluting with CH_2Cl_2/EtOAc, 1:1 to 0:1 gave diallylic alcohol **298** as a white solid (21 mg, 67%): R_f = 0.40 (EtOAc): ^{1}H NMR ($CDCl_3$, 250 MHz) δ 6.31 (dd, J = 9.8, 2.7 Hz, 2 H), 6.14 (dd, J = 9.8, 1.8 Hz, 2 H), 4.83 (ddd, J = 7.0, 2.7, 1.8 Hz, 2 H), 4.77 (d, J = 7.0 Hz, 2 H), 1.84 (s, 1 H), 1.68 (s, 6 H), 1.47 (s, 6 H); ^{13}C NMR ($CDCl_3$, 100 MHz) δ 133.2 (2 C), 130.7 (2 C), 118.8, 111.3 (2 C), 71.4 (2 C), 70.6, 46.8 (2 C), 29.7, 26.2 (2 C), 24.6 (2 C); IR ($CHCl_3$) 3594, 2248, 1592, 1459, 1386, 1260, 1207, 1159, 1084 cm^{-1}; MS (CI+, NH_3) *m/z* 337 $(M + NH_4)^+$, 320 $(M + H)^+$, 304, 279, 272, 267; HRMS (CI+, NH_3) calculated for $C_{17}H_{25}N_2O_5$ $(M + NH_4)^+$ 337.1763, found 337.1753.

Racemic epoxidation of *diallylic alcohol* (298).

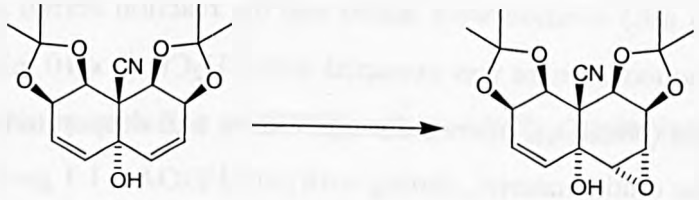

298 299

To a solution of diallylic alcohol **298** (21 mg, 0.066 mmol) in CH_2Cl_2 (1.5 mL) at room temperature under nitrogen was added ^{t}BuOOH (0.030 mL, 0.115 mmol) followed by a solution of $VO(acac)_2$ (5 mg, 0.02 mmol) in CH_2Cl_2 (0.5 mL), and the reaction monitored by TLC. After 20 hours saturated aqueous Na_2SO_3 (0.2 mL) solution was added and the mixture

stirred for 10 minutes. The organic phase was dried (Na_2SO_3) and evaporated to dryness to give a crude residue. Column chromatography on alumina, eluting with a solvent gradient of CH_2Cl_2 to EtOAc/MeOH, 1:0 to 9:1 gave monoepoxide **299** as a white solid (12 mg, 54%): R_f = 0.55 (EtOAc): ^{1}H NMR ($CDCl_3$, 250 MHz) δ 6.36 (dd, J = 10.1, 3.4 Hz, 1 H), 6.13 (dd, J = 10.1, 1.8 Hz, 1 H), 4.79 (ddd, J = 7.0, 3.4, 1.8 Hz, 1 H), 4.61 (d, J = 7.0 Hz, 1 H), 4.60 (d, J = 6.7 Hz, 1 H), 4.43 (d, J = 6.7 Hz, 1 H), 3.82 (d, J = 3.7 Hz, 1 H), 3.62 (d, J = 3.7 Hz, 1 H), 2.73 (s, 1 H), 1.67 (s, 6 H), 1.45 (s, 3 H), 1.42 (s, 3 H); ^{13}C NMR ($CDCl_3$, 63 MHz) δ 131.7, 129.6, 118.1, 111.3, 110.7, 77.9, 76.8, 71.2, 70.7, 68.2, 57.9, 55.4, 47.5, 26.3, 25.8, 24.8, 24.4; MS (CI+, NH_3) *m/z* 353 $(M + NH_4)^+$, 336 $(M + H)^+$, 320, 295, 279, 272, 267; HRMS (CI+, NH_3) calculated for $C_{17}H_{22}N_2O_6$ $(M + H)^+$ 336.1447, found 336.1436.

Asymmetric epoxidation of *diallylic alcohol* (298) employing L-(+)-DIPT.

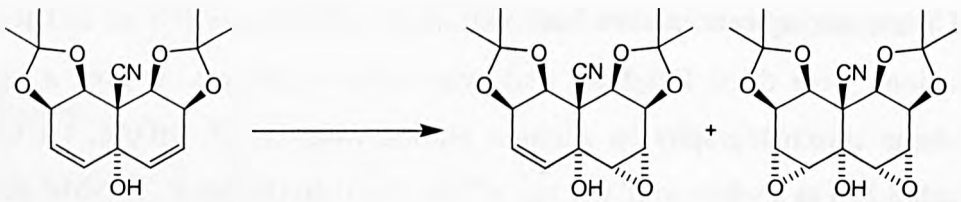

298 **(–)-299** **335**

A 25 mL pear-shaped flask was charged with $Zr(O^iPr)_4{\cdot}^iPrOH$ (109 mg, 0.282 mmol), 4 Å MS, and a magnetic stirrer bar, and the flask was flushed with nitrogen and cooled to –20°C with a CCl_4/dry ice bath. CH_2Cl_2 (5 mL) was added and the solution stirred for 30 minutes at –20°C. L-(+)-diisopropyl tartrate (0.065 mL, 0.31 mmol) and ^{t}BuOOH (0.085 mL, 0.32 mmol) were added and the solution stirred for a further 30 minutes at –20°C. A solution of diallylic alcohol **298** (30 mg, 0.094 mmol) in CH_2Cl_2 (5 mL) was added and the reaction placed in a freezer and monitored by TLC. After 69 hours H_2O (2.5 mL) and saturated aqueous Na_2SO_3 (2.5 mL) solution were added and the reaction stirred at room temperature for 30 minutes. The aqueous phase was extracted with CH_2Cl_2 (3 × 10 mL) and the combined organic fractions dried (Na_2SO_4), filtered through Celite, and evaporated to dryness. Column chromatography of the crude material, eluting with petrol/EtOAc, 1:1 gave:

Bis-epoxide **335** as a white solid (6 mg, 19%): R_f = 0.56 (EtOAc); ^{1}H NMR ($CDCl_3$, 250 MHz) δ 4.64 (d, J = 6.4 Hz, 2 H), 4.35 (d, J = 6.4 Hz, 1 H), 3.82 (d, J = 3.7 Hz, 2 H), 3.67 (d, J = 3.7 Hz, 2 H), 2.68 (s, 1 H), 1.67 (s, 6 H), 1.41 (s, 6 H).

Monoepoxide **(–)-299** as a white solid (17 mg, 54%): R_f = 0.54 (EtOAc); $[\alpha]_D$ –29.6° (c =

1.12, $CHCl_3$); Chiralpak-AD (25 × 0.46 cm), 90:10 hexane:IPA, 1 mL min^{-1}, thermostatic 10°C, detect by UV (210 nm). Retention times: **(+)-299** 25.5, **(–)-299** 30.2 min. Ee = >95%, second eluting peak in excess; analytical data as previously reported.

Diallylic alcohol **298** as a white solid (7 mg, 24%): R_f = 0.42 (EtOAc); analytical data as previously reported.

Asymmetric epoxidation of *diallylic alcohol* (298) employing D-(–)-DIPT.

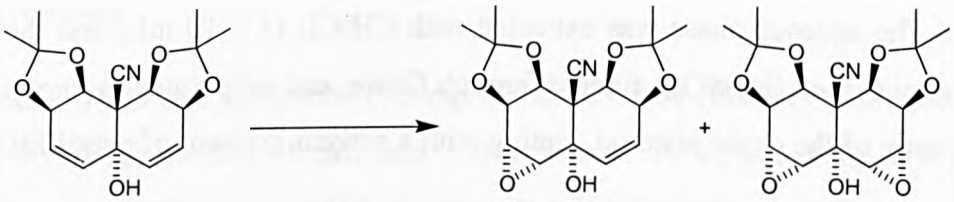

Reaction procedure identical to that detailed above but employing D-(–)-DIPT in place of L-(+)-DIPT. Column chromatography of the crude material, eluting with a solvent gradient of petrol/EtOAc, 1:0 to 1:1 gave:

Bis-epoxide **335** as a white solid (7 mg, 21%): R_f = 0.56 (EtOAc); analytical data as previously reported.

Monoepoxide **(+)-299** as a white solid (14 mg, 44%): R_f = 0.54 (EtOAc); $[\alpha]_D$ +30.5° (*c* = 0.66, $CHCl_3$); HPLC assay: Chiralpak-AD (25 × 0.46 cm), 90:10 hexane:IPA, 1 mL min^{-1}, thermostatic 10°C, detect by UV (210 nm). Retention times: **(+)-299** 25.5, **(–)-299** 30.2 min. Ee = >95%, first eluting peak in excess; analytical data as previously reported.

Diallylic alcohol **298** as a white solid (6 mg, 20%): R_f = 0.42 (EtOAc); analytical data as previously reported.

Sharpless asymmetric epoxidation of *diallylic alcohol* (298) employing L-(+)-DIPT.

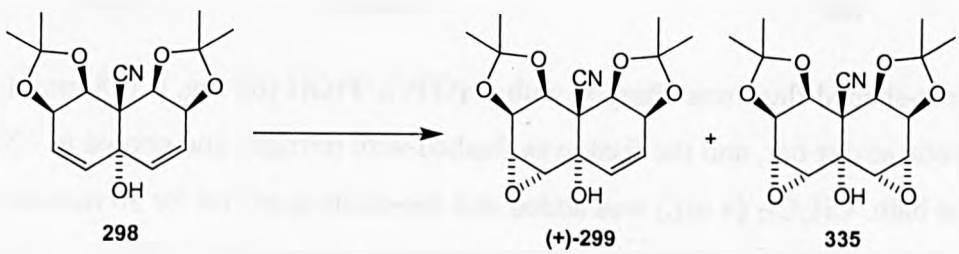

A 10 mL pear-shaped flask was charged with $Ti(O^iPr)_4$ (0.028 mL, 0.094 mmol), 4 Å MS, and a magnetic stirrer bar, and the flask was flushed with nitrogen and cooled to –20°C with a CCl_4/dry ice bath. CH_2Cl_2 (2 mL) was added and the solution stirred for 30 minutes at –20°C. L-(+)-diisopropyl tartrate (0.022 mL, 0.103 mmol) and ^tBuOOH (0.028 mL, 0.107 mmol) were added and the solution stirred for a further 30 minutes at –20°C. A solution of diallylic alcohol **298** (10 mg, 0.031 mmol) in CH_2Cl_2 (2 mL) was added and the reaction placed in a freezer and monitored by TLC. After 70 hours and 40 minutes H_2O (1 mL) and saturated aqueous Na_2SO_3 (1 mL) solution were added and the reaction stirred at room temperature for 30 minutes. The aqueous phase was extracted with CH_2Cl_2 (3 × 10 mL) and the combined organic fractions dried (Na_2SO_4), filtered through Celite, and evaporated to dryness. Column chromatography of the crude material, eluting with a solvent gradient of petrol/EtOAc, 1:0 to 1:1 gave:

Bis-epoxide **335** as a white solid (0.8 mg, 7%): R_f = 0.59 (EtOAc); analytical data as previously reported.

Monoepoxide **(+)-299** as a white solid (4.2 mg, 40%): R_f = 0.57 (EtOAc); HPLC assay: Chiralpak-AD (25 × 0.46 cm), 90:10 hexane:IPA, 1 mL min^{-1}, thermostatic 10°C, detect by UV (210 nm). Retention times: **(+)-299** 25.5, **(–)-299** 30.2 min. Ee = 13.8%, first eluting peak in excess; analytical data as previously reported.

Diallylic alcohol **298** as a white solid (4 mg, 40%): R_f = 0.44 (EtOAc); analytical data as previously reported.

Asymmetric epoxidation of *diallylic alcohol* (298) employing L-(+)-DIPT.

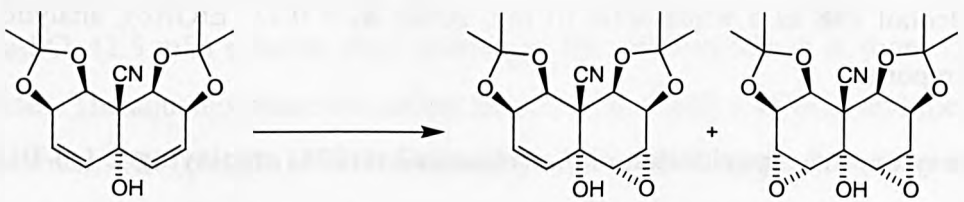

298 **(–)-299** **335**

A 25 mL pear-shaped flask was charged with $Zr(O^iPr)_4 \cdot {}^iPrOH$ (69 mg, 0.178 mmol), 4 Å MS, and a magnetic stirrer bar, and the flask was flushed with nitrogen and cooled to –20°C with a CCl_4/dry ice bath. CH_2Cl_2 (4 mL) was added and the solution stirred for 30 minutes at –20°C. L-(+)-diisopropyl tartrate (0.041 mL, 0.197 mmol) and ^tBuOOH (0.054 mL, 0.203 mmol) were added and the solution stirred for a further 30 minutes at –20°C. A solution of diallylic

alcohol **298** (19 mg, 0.060 mmol) in CH_2Cl_2 (4 mL) was added and the reaction placed in a freezer and monitored by TLC. After 24 hours H_2O (2.5 mL) and saturated aqueous Na_2SO_3 (2.5 mL) solution were added and the reaction stirred at room temperature for 30 minutes. The aqueous phase was extracted with CH_2Cl_2 (3 × 10 mL) and the combined organic fractions dried (Na_2SO_4), filtered through Celite, and evaporated to dryness. Column chromatography of the crude material, eluting with a solvent gradient of petrol/EtOAc, 1:0 to 1:1 gave:

Bis-epoxide **335** as a white solid (1.7 mg, 8%): R_f = 0.59 (EtOAc); analytical data as previously reported.

Monoepoxide **(–)-299** as a white solid (7.3 mg, 37%): R_f = 0.57 (EtOAc); Chiralpak-AD (25 × 0.46 cm), 90:10 hexane:IPA, 1 mL min^{-1}, thermostatic 10°C, detect by UV (210 nm). Retention times: **(+)-299** 25.5, **(–)-299** 30.2 min. Ee = 81.3%, second eluting peak in excess; analytical data as previously reported.

Diallylic alcohol **298** as a white solid (5 mg, 26%): R_f = 0.45 (EtOAc); analytical data as previously reported.

BLANK PAGE IN ORIGINAL

References

(1) Magnuson, S. R. *Tetrahedron* **1995**, *51*, 2167-2213.

(2) Poss, C. S.; Schreiber, S. L. *Acc. Chem. Res.* **1994**, *27*, 9-17.

(3) Schreiber, S. L.; Schreiber, T. S.; Smith, D. B. *J. Am. Chem. Soc.* **1987**, *109*, 1525-1529.

(4) Seebach, D.; Hungerbühler, E. *Modern Synthetic Methods*; Scheffold, R., Ed; Salle and Sauerländer: Frankfurt/Aarau, 1980, pp 91.

(5) Ward, R. S. *Chem. Soc. Rev.* **1990**, *19*, 1-19.

(6) Willis, M. C. *J. Chem. Soc., Perkin Trans. 1* **1999**, 1765-1784.

(7) Maier, M. *Group Selective Reactions*; Waldmann, H., Ed.; VCH: Weinheim, 1995, pp 203.

(8) Theisen, P. D.; Heathcock, C. H. *J. Org. Chem.* **1993**, *58*, 142-146.

(9) Theisen, P. D.; Heathcock, C. H. *J. Org. Chem.* **1988**, *53*, 2374-2378.

(10) Jaeschke, G.; Seebach, D. *J. Org. Chem.* **1998**, *63*, 1190-1197.

(11) Ramon, D. J.; Guillena, G.; Seebach, D. *Helv. Chim. Acta* **1996**, *79*, 875-894.

(12) Real, S. D.; Kronenthal, D. R.; Wu, H. Y. *Tetrahedron Lett.* **1993**, *34*, 8063-8066.

(13) Matsuki, K.; Inoue, H.; Ishida, A.; Takeda, M.; Nakagawa, M.; Hino, T. *Heterocycles* **1993**, *36*, 937-940.

(14) Matsuki, K.; Inoue, H.; Ishida, A.; Takeda, M.; Nakagawa, M.; Hino, T. *Chem. Pharm. Bull.* **1994**, *42*, 9-18.

(15) Kang, J. Y.; Lee, J. W.; Kim, J. I.; Pyun, C. *Tetrahedron Lett.* **1995**, *36*, 4265-4268.

(16) Kang, J. Y.; Lee, C. W.; Lim, G. J.; Cho, B. T. *Tetrahedron: Asymmetry* **1999**, *10*, 657-660.

(17) Romagnoli, R.; Roos, E. C.; Hiemstra, H.; Moolenaar, M. J.; Speckamp, W. N.; Kaptein, B.; Schoemaker, H. E. *Tetrahedron Lett.* **1994**, *35*, 1087-1090.

(18) Ostendorf, M.; Romagnoli, R.; Pereiro, I. C.; Roos, E. C.; Moolenaar, M. J.; Speckamp, W. N.; Hiemstra, H. *Tetrahedron: Asymmetry* **1997**, *8*, 1773-1789.

(19) Martinez, L. E.; Leighton, J. L.; Carsten, D. H.; Jacobsen, E. N. *J. Am. Chem. Soc.* **1995**, *117*, 5897-5898.

(20) Cole, B. M.; Shimizu, K. D.; Krueger, C. A.; Harrity, J. P. A.; Snapper, M. L.; Hoveyda, A. H. *Angew. Chem., Int. Ed. Engl.* **1996**, *35*, 1668-1671.

(21) Hayashi, M.; Ono, K.; Hoshimi, H.; Oguni, N. *J. Chem. Soc., Chem. Commun.* **1994**, 2699-2700.

(22) Hayashi, M.; Ono, K.; Hoshimi, H.; Oguni, N. *Tetrahedron* **1996**, *52*, 7817-7832.

(23) Hoppe, D.; Hense, T. *Angew. Chem., Int. Ed. Engl.* **1997**, *36*, 2283-2316.

(24) Hodgson, D. M.; Gibbs, A. R.; Lee, G. P. *Tetrahedron* **1996**, *52*, 14361-14384.

(25) O'Brien, P. *J. Chem. Soc., Perkin Trans. 1* **1998**, 1439-1457.

(26) Cox, P. J.; Simpkins, N. S. *Tetrahedron: Asymmetry* **1991**, *2*, 1-26.

(27) Asami, M. *J. Synth. Org. Chem. Japan* **1996**, *54*, 188-199.

(28) Bhuniya, D.; Gupta, A. D.; Singh, V. K. *Tetrahedron Lett.* **1995**, *36*, 2847-2850.

(29) Bhuniya, D.; Gupta, A. D.; Singh, V. K. *J. Org. Chem.* **1996**, *61*, 6108-6113.

(30) Asami, M.; Ishizaki, T.; Inoue, S. *Tetrahedron: Asymmetry* **1994**, *5*, 793-796.

(31) Sodergren, M. J.; Bertilsson, S. K.; Andersson, P. G. *J. Am. Chem. Soc.* **2000**, *122*, 6610-6618.

(32) Hodgson, D. M.; Lee, G. P. *J. Chem. Soc., Chem. Commun.* **1996**, 1015-1016.

(33) Schreiber, S. L.; Goulet, M. T.; Schulte, G. *J. Am. Chem. Soc.* **1987**, *109*, 4718-4720.

(34) Poss, C. S.; Rychnovsky, S. D.; Schreiber, S. L. *J. Am. Chem. Soc.* **1993**, *115*, 3360-3361.

(35) Honda, T.; Mizutani, H.; Kanai, K. *J. Chem. Soc. Perkin Trans. 1* **1996**, 1729-1739.

(36) Yang, Z.-C.; Jiang, X.-B.; Wang, Z.-M.; Zhou, W.-S. *J. Chem. Soc., Chem. Commun.* **1995**, 2389-2390.

(37) Hatakeyama, S.; Sakurai, K.; Takano, S. *J. Chem. Soc., Chem. Commun.* **1985**, 1759-1761.

(38) Hatakeyama, S.; Sakurai, K.; Takano, S. *Tetrahedron Lett.* **1986**, *27*, 4485-4488.

(39) Hatakeyama, S.; Satoh, K.; Takano, S. *Tetrahedron Lett.* **1993**, *34*, 7425-7428.

(40) Jager, V.; Schroter, D.; Koppenhoefer, B. *Tetrahedron* **1991**, *47*, 2195-2210.

(41) Babine, R. E. *Tetrahedron Lett.* **1986**, *27*, 5791-5794.

(42) Hafele, B.; Schroter, D.; Jager, V. *Angew. Chemie., Int. Ed. Engl.* **1986**, *25*, 87-89.

(43) Sharpless, K. B.; Behrens, C. H.; Katsuki, T.; Lee, A. W. M.; Martin, V. S.; Takatani, M.; Viti, S. M.; Walker, F. J.; Woodard, S. S. *Pure Appl. Chem.* **1983**, *55*, 589-604.

(44) Ibuka, T.; Tanaka, M.; Yamamoto, Y. *J. Chem. Soc., Chem. Commun.* **1989**, 967-969.

(45) Angelaud, R.; Landais, Y.; Schenk, K. *Tetrahedron Lett.* **1997**, *38*, 1407-1410.

(46) Tamao, K.; Tohma, T.; Inui, N.; Nakayama, O.; Ito, Y. *Tetrahedron Lett.* **1990**, *31*, 7333-7336.

(47) La, D. S.; Alexander, J. B.; Cefalo, D. R.; Graf, D. D.; Hoveyda, A. H.; Schrock, R. R. *J. Am. Chem. Soc.* **1998**, *120*, 9720-9721.

(48) Takano, S.; Yoshimitsu, T.; Ogasawara, K. *J. Org. Chem.* **1994**, *59*, 54-57.

(49) Inoue, T.; Kitagawa, O.; Saito, A.; Taguchi, T. *J. Org. Chem.* **1997**, *62*, 7384-7389.

(50) Greene, A. E.; Luche, M. J.; Serra, A. A. *J. Org. Chem.* **1985**, *50*, 3957-3962.

(51) Partridge, J. J.; Chadha, N. K.; Uskovic, M. R. *J. Am. Chem. Soc.* **1973**, *95*, 7171-7172.

(52) Partridge, J. J.; Chadha, N. K.; Uskovic, M. R. *Org. Synth.* **1985**, *63*, 44-56.

(53) Mikami, K.; Yoshida, A.; Matsumoto, Y. *Tetrahedron Lett.* **1996**, *37*, 8515-8518.

(54) Mikami, K.; Narisawa, S.; Shimizu, M.; Terada, M. *J. Am. Chem. Soc.* **1992**, *114*, 6566-6568.

(55) Harada, T.; Oku, A. *Synlett* **1994**, 95-104.

(56) Harada, T.; Ikemura, Y.; Nakajima, H.; Ohnishi, T.; Oku, A. *Chem. Lett.* **1990**, 1441-1444.

(57) Harada, T.; Hayashiya, T.; Wada, I.; Iwaake, N.; Oku, A. *J. Am. Chem. Soc.* **1987**, *109*, 527-532.

(58) Maezaki, N.; Sakamoto, A.; Nagahashi, N.; Soejima, M.; Li, Y. X.; Imamura, T.; Kojima, N.; Ohishi, H.; Sakaguchi, K.; Iwata, C.; Tanaka, T. *J. Org. Chem.* **2000**, *65*, 3284-3291.

(59) Kinugasa, M.; Harada, T.; Oku, A. *J. Am. Chem. Soc.* **1997**, *119*, 9067-9068.

(60) Kinugasa, M.; Harada, T.; Oku, A. *Tetrahedron Lett.* **1998**, *39*, 4529-4532.

(61) Fujioka, H.; Nagatomi, Y.; Kitagawa, H.; Kita, Y. *J. Am. Chem. Soc.* **1997**, *119*, 12016-12017.

(62) Fujioka, H.; Nagatomi, Y.; Kotoku, N.; Kitagawa, H.; Kita, Y. *Tetrahedron Lett.* **1998**, *39*, 7309-7312.

(63) Boons, G. J.; Entwistle, D. A.; Ley, S. V.; Woods, M. *Tetrahedron Lett.* **1993**, *34*, 5649-5652.

(64) Ruble, J. C.; Tweddell, J.; Fu, G. C. *J. Org. Chem.* **1998**, *63*, 2794-2795.

(65) Oriyama, T.; Imai, K.; Sano, T.; Hosoya, T. *Tetrahedron Lett.* **1998**, *39*, 3529-3532.

(66) Oriyama, T.; Imai, K.; Hosoya, T.; Sano, T. *Tetrahedron Lett.* **1998**, *39*, 397-400.

(67) Waldmann, H. *Enantioselective Protonation and Deprotonation*; Waldmann, H., Ed.; VCH: Weinheim, 1995, pp 19.

(68) Shirai, R.; Tanaka, M.; Koga, K. *J. Am. Chem. Soc.* **1986**, *108*, 543-545.

(69) Kim, H. D.; Kawasaki, H.; Nakajima, M.; Koga, K. *Tetrahedron Lett.* **1989**, *30*, 6537-6540.

(70) Naruse, Y.; Yamamoto, H. *Tetrahedron Lett.* **1986**, *27*, 1363-1366.

(71) Naruse, Y.; Yamamoto, H. *Tetrahedron* **1988**, *44*, 6021-6029.

(72) Fujisawa, T.; Watanabe, M.; Sato, T. *Chem. Lett.* **1984**, 2055-2058.

(73) Cohen, N. *Acc. Chem. Res.* **1976**, *9*, 412-417.

(74) Hajos, Z. G. *J. Org. Chem.* **1974**, *39*, 1615-1621.

(75) Eder, U.; Sauer, G.; Wiechert, R. *Angew. Chem., Int. Ed. Engl.* **1971**, *10*, 496-497.

(76) Hanessian, S.; Beaudoin, S. *Tetrahedron Lett.* **1992**, *33*, 7655-7658.

(77) Hanessian, S.; Delorme, D.; Beaudoin, S.; Leblanc, Y. *J. Am. Chem. Soc.* **1984**, *106*, 5754-5756.

(78) Arai, S.; Hamaguchi, S.; Shioiri, T. *Tetrahedron Lett.* **1998**, *39*, 2997-3000.

(79) Aube, J.; Wang, Y. G.; Hammond, M.; Tanol, M.; Takusagawa, F.; Vandervelde, D. *J. Am. Chem. Soc.* **1990**, *112*, 4879-4891.

(80) Gracias, V.; Milligan, G. L.; Aube, J. *J. Am. Chem. Soc.* **1995**, *117*, 8047-8048.

(81) Roush, W. R.; Park, J. C. *Tetrahedron Lett.* **1990**, *31*, 4707-4710.

(82) Roush, W. R.; Park, J. C. *J. Org. Chem.* **1990**, *55*, 1143-1144.

(83) Takemoto, Y.; Baba, Y.; Noguchi, I.; Iwata, C. *Tetrahedron Lett.* **1996**, *37*, 3345-3346.

(84) Kann, N.; Rein, T. *J. Org. Chem.* **1993**, *58*, 3802-3804.

(85) Oppolzer, W.; Debrabander, J.; Walther, E.; Bernardinelli, G. *Tetrahedron Lett.* **1995**, *36*, 4413-4416.

(86) Misumi, A.; Iwanaga, K.; Furuta, K.; Yamamoto, H. *J. Am. Chem. Soc.* **1985**, *107*, 3343-3345.

(87) Sakamoto, A.; Yamamoto, Y.; Oda, J. *J. Am. Chem. Soc.* **1987**, *109*, 7188-7189.

(88) Yamamoto, Y.; Sakamoto, A.; Nishioka, T.; Oda, J.; Fukazawa, Y. *J. Org. Chem.* **1991**, *56*, 1112-1119.

(89) Fuji, K.; Node, M.; Terada, S.; Murata, M.; Nagasawa, H.; Taga, T.; Machida, K. *J. Am. Chem. Soc.* **1985**, *107*, 6404-6406.

(90) Ihara, M.; Takahashi, M.; Taniguchi, N.; Yasui, K.; Fukumoto, K.; Kametani, T. *J. Chem. Soc., Perkin Trans. 1* **1989**, 897-903.

(91) Kashihara, H.; Suemune, H.; Kawahara, T.; Sakai, K. *Tetrahedron Lett.* **1987**, *28*, 6489-6492.

(92) Paetow, M.; Ahrens, H.; Hoppe, D. *Tetrahedron Lett.* **1992**, *33*, 5323-5326.

(93) Hiroya, K.; Ogasawara, K. *J. Chem. Soc., Chem. Commun.* **1995**, 2205-2206.

(94) Trost, B. M.; Cook, G. R. *Tetrahedron Lett.* **1996**, *37*, 7485-7488.

(95) Trost, B. M.; Patterson, D. E. *J. Org. Chem.* **1998**, *63*, 1339-1341.

(96) Hayashi, T.; Niizuma, S.; Kamikawa, T.; Suzuki, N.; Uozumi, Y. *J. Am. Chem. Soc.* **1995**, *117*, 9101-9102.

(97) Kamikawa, T.; Uozumi, Y.; Hayashi, T. *Tetrahedron Lett.* **1996**, *37*, 3161-3164.

(98) Chong, J. M.; Sokoll, K. K. *Tetrahedron Lett.* **1992**, *33*, 879-882.

(99) Duhamel, L.; Ravard, A.; Plaquevent, J. C. *Tetrahedron: Asymmetry* **1990**, *1*, 347-350.

(100) Doyle, M. P.; Dyatkin, A. B.; Roos, G. H. P.; Canas, F.; Pierson, D. A.; Vanbasten, A.; Muller, P.; Polleux, P. *J. Am. Chem. Soc.* **1994**, *116*, 4507-4508.

(101) Miyafuji, A.; Katsuki, T. *Tetrahedron* **1998**, *54*, 10339-10348.

(102) Punniyamurthy, T.; Miyafuji, A.; Katsuki, T. *Tetrahedron Lett.* **1998**, *39*, 8295-8298.

(103) Taylor, E. C.; Paudler, W. W. *Tetrahedron Lett.* **1960**, 1-3.

(104) Ayer, W. A.; Hayatsu, R.; de Mayo, P.; Reid, S. T.; Stothers, J. B. *Tetrahedron Lett.* **1961**, 648-653.

(105) Slomp, G.; MacKellar, F. A.; Paquette, L. A. *J. Am. Chem. Soc.* **1961**, *83*, 4472-4473.

(106) Taylor, E. C.; Kan, R. O.; Paudler, W. W. *J. Am. Chem. Soc.* **1961**, *83*, 4484-4485.

(107) Paquette, L. A.; Slomp, G. *J. Am. Chem. Soc.* **1963**, *85*, 765-769.

(108) Sharp IV, L. J.; Hammond, G. S. *Mol. Photochem.* **1970**, *2*, 225-250.

(109) Dilling, W. L.; Tefertiller, N. B.; Mitchell, A. B. *Mol. Photochem.* **1973**, *5*, 371-409.

(110) Corey, E. J.; Streith, J. *J. Am. Chem. Soc.* **1964**, *86*, 950-951.

(111) Nakamura, Y.; Kato, T.; Morita, Y. *J. Chem. Soc., Perkin Trans. 1* **1982**, 1187-1191.

(112) Matsushima, R.; Terada, K. *J. Chem. Soc., Perkin Trans. 2* **1985**, 1445-1448.

(113) Sieburth, S. M.; Cunard, N. T. *Tetrahedron* **1996**, *52*, 6251-6282.

(114) Sieburth, S. M.; Chen, J.; Ravindran, K.; Chen, J.-I. *J. Am. Chem. Soc.* **1996**, *118*, 10803-10810.

(115) Sieburth, S. M.; Ravindran, K. *Tetrahedron Lett.* **1994**, *35*, 3861-3864.

(116) Sieburth, S. M.; McGee, K. F., Jr.; Al-Tel, T. H. *Tetrahedron Lett.* **1999**, *40*, 4007-4010.

(117) Sieburth, S. M.; McGee, K. F., Jr.; Al-Tel, T. H. *J. Am. Chem. Soc.* **1998**, *120*, 587-588.

(118) Sieburth, S. M.; Al-Tel, T. H. *Book of Abstracts, 212th ACS National Meeting, Orlando, FL, August 25-29* **1996**, ORGN-419.

(119) Taylor, S. J. C.; McCague, R.; Wisdom, R.; Lee, C.; Dickson, K.; Ruecroft, G.; O'Brien, F.; Littlechild, J.; Bevan, J.; Roberts, S. M.; Evans, C. T. *Tetrahedron: Asymmetry* **1993**, *4*, 1117-1128.

(120) Taylor, E. C.; Kan, R. O. *J. Am. Chem. Soc.* **1963**, *85*, 776-784.

(121) Nakano, H.; Iwasa, K.; Okuyama, Y.; Hongo, K. *Tetrahedron: Asymmetry* **1996**, *7*, 2381-2386.

(122) Nakano, H.; Okuyama, Y.; Iwasa, K.; Hongo, H. *Tetrahedron: Asymmetry* **1994**, *5*, 1155-1156.

(123) Testa, E.; Pifferi, G.; Fontanella, L.; Aresi, V. *Liebigs Ann. Chem.* **1966**, *696*, 108-115.

(124) Somekawa, K.; Okuhira, H.; Sendayama, M.; Suishu, T.; Shimo, T. *J. Org. Chem.* **1992**, *57*, 5708-5712.

(125) Jouglet, B.; Rousseau, G. *Tetrahedron Lett.* **1993**, *34*, 2307-2310.

(126) Ho, P.-T. *Tetrahedron Lett.* **1978**, 1623-1626.

(127) Ishihara, K.; Kubota, M.; Kurihara, H.; Yamamoto, H. *J. Am. Chem. Soc.* **1995**, *117*, 4413-4414.

(128) Nakano, H.; Iwasa, K.; Kabuto, C.; Matsuzaki, H.; Hongo, H. *Chem. Pharm. Bull.* **1995**, *43*, 1254-1256.

(129) Davis, A. P.; Midland, M. M.; Morell, L. A. *Reduction with Metal Hydrides*; Helmchen, G., Hoffman, R. W., Mulzer, J. and Schaumann, E., Ed.; Thieme: Stuttgart, 1996; Vol. 7, pp 3988-4066.

(130) Nishizawa, M.; Noyori, R. *Reduction of C=X to CHXH by Chirally Modified Hydride Reagents* in *Comprehensive Organic Synthesis*; Trost, B. M., Ed., 1991; Vol. 8, pp 159-182.

(131) Corey, E. J.; Helal, C. J. *Angew. Chem., Int. Ed. Engl.* **1998**, *37*, 1987-2012.

(132) Noyori, R.; Tomino, I.; Tanimoto, Y.; Nishizawa, M. *J. Am. Chem. Soc.* **1984**, *106*, 6709-6716.

(133) Noyori, R.; Tomino, I.; Yamada, M.; Nishizawa, M. *J. Am. Chem. Soc.* **1984**, *106*, 6717-6725.

(134) Langa, F.; DelaCruz, P.; DelaHoz, A.; DiazOrtiz, A.; DiezBarra, E. *Contemporary Organic Synthesis* **1997**, *4*, 373-386.

(135) Almena, I.; DiazOrtiz, A.; DiezBarra, E.; DelaHoz, A.; Loupy, A. *Chem. Lett.* **1996**, 333-334.

(136) Winterfeldt, E. *Synthesis* **1975**, 617-630.

(137) Laing, M. *Proc. Chem. Soc.* **1964**, 343.

(138) Mori, M.; Uozumi, Y.; Kimura, M.; Ban, Y. *Tetrahedron* **1986**, *42*, 3793-3806.

(139) Spivey, A. C.; Frampton, C. S.; Battersby, A. R. *J. Chem. Soc., Perkin Trans. 1* **1996**, 2103-2110.

(140) Evans, D. A.; Carter, P. H.; Dinsmore, C. J.; Barrow, J. C.; Katz, J. L.; Kung, D. W. *Tetrahedron Lett.* **1997**, *38*, 4535-4538.

(141) Husain, M. I.; Shukla, S. *Indian J. Chem., Sect. B* **1986**, *25*, 983-985.

(142) Grehn, L.; Gunnarsson, K.; Ragnarsson, U. *Acta Chem. Scand., Ser. B* **1986**, *40*, 745-750.

(143) Flynn, D. L.; Zelle, R. E.; Grieco, P. A. *J. Org. Chem.* **1983**, *48*, 2424-2426.

(144) Dieter, R. K.; Sharma, R. R. *J. Org. Chem.* **1996**, *61*, 4180-4184.

(145) Saari, W. S.; Fisher, T. E. *Synthesis* **1990**, 453-454.

(146) Trost, B. M.; Li, Y. *J. Am. Chem. Soc.* **1996**, *118*, 6625-6633.

(147) Sieburth, S. M.; Rucando, D.; Lin, C.-H. *J. Org. Chem.* **1999**, *64*, 954-959.

(148) Krishnamurthy, S.; Vogel, F.; Brown, H. C. *J. Org. Chem.* **1977**, *42*, 2534-2536.

(149) Corey, E. J.; Bakshi, R. K.; Shibata, S. *J. Am. Chem. Soc.* **1987**, *109*, 5551-5553.

(150) Xavier, L. C.; Mohan, J. J.; Mathre, D. J.; Thompson, J. D.; Carroll, J. D.; Corley, E. G.; Desmond, R. *Org. Synth.* **1996**, *74*, 50-71.

(151) Jones, D. K.; Liotta, D. C.; Shinkai, I.; Mathre, D. J. *J. Org. Chem.* **1993**, *58*, 799-801.

(152) Dale, J. A.; Dull, D. L.; Mosher, H. S. *J. Org. Chem.* **1969**, *34*, 2543-2549.

(153) Ward, D. E.; Rhee, C. K. *Tetrahedron Lett.* **1991**, *32*, 7165-7166.

(154) Zhang, F. Y.; Yip, C. W.; Chan, A. S. C. *Tetrahedron: Asymmetry* **1996**, *7*, 3135-3140.

(155) Corey, E. J.; Cheng, X. M.; Cimprich, K. A.; Sarshar, S. *Tetrahedron Lett.* **1991**, *32*, 6835-6838.

(156) Sisko, J.; Henry, J. R.; Weinreb, S. M. *J. Org. Chem.* **1993**, *58*, 4945-4951.

(157) Katagiri, N.; Muto, M.; Nomura, M.; Higashikawa, T.; Kaneko, C. *Chem. Pharm. Bull.* **1991**, *39*, 1112-1122.

(158) Posner, G. H.; Vinader, V.; Afarinkia, K. *J. Org. Chem.* **1992**, *57*, 4088-4097.

(159) Szeja, W. *Synthesis* **1979**, 822-823.

(160) Abu-Zeid, Y. M.; Abu-Elela, Z. *Proc. Pharm. Soc. Egypt, Sci. Ed.* **1957**, *39*, 57-61.

(161) Cristol, S. J.; Harrington, K.; Singer, M. S. *J. Am. Chem. Soc.* **1966**, *88*.

(162) Edwards, G. L.; Muldoon, C. A.; Sinclair, D. J. *Tetrahedron* **1996**, *52*, 7779-7788.

(163) Craine, L.; Raban, M. *Chem. Rev.* **1989**, *89*, 689-712.

(164) Davis, F. A.; Nadir, U. K. *Org. Prep. Proc. Int.* **1979**, *11*, 33-51.

(165) Wilson, L. J.; Liotta, D. C. *J. Org. Chem.* **1992**, *57*, 1948-1950.

(166) Renga, J. M.; Wang, P. C. *Tetrahedron Lett.* **1985**, *26*, 1175-1178.

(167) Cantrill, A. A.; Sweeney, J. B. *Synlett* **1995**, 1277-9.

(168) Osborn, H. M. I.; Sweeney, J. B.; Howson, B. *Synlett* **1994**, 145-7.

(169) Thorsen, M.; Yde, B.; Pedersen, U.; Clausen, K.; Lawesson, S. O. *Tetrahedron* **1983**, *39*, 3429-3435.

(170) Knapp, S.; Ornaf, R. M.; Rodriques, K. E. *J. Am. Chem. Soc.* **1983**, *105*, 5494-5495.

(171) Kam, B. L.; Oppenheimer, N. J. *J. Org. Chem.* **1981**, *46*, 3268-3272.

(172) Faith, W. C.; Booth, C. A.; Foxman, B. M.; Snider, B. B. *J. Org. Chem.* **1985**, *50*, 1983-1985.

(173) Eames, J.; Mitchell, H. J.; Nelson, A.; O'Brien, P.; Warren, S.; Wyatt, P. *Tetrahedron Lett.* **1995**, *36*, 1719-1722.

(174) Adam, W.; Bialas, J.; Hadjiarapoglou, L. *Chem. Ber.* **1991**, *124*, 2377-2377.

(175) Kishi, Y.; Aratani, M.; Tanino, H.; Fukuyama, T.; Goto, T. *J. Chem. Soc., Chem. Commun.* **1972**.

(176) Cooper, M. S.; Heaney, H.; Newbold, A. J.; Sanderson, W. R. *Synlett* **1990**, 533-535.

(177) Burgi, H. B.; Dunitz, J. D.; Lehn, J. M.; Wipff, G. *Tetrahedron* **1974**, *30*, 1563.

(178) Jacobsen, E. N.; Zhang, W.; Muci, A. R.; Ecker, J. R.; Deng, L. *J. Am. Chem. Soc.* **1991**, *113*, 7063-7064.

(179) Nishiyama, H.; Yamaguchi, S.; Kondo, M.; Itoh, K. *J. Org. Chem.* **1992**, *57*, 4306-4309.

(180) Schwink, L.; Knochel, P. *Chem. Eur. J.* **1998**, *4*, 950-968.

(181) Panday, S. K.; Griffartbrunet, D.; Langlois, N. *Tetrahedron Lett.* **1994**, *35*, 6673-6676.

(182) He, F.; Bo, Y. X.; Altom, J. D.; Corey, E. J. *J. Am. Chem. Soc.* **1999**, *121*, 6771-6772.

(183) Munoz, O.; Penaloza, A.; Gonzalez, A. G.; Ravelo, A. G.; Bazzocchi, I. L.; Alvarenga, N. L. *The Celastraceae from Latin America Chemistry and Biological Activity*; Atta-ur-Rahman, Ed.; Elsevier, **1996**; Vol. 18, pp 739-783.

(184) Szendrei, K. *Bull. Narc.* **1980**, *32*, 5.

(185) Zheng, Y. L.; Xu, Y.; Lin, J. F. *Acta Pharm. Sinica* **1989**, *24*, 568-572.

(186) Beroza, M.; Bottger, G. T. *J. Econom. Entomol.* **1954**, *47*, 188-189.

(187) Kuo, Y. H.; Kuo, L. M. Y. *Phytochemistry* **1997**, *44*, 1275-1281.

(188) Wakabayashi, N.; Wu, W. J.; Waters, R. M.; Redfern, R. E.; Mills, G. D. J.; Demilo, A. B.; Lusby, W. R.; Andrzejewski, D. *J. Nat. Prod.* **1988**, *51*, 537-542.

(189) Duan, H.; Takaishi, Y.; Imakura, Y.; Jia, Y.; Li, T.; Consentino, L. M.; Lee, K.-H. *J. Nat. Prod.* **2000**, *63*, 357-361.

(190) Duan, H.; Takaishi, Y.; Bando, M.; Kido, M.; Imakura, Y.; Lee, K.-H. *Tetrahedron Lett.* **1999**, *40*, 2969-2972.

(191) Katsuki, T.; Martin, V. S. *Org. React.* **1996**, *48*, 1-299.

(192) Sharpless, K. B.; Katsuki, T. *J. Am. Chem. Soc.* **1980**, *102*, 5976-5978.

(193) Vogel, E.; Klug, W.; Breuer, A. *Org. Synth.* **1974**, *54*, 11 - 18.

(194) Vogel, E.; Klug, W.; Breuer, A. *Org. Synth.* **1976**, *55*, 86 - 90.

(195) Nagata, W.; Yoshioka, M.; Okumura, T. *Tetrahedron Lett.* **1966**, *8*, 847-852.

(196) Sharpless, K. B.; Michaelson, R. C. *J. Am. Chem. Soc.* **1973**, *95*, 6136-6137.

(197) Palumbo, G.; Ferreri, C.; Caputo, R. *Tetrahedron Lett.* **1983**, *24*, 1307 - 1310.

(198) Murata, S.; Suzuki, M.; Noyori, R. *J. Am. Chem. Soc.* **1979**, *101*, 2738 - 2739.

(199) Detty, M. R. *J. Org. Chem.* **1980**, *45*, 924-927.

(200) Detty, M. R.; Seidler, M. D. *J. Org. Chem.* **1981**, *46*, 1283 - 1292.

(201) Cha, J. K.; Christ, W. J.; Kishi, Y. *Tetrahedron* **1984**, *40*, 2247-2255.

(202) Saito, S.; Morikawa, Y.; Moriwake, T. *J. Org. Chem.* **1990**, *55*, 5424-5426.

(203) VanRheenan, V.; Kelly, R. C.; Cha, D. Y. *Tetrahedron Lett.* **1976**, 1973-1976.

(204) Kolb, H. C.; VanNieuwenhze, M. S.; Sharpless, K. B. *Chem. Rev.* **1994**, *94*, 2483.

(205) Gao, Y.; Hanson, R. M.; Klunder, J. M.; Ko, S. Y.; Masamune, H.; Sharpless, K. B. *J. Am. Chem. Soc.* **1987**, *109*, 5765-5780.

(206) Lu, L. D.-L.; Johnson, R. A.; Finn, M. G.; Sharpless, K. B. *J. Org. Chem.* **1984**, *49*, 731-733.

(207) Yang, Z.-C.; Jiang, X.-B.; Wang, Z.-M.; Zhou, W.-S. *J. Chem. Soc., Perkin Trans. 1* **1997**, 317-321.

(208) Dittmer, D. C.; Discordia, R. P.; Zhang, Y. Z.; Murphy, C. K.; Kumar, A.; Pepito, A. S.; Wang, Y. S. *J. Org. Chem.* **1993**, *58*, 718-731.

(209) Takano, S.; Iwabuchi, Y.; Ogasawara, K. *Tetrahedron Lett.* **1991**, *32*, 3527-3528.

(210) Ikegami, S.; Katsuki, T.; Yamaguchi, M. *Chem. Lett.* **1987**, 83-84.

(211) Bonchio, M.; Licini, G.; Di Furia, F.; Mantovani, S.; Modena, G.; Nugent, W. A. *J. Org. Chem.* **1999**, *64*, 1326-1330.

(212) Bajwa, J. S.; Anderson, R. C. *Tetrahedron Lett.* **1991**, *32*, 3021-3024.

(213) Ciaccio, J. A.; Heller, E.; Talbot, A. *Synlett* **1991**, 248-250.

(214) Iranpoor, N.; Kazemi, F.; Salehi, P. *Synth. Commun.* **1997**, *27*, 1247-1258.

(215) Gypser, A.; Michel, D.; Nirschl, D. S.; Sharpless, K. B. *J. Org. Chem.* **1998**, *63*, 7322-7327.

(216) Iwasawa, N.; Kato, T.; Narasaka, K. *Chem. Lett.* **1988**, 1721-1724.

(217) Kusama, H.; Hara, R.; Kawahara, S.; Nishimori, T.; Kashima, H.; Nakamura, N.; Morihira, K.; Kuwajima, I. *J. Am. Chem. Soc.* **2000**, *122*, 3811-3820.

(218) Morihira, K.; Hara, R.; Kawahara, S.; Nishimori, T.; Nakamura, N.; Kusama, H.; Kuwajima, I. *J. Am. Chem. Soc.* **1998**, *120*, 12980-12981.

(219) Still, W. C.; Kahn, M.; Mitra, M. *J. Org. Chem.* **1978**, *43*, 2923.

(220) Kurita, J.; Yoneda, T.; Kakusawa, N.; Tsuchiya, T. *Chem. Pharm. Bull.* **1990**, *38*, 2911-2918.

(221) Posner, G. H.; Switzer, C. *J. Org. Chem.* **1987**, *52*, 1642-4.

(222) Kurzer, F. *Org. Synth.* **1954**, *34*, 93-96.

(223) Kurzer, F.; Powell, J. R. *Org. Synth.* **1955**, *35*, 99-101.

(224) Nishiyama, H.; Kondo, M.; Nakamura, T.; Itoh, K. *Organometallics* **1991**, *10*, 500-508.

(225) Perrin, D. D.; Armarego, W. L. F. *Purification of Laboratory Chemicals*; 3rd Ed. ed.; Pergamon Press: London, 1988.

Appenidces

Appendix 1: Purification of solvents

All solvents were distilled before use. 'Petrol' refers to the fraction of light petroleum-ether boiling between 40–60°C. Commercial grade solvents used for flash chromatography were distilled before use. Anhydrous solvents were obtained as follows:[225]

Acetone	Stirred over K_2CO_3 under nitrogen for 24 h, distilled, and stored over 4Å MS under nitrogen.
Acetonitrile	Stirred over CaH_2 under nitrogen for 24 h, distilled, and stored over 4 Å MS under nitrogen.
Benzene	Distilled from sodium metal under nitrogen immediately prior to use.
Carbon tetrachloride	Careful fractional distillation prior to use.
Chloroform	Washed with water, dried with K_2CO_3, filtered, refluxed over $CaCl_2$ for 6 h, then distilled immediately prior to use.
Dichloromethane	Distilled from CaH_2 under nitrogen immediately prior to use.
Diethyl ether	Distilled from sodium/benzophenone ketyl under nitrogen immediately prior to use.
Dimethylformamide	Stirred over CaH_2 under nitrogen for 24 h, distilled under reduced pressure, and stored over 4 Å MS under nitrogen.
Dimethylsulfoxide	Distilled from CaH_2 under nitrogen prior to use.
1,4-Dioxane	Distilled from sodium/benzophenone ketyl under nitrogen immediately prior to use.
Ethanol	Distilled from $Mg(OEt)_2$ under nitrogen immediately prior to use.
Ethyl acetate	Stirred over CaH_2 under nitrogen for 24 h, distilled, and stored over 4 Å MS under nitrogen.
Methanol	Distilled from $Mg(OMe)_2$ under nitrogen immediately prior to use.

Pyridine	Pyridine was refluxed with calcium hydride for 24 h, distilled, and stored over 4 Å MS.
Tetrahydrofuran	Distilled from sodium/benzophenone ketyl under nitrogen immediately prior to use.
Toluene	Distilled from sodium metal under nitrogen immediately prior to use.

Appendix 2: Purification of reagents

All chemicals were handled in accordance with COSHH regulations. All reagents were used as commercially supplied unless specified below:[225]

Acetic anhydride

Anhydrous acetic anhydride was prepared by distillation from quinoline (1% by volume).

Acetyl chloride

Acetyl chloride was refluxed with phosphorus pentachloride for 3 h, and then distilled.

Benzoyl chloride

Benzoyl chloride was refluxed with thionyl chloride (1:1) for 4 h, and then distilled under reduced pressure.

Benzyl bromide

Benzyl bromide was distilled from calcium chloride under reduced pressure, in the dark.

n-Butyl lithium

Solutions of ^{n}BuLi were used as supplied by Aldrich and titrated with diphenylacetic acid immediately prior to use.

meta-Chloroperbenzoic acid

meta-Chloroperbenzoic acid was recrystallised from CH_2Cl_2, and stored at 0°C.

Diisopropylethylamine

Diisopropylethylamine was distilled from CaH_2.

Dimethyldioxirane

Dimethyldioxirane was prepared by the method of Adam and stored in a freezer over 4 Å MS.

Lithium diisopropylamine

Lithium diisopropylamine was prepared by mixing equal amounts of ^{n}BuLi and diisopropylamine in anhydrous THF at -78°C and warming to 0°C.

Methanesulfonyl chloride

Methanesulfonyl chloride was distilled from phosphorus pentoxide under reduced pressure.

Potassium *tert*-butoxide

Potassium *tert*-butoxide was sublimed (220°C/1 mm Hg) prior to use.

Thionyl chloride

Thionyl chloride was distilled from quinoline and then re-distilled prior to use.

***para*-Toluenesulfonic acid**

Anhydrous *para*-toluenesulfonic acid was obtained by azeotropic distillation with benzene, crystallisation from chloroform, and drying under high vacuum.

Triethylamine

Triethylamine was stirred over calcium hydride for 24 h, distilled, and stored over 4 Å MS.

Triphenylphosphine

Triphenylphosphine was crystallised from petrol, and dried under high vacuum.

Appendix 3: X-ray crystal data

X-ray crystal structure data for *N*-Boc tetrahydro dimer (227)

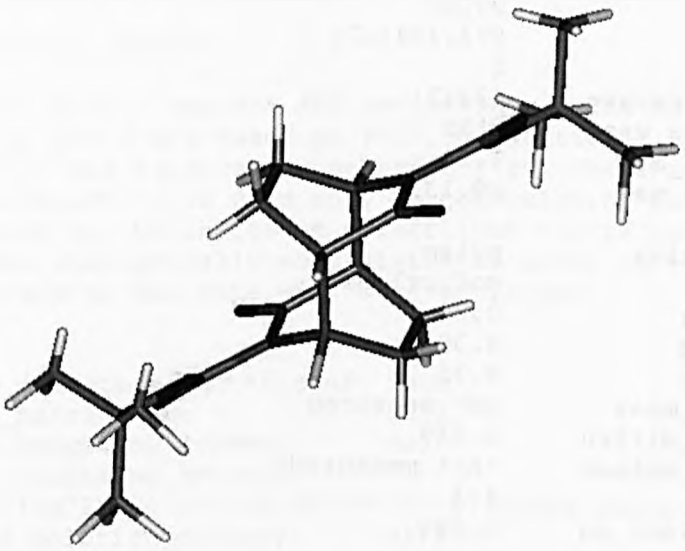

227

```
data_csf73s

_audit_creation_method            SHELXL-97
_chemical_name_systematic
;
 ?
;
_chemical_name_common             ?
_chemical_melting_point           ?
_chemical_formula_moiety          ?
_chemical_formula_sum
 'C20 H30 N2 O6'
_chemical_formula_weight          394.46

loop_
 _atom_type_symbol
 _atom_type_description
 _atom_type_scat_dispersion_real
 _atom_type_scat_dispersion_imag
 _atom_type_scat_source
 'C'  'C'   0.0033   0.0016
 'International Tables Vol C Tables 4.2.6.8 and 6.1.1.4'
 'H'  'H'   0.0000   0.0000
 'International Tables Vol C Tables 4.2.6.8 and 6.1.1.4'
 'N'  'N'   0.0061   0.0033
 'International Tables Vol C Tables 4.2.6.8 and 6.1.1.4'
 'O'  'O'   0.0106   0.0060
 'International Tables Vol C Tables 4.2.6.8 and 6.1.1.4'

_symmetry_cell_setting            Monoclinic
_symmetry_space_group_name_H-M    P2(1)/n

loop_
 _symmetry_equiv_pos_as_xyz
 'x, y, z'
 '-x+1/2, y+1/2, -z+1/2'
 '-x, -y, -z'
```

```
 'x-1/2, -y-1/2, z-1/2'

_cell_length_a                      6.210
_cell_length_b                      25.8518(2)
_cell_length_c                      6.45690(10)
_cell_angle_alpha                   90.00
_cell_angle_beta                    110.3090(10)
_cell_angle_gamma                   90.00
_cell_volume                        972.164(17)
_cell_formula_units_Z               2
_cell_measurement_temperature       123(2)
_cell_measurement_reflns_used       8192
_cell_measurement_theta_min         1.58
_cell_measurement_theta_max         29.13

_exptl_crystal_description          prism
_exptl_crystal_colour               colourless
_exptl_crystal_size_max             0.20
_exptl_crystal_size_mid             0.30
_exptl_crystal_size_min             0.35
_exptl_crystal_density_meas         not_measured
_exptl_crystal_density_diffrn       1.348
_exptl_crystal_density_method       'not measured'
_exptl_crystal_F_000                424
_exptl_absorpt_coefficient_mu       0.099
_exptl_absorpt_correction_type      none
_exptl_absorpt_correction_T_min     ?
_exptl_absorpt_correction_T_max     ?
_exptl_absorpt_process_details      ?

_exptl_special_details
;
 ?
;

_diffrn_ambient_temperature             123(1)
_diffrn_radiation_wavelength            0.71073
_diffrn_radiation_type                  MoK\a
_diffrn_radiation_source                'fine-focus sealed tube'
_diffrn_radiation_monochromator         graphite
_diffrn_measurement_device_type         'Bruker AXS 1K CCD area detector'
_diffrn_measurement_method              'narrow frame \w scans'
_diffrn_detector_area_resol_mean        8.192
_diffrn_standards_number                'see text'
_diffrn_standards_interval_count        ?
_diffrn_standards_interval_time         ?
_diffrn_standards_decay_%               none
_diffrn_reflns_number                   9608
_diffrn_reflns_av_R_equivalents         0.0163
_diffrn_reflns_av_sigmaI/netI           0.0112
_diffrn_reflns_limit_h_min              -7
_diffrn_reflns_limit_h_max              7
_diffrn_reflns_limit_k_min              -32
_diffrn_reflns_limit_k_max              32
_diffrn_reflns_limit_l_min              -8
_diffrn_reflns_limit_l_max               8
_diffrn_reflns_theta_min                1.58
_diffrn_reflns_theta_max                26.37
_diffrn_reflns_theta_full               26.37
_diffrn_measured_fraction_theta_full    0.998
_reflns_number_total                    1977
_reflns_number_gt                       1914
   _reflns_threshold_expression            >2sigma(I)
```

```
_computing_data_collection          'SMART (Bruker AXS, 1995)'
_computing_cell_refinement          'SMART & SAINT (Bruker AXS, 1995)'
_computing_data_reduction           'SAINT (Bruker AXS, 1995)'
_computing_structure_solution       'SHELXTL (Sheldrick, 1994)'
_computing_structure_refinement     'SHELXTL (Sheldrick, 1994)'
_computing_molecular_graphics       'SHELXTL (Sheldrick, 1994)'
_computing_publication_material     'SHELXTL (Sheldrick, 1994)'

_refine_special_details
;
 Refinement of F^2^ against ALL reflections.  The weighted R-factor wR and
 goodness of fit S are based on F^2^, conventional R-factors R are based
 on F, with F set to zero for negative F^2^. The threshold expression of
 F^2^ > 2sigma(F^2^) is used only for calculating R-factors(gt) etc. and is
 not relevant to the choice of reflections for refinement.  R-factors based
 on F^2^ are statistically about twice as large as those based on F, and R-
 factors based on ALL data will be even larger.
;

_refine_ls_structure_factor_coef  Fsqd
_refine_ls_matrix_type            full
_refine_ls_weighting_scheme       calc
_refine_ls_weighting_details
 'calc w=1/[\s^2^(Fo^2^)+(0.0770P)^2^+0.3500P] where P=(Fo^2^+2Fc^2^)/3'
_atom_sites_solution_primary      direct
_atom_sites_solution_secondary    difmap
_atom_sites_solution_hydrogens    geom
_refine_ls_hydrogen_treatment     mixed
_refine_ls_extinction_method      none
_refine_ls_extinction_coef        none
_refine_ls_number_reflns          1977
_refine_ls_number_parameters      187
_refine_ls_number_restraints      0
_refine_ls_R_factor_all           0.0366
_refine_ls_R_factor_gt            0.0356
_refine_ls_wR_factor_ref          0.1083
_refine_ls_wR_factor_gt           0.1072
_refine_ls_goodness_of_fit_ref    1.001
_refine_ls_restrained_S_all       1.001
_refine_ls_shift/su_max           0.000
_refine_ls_shift/su_mean          0.000
_refine_diff_density_max          0.379
_refine_diff_density_min         -0.243
_refine_diff_density_rms          0.077

loop_
 _atom_site_label
 _atom_site_type_symbol
 _atom_site_fract_x
 _atom_site_fract_y
 _atom_site_fract_z
 _atom_site_U_iso_or_equiv
 _atom_site_adp_type
 _atom_site_occupancy
 _atom_site_symmetry_multiplicity
 _atom_site_calc_flag
 _atom_site_refinement_flags
 _atom_site_disorder_assembly
 _atom_site_disorder_group
O1 O 0.58701(14) 0.05892(3) 0.66166(13) 0.0172(2) Uani 1 1 d . . .
O2 O 0.87525(15) 0.13225(3) 0.60162(15) 0.0214(2) Uani 1 1 d . . .
O3 O 1.22931(14) 0.12087(3) 0.86262(13) 0.0162(2) Uani 1 1 d . . .
```

```
N1 N 0.98377(15) 0.05425(4) 0.78733(14) 0.0122(2) Uani 1 1 d . . .
C1 C 0.76285(18) 0.03461(4) 0.74965(17) 0.0122(2) Uani 1 1 d . . .
C2 C 1.18467(18) 0.02131(4) 0.90795(17) 0.0112(2) Uani 1 1 d . . .
H2A H 1.312(2) 0.0376(5) 0.886(2) 0.009(3) Uiso 1 1 d . . .
C3 C 1.15361(18) -0.03191(4) 0.79482(17) 0.0130(2) Uani 1 1 d . . .
H3A H 1.181(3) -0.0273(6) 0.656(3) 0.020(4) Uiso 1 1 d . . .
H3B H 1.273(3) -0.0542(6) 0.885(2) 0.014(3) Uiso 1 1 d . . .
C4 C 0.91341(19) -0.05540(4) 0.74988(18) 0.0133(3) Uani 1 1 d . . .
H4A H 0.834(3) -0.0598(6) 0.590(3) 0.020(4) Uiso 1 1 d . . .
H4B H 0.923(2) -0.0899(6) 0.814(2) 0.014(3) Uiso 1 1 d . . .
C5 C 0.76123(18) -0.02038(4) 0.83417(17) 0.0119(2) Uani 1 1 d . . .
H5A H 0.603(2) -0.0309(5) 0.765(2) 0.012(3) Uiso 1 1 d . . .
C6 C 1.01703(19) 0.10640(4) 0.73628(18) 0.0141(2) Uani 1 1 d . . .
C7 C 1.3183(2) 0.17332(4) 0.8415(2) 0.0181(3) Uani 1 1 d . . .
C8 C 1.1806(2) 0.21324(5) 0.9166(2) 0.0243(3) Uani 1 1 d . . .
H8A H 1.189(3) 0.2052(7) 1.068(3) 0.038(5) Uiso 1 1 d . . .
H8B H 1.251(3) 0.2478(7) 0.925(3) 0.036(5) Uiso 1 1 d . . .
H8C H 1.022(3) 0.2146(7) 0.818(3) 0.032(4) Uiso 1 1 d . . .
C9 C 1.5653(2) 0.17003(5) 1.0014(2) 0.0255(3) Uani 1 1 d . . .
H9A H 1.568(3) 0.1616(7) 1.152(3) 0.035(4) Uiso 1 1 d . . .
H9B H 1.640(3) 0.2035(7) 1.007(3) 0.036(5) Uiso 1 1 d . . .
H9C H 1.652(3) 0.1443(7) 0.949(3) 0.033(4) Uiso 1 1 d . . .
C10 C 1.3139(2) 0.18191(5) 0.6060(2) 0.0235(3) Uani 1 1 d . . .
H10A H 1.394(3) 0.2156(7) 0.602(3) 0.039(5) Uiso 1 1 d . . .
H10B H 1.156(3) 0.1846(7) 0.499(3) 0.031(4) Uiso 1 1 d . . .
H10C H 1.390(3) 0.1532(7) 0.562(3) 0.034(4) Uiso 1 1 d . . .

loop_
 _atom_site_aniso_label
 _atom_site_aniso_U_11
 _atom_site_aniso_U_22
 _atom_site_aniso_U_33
 _atom_site_aniso_U_23
 _atom_site_aniso_U_13
 _atom_site_aniso_U_12
O1 0.0118(4) 0.0213(4) 0.0170(4) 0.0030(3) 0.0032(3) 0.0031(3)
O2 0.0179(4) 0.0204(4) 0.0230(5) 0.0080(3) 0.0035(4) 0.0021(3)
O3 0.0147(4) 0.0139(4) 0.0188(4) 0.0022(3) 0.0043(3) -0.0025(3)
N1 0.0099(5) 0.0147(5) 0.0114(4) 0.0014(3) 0.0030(4) 0.0009(3)
C1 0.0113(5) 0.0175(5) 0.0083(5) -0.0016(4) 0.0038(4) 0.0000(4)
C2 0.0085(5) 0.0144(5) 0.0109(5) 0.0013(4) 0.0036(4) 0.0008(4)
C3 0.0115(5) 0.0172(5) 0.0107(5) -0.0005(4) 0.0046(4) 0.0011(4)
C4 0.0126(5) 0.0152(5) 0.0122(5) -0.0023(4) 0.0043(4) -0.0010(4)
C5 0.0086(5) 0.0162(5) 0.0101(5) -0.0006(4) 0.0023(4) -0.0011(4)
C6 0.0141(5) 0.0169(5) 0.0126(5) 0.0006(4) 0.0064(4) 0.0006(4)
C7 0.0200(6) 0.0111(5) 0.0243(6) 0.0005(4) 0.0093(5) -0.0027(4)
C8 0.0280(7) 0.0172(6) 0.0298(7) -0.0021(5) 0.0128(6) 0.0018(5)
C9 0.0198(6) 0.0179(6) 0.0363(7) -0.0022(5) 0.0064(5) -0.0052(5)
C10 0.0283(7) 0.0187(6) 0.0284(7) 0.0041(5) 0.0158(6) -0.0010(5)

_geom_special_details
;
 All esds (except the esd in the dihedral angle between two l.s. planes)
 are estimated using the full covariance matrix.  The cell esds are taken
 into account individually in the estimation of esds in distances, angles
 and torsion angles; correlations between esds in cell parameters are only
 used when they are defined by crystal symmetry.  An approximate
(isotropic)
 treatment of cell esds is used for estimating esds involving l.s. planes.
;

loop_
    _geom_bond_atom_site_label_1
```

```
  _geom_bond_atom_site_label_2
  _geom_bond_distance
  _geom_bond_site_symmetry_2
  _geom_bond_publ_flag
 O1 C1 1.2164(14) . ?
 O2 C6 1.2026(14) . ?
 O3 C6 1.3404(14) . ?
 O3 C7 1.4881(13) . ?
 N1 C1 1.4027(14) . ?
 N1 C6 1.4199(14) . ?
 N1 C2 1.4879(13) . ?
 C1 C5 1.5240(15) . ?
 C2 C3 1.5382(14) . ?
 C2 C5 1.5805(14) 3_757 ?
 C2 H2A 0.948(15) . ?
 C3 C4 1.5420(15) . ?
 C3 H3A 0.974(16) . ?
 C3 H3B 0.960(15) . ?
 C4 C5 1.5381(15) . ?
 C4 H4A 0.982(16) . ?
 C4 H4B 0.976(15) . ?
 C5 C2 1.5805(14) 3_757 ?
 C5 H5A 0.966(14) . ?
 C7 C8 1.5230(17) . ?
 C7 C9 1.5256(17) . ?
 C7 C10 1.5277(17) . ?
 C8 H8A 0.98(2) . ?
 C8 H8B 0.988(19) . ?
 C8 H8C 0.970(19) . ?
 C9 H9A 0.988(19) . ?
 C9 H9B 0.977(19) . ?
 C9 H9C 0.987(19) . ?
 C10 H10A 1.010(19) . ?
 C10 H10B 0.988(18) . ?
 C10 H10C 0.975(19) . ?

 loop_
  _geom_angle_atom_site_label_1
  _geom_angle_atom_site_label_2
  _geom_angle_atom_site_label_3
  _geom_angle
  _geom_angle_site_symmetry_1
  _geom_angle_site_symmetry_3
  _geom_angle_publ_flag
C6 O3 C7 121.09(9) . . ?
C1 N1 C6 121.05(9) . . ?
C1 N1 C2 118.40(9) . . ?
C6 N1 C2 120.12(9) . . ?
O1 C1 N1 124.01(10) . . ?
O1 C1 C5 122.20(10) . . ?
N1 C1 C5 113.78(9) . . ?
N1 C2 C3 108.61(8) . . ?
N1 C2 C5 113.15(8) . 3_757 ?
C3 C2 C5 115.62(9) . 3_757 ?
N1 C2 H2A 105.0(8) . . ?
C3 C2 H2A 107.4(8) . . ?
C5 C2 H2A 106.3(8) 3_757 . ?
C2 C3 C4 113.29(9) . . ?
C2 C3 H3A 107.0(9) . . ?
C4 C3 H3A 110.0(9) . . ?
C2 C3 H3B 107.9(9) . . ?
C4 C3 H3B 111.6(9) . . ?
H3A C3 H3B 106.7(12) . . ?
```

```
C5 C4 C3 112.00(9) . . ?
C5 C4 H4A 106.9(9) . . ?
C3 C4 H4A 110.3(9) . . ?
C5 C4 H4B 110.1(8) . . ?
C3 C4 H4B 111.5(8) . . ?
H4A C4 H4B 105.7(12) . . ?
C1 C5 C4 109.94(9) . . ?
C1 C5 C2 111.47(8) . 3_757 ?
C4 C5 C2 115.58(9) . 3_757 ?
C1 C5 H5A 103.3(8) . . ?
C4 C5 H5A 108.9(8) . . ?
C2 C5 H5A 106.9(8) 3_757 . ?
O2 C6 O3 127.13(11) . . ?
O2 C6 N1 124.50(10) . . ?
O3 C6 N1 108.37(9) . . ?
O3 C7 C8 108.72(9) . . ?
O3 C7 C9 101.85(9) . . ?
C8 C7 C9 111.47(11) . . ?
O3 C7 C10 110.17(9) . . ?
C8 C7 C10 113.61(10) . . ?
C9 C7 C10 110.36(11) . . ?
C7 C8 H8A 109.5(11) . . ?
C7 C8 H8B 110.3(11) . . ?
H8A C8 H8B 105.4(15) . . ?
C7 C8 H8C 111.8(11) . . ?
H8A C8 H8C 110.4(15) . . ?
H8B C8 H8C 109.4(15) . . ?
C7 C9 H9A 110.3(10) . . ?
C7 C9 H9B 109.1(10) . . ?
H9A C9 H9B 108.4(15) . . ?
C7 C9 H9C 110.3(11) . . ?
H9A C9 H9C 111.3(15) . . ?
H9B C9 H9C 107.4(15) . . ?
C7 C10 H10A 108.4(11) . . ?
C7 C10 H10B 112.2(10) . . ?
H10A C10 H10B 107.5(14) . . ?
C7 C10 H10C 109.6(11) . . ?
H10A C10 H10C 110.7(15) . . ?
H10B C10 H10C 108.4(15) . . ?

loop_
 _geom_torsion_atom_site_label_1
 _geom_torsion_atom_site_label_2
 _geom_torsion_atom_site_label_3
 _geom_torsion_atom_site_label_4
 _geom_torsion
 _geom_torsion_site_symmetry_1
 _geom_torsion_site_symmetry_2
 _geom_torsion_site_symmetry_3
 _geom_torsion_site_symmetry_4
 _geom_torsion_publ_flag
C6 N1 C1 O1 4.21(16) . . . . ?
C2 N1 C1 O1 176.65(9) . . . . ?
C6 N1 C1 C5 -174.51(9) . . . . ?
C2 N1 C1 C5 -2.06(13) . . . . ?
C1 N1 C2 C3 52.12(12) . . . . ?
C6 N1 C2 C3 -135.36(9) . . . . ?
C1 N1 C2 C5 -77.69(11) . . . 3_757 ?
C6 N1 C2 C5 94.83(11) . . . 3_757 ?
N1 C2 C3 C4 -48.23(11) . . . . ?
C5 C2 C3 C4 80.22(11) 3_757 . . . ?
C2 C3 C4 C5 -1.30(13) . . . . ?
   O1 C1 C5 C4 130.76(10) . . . . ?
```

```
N1 C1 C5 C4 -50.50(12) . . . . ?
O1 C1 C5 C2 -99.72(12) . . . 3_757 ?
N1 C1 C5 C2 79.02(11) . . . 3_757 ?
C3 C4 C5 C1 50.54(12) . . . . ?
C3 C4 C5 C2 -76.72(11) . . . 3_757 ?
C7 O3 C6 O2 -2.15(17) . . . . ?
C7 O3 C6 N1 177.90(9) . . . . ?
C1 N1 C6 O2 -24.41(16) . . . . ?
C2 N1 C6 O2 163.27(10) . . . . ?
C1 N1 C6 O3 155.54(9) . . . . ?
C2 N1 C6 O3 -16.77(13) . . . . ?
C6 O3 C7 C8 66.36(13) . . . . ?
C6 O3 C7 C9 -175.86(10) . . . . ?
C6 O3 C7 C10 -58.73(13) . . . . ?
```

X-ray crystal structure data for racemic *N*-Boc tetrahydro monolactamol (±)-(229)

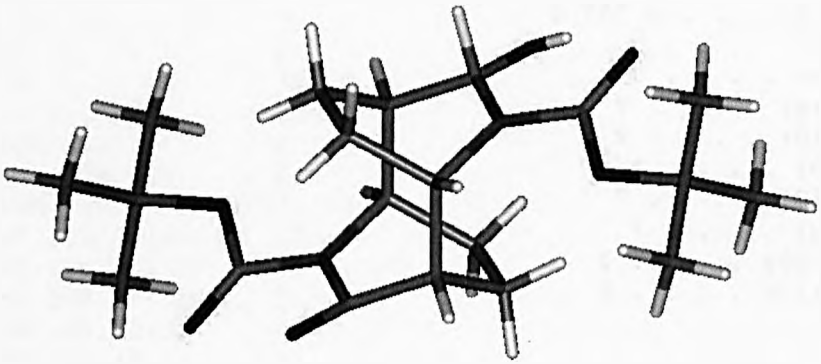

(±)-229

```
data_csf89s

_audit_creation_method            SHELXL-97
_chemical_name_systematic
;
 ?
;
_chemical_name_common             ?
_chemical_melting_point           ?
_chemical_formula_moiety          ?
_chemical_formula_sum
 'C20 H32 N2 O6'
_chemical_formula_weight          396.48

loop_
 _atom_type_symbol
 _atom_type_description
 _atom_type_scat_dispersion_real
 _atom_type_scat_dispersion_imag
 _atom_type_scat_source
 'C'  'C'   0.0033   0.0016
 'International Tables Vol C Tables 4.2.6.8 and 6.1.1.4'
 'H'  'H'   0.0000   0.0000
 'International Tables Vol C Tables 4.2.6.8 and 6.1.1.4'
 'N'  'N'   0.0061   0.0033
 'International Tables Vol C Tables 4.2.6.8 and 6.1.1.4'
 'O'  'O'   0.0106   0.0060
 'International Tables Vol C Tables 4.2.6.8 and 6.1.1.4'

_symmetry_cell_setting            Triclinic
_symmetry_space_group_name_H-M    P-1

loop_
 _symmetry_equiv_pos_as_xyz
 'x, y, z'
 '-x, -y, -z'

_cell_length_a                    6.3279(4)
_cell_length_b                    6.6972(4)
_cell_length_c                    13.1666(8)
_cell_angle_alpha                 81.172(2)
_cell_angle_beta                  84.624(2)
_cell_angle_gamma                 67.344(2)
_cell_volume                      508.47(5)
_cell_formula_units_Z             1
_cell_measurement_temperature     123(1)
```

```
_cell_measurement_reflns_used      2015
_cell_measurement_theta_min        3.13
_cell_measurement_theta_max        29.13

_exptl_crystal_description         Prism
_exptl_crystal_colour              Colourless
_exptl_crystal_size_max            0.20
_exptl_crystal_size_mid            0.20
_exptl_crystal_size_min            0.10
_exptl_crystal_density_meas        ?
_exptl_crystal_density_diffrn      1.295
_exptl_crystal_density_method      'not measured'
_exptl_crystal_F_000               214
_exptl_absorpt_coefficient_mu      0.095
_exptl_absorpt_correction_type     none
_exptl_absorpt_correction_T_min    ?
_exptl_absorpt_correction_T_max    ?
_exptl_absorpt_process_details     ?

_exptl_special_details
;
 ?
;

_diffrn_ambient_temperature             123(1)
_diffrn_radiation_wavelength            0.71073
_diffrn_radiation_type                  MoK\a
_diffrn_radiation_source                'fine-focus sealed tube'
_diffrn_radiation_monochromator         graphite
_diffrn_measurement_device_type         'Bruker AXS 1K CCD area detector'
_diffrn_measurement_method              'narrow frame \w scans'
_diffrn_detector_area_resol_mean        8.192
_diffrn_standards_number                'see text'
_diffrn_standards_interval_count        ?
_diffrn_standards_interval_time         ?
_diffrn_standards_decay_%               none
_diffrn_reflns_number                   5325
_diffrn_reflns_av_R_equivalents         0.0319
_diffrn_reflns_av_sigmaI/netI           0.0499
_diffrn_reflns_limit_h_min              -7
_diffrn_reflns_limit_h_max              7
_diffrn_reflns_limit_k_min              -8
_diffrn_reflns_limit_k_max              8
_diffrn_reflns_limit_l_min              -16
_diffrn_reflns_limit_l_max              16
_diffrn_reflns_theta_min                3.13
_diffrn_reflns_theta_max                26.37
_diffrn_reflns_theta_full               26.37
_diffrn_measured_fraction_theta_full    0.994
_reflns_number_total                    2067
_reflns_number_gt                       1410
_reflns_threshold_expression            >2sigma(I)

_computing_data_collection          'SMART (Bruker AXS, 1995)'
_computing_cell_refinement          'SMART & SAINT (Bruker AXS, 1995)'
_computing_data_reduction           'SAINT (Bruker AXS, 1995)'
_computing_structure_solution       'SHELXTL (Sheldrick, 1994)'
_computing_structure_refinement     'SHELXTL (Sheldrick, 1994)'
_computing_molecular_graphics       'SHELXTL (Sheldrick, 1994)'
_computing_publication_material     'SHELXTL (Sheldrick, 1994)'

_refine_special_details
;
```

```
  The molecule is disordered about the inversion centre such that the
  asymmetric unit contains both the C==O and C---OH bond.
  Refinement of F^2^ against ALL reflections.  The weighted R-factor wR and
  goodness of fit S are based on F^2^, conventional R-factors R are based
  on F, with F set to zero for negative F^2^. The threshold expression of
  F^2^ > 2sigma(F^2^) is used only for calculating R-factors(gt) etc. and is
  not relevant to the choice of reflections for refinement.  R-factors based
  on F^2^ are statistically about twice as large as those based on F, and R-
  factors based on ALL data will be even larger.
;

_refine_ls_structure_factor_coef  Fsqd
_refine_ls_matrix_type            full
_refine_ls_weighting_scheme       calc
_refine_ls_weighting_details
 'calc w=1/[\s^2^(Fo^2^)+(0.1000P)^2^+0.1000P] where P=(Fo^2^+2Fc^2^)/3'
_atom_sites_solution_primary      direct
_atom_sites_solution_secondary    difmap
_atom_sites_solution_hydrogens    geom
_refine_ls_hydrogen_treatment     mixed
_refine_ls_extinction_method      none
_refine_ls_extinction_coef        ?
_refine_ls_number_reflns          2067
_refine_ls_number_parameters      146
_refine_ls_number_restraints      0
_refine_ls_R_factor_all           0.0857
_refine_ls_R_factor_gt            0.0603
_refine_ls_wR_factor_ref          0.1659
_refine_ls_wR_factor_gt           0.1578
_refine_ls_goodness_of_fit_ref    0.999
_refine_ls_restrained_S_all       0.999
_refine_ls_shift/su_max           1.188
_refine_ls_shift/su_mean          0.016
_refine_diff_density_max          0.289
_refine_diff_density_min         -0.254
_refine_diff_density_rms          0.060

loop_
 _atom_site_label
 _atom_site_type_symbol
 _atom_site_fract_x
 _atom_site_fract_y
 _atom_site_fract_z
 _atom_site_U_iso_or_equiv
 _atom_site_adp_type
 _atom_site_occupancy
 _atom_site_symmetry_multiplicity
 _atom_site_calc_flag
 _atom_site_refinement_flags
 _atom_site_disorder_assembly
 _atom_site_disorder_group
O1 O -0.4117(3) 0.3431(5) 0.88703(18) 0.0642(8) Uani 1 1 d . . .
H1B H -0.390(8) 0.395(7) 0.845(3) 0.000(12) Uiso 0.50 1 d P . .
O2 O -0.1363(3) 0.4713(3) 0.74798(15) 0.0521(6) Uani 1 1 d . . .
O3 O 0.2299(3) 0.2248(3) 0.76189(11) 0.0318(5) Uani 1 1 d . . .
N1 N -0.0155(3) 0.2400(3) 0.89623(14) 0.0268(5) Uani 1 1 d . . .
C1 C -0.2403(4) 0.2824(4) 0.9409(2) 0.0340(6) Uani 1 1 d . . .
H1A H -0.280(8) 0.448(8) 0.965(3) 0.026(12) Uiso 0.50 1 d P . .
C2 C -0.2406(4) 0.1525(4) 1.04512(18) 0.0284(6) Uani 1 1 d . . .
H2A H -0.399(4) 0.213(4) 1.0715(17) 0.029(6) Uiso 1 1 d . . .
C3 C -0.0923(4) 0.2022(4) 1.11499(19) 0.0332(6) Uani 1 1 d . . .
H3A H -0.0744 0.1041 1.1807 0.040 Uiso 1 1 calc R . .
   H3B H -0.1703 0.3542 1.1305 0.040 Uiso 1 1 calc R . .
```

```
 C4 C 0.1454(4) 0.1725(4) 1.06508(17) 0.0258(5) Uani 1 1 d . . .
 H4A H 0.1665 0.3129 1.0587 0.031 Uiso 1 1 calc R . .
 H4B H 0.2637 0.0646 1.1109 0.031 Uiso 1 1 calc R . .
 C5 C 0.1823(3) 0.0961(4) 0.95876(17) 0.0227(5) Uani 1 1 d . . .
 H5A H 0.305(4) 0.135(4) 0.9246(16) 0.020(5) Uiso 1 1 d . . .
 C6 C 0.0129(4) 0.3269(4) 0.79620(19) 0.0316(6) Uani 1 1 d . . .
 C7 C 0.3060(5) 0.2801(4) 0.65523(18) 0.0431(7) Uani 1 1 d . . .
 C8 C 0.5560(5) 0.1241(5) 0.6539(2) 0.0581(9) Uani 1 1 d . . .
 H8A H 0.6383 0.1568 0.7044 0.087 Uiso 1 1 calc R . .
 H8B H 0.6260 0.1416 0.5852 0.087 Uiso 1 1 calc R . .
 H8C H 0.5645 -0.0264 0.6711 0.087 Uiso 1 1 calc R . .
 C9 C 0.2851(6) 0.5152(5) 0.6388(2) 0.0592(9) Uani 1 1 d . . .
 H9A H 0.1235 0.6111 0.6452 0.089 Uiso 1 1 calc R . .
 H9B H 0.3466 0.5482 0.5700 0.089 Uiso 1 1 calc R . .
 H9C H 0.3717 0.5389 0.6906 0.089 Uiso 1 1 calc R . .
 C10 C 0.1694(6) 0.2289(5) 0.5808(2) 0.0626(9) Uani 1 1 d . . .
 H10A H 0.0079 0.3259 0.5861 0.094 Uiso 1 1 calc R . .
 H10B H 0.1829 0.0769 0.5979 0.094 Uiso 1 1 calc R . .
 H10C H 0.2294 0.2509 0.5104 0.094 Uiso 1 1 calc R . .

 loop_
  _atom_site_aniso_label
  _atom_site_aniso_U_11
  _atom_site_aniso_U_22
  _atom_site_aniso_U_33
  _atom_site_aniso_U_23
  _atom_site_aniso_U_13
  _atom_site_aniso_U_12
O1 0.0168(10) 0.121(2) 0.0362(13) -0.0205(14) -0.0041(10) -0.0014(11)
O2 0.0443(12) 0.0459(12) 0.0497(12) -0.0059(9) -0.0195(9) 0.0048(9)
O3 0.0264(9) 0.0372(10) 0.0269(9) -0.0008(7) 0.0039(7) -0.0089(7)
N1 0.0133(9) 0.0321(11) 0.0307(10) -0.0078(8) 0.0007(8) -0.0027(8)
C1 0.0122(11) 0.0242(13) 0.0594(17) 0.0016(11) -0.0010(11) -0.0028(9)
C2 0.0120(10) 0.0293(13) 0.0436(14) -0.0153(10) 0.0096(10) -0.0060(9)
C3 0.0257(12) 0.0391(14) 0.0405(14) -0.0221(11) 0.0109(10) -0.0148(11)
C4 0.0191(11) 0.0253(12) 0.0339(12) -0.0091(9) 0.0014(9) -0.0080(9)
C5 0.0122(10) 0.0254(12) 0.0291(12) -0.0035(9) 0.0009(9) -0.0059(9)
C6 0.0242(12) 0.0304(13) 0.0367(13) -0.0086(10) -0.0053(10) -0.0039(10)
C7 0.0605(18) 0.0450(16) 0.0219(13) -0.0028(11) 0.0070(12) -0.0204(14)
C8 0.059(2) 0.066(2) 0.0420(16) -0.0116(14) 0.0267(15) -0.0211(16)
C9 0.096(3) 0.055(2) 0.0300(15) -0.0014(13) 0.0150(15) -0.0369(18)
C10 0.094(3) 0.057(2) 0.0342(16) -0.0101(14) -0.0086(16) -0.0231(18)

_geom_special_details
;
 All esds (except the esd in the dihedral angle between two l.s. planes)
 are estimated using the full covariance matrix.  The cell esds are taken
 into account individually in the estimation of esds in distances, angles
 and torsion angles; correlations between esds in cell parameters are only
 used when they are defined by crystal symmetry.  An approximate
(isotropic)
 treatment of cell esds is used for estimating esds involving l.s. planes.
;

loop_
 _geom_bond_atom_site_label_1
 _geom_bond_atom_site_label_2
 _geom_bond_distance
 _geom_bond_site_symmetry_2
 _geom_bond_publ_flag
O1 C1 1.250(3) . ?
O1 H1B 0.64(4) . ?
O2 C6 1.204(3) . ?
```

```
O3 C6 1.346(3) . ?
O3 C7 1.481(3) . ?
N1 C6 1.381(3) . ?
N1 C1 1.426(3) . ?
N1 C5 1.481(3) . ?
C1 C2 1.508(3) . ?
C1 H1B 1.56(4) . ?
C1 H1A 1.12(5) . ?
C2 C3 1.528(3) . ?
C2 C5 1.568(3) 2_557 ?
C2 H2A 0.98(2) . ?
C3 C4 1.536(3) . ?
C3 H3A 0.9900 . ?
C3 H3B 0.9900 . ?
C4 C5 1.531(3) . ?
C4 H4A 0.9900 . ?
C4 H4B 0.9900 . ?
C5 C2 1.568(3) 2_557 ?
C5 H5A 0.96(2) . ?
C7 C9 1.512(4) . ?
C7 C10 1.522(4) . ?
C7 C8 1.524(4) . ?
C8 H8A 0.9800 . ?
C8 H8B 0.9800 . ?
C8 H8C 0.9800 . ?
C9 H9A 0.9800 . ?
C9 H9B 0.9800 . ?
C9 H9C 0.9800 . ?
C10 H10A 0.9800 . ?
C10 H10B 0.9800 . ?
C10 H10C 0.9800 . ?

loop_
 _geom_angle_atom_site_label_1
 _geom_angle_atom_site_label_2
 _geom_angle_atom_site_label_3
 _geom_angle
 _geom_angle_site_symmetry_1
 _geom_angle_site_symmetry_3
 _geom_angle_publ_flag
C1 O1 H1B 107(4) . . ?
C6 O3 C7 121.20(19) . . ?
C6 N1 C1 119.98(18) . . ?
C6 N1 C5 121.84(17) . . ?
C1 N1 C5 118.15(18) . . ?
O1 C1 N1 121.8(2) . . ?
O1 C1 C2 119.2(2) . . ?
N1 C1 C2 112.95(18) . . ?
O1 C1 H1B 22.9(16) . . ?
N1 C1 H1B 101.2(17) . . ?
C2 C1 H1B 142.2(16) . . ?
O1 C1 H1A 95(2) . . ?
N1 C1 H1A 100(2) . . ?
C2 C1 H1A 10 (2) . . ?
H1B C1 H1A 89(3) . . ?
C1 C2 C3 108.28(19) . . ?
C1 C2 C5 113.94(19) . 2_557 ?
C3 C2 C5 115.18(19) . 2_557 ?
C1 C2 H2A 104.6(13) . . ?
C3 C2 H2A 107.5(14) . . ?
C5 C2 H2A 106.6(14) 2_557 . ?
C2 C3 C4 111.82(18) . . ?
   C2 C3 H3A 109.3 . . ?
```

```
  C4 C3 H3A 109.3 . . ?
  C2 C3 H3B 109.3 . . ?
  C4 C3 H3B 109.3 . . ?
  H3A C3 H3B 107.9 . . ?
  C5 C4 C3 113.60(18) . . ?
  C5 C4 H4A 108.8 . . ?
  C3 C4 H4A 108.8 . . ?
  C5 C4 H4B 108.8 . . ?
  C3 C4 H4B 108.8 . . ?
  H4A C4 H4B 107.7 . . ?
  N1 C5 C4 108.11(17) . . ?
  N1 C5 C2 112.92(18) . 2_557 ?
  C4 C5 C2 117.25(18) . 2_557 ?
  N1 C5 H5A 101.9(13) . . ?
  C4 C5 H5A 106.4(13) . . ?
  C2 C5 H5A 108.9(13) 2_557 . ?
  O2 C6 O3 126.0(2) . . ?
  O2 C6 N1 124.4(2) . . ?
  O3 C6 N1 109.65(18) . . ?
  O3 C7 C9 109.7(2) . . ?
  O3 C7 C10 109.0(2) . . ?
  C9 C7 C10 113.5(2) . . ?
  O3 C7 C8 101.5(2) . . ?
  C9 C7 C8 111.4(3) . . ?
  C10 C7 C8 111.2(2) . . ?
  C7 C8 H8A 109.5 . . ?
  C7 C8 H8B 109.5 . . ?
  H8A C8 H8B 109.5 . . ?
  C7 C8 H8C 109.5 . . ?
  H8A C8 H8C 109.5 . . ?
  H8B C8 H8C 109.5 . . ?
  C7 C9 H9A 109.5 . . ?
  C7 C9 H9B 109.5 . . ?
  H9A C9 H9B 109.5 . . ?
  C7 C9 H9C 109.5 . . ?
  H9A C9 H9C 109.5 . . ?
  H9B C9 H9C 109.5 . . ?
  C7 C10 H10A 109.5 . . ?
  C7 C10 H10B 109.5 . . ?
  H10A C10 H10B 109.5 . . ?
  C7 C10 H10C 109.5 . . ?
  H10A C10 H10C 109.5 . . ?
  H10B C10 H10C 109.5 . . ?

  loop_
   _geom_torsion_atom_site_label_1
   _geom_torsion_atom_site_label_2
   _geom_torsion_atom_site_label_3
   _geom_torsion_atom_site_label_4
   _geom_torsion
   _geom_torsion_site_symmetry_1
   _geom_torsion_site_symmetry_2
   _geom_torsion_site_symmetry_3
   _geom_torsion_site_symmetry_4
   _geom_torsion_publ_flag
C6 N1 C1 O1 20.1(4) . . . . ?
C5 N1 C1 O1 -158.0(3) . . . . ?
C6 N1 C1 C2 172.6(2) . . . . ?
C5 N1 C1 C2 -5.5(3) . . . . ?
O1 C1 C2 C3 -150.0(2) . . . . ?
N1 C1 C2 C3 56.7(2) . . . . ?
O1 C1 C2 C5 80.4(3) . . . 2_557 ?
N1 C1 C2 C5 -72.8(2) . . . 2_557 ?
```

```
C1 C2 C3 C4 -51.7(2) . . . . ?
C5 C2 C3 C4 77.2(2) 2_557 . . . ?
C2 C3 C4 C5 -1.2(3) . . . . ?
C6 N1 C5 C4 133.9(2) . . . . ?
C1 N1 C5 C4 -48.0(2) . . . . ?
C6 N1 C5 C2 -94.7(2) . . . 2_557 ?
C1 N1 C5 C2 83.4(2) . . . 2_557 ?
C3 C4 C5 N1 50.0(2) . . . . ?
C3 C4 C5 C2 -79.0(2) . . . 2_557 ?
C7 O3 C6 O2 -1.8(4) . . . . ?
C7 O3 C6 N1 177.8(2) . . . . ?
C1 N1 C6 O2 14.8(4) . . . . ?
C5 N1 C6 O2 -167.2(2) . . . . ?
C1 N1 C6 O3 -164.84(19) . . . . ?
C5 N1 C6 O3 13.2(3) . . . . ?
C6 O3 C7 C9 62.5(3) . . . . ?
C6 O3 C7 C10 -62.2(3) . . . . ?
C6 O3 C7 C8 -179.6(2) . . . . ?
```

X-ray crystal structure data for homochiral *N*-Boc tetrahydro monolactamol (+)-(229)

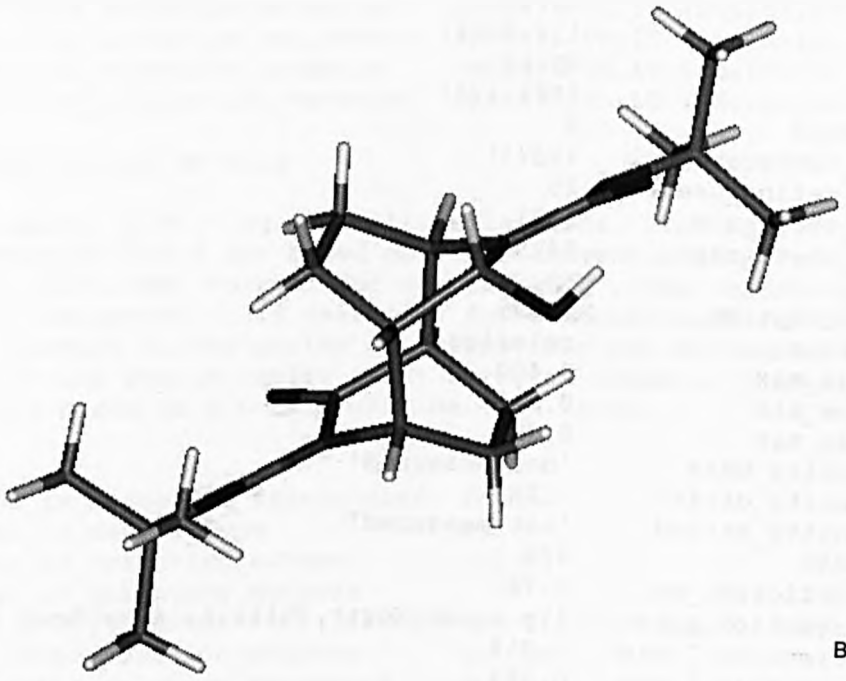

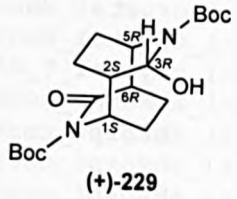

(+)-229

```
data_csf104a

_audit_creation_method            SHELXL-97
_chemical_name_systematic
;
 ?
;
_chemical_name_common             ?
_chemical_melting_point           ?
_chemical_formula_moiety          'C20 H32 N2 O6'
_chemical_formula_sum
 'C20 H32 N2 O6'
_chemical_formula_weight          396.48

loop_
 _atom_type_symbol
 _atom_type_description
 _atom_type_scat_dispersion_real
 _atom_type_scat_dispersion_imag
 _atom_type_scat_source
 'C'  'C'   0.0181   0.0091
 'International Tables Vol C Tables 4.2.6.8 and 6.1.1.4'
 'H'  'H'   0.0000   0.0000
 'International Tables Vol C Tables 4.2.6.8 and 6.1.1.4'
 'N'  'N'   0.0311   0.0180
 'International Tables Vol C Tables 4.2.6.8 and 6.1.1.4'
 'O'  'O'   0.0492   0.0322
 'International Tables Vol C Tables 4.2.6.8 and 6.1.1.4'

_symmetry_cell_setting            Monoclinic
_symmetry_space_group_name_H-M    'P 21'

loop_
 _symmetry_equiv_pos_as_xyz
 'x, y, z'
 '-x, y+1/2, -z'
```

```
_cell_length_a                      6.332(4)
_cell_length_b                      26.000(4)
_cell_length_c                      6.720(3)
_cell_angle_alpha                   90.00
_cell_angle_beta                    112.63(4)
_cell_angle_gamma                   90.00
_cell_volume                        1021.1(8)
_cell_formula_units_Z               2
_cell_measurement_temperature       123(1)
_cell_measurement_reflns_used       25
_cell_measurement_theta_min         53.1
_cell_measurement_theta_max         54.9

_exptl_crystal_description          prism
_exptl_crystal_colour               colorless
_exptl_crystal_size_max             0.400
_exptl_crystal_size_mid             0.350
_exptl_crystal_size_min             0.300
_exptl_crystal_density_meas         'not measured'
_exptl_crystal_density_diffrn       1.289
_exptl_crystal_density_method       'not measured'
_exptl_crystal_F_000                428
_exptl_absorpt_coefficient_mu       0.781
_exptl_absorpt_correction_type      '\y scans(North,Phillips & Mathews,1968)'
_exptl_absorpt_correction_T_min     0.916
_exptl_absorpt_correction_T_max     0.999
_exptl_absorpt_process_details      ?

_exptl_special_details
;
 ?
;

_diffrn_ambient_temperature             123(1)
_diffrn_radiation_wavelength            1.54178
_diffrn_radiation_type                  CuK\a
_diffrn_radiation_source                'Rigaku RU200 Rotating Cu Anode'
_diffrn_radiation_monochromator         graphite
_diffrn_measurement_device_type         Rigaku AFC7R
_diffrn_measurement_method              \w-2\q
_diffrn_standards_number                3
_diffrn_standards_interval_count        150
_diffrn_standards_decay_%               2.32
_diffrn_reflns_number                   4008
_diffrn_reflns_av_R_equivalents         0.0140
_diffrn_reflns_av_sigmaI/netI           0.0087
_diffrn_reflns_limit_h_min              -7
_diffrn_reflns_limit_h_max              7
_diffrn_reflns_limit_k_min              -31
_diffrn_reflns_limit_k_max              31
_diffrn_reflns_limit_l_min              -7
_diffrn_reflns_limit_l_max              7
_diffrn_reflns_theta_min                3.40
_diffrn_reflns_theta_max                67.45
_diffrn_measured_fraction_theta_max     0.983
_diffrn_reflns_theta_full               67.45
_diffrn_measured_fraction_theta_full    0.983

_reflns_number_total                    3589
_reflns_number_gt                       3585
_reflns_threshold_expression            >2sigma(I)
```

```
_computing_data_collection      'Rigaku/AFC Diffractometer Control, (MSC,
1992)'
_computing_cell_refinement      'Rigaku/AFC Diffractometer Control, (MSC,
1992)'
_computing_data_reduction       'teXsan V1.7,(MSC, 1997)'
_computing_structure_solution   'SHELXTL V5.10 (Sheldrick, 1997)'
_computing_structure_refinement 'SHELXTL V5.10 (Sheldrick, 1997)'
_computing_molecular_graphics   'SHELXTL V5.10 (Sheldrick, 1997)'
_computing_publication_material 'SHELXTL V5.10 (Sheldrick, 1997)'

_refine_special_details
;
 Refinement of F^2^ against ALL reflections.  The weighted R-factor wR and
 goodness of fit S are based on F^2^, conventional R-factors R are based
 on F, with F set to zero for negative F^2^. The threshold expression of
 F^2^ > 2sigma(F^2^) is used only for calculating R-factors(gt) etc. and is
 not relevant to the choice of reflections for refinement.  R-factors based
 on F^2^ are statistically about twice as large as those based on F, and R-
 factors based on ALL data will be even larger.
;

_refine_ls_structure_factor_coef  Fsqd
_refine_ls_matrix_type            full
_refine_ls_weighting_scheme       calc
_refine_ls_weighting_details
 'calc w=1/[\s^2^(Fo^2^)+(0.0850P)^2^+0.4000P] where P=(Fo^2^+2Fc^2^)/3'
_atom_sites_solution_primary      direct
_atom_sites_solution_secondary    difmap
_atom_sites_solution_hydrogens    geom
_refine_ls_hydrogen_treatment     mixed
_refine_ls_extinction_method      none
_refine_ls_extinction_coef        none
_refine_ls_abs_structure_details
 'Flack H D (1983), Acta Cryst. A39, 876-881'
_refine_ls_abs_structure_Flack    0.14(19)
_refine_ls_number_reflns          3589
_refine_ls_number_parameters      295
_refine_ls_number_restraints      1
_refine_ls_R_factor_all           0.0418
_refine_ls_R_factor_gt            0.0417
_refine_ls_wR_factor_ref          0.1177
_refine_ls_wR_factor_gt           0.1177
_refine_ls_goodness_of_fit_ref    1.009
_refine_ls_restrained_S_all       1.008
_refine_ls_shift/su_max           0.001
_refine_ls_shift/su_mean          0.000
_refine_diff_density_max          0.193
_refine_diff_density_min         -0.216
_refine_diff_density_rms          0.049

loop_
 _atom_site_label
 _atom_site_type_symbol
 _atom_site_fract_x
 _atom_site_fract_y
 _atom_site_fract_z
 _atom_site_U_iso_or_equiv
 _atom_site_adp_type
 _atom_site_occupancy
 _atom_site_symmetry_multiplicity
 _atom_site_calc_flag
 _atom_site_refinement_flags
 _atom_site_disorder_assembly
```

```
  _atom_site_disorder_group
O1 O 0.6381(3) 0.79456(7) 0.5243(3) 0.0309(4) Uani 1 1 d . . .
H1B H 0.636(4) 0.8201(11) 0.605(4) 0.023(6) Uiso 1 1 d . . .
O2 O -0.2069(3) 0.68156(6) -0.0908(3) 0.0319(4) Uani 1 1 d . . .
O3 O 0.3960(3) 0.86265(6) 0.6459(3) 0.0339(4) Uani 1 1 d . . .
O4 O 0.0180(3) 0.85976(6) 0.4204(3) 0.0311(4) Uani 1 1 d . . .
O5 O 0.0767(3) 0.61186(7) -0.1617(3) 0.0369(4) Uani 1 1 d . . .
O6 O 0.4317(3) 0.62229(6) 0.0986(2) 0.0288(4) Uani 1 1 d . . .
N1 N 0.2382(3) 0.79078(7) 0.4542(3) 0.0229(4) Uani 1 1 d . . .
N2 N 0.1860(3) 0.68803(7) 0.0288(3) 0.0234(4) Uani 1 1 d . . .
C1 C 0.4413(3) 0.71402(8) 0.4113(3) 0.0225(4) Uani 1 1 d . . .
H1A H 0.5949 0.6972 0.4756 0.026(6) Uiso 1 1 calc R . .
C2 C 0.4600(3) 0.76399(9) 0.5341(3) 0.0240(4) Uani 1 1 d . . .
H2A H 0.4981 0.7551 0.6889 0.018(5) Uiso 1 1 calc R . .
C3 C 0.0288(3) 0.76086(8) 0.3343(3) 0.0219(4) Uani 1 1 d . . .
H3A H -0.0999 0.7787 0.3572 0.024(6) Uiso 1 1 calc R . .
C4 C 0.0517(3) 0.70763(9) 0.4399(3) 0.0236(4) Uani 1 1 d . . .
H4A H -0.0789 0.6860 0.3501 0.022(6) Uiso 1 1 calc R . .
H4B H 0.0422 0.7117 0.5827 0.025(6) Uiso 1 1 calc R . .
C5 C 0.2762(3) 0.67959(9) 0.4695(3) 0.0264(5) Uani 1 1 d . . .
H5A H 0.3517 0.6683 0.6214 0.032(7) Uiso 1 1 calc R . .
H5B H 0.2406 0.6485 0.3773 0.027(6) Uiso 1 1 calc R . .
C6 C -0.0345(3) 0.76002(9) 0.0831(3) 0.0237(4) Uani 1 1 d . . .
H6A H -0.1959 0.7725 0.0143 0.022(6) Uiso 1 1 calc R . .
C7 C -0.0313(3) 0.70629(9) -0.0045(3) 0.0240(4) Uani 1 1 d . . .
C8 C 0.3869(3) 0.71995(8) 0.1626(3) 0.0207(4) Uani 1 1 d . . .
H8A H 0.5216 0.7052 0.1398 0.013(5) Uiso 1 1 calc R . .
C9 C 0.3514(4) 0.77397(8) 0.0626(3) 0.0237(4) Uani 1 1 d . . .
H9A H 0.3818 0.7727 -0.0713 0.019(6) Uiso 1 1 calc R . .
H9B H 0.4651 0.7975 0.1639 0.012(5) Uiso 1 1 calc R . .
C10 C 0.1108(4) 0.79632(9) 0.0087(3) 0.0258(4) Uani 1 1 d . . .
H10A H 0.1234 0.8301 0.0806 0.019(5) Uiso 1 1 calc R . .
H10B H 0.0351 0.8018 -0.1488 0.018(6) Uiso 1 1 calc R . .
C11 C 0.2296(4) 0.83982(9) 0.5177(3) 0.0263(5) Uani 1 1 d . . .
C12 C -0.0309(5) 0.91416(9) 0.4471(5) 0.0364(6) Uani 1 1 d . . .
C13 C -0.2816(5) 0.91832(11) 0.2987(6) 0.0506(7) Uani 1 1 d . . .
H13A H -0.2997 0.9095 0.1512 0.061(11) Uiso 1 1 calc R . .
H13B H -0.3348 0.9536 0.3020 0.074(12) Uiso 1 1 calc R . .
H13C H -0.3720 0.8945 0.3472 0.049(9) Uiso 1 1 calc R . .
C14 C 0.0045(6) 0.92416(11) 0.6813(5) 0.0489(7) Uani 1 1 d . . .
H14A H -0.0852 0.8994 0.7262 0.065(10) Uiso 1 1 calc R . .
H14B H -0.0457 0.9592 0.6953 0.077(12) Uiso 1 1 calc R . .
H14C H 0.1671 0.9204 0.7730 0.13(2) Uiso 1 1 calc R . .
C15 C 0.1160(5) 0.94880(11) 0.3707(5) 0.0434(6) Uani 1 1 d . . .
H15A H 0.1052 0.9376 0.2279 0.045(8) Uiso 1 1 calc R . .
H15B H 0.2756 0.9468 0.4727 0.066(11) Uiso 1 1 calc R . .
H15C H 0.0620 0.9844 0.3624 0.057(10) Uiso 1 1 calc R . .
C16 C 0.2194(4) 0.63705(9) -0.0260(3) 0.0257(5) Uani 1 1 d . . .
C17 C 0.5164(4) 0.57016(9) 0.0778(4) 0.0330(5) Uani 1 1 d . . .
C18 C 0.7614(4) 0.57259(10) 0.2414(5) 0.0430(6) Uani 1 1 d . . .
H18A H 0.7617 0.5808 0.3838 0.058(10) Uiso 1 1 calc R . .
H18B H 0.8449 0.5993 0.1987 0.050(9) Uiso 1 1 calc R . .
H18C H 0.8358 0.5393 0.2472 0.086(14) Uiso 1 1 calc R . .
C19 C 0.5112(5) 0.56203(10) -0.1470(5) 0.0393(6) Uani 1 1 d . . .
H19A H 0.5923 0.5903 -0.1836 0.043(8) Uiso 1 1 calc R . .
H19B H 0.3521 0.5612 -0.2506 0.045(8) Uiso 1 1 calc R . .
H19C H 0.5860 0.5294 -0.1525 0.075(12) Uiso 1 1 calc R . .
C20 C 0.3780(5) 0.53050(10) 0.1426(5) 0.0424(6) Uani 1 1 d . . .
H20A H 0.3775 0.5395 0.2840 0.053(9) Uiso 1 1 calc R . .
H20B H 0.4468 0.4964 0.1500 0.066(11) Uiso 1 1 calc R . .
H20C H 0.2205 0.5300 0.0354 0.043(8) Uiso 1 1 calc R . .

  loop_
```

```
   _atom_site_aniso_label
   _atom_site_aniso_U_11
   _atom_site_aniso_U_22
   _atom_site_aniso_U_33
   _atom_site_aniso_U_23
   _atom_site_aniso_U_13
   _atom_site_aniso_U_12
  O1 0.0186(7) 0.0382(8) 0.0343(8) -0.0054(7) 0.0083(6) -0.0040(6)
  O2 0.0201(7) 0.0365(8) 0.0333(8) 0.0018(7) 0.0039(6) -0.0044(6)
  O3 0.0259(8) 0.0375(9) 0.0323(8) -0.0087(7) 0.0046(7) -0.0065(7)
  O4 0.0241(8) 0.0262(8) 0.0401(9) -0.0032(7) 0.0091(7) 0.0036(6)
  O5 0.0296(9) 0.0374(9) 0.0366(9) -0.0082(7) 0.0049(7) -0.0040(7)
  O6 0.0267(8) 0.0264(8) 0.0297(8) -0.0030(6) 0.0068(6) 0.0033(6)
  N1 0.0153(8) 0.0301(9) 0.0218(8) -0.0001(7) 0.0056(7) -0.0003(7)
  N2 0.0192(8) 0.0292(9) 0.0195(8) -0.0005(7) 0.0051(7) 0.0016(7)
  C1 0.0170(9) 0.0320(11) 0.0165(9) 0.0029(8) 0.0043(7) 0.0030(8)
  C2 0.0152(9) 0.0378(12) 0.0174(9) -0.0025(8) 0.0045(7) 0.0014(8)
  C3 0.0157(9) 0.0295(10) 0.0191(10) -0.0009(8) 0.0051(7) -0.0005(8)
  C4 0.0190(9) 0.0313(10) 0.0202(9) 0.0023(9) 0.0072(7) 0.0007(8)
  C5 0.0216(10) 0.0333(11) 0.0238(10) 0.0068(9) 0.0082(8) 0.0030(8)
  C6 0.0135(9) 0.0325(11) 0.0217(10) 0.0025(8) 0.0030(7) 0.0040(8)
  C7 0.0185(10) 0.0338(10) 0.0163(8) 0.0007(8) 0.0029(7) -0.0005(8)
  C8 0.0166(9) 0.0274(10) 0.0179(10) -0.0020(8) 0.0064(7) -0.0008(8)
  C9 0.0232(10) 0.0278(10) 0.0193(9) 0.0024(8) 0.0072(8) -0.0005(8)
  C10 0.0264(10) 0.0291(10) 0.0209(10) 0.0047(8) 0.0080(8) 0.0027(8)
  C11 0.0215(11) 0.0334(12) 0.0238(10) 0.0014(9) 0.0084(9) -0.0010(8)
  C12 0.0402(13) 0.0225(11) 0.0518(15) 0.0002(10) 0.0237(12) 0.0037(9)
  C13 0.0384(15) 0.0331(13) 0.082(2) 0.0133(14) 0.0248(14) 0.0125(11)
  C14 0.0646(19) 0.0339(14) 0.0627(19) -0.0061(13) 0.0405(16) -0.0010(12)
  C15 0.0467(15) 0.0346(13) 0.0543(15) 0.0029(12) 0.0254(13) -0.0025(11)
  C16 0.0230(10) 0.0306(11) 0.0215(10) -0.0016(9) 0.0063(8) -0.0011(8)
  C17 0.0309(12) 0.0259(11) 0.0412(13) -0.0019(10) 0.0127(10) 0.0019(9)
  C18 0.0330(13) 0.0311(12) 0.0558(16) 0.0009(11) 0.0070(12) 0.0084(10)
  C19 0.0434(14) 0.0312(12) 0.0491(15) -0.0069(11) 0.0242(12) -0.0013(11)
  C20 0.0441(15) 0.0356(14) 0.0473(15) 0.0032(11) 0.0172(12) -0.0037(11)

 _geom_special_details
 ;
  All esds (except the esd in the dihedral angle between two l.s. planes)
  are estimated using the full covariance matrix.  The cell esds are taken
  into account individually in the estimation of esds in distances, angles
  and torsion angles; correlations between esds in cell parameters are only
  used when they are defined by crystal symmetry.  An approximate
 (isotropic)
  treatment of cell esds is used for estimating esds involving l.s. planes.
 ;

 loop_
  _geom_bond_atom_site_label_1
  _geom_bond_atom_site_label_2
  _geom_bond_distance
  _geom_bond_site_symmetry_2
  _geom_bond_publ_flag
 O1 C2 1.402(3) . yes
 O2 C7 1.221(3) . yes
 O3 C11 1.227(3) . yes
 O4 C11 1.348(3) . yes
 O4 C12 1.473(3) . yes
 O5 C16 1.201(3) . yes
 O6 C16 1.338(3) . yes
 O6 C17 1.484(3) . yes
 N1 C11 1.352(3) . yes
 N1 C2 1.471(3) . yes
```

```
N1 C3 1.480(3) . yes
N2 C7 1.390(3) . yes
N2 C16 1.413(3) . yes
N2 C8 1.495(3) . yes
C1 C2 1.519(3) . yes
C1 C5 1.537(3) . yes
C1 C8 1.579(3) . yes
C3 C4 1.537(3) . yes
C3 C6 1.578(3) . yes
C4 C5 1.541(3) . yes
C6 C7 1.519(3) . yes
C6 C10 1.530(3) . yes
C8 C9 1.536(3) . yes
C9 C10 1.538(3) . yes
C12 C15 1.519(4) . yes
C12 C13 1.519(4) . yes
C12 C14 1.525(4) . yes
C17 C19 1.514(4) . yes
C17 C18 1.519(3) . yes
C17 C20 1.521(3) . yes
O1 H1B 0.86(3) . yes
C1 H1A 1.0000 . no
C2 H2A 1.0000 . no
C3 H3A 1.0000 . no
C4 H4A 0.9900 . no
C4 H4B 0.9900 . no
C5 H5A 0.9900 . no
C5 H5B 0.9900 . no
C6 H6A 1.0000 . no
C8 H8A 1.0000 . no
C9 H9A 0.9900 . no
C9 H9B 0.9900 . no
C10 H10A 0.9900 . no
C10 H10B 0.9900 . no
C13 H13A 0.9800 . no
C13 H13B 0.9800 . no
C13 H13C 0.9800 . no
C14 H14A 0.9800 . no
C14 H14B 0.9800 . no
C14 H14C 0.9800 . no
C15 H15A 0.9800 . no
C15 H15B 0.9800 . no
C15 H15C 0.9800 . no
C18 H18A 0.9800 . no
C18 H18B 0.9800 . no
C18 H18C 0.9800 . no
C19 H19A 0.9800 . no
C19 H19B 0.9800 . no
C19 H19C 0.9800 . no
C20 H20A 0.9800 . no
C20 H20B 0.9800 . no
C20 H20C 0.9800 . no

loop_
 _geom_angle_atom_site_label_1
 _geom_angle_atom_site_label_2
 _geom_angle_atom_site_label_3
 _geom_angle
 _geom_angle_site_symmetry_1
 _geom_angle_site_symmetry_3
 _geom_angle_publ_flag
C11 O4 C12 121.77(18) . . yes
   C16 O6 C17 121.03(17) . . yes
```

```
C11 N1 C2 118.69(18) . . yes
C11 N1 C3 122.07(17) . . yes
C2 N1 C3 118.62(18) . . yes
C7 N2 C16 121.10(18) . . yes
C7 N2 C8 117.89(17) . . yes
C16 N2 C8 119.96(16) . . yes
C2 C1 C5 106.15(16) . . yes
C2 C1 C8 115.55(17) . . yes
C5 C1 C8 115.69(17) . . yes
O1 C2 N1 112.73(19) . . yes
O1 C2 C1 110.79(16) . . yes
N1 C2 C1 110.05(16) . . yes
N1 C3 C4 108.46(16) . . yes
N1 C3 C6 113.28(16) . . yes
C4 C3 C6 114.93(17) . . yes
C3 C4 C5 113.83(17) . . yes
C1 C5 C4 112.07(18) . . yes
C7 C6 C10 109.95(18) . . yes
C7 C6 C3 113.07(17) . . yes
C10 C6 C3 113.81(17) . . yes
O2 C7 N2 124.1(2) . . yes
O2 C7 C6 121.53(19) . . yes
N2 C7 C6 114.31(18) . . yes
N2 C8 C9 107.29(16) . . yes
N2 C8 C1 111.79(16) . . yes
C9 C8 C1 119.23(16) . . yes
C8 C9 C10 114.39(17) . . yes
C6 C10 C9 110.84(18) . . yes
O3 C11 O4 125.4(2) . . yes
O3 C11 N1 123.3(2) . . yes
O4 C11 N1 111.30(18) . . yes
O4 C12 C15 110.1(2) . . yes
O4 C12 C13 101.8(2) . . yes
C15 C12 C13 110.9(2) . . yes
O4 C12 C14 109.6(2) . . yes
C15 C12 C14 112.5(2) . . yes
C13 C12 C14 111.5(2) . . yes
O5 C16 O6 126.9(2) . . yes
O5 C16 N2 124.4(2) . . yes
O6 C16 N2 108.73(17) . . yes
O6 C17 C19 110.60(19) . . yes
O6 C17 C18 101.49(18) . . yes
C19 C17 C18 110.6(2) . . yes
O6 C17 C20 108.9(2) . . yes
C19 C17 C20 113.4(2) . . yes
C18 C17 C20 111.2(2) . . yes
C2 O1 H1B 101.7(17) . . yes
C2 C1 H1A 106.2 . . no
C5 C1 H1A 106.2 . . no
C8 C1 H1A 106.2 . . no
O1 C2 H2A 107.7 . . no
N1 C2 H2A 107.7 . . no
C1 C2 H2A 107.7 . . no
N1 C3 H3A 106.5 . . no
C4 C3 H3A 106.5 . . no
C6 C3 H3A 106.5 . . no
C3 C4 H4A 108.8 . . no
C5 C4 H4A 108.8 . . no
C3 C4 H4B 108.8 . . no
C5 C4 H4B 108.8 . . no
H4A C4 H4B 107.7 . . no
C1 C5 H5A 109.2 . . no
C4 C5 H5A 109.2 . . no
```

```
C1 C5 H5B 109.2 . . no
C4 C5 H5B 109.2 . . no
H5A C5 H5B 107.9 . . no
C7 C6 H6A 106.5 . . no
C10 C6 H6A 106.5 . . no
C3 C6 H6A 106.5 . . no
N2 C8 H8A 105.9 . . no
C9 C8 H8A 105.9 . . no
C1 C8 H8A 105.9 . . no
C8 C9 H9A 108.7 . . no
C10 C9 H9A 108.7 . . no
C8 C9 H9B 108.7 . . no
C10 C9 H9B 108.7 . . no
H9A C9 H9B 107.6 . . no
C6 C10 H10A 109.5 . . no
C9 C10 H10A 109.5 . . no
C6 C10 H10B 109.5 . . no
C9 C10 H10B 109.5 . . no
H10A C10 H10B 108.1 . . no
C12 C13 H13A 109.5 . . no
C12 C13 H13B 109.5 . . no
H13A C13 H13B 109.5 . . no
C12 C13 H13C 109.5 . . no
H13A C13 H13C 109.5 . . no
H13B C13 H13C 109.5 . . no
C12 C14 H14A 109.5 . . no
C12 C14 H14B 109.5 . . no
H14A C14 H14B 109.5 . . no
C12 C14 H14C 109.5 . . no
H14A C14 H14C 109.5 . . no
H14B C14 H14C 109.5 . . no
C12 C15 H15A 109.5 . . no
C12 C15 H15B 109.5 . . no
H15A C15 H15B 109.5 . . no
C12 C15 H15C 109.5 . . no
H15A C15 H15C 109.5 . . no
H15B C15 H15C 109.5 . . no
C17 C18 H18A 109.5 . . no
C17 C18 H18B 109.5 . . no
H18A C18 H18B 109.5 . . no
C17 C18 H18C 109.5 . . no
H18A C18 H18C 109.5 . . no
H18B C18 H18C 109.5 . . no
C17 C19 H19A 109.5 . . no
C17 C19 H19B 109.5 . . no
H19A C19 H19B 109.5 . . no
C17 C19 H19C 109.5 . . no
H19A C19 H19C 109.5 . . no
H19B C19 H19C 109.5 . . no
C17 C20 H20A 109.5 . . no
C17 C20 H20B 109.5 . . no
H20A C20 H20B 109.5 . . no
C17 C20 H20C 109.5 . . no
H20A C20 H20C 109.5 . . no
H20B C20 H20C 109.5 . . no

loop_
 _geom_torsion_atom_site_label_1
 _geom_torsion_atom_site_label_2
 _geom_torsion_atom_site_label_3
 _geom_torsion_atom_site_label_4
 _geom_torsion
    _geom_torsion_site_symmetry_1
```

```
  _geom_torsion_site_symmetry_2
  _geom_torsion_site_symmetry_3
  _geom_torsion_site_symmetry_4
  _geom_torsion_publ_flag
 C11 N1 C2 O1 -44.8(2) . . . . no
 C3 N1 C2 O1 144.08(17) . . . . no
 C11 N1 C2 C1 -169.01(17) . . . . no
 C3 N1 C2 C1 19.8(2) . . . . no
 C5 C1 C2 O1 169.11(16) . . . . no
 C8 C1 C2 O1 -61.2(2) . . . . no
 C5 C1 C2 N1 -65.5(2) . . . . no
 C8 C1 C2 N1 64.2(2) . . . . no
 C11 N1 C3 C4 -132.56(19) . . . . no
 C2 N1 C3 C4 38.3(2) . . . . no
 C11 N1 C3 C6 98.6(2) . . . . no
 C2 N1 C3 C6 -90.6(2) . . . . no
 N1 C3 C4 C5 -51.7(2) . . . . no
 C6 C3 C4 C5 76.3(2) . . . . no
 C2 C1 C5 C4 50.7(2) . . . . no
 C8 C1 C5 C4 -78.9(2) . . . . no
 C3 C4 C5 C1 6.9(2) . . . . no
 N1 C3 C6 C7 118.01(19) . . . . no
 C4 C3 C6 C7 -7.5(2) . . . . no
 N1 C3 C6 C10 -8.4(2) . . . . no
 C4 C3 C6 C10 -133.85(18) . . . . no
 C16 N2 C7 O2 -3.7(3) . . . . no
 C8 N2 C7 O2 -171.94(19) . . . . no
 C16 N2 C7 C6 174.29(18) . . . . no
 C8 N2 C7 C6 6.0(2) . . . . no
 C10 C6 C7 O2 -132.7(2) . . . . no
 C3 C6 C7 O2 98.8(2) . . . . no
 C10 C6 C7 N2 49.2(2) . . . . no
 C3 C6 C7 N2 -79.2(2) . . . . no
 C7 N2 C8 C9 -54.4(2) . . . . no
 C16 N2 C8 C9 137.16(18) . . . . no
 C7 N2 C8 C1 78.0(2) . . . . no
 C16 N2 C8 C1 -90.4(2) . . . . no
 C2 C1 C8 N2 -127.64(18) . . . . no
 C5 C1 C8 N2 -2.8(2) . . . . no
 C2 C1 C8 C9 -1.4(2) . . . . no
 C5 C1 C8 C9 123.4(2) . . . . no
 N2 C8 C9 C10 47.2(2) . . . . no
 C1 C8 C9 C10 -81.1(2) . . . . no
 C7 C6 C10 C9 -52.3(2) . . . . no
 C3 C6 C10 C9 75.7(2) . . . . no
 C8 C9 C10 C6 3.8(2) . . . . no
 C12 O4 C11 O3 5.0(3) . . . . no
 C12 O4 C11 N1 -174.24(19) . . . . no
 C2 N1 C11 O3 -3.1(3) . . . . no
 C3 N1 C11 O3 167.8(2) . . . . no
 C2 N1 C11 O4 176.24(17) . . . . no
 C3 N1 C11 O4 -12.9(3) . . . . no
 C11 O4 C12 C15 58.9(3) . . . . no
 C11 O4 C12 C13 176.6(2) . . . . no
 C11 O4 C12 C14 -65.3(3) . . . . no
 C17 O6 C16 O5 0.5(3) . . . . no
 C17 O6 C16 N2 179.94(18) . . . . no
 C7 N2 C16 O5 25.7(3) . . . . no
 C8 N2 C16 O5 -166.3(2) . . . . no
 C7 N2 C16 O6 -153.75(18) . . . . no
 C8 N2 C16 O6 14.3(3) . . . . no
 C16 O6 C17 C19 60.4(3) . . . . no
 C16 O6 C17 C18 177.8(2) . . . . no
```

```
C16 O6 C17 C20 -64.9(3) . . . . no

loop_
 _geom_hbond_atom_site_label_D
 _geom_hbond_atom_site_label_H
 _geom_hbond_atom_site_label_A
 _geom_hbond_distance_DH
 _geom_hbond_distance_HA
 _geom_hbond_distance_DA
 _geom_hbond_angle_DHA
 _geom_hbond_site_symmetry_A
O1 H1B O3  0.86(3) 1.98(3) 2.668(3) 136(2) .
```

X-ray crystal structure data for α-methyl *N*-Boc tetrahydro dimer (275)

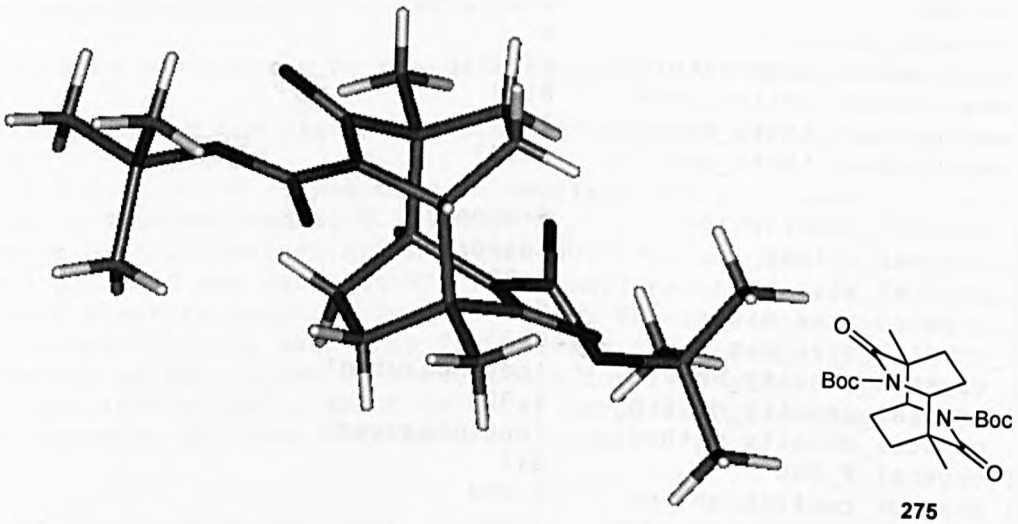

275

```
data_csf67s

_audit_creation_method            SHELXL-97
_chemical_name_systematic
;
 ?
;
_chemical_name_common             ?
_chemical_melting_point           ?
_chemical_formula_moiety          ?
_chemical_formula_sum
 'C22 H34 N2 O6'
_chemical_formula_weight          422.51

loop_
 _atom_type_symbol
 _atom_type_description
 _atom_type_scat_dispersion_real
 _atom_type_scat_dispersion_imag
 _atom_type_scat_source
 'C'  'C'   0.0033   0.0016
 'International Tables Vol C Tables 4.2.6.8 and 6.1.1.4'
 'H'  'H'   0.0000   0.0000
 'International Tables Vol C Tables 4.2.6.8 and 6.1.1.4'
 'N'  'N'   0.0061   0.0033
 'International Tables Vol C Tables 4.2.6.8 and 6.1.1.4'
 'O'  'O'   0.0106   0.0060
 'International Tables Vol C Tables 4.2.6.8 and 6.1.1.4'

_symmetry_cell_setting            Monoclinic
_symmetry_space_group_name_H-M    P2(1)/n

loop_
 _symmetry_equiv_pos_as_xyz
 'x, y, z'
 '-x+1/2, y+1/2, -z+1/2'
 '-x, -y, -z'
 'x-1/2, -y-1/2, z-1/2'

_cell_length_a                    10.0383(1)
_cell_length_b                    10.5380(1)
```

```
_cell_length_c                      20.4030(1)
_cell_angle_alpha                   90.000
_cell_angle_beta                    90.261(10)
_cell_angle_gamma                   90.000
_cell_volume                        2158.28(3)
_cell_formula_units_Z               4
_cell_measurement_temperature       123(1)
_cell_measurement_reflns_used       8192
_cell_measurement_theta_min         1.00
_cell_measurement_theta_max         26.37

_exptl_crystal_description          Fragment
_exptl_crystal_colour               Colourless
_exptl_crystal_size_max             0.20
_exptl_crystal_size_mid             0.30
_exptl_crystal_size_min             0.35
_exptl_crystal_density_meas         'not_measured'
_exptl_crystal_density_diffrn       1.300
_exptl_crystal_density_method       'not measured'
_exptl_crystal_F_000                912
_exptl_absorpt_coefficient_mu       0.094
_exptl_absorpt_correction_type      none
_exptl_absorpt_correction_T_min     ?
_exptl_absorpt_correction_T_max     ?
_exptl_absorpt_process_details      ?

_exptl_special_details
;
 ?
;

_diffrn_ambient_temperature             123(1)
_diffrn_radiation_wavelength            0.71073
_diffrn_radiation_type                  MoK\a
_diffrn_radiation_source                'fine-focus sealed tube'
_diffrn_radiation_monochromator         graphite
_diffrn_measurement_device_type         'Bruker AXS 1K CCD area detector'
_diffrn_measurement_method              'narrow frame \w scans'
_diffrn_detector_area_resol_mean        8.192
_diffrn_standards_number                'see text'
_diffrn_standards_interval_count        ?
_diffrn_standards_interval_time         ?
_diffrn_standards_decay_%               none
_diffrn_reflns_number                   22016
_diffrn_reflns_av_R_equivalents         0.0670
_diffrn_reflns_av_sigmaI/netI           0.0475
_diffrn_reflns_limit_h_min              -12
_diffrn_reflns_limit_h_max              12
_diffrn_reflns_limit_k_min              -13
_diffrn_reflns_limit_k_max              13
_diffrn_reflns_limit_l_min              -25
_diffrn_reflns_limit_l_max              25
_diffrn_reflns_theta_min                1.00
_diffrn_reflns_theta_max                26.37
_diffrn_reflns_theta_full               26.37
_diffrn_measured_fraction_theta_full    1.000
_reflns_number_total                    4422
_reflns_number_gt                       3830
_reflns_threshold_expression            >2sigma(I)

_computing_data_collection          'SMART (Bruker AXS, 1995)'
_computing_cell_refinement          'SMART & SAINT (Bruker AXS, 1995)'
   _computing_data_reduction           'SAINT (Bruker AXS, 1995)'
```

```
_computing_structure_solution     'SHELXTL (Sheldrick, 1994)'
_computing_structure_refinement   'SHELXTL (Sheldrick, 1994)'
_computing_molecular_graphics     'SHELXTL (Sheldrick, 1994)'
_computing_publication_material   'SHELXTL (Sheldrick, 1994)'

_refine_special_details
;
 The structure was twinned by pseudo-merohedry:  The \b angle being close
to
 90\% was emulating the higher orthorhombic crystal system and the twin
operator
 TWIN 1 0 0 0 -1 0 0 0 -1 was used to complete the refinement.  The batch
 scalefactor BASF refined to 0.36650.
 Refinement of F^2^ against ALL reflections.  The weighted R-factor wR and
 goodness of fit S are based on F^2^, conventional R-factors R are based
 on F, with F set to zero for negative F^2^. The threshold expression of
 F^2^ > 2sigma(F^2^) is used only for calculating R-factors(gt) etc. and is
 not relevant to the choice of reflections for refinement.  R-factors based
 on F^2^ are statistically about twice as large as those based on F, and R-
 factors based on ALL data will be even larger.
;

_refine_ls_structure_factor_coef  Fsqd
_refine_ls_matrix_type            full
_refine_ls_weighting_scheme       calc
_refine_ls_weighting_details
 'calc w=1/[\s^2^(Fo^2^)+(0.0975P)^2^+0.0000P] where P=(Fo^2^+2Fc^2^)/3'
_atom_sites_solution_primary      direct
_atom_sites_solution_secondary    difmap
_atom_sites_solution_hydrogens    geom
_refine_ls_hydrogen_treatment     mixed
_refine_ls_extinction_method      none
_refine_ls_extinction_coef        none
_refine_ls_number_reflns          4422
_refine_ls_number_parameters      280
_refine_ls_number_restraints      0
_refine_ls_R_factor_all           0.0565
_refine_ls_R_factor_gt            0.0505
_refine_ls_wR_factor_ref          0.1383
_refine_ls_wR_factor_gt           0.1324
_refine_ls_goodness_of_fit_ref    1.015
_refine_ls_restrained_S_all       1.015
_refine_ls_shift/su_max           0.000
_refine_ls_shift/su_mean          0.000
_refine_diff_density_max          0.330
_refine_diff_density_min         -0.333
_refine_diff_density_rms          0.064

loop_
 _atom_site_label
 _atom_site_type_symbol
 _atom_site_fract_x
 _atom_site_fract_y
 _atom_site_fract_z
 _atom_site_U_iso_or_equiv
 _atom_site_adp_type
 _atom_site_occupancy
 _atom_site_symmetry_multiplicity
 _atom_site_calc_flag
 _atom_site_refinement_flags
 _atom_site_disorder_assembly
 _atom_site_disorder_group
O1 O 0.03044(15) 0.91285(14) 0.06315(8) 0.0237(4) Uani 1 1 d . . .
```

```
O2 O 0.42874(16) 0.97473(15) 0.09411(8) 0.0258(4) Uani 1 1 d . . .
O3 O 0.22464(17) 0.97963(17) 0.13760(9) 0.0294(4) Uani 1 1 d . . .
O4 O 0.43111(17) 0.60792(15) -0.10582(9) 0.0278(4) Uani 1 1 d . . .
O5 O 0.06086(16) 0.50740(16) -0.11402(9) 0.0297(4) Uani 1 1 d . . .
O6 O 0.26170(15) 0.41340(14) -0.11944(8) 0.0221(4) Uani 1 1 d . . .
N1 N 0.25170(18) 0.89602(16) 0.03679(9) 0.0183(4) Uani 1 1 d . . .
N2 N 0.23506(18) 0.58029(16) -0.05234(9) 0.0188(4) Uani 1 1 d . . .
C1 C 0.1160(2) 0.86714(19) 0.02989(11) 0.0182(4) Uani 1 1 d . . .
C2 C 0.0863(2) 0.7704(2) -0.02408(11) 0.0198(5) Uani 1 1 d . . .
C3 C 0.1408(2) 0.8225(2) -0.08870(11) 0.0217(5) Uani 1 1 d . . .
H3A H 0.0789 0.8877 -0.1059 0.026 Uiso 1 1 calc R . .
H3B H 0.1449 0.7528 -0.1212 0.026 Uiso 1 1 calc R . .
C4 C 0.2800(2) 0.8811(2) -0.08095(11) 0.0222(5) Uani 1 1 d . . .
H4A H 0.3384 0.8469 -0.1157 0.027 Uiso 1 1 calc R . .
H4B H 0.2732 0.9739 -0.0875 0.027 Uiso 1 1 calc R . .
C5 C 0.3444(2) 0.85603(19) -0.01478(11) 0.0187(5) Uani 1 1 d . . .
H5A H 0.4216 0.9157 -0.0119 0.022 Uiso 1 1 calc R . .
C6 C -0.0650(2) 0.7558(2) -0.02995(12) 0.0242(5) Uani 1 1 d . . .
H6A H -0.1050 0.8382 -0.0407 0.036 Uiso 1 1 calc R . .
H6B H -0.1009 0.7253 0.0118 0.036 Uiso 1 1 calc R . .
H6C H -0.0861 0.6947 -0.0647 0.036 Uiso 1 1 calc R . .
C7 C 0.3109(2) 0.95469(19) 0.09186(11) 0.0199(5) Uani 1 1 d . . .
C8 C 0.2703(2) 1.0339(2) 0.20105(12) 0.0279(5) Uani 1 1 d . . .
C9 C 0.3659(3) 0.9438(2) 0.23454(13) 0.0307(6) Uani 1 1 d . . .
H9A H 0.3283 0.8580 0.2342 0.046 Uiso 1 1 calc R . .
H9B H 0.3803 0.9711 0.2799 0.046 Uiso 1 1 calc R . .
H9C H 0.4510 0.9439 0.2112 0.046 Uiso 1 1 calc R . .
C10 C 0.1417(3) 1.0443(4) 0.23767(15) 0.0480(8) Uani 1 1 d . . .
H10A H 0.1040 0.9594 0.2441 0.072 Uiso 1 1 calc R . .
H10B H 0.0788 1.0964 0.2124 0.072 Uiso 1 1 calc R . .
H10C H 0.1580 1.0839 0.2804 0.072 Uiso 1 1 calc R . .
C11 C 0.3320(3) 1.1634(2) 0.19002(15) 0.0379(7) Uani 1 1 d . . .
H11A H 0.4156 1.1538 0.1659 0.057 Uiso 1 1 calc R . .
H11B H 0.3499 1.2037 0.2324 0.057 Uiso 1 1 calc R . .
H11C H 0.2703 1.2163 0.1646 0.057 Uiso 1 1 calc R . .
C12 C 0.3626(2) 0.63078(19) -0.05959(11) 0.0192(4) Uani 1 1 d . . .
C13 C 0.4044(2) 0.7193(2) -0.00398(11) 0.0186(4) Uani 1 1 d . . .
C14 C 0.3632(2) 0.66002(19) 0.06133(11) 0.0204(5) Uani 1 1 d . . .
H14A H 0.3834 0.7203 0.0972 0.025 Uiso 1 1 calc R . .
H14B H 0.4165 0.5823 0.0690 0.025 Uiso 1 1 calc R . .
C15 C 0.2144(2) 0.6259(2) 0.06323(11) 0.0210(5) Uani 1 1 d . . .
H15A H 0.2048 0.5379 0.0796 0.025 Uiso 1 1 calc R . .
H15B H 0.1690 0.6829 0.0946 0.025 Uiso 1 1 calc R . .
C16 C 0.1456(2) 0.63648(19) -0.00368(11) 0.0194(5) Uani 1 1 d . . .
H16A H 0.0673 0.5780 -0.0014 0.023 Uiso 1 1 calc R . .
C17 C 0.5564(2) 0.7317(2) -0.00614(12) 0.0243(5) Uani 1 1 d . . .
H17A H 0.5970 0.6478 -0.0007 0.036 Uiso 1 1 calc R . .
H17B H 0.5864 0.7877 0.0293 0.036 Uiso 1 1 calc R . .
H17C H 0.5830 0.7676 -0.0484 0.036 Uiso 1 1 calc R . .
C18 C 0.1762(2) 0.4991(2) -0.09890(12) 0.0213(5) Uani 1 1 d . . .
C19 C 0.2381(2) 0.3451(2) -0.18173(11) 0.0205(5) Uani 1 1 d . . .
C20 C 0.3618(2) 0.2656(2) -0.18780(12) 0.0267(5) Uani 1 1 d . . .
H20A H 0.4405 0.3205 -0.1857 0.040 Uiso 1 1 calc R . .
H20B H 0.3604 0.2205 -0.2298 0.040 Uiso 1 1 calc R . .
H20C H 0.3651 0.2039 -0.1519 0.040 Uiso 1 1 calc R . .
C21 C 0.1153(3) 0.2624(2) -0.17825(15) 0.0346(6) Uani 1 1 d . . .
H21A H 0.0359 0.3161 -0.1747 0.052 Uiso 1 1 calc R . .
H21B H 0.1214 0.2070 -0.1398 0.052 Uiso 1 1 calc R . .
H21C H 0.1089 0.2104 -0.2180 0.052 Uiso 1 1 calc R . .
C22 C 0.2306(3) 0.4431(3) -0.23568(13) 0.0359(6) Uani 1 1 d . . .
H22A H 0.3095 0.4977 -0.2337 0.054 Uiso 1 1 calc R . .
H22B H 0.1503 0.4948 -0.2301 0.054 Uiso 1 1 calc R . .
   H22C H 0.2271 0.4002 -0.2783 0.054 Uiso 1 1 calc R . .
```

```
loop_
 _atom_site_aniso_label
 _atom_site_aniso_U_11
 _atom_site_aniso_U_22
 _atom_site_aniso_U_33
 _atom_site_aniso_U_23
 _atom_site_aniso_U_13
 _atom_site_aniso_U_12
O1 0.0201(8) 0.0179(8) 0.0331(9) -0.0044(7) 0.0011(7) 0.0007(6)
O2 0.0222(8) 0.0233(8) 0.0320(9) -0.0055(7) 0.0002(7) -0.0061(7)
O3 0.0214(8) 0.0338(9) 0.0330(9) -0.0122(8) -0.0017(7) -0.0008(7)
O4 0.0253(8) 0.0228(8) 0.0352(10) -0.0069(7) 0.0062(8) -0.0030(7)
O5 0.0206(8) 0.0241(9) 0.0443(10) -0.0121(7) -0.0061(8) 0.0019(7)
O6 0.0246(8) 0.0131(7) 0.0286(8) -0.0049(6) -0.0038(7) 0.0034(6)
N1 0.0171(9) 0.0101(8) 0.0276(10) -0.0015(7) -0.0002(8) -0.0007(7)
N2 0.0179(9) 0.0110(8) 0.0274(10) -0.0033(7) -0.0014(8) 0.0009(7)
C1 0.0193(10) 0.0108(9) 0.0245(11) 0.0034(8) -0.0005(9) 0.0003(8)
C2 0.0178(11) 0.0128(10) 0.0287(12) -0.0029(9) -0.0030(9) 0.0006(8)
C3 0.0231(11) 0.0149(10) 0.0269(12) -0.0012(9) -0.0039(10) 0.0017(9)
C4 0.0226(11) 0.0157(10) 0.0282(12) 0.0039(9) -0.0012(9) -0.0006(9)
C5 0.0199(11) 0.0107(10) 0.0254(12) -0.0010(8) 0.0014(9) -0.0022(8)
C6 0.0183(11) 0.0186(11) 0.0358(13) -0.0051(10) -0.0041(10) 0.0003(9)
C7 0.0208(11) 0.0108(9) 0.0279(11) -0.0008(9) -0.0015(9) -0.0009(8)
C8 0.0242(12) 0.0291(12) 0.0304(13) -0.0105(10) -0.0040(10) 0.0027(10)
C9 0.0305(13) 0.0267(12) 0.0348(13) 0.0008(10) -0.0018(11) 0.0007(11)
C10 0.0269(14) 0.080(2) 0.0375(15) -0.0239(16) -0.0012(13) 0.0063(14)
C11 0.0529(18) 0.0200(12) 0.0407(15) -0.0082(11) -0.0088(13) 0.0069(12)
C12 0.0178(10) 0.0117(9) 0.0280(12) 0.0011(9) -0.0022(9) 0.0003(8)
C13 0.0166(11) 0.0141(10) 0.0251(11) -0.0020(9) -0.0011(9) -0.0006(8)
C14 0.0213(11) 0.0143(10) 0.0257(12) 0.0009(8) -0.0028(10) 0.0001(8)
C15 0.0226(11) 0.0114(9) 0.0289(12) 0.0029(9) 0.0027(10) -0.0005(8)
C16 0.0175(10) 0.0099(9) 0.0308(12) -0.0013(8) 0.0010(9) -0.0022(8)
C17 0.0163(11) 0.0217(11) 0.0349(13) -0.0016(10) -0.0011(10) 0.0001(9)
C18 0.0211(11) 0.0142(10) 0.0286(12) -0.0021(9) -0.0025(9) 0.0010(8)
C19 0.0205(10) 0.0158(10) 0.0252(11) -0.0046(9) -0.0017(9) -0.0001(8)
C20 0.0256(12) 0.0207(11) 0.0339(13) -0.0073(10) -0.0037(10) 0.0032(10)
C21 0.0263(13) 0.0252(12) 0.0524(16) -0.0162(12) 0.0030(12) -0.0088(10)
C22 0.0431(16) 0.0320(14) 0.0325(14) 0.0033(11) -0.0018(13) 0.0106(12)

_geom_special_details
;
 All esds (except the esd in the dihedral angle between two l.s. planes)
 are estimated using the full covariance matrix.  The cell esds are taken
 into account individually in the estimation of esds in distances, angles
 and torsion angles; correlations between esds in cell parameters are only
 used when they are defined by crystal symmetry.  An approximate
(isotropic)
 treatment of cell esds is used for estimating esds involving l.s. planes.
;

loop_
 _geom_bond_atom_site_label_1
 _geom_bond_atom_site_label_2
 _geom_bond_distance
 _geom_bond_site_symmetry_2
 _geom_bond_publ_flag
O1 C1 1.198(3) . ?
O2 C7 1.202(3) . ?
O3 C7 1.303(3) . ?
O3 C8 1.486(3) . ?
O4 C12 1.195(3) . ?
O5 C18 1.200(3) . ?
```

```
O6 C18 1.316(3) . ?
O6 C19 1.479(3) . ?
N1 C1 1.403(3) . ?
N1 C7 1.411(3) . ?
N1 C5 1.469(3) . ?
N2 C12 1.395(3) . ?
N2 C18 1.407(3) . ?
N2 C16 1.467(3) . ?
C1 C2 1.529(3) . ?
C2 C6 1.531(3) . ?
C2 C3 1.532(3) . ?
C2 C16 1.587(3) . ?
C3 C4 1.535(3) . ?
C3 H3A 0.9900 . ?
C3 H3B 0.9900 . ?
C4 C5 1.517(3) . ?
C4 H4A 0.9900 . ?
C4 H4B 0.9900 . ?
C5 C13 1.577(3) . ?
C5 H5A 1.0000 . ?
C6 H6A 0.9800 . ?
C6 H6B 0.9800 . ?
C6 H6C 0.9800 . ?
C8 C10 1.499(4) . ?
C8 C9 1.510(3) . ?
C8 C11 1.516(4) . ?
C9 H9A 0.9800 . ?
C9 H9B 0.9800 . ?
C9 H9C 0.9800 . ?
C10 H10A 0.9800 . ?
C10 H10B 0.9800 . ?
C10 H10C 0.9800 . ?
C11 H11A 0.9800 . ?
C11 H11B 0.9800 . ?
C11 H11C 0.9800 . ?
C12 C13 1.526(3) . ?
C13 C14 1.530(3) . ?
C13 C17 1.532(3) . ?
C14 C15 1.537(3) . ?
C14 H14A 0.9900 . ?
C14 H14B 0.9900 . ?
C15 C16 1.531(3) . ?
C15 H15A 0.9900 . ?
C15 H15B 0.9900 . ?
C16 H16A 1.0000 . ?
C17 H17A 0.9800 . ?
C17 H17B 0.9800 . ?
C17 H17C 0.9800 . ?
C19 C20 1.504(3) . ?
C19 C22 1.511(3) . ?
C19 C21 1.512(3) . ?
C20 H20A 0.9800 . ?
C20 H20B 0.9800 . ?
C20 H20C 0.9800 . ?
C21 H21A 0.9800 . ?
C21 H21B 0.9800 . ?
C21 H21C 0.9800 . ?
C22 H22A 0.9800 . ?
C22 H22B 0.9800 . ?
C22 H22C 0.9800 . ?

loop_
    _geom_angle_atom_site_label_1
```

```
_geom_angle_atom_site_label_2
_geom_angle_atom_site_label_3
_geom_angle
_geom_angle_site_symmetry_1
_geom_angle_site_symmetry_3
_geom_angle_publ_flag
C7 O3 C8 119.88(18) . . ?
C18 O6 C19 120.34(17) . . ?
C1 N1 C7 125.48(19) . . ?
C1 N1 C5 118.94(18) . . ?
C7 N1 C5 115.46(17) . . ?
C12 N2 C18 122.92(19) . . ?
C12 N2 C16 118.89(17) . . ?
C18 N2 C16 116.47(18) . . ?
O1 C1 N1 123.7(2) . . ?
O1 C1 C2 122.6(2) . . ?
N1 C1 C2 113.77(18) . . ?
C1 C2 C6 108.27(18) . . ?
C1 C2 C3 108.19(17) . . ?
C6 C2 C3 109.08(19) . . ?
C1 C2 C16 109.42(18) . . ?
C6 C2 C16 107.58(17) . . ?
C3 C2 C16 114.15(18) . . ?
C2 C3 C4 112.59(19) . . ?
C2 C3 H3A 109.1 . . ?
C4 C3 H3A 109.1 . . ?
C2 C3 H3B 109.1 . . ?
C4 C3 H3B 109.1 . . ?
H3A C3 H3B 107.8 . . ?
C5 C4 C3 113.93(18) . . ?
C5 C4 H4A 108.8 . . ?
C3 C4 H4A 108.8 . . ?
C5 C4 H4B 108.8 . . ?
C3 C4 H4B 108.8 . . ?
H4A C4 H4B 107.7 . . ?
N1 C5 C4 108.58(18) . . ?
N1 C5 C13 113.87(17) . . ?
C4 C5 C13 116.38(18) . . ?
N1 C5 H5A 105.7 . . ?
C4 C5 H5A 105.7 . . ?
C13 C5 H5A 105.7 . . ?
C2 C6 H6A 109.5 . . ?
C2 C6 H6B 109.5 . . ?
H6A C6 H6B 109.5 . . ?
C2 C6 H6C 109.5 . . ?
H6A C6 H6C 109.5 . . ?
H6B C6 H6C 109.5 . . ?
O2 C7 O3 126.5(2) . . ?
O2 C7 N1 121.2(2) . . ?
O3 C7 N1 112.31(18) . . ?
O3 C8 C10 101.5(2) . . ?
O3 C8 C9 110.20(19) . . ?
C10 C8 C9 111.6(2) . . ?
O3 C8 C11 110.0(2) . . ?
C10 C8 C11 111.2(2) . . ?
C9 C8 C11 112.0(2) . . ?
C8 C9 H9A 109.5 . . ?
C8 C9 H9B 109.5 . . ?
H9A C9 H9B 109.5 . . ?
C8 C9 H9C 109.5 . . ?
H9A C9 H9C 109.5 . . ?
H9B C9 H9C 109.5 . . ?
C8 C10 H10A 109.5 . . ?
```

```
C8 C10 H10B 109.5 . . ?
H10A C10 H10B 109.5 . . ?
C8 C10 H10C 109.5 . . ?
H10A C10 H10C 109.5 . . ?
H10B C10 H10C 109.5 . . ?
C8 C11 H11A 109.5 . . ?
C8 C11 H11B 109.5 . . ?
H11A C11 H11B 109.5 . . ?
C8 C11 H11C 109.5 . . ?
H11A C11 H11C 109.5 . . ?
H11B C11 H11C 109.5 . . ?
O4 C12 N2 122.6(2) . . ?
O4 C12 C13 123.57(19) . . ?
N2 C12 C13 113.80(19) . . ?
C12 C13 C14 108.87(17) . . ?
C12 C13 C17 107.54(18) . . ?
C14 C13 C17 109.43(18) . . ?
C12 C13 C5 110.55(18) . . ?
C14 C13 C5 112.99(17) . . ?
C17 C13 C5 107.31(17) . . ?
C13 C14 C15 112.56(18) . . ?
C13 C14 H14A 109.1 . . ?
C15 C14 H14A 109.1 . . ?
C13 C14 H14B 109.1 . . ?
C15 C14 H14B 109.1 . . ?
H14A C14 H14B 107.8 . . ?
C16 C15 C14 113.28(18) . . ?
C16 C15 H15A 108.9 . . ?
C14 C15 H15A 108.9 . . ?
C16 C15 H15B 108.9 . . ?
C14 C15 H15B 108.9 . . ?
H15A C15 H15B 107.7 . . ?
N2 C16 C15 107.36(17) . . ?
N2 C16 C2 114.32(18) . . ?
C15 C16 C2 117.77(17) . . ?
N2 C16 H16A 105.4 . . ?
C15 C16 H16A 105.4 . . ?
C2 C16 H16A 105.4 . . ?
C13 C17 H17A 109.5 . . ?
C13 C17 H17B 109.5 . . ?
H17A C17 H17B 109.5 . . ?
C13 C17 H17C 109.5 . . ?
H17A C17 H17C 109.5 . . ?
H17B C17 H17C 109.5 . . ?
O5 C18 O6 126.8(2) . . ?
O5 C18 N2 122.1(2) . . ?
O6 C18 N2 111.07(19) . . ?
O6 C19 C20 102.28(18) . . ?
O6 C19 C22 107.52(18) . . ?
C20 C19 C22 111.0(2) . . ?
O6 C19 C21 111.60(19) . . ?
C20 C19 C21 110.88(19) . . ?
C22 C19 C21 113.0(2) . . ?
C19 C20 H20A 109.5 . . ?
C19 C20 H20B 109.5 . . ?
H20A C20 H20B 109.5 . . ?
C19 C20 H20C 109.5 . . ?
H20A C20 H20C 109.5 . . ?
H20B C20 H20C 109.5 . . ?
C19 C21 H21A 109.5 . . ?
C19 C21 H21B 109.5 . . ?
H21A C21 H21B 109.5 . . ?
   C19 C21 H21C 109.5 . . ?
```

```
H21A C21 H21C 109.5 . . ?
H21B C21 H21C 109.5 . . ?
C19 C22 H22A 109.5 . . ?
C19 C22 H22B 109.5 . . ?
H22A C22 H22B 109.5 . . ?
C19 C22 H22C 109.5 . . ?
H22A C22 H22C 109.5 . . ?
H22B C22 H22C 109.5 . . ?

loop_
 _geom_torsion_atom_site_label_1
 _geom_torsion_atom_site_label_2
 _geom_torsion_atom_site_label_3
 _geom_torsion_atom_site_label_4
 _geom_torsion
 _geom_torsion_site_symmetry_1
 _geom_torsion_site_symmetry_2
 _geom_torsion_site_symmetry_3
 _geom_torsion_site_symmetry_4
 _geom_torsion_publ_flag
C7 N1 C1 O1 16.9(3) . . . . ?
C5 N1 C1 O1 -167.3(2) . . . . ?
C7 N1 C1 C2 -162.70(19) . . . . ?
C5 N1 C1 C2 13.1(3) . . . . ?
O1 C1 C2 C6 4.9(3) . . . . ?
N1 C1 C2 C6 -175.52(18) . . . . ?
O1 C1 C2 C3 123.0(2) . . . . ?
N1 C1 C2 C3 -57.4(2) . . . . ?
O1 C1 C2 C16 -112.1(2) . . . . ?
N1 C1 C2 C16 67.5(2) . . . . ?
C1 C2 C3 C4 43.4(2) . . . . ?
C6 C2 C3 C4 161.02(18) . . . . ?
C16 C2 C3 C4 -78.6(2) . . . . ?
C2 C3 C4 C5 9.8(3) . . . . ?
C1 N1 C5 C4 42.1(2) . . . . ?
C7 N1 C5 C4 -141.67(18) . . . . ?
C1 N1 C5 C13 -89.3(2) . . . . ?
C7 N1 C5 C13 86.9(2) . . . . ?
C3 C4 C5 N1 -53.2(2) . . . . ?
C3 C4 C5 C13 76.8(2) . . . . ?
C8 O3 C7 O2 -2.5(3) . . . . ?
C8 O3 C7 N1 176.04(18) . . . . ?
C1 N1 C7 O2 179.1(2) . . . . ?
C5 N1 C7 O2 3.1(3) . . . . ?
C1 N1 C7 O3 0.5(3) . . . . ?
C5 N1 C7 O3 -175.48(18) . . . . ?
C7 O3 C8 C10 -179.1(2) . . . . ?
C7 O3 C8 C9 -60.7(3) . . . . ?
C7 O3 C8 C11 63.2(3) . . . . ?
C18 N2 C12 O4 -0.4(3) . . . . ?
C16 N2 C12 O4 -164.9(2) . . . . ?
C18 N2 C12 C13 178.37(19) . . . . ?
C16 N2 C12 C13 13.9(3) . . . . ?
O4 C12 C13 C14 -137.9(2) . . . . ?
N2 C12 C13 C14 43.3(2) . . . . ?
O4 C12 C13 C17 -19.4(3) . . . . ?
N2 C12 C13 C17 161.76(18) . . . . ?
O4 C12 C13 C5 97.4(2) . . . . ?
N2 C12 C13 C5 -81.4(2) . . . . ?
N1 C5 C13 C12 117.3(2) . . . . ?
C4 C5 C13 C12 -10.2(2) . . . . ?
N1 C5 C13 C14 -5.0(2) . . . . ?
C4 C5 C13 C14 -132.5(2) . . . . ?
```

```
N1 C5 C13 C17 -125.7(2) . . . . ?
C4 C5 C13 C17 106.8(2) . . . . ?
C12 C13 C14 C15 -54.1(2) . . . . ?
C17 C13 C14 C15 -171.38(18) . . . . ?
C5 C13 C14 C15 69.1(2) . . . . ?
C13 C14 C15 C16 10.1(2) . . . . ?
C12 N2 C16 C15 -58.8(2) . . . . ?
C18 N2 C16 C15 135.67(19) . . . . ?
C12 N2 C16 C2 73.8(2) . . . . ?
C18 N2 C16 C2 -91.7(2) . . . . ?
C14 C15 C16 N2 43.2(2) . . . . ?
C14 C15 C16 C2 -87.5(2) . . . . ?
C1 C2 C16 N2 -125.71(19) . . . . ?
C6 C2 C16 N2 116.9(2) . . . . ?
C3 C2 C16 N2 -4.3(3) . . . . ?
C1 C2 C16 C15 1.7(3) . . . . ?
C6 C2 C16 C15 -115.7(2) . . . . ?
C3 C2 C16 C15 123.1(2) . . . . ?
C19 O6 C18 O5 22.5(4) . . . . ?
C19 O6 C18 N2 -160.71(18) . . . . ?
C12 N2 C18 O5 -139.5(2) . . . . ?
C16 N2 C18 O5 25.3(3) . . . . ?
C12 N2 C18 O6 43.5(3) . . . . ?
C16 N2 C18 O6 -151.61(18) . . . . ?
C18 O6 C19 C20 176.37(19) . . . . ?
C18 O6 C19 C22 59.4(3) . . . . ?
C18 O6 C19 C21 -65.0(3) . . . . ?
```

X-ray crystal structure data for α-methyl *N*-Boc tetrahydro dilactamol (285)

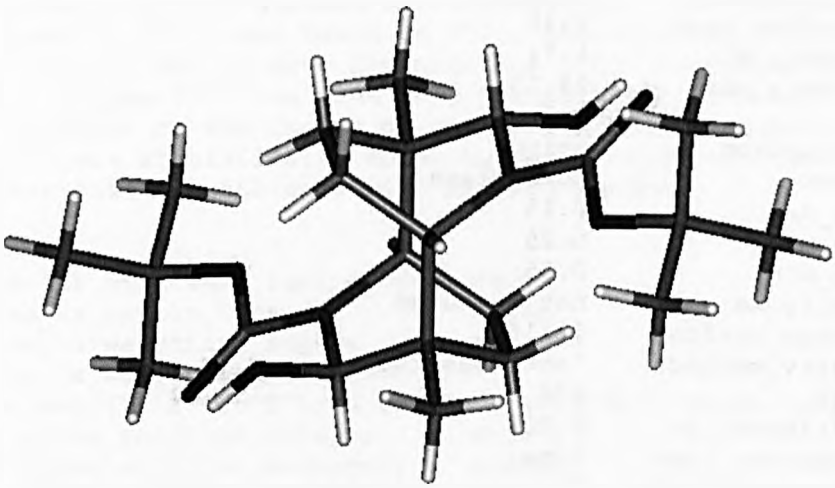

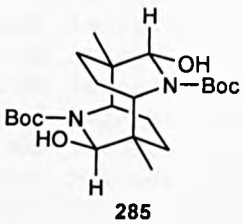

285

```
data_csf74s

_audit_creation_method            SHELXL-97
_chemical_name_systematic
;
 ?
;
_chemical_name_common             ?
_chemical_melting_point           ?
_chemical_formula_moiety          ?
_chemical_formula_sum
 'C22 H38 N2 O6'
_chemical_formula_weight          426.54

loop_
 _atom_type_symbol
 _atom_type_description
 _atom_type_scat_dispersion_real
 _atom_type_scat_dispersion_imag
 _atom_type_scat_source
 'C'  'C'   0.0033   0.0016
 'International Tables Vol C Tables 4.2.6.8 and 6.1.1.4'
 'H'  'H'   0.0000   0.0000
 'International Tables Vol C Tables 4.2.6.8 and 6.1.1.4'
 'N'  'N'   0.0061   0.0033
 'International Tables Vol C Tables 4.2.6.8 and 6.1.1.4'
 'O'  'O'   0.0106   0.0060
 'International Tables Vol C Tables 4.2.6.8 and 6.1.1.4'

_symmetry_cell_setting            Triclinic
_symmetry_space_group_name_H-M    P-1

loop_
 _symmetry_equiv_pos_as_xyz
 'x, y, z'
 '-x, -y, -z'

_cell_length_a                    9.3330(17)
_cell_length_b                    10.677(2)
_cell_length_c                    12.256(4)
_cell_angle_alpha                 72.454(15)
```

```
_cell_angle_beta                    88.891(18)
_cell_angle_gamma                   87.200(13)
_cell_volume                        1163.0(5)
_cell_formula_units_Z               2
_cell_measurement_temperature       123(1)
_cell_measurement_reflns_used       7745
_cell_measurement_theta_min         1.74
_cell_measurement_theta_max         29.13

_exptl_crystal_description          prism
_exptl_crystal_colour               colourless
_exptl_crystal_size_max             0.15
_exptl_crystal_size_mid             0.25
_exptl_crystal_size_min             0.55
_exptl_crystal_density_meas         not_measured
_exptl_crystal_density_diffrn       1.218
_exptl_crystal_density_method       'not measured'
_exptl_crystal_F_000                464
_exptl_absorpt_coefficient_mu       0.088
_exptl_absorpt_correction_type      none
_exptl_absorpt_correction_T_min     ?
_exptl_absorpt_correction_T_max     ?
_exptl_absorpt_process_details      ?

_exptl_special_details
;
 ?
;

_diffrn_ambient_temperature             123(1)
_diffrn_radiation_wavelength            0.71073
_diffrn_radiation_type                  MoK\a
_diffrn_radiation_source                'fine-focus sealed tube'
_diffrn_radiation_monochromator         graphite
_diffrn_measurement_device_type         'Bruker AXS 1K CCD area detector'
_diffrn_measurement_method              'narrow frame \w scans'
_diffrn_detector_area_resol_mean        8.192
_diffrn_standards_number                'see text'
_diffrn_standards_interval_count        ?
_diffrn_standards_interval_time         ?
_diffrn_standards_decay_%               none
_diffrn_reflns_number                   11721
_diffrn_reflns_av_R_equivalents         0.0380
_diffrn_reflns_av_sigmaI/netI           0.0512
_diffrn_reflns_limit_h_min              -11
_diffrn_reflns_limit_h_max              11
_diffrn_reflns_limit_k_min              -13
_diffrn_reflns_limit_k_max              13
_diffrn_reflns_limit_l_min              -15
_diffrn_reflns_limit_l_max              15
_diffrn_reflns_theta_min                1.74
_diffrn_reflns_theta_max                26.37
_diffrn_reflns_theta_full               26.37
_diffrn_measured_fraction_theta_full    0.992
_reflns_number_total                    4716
_reflns_number_gt                       3497
_reflns_threshold_expression            >2sigma(I)

_computing_data_collection          'SMART (Bruker AXS, 1995)'
_computing_cell_refinement          'SMART & SAINT (Bruker AXS, 1995)'
_computing_data_reduction           'SAINT (Bruker AXS, 1995)'
_computing_structure_solution       'SHELXTL (Sheldrick, 1994)'
   _computing_structure_refinement   'SHELXTL (Sheldrick, 1994)'
```

```
_computing_molecular_graphics     'SHELXTL (Sheldrick, 1994)'
_computing_publication_material   'SHELXTL (Sheldrick, 1994)'

_refine_special_details
;
 Refinement of F^2^ against ALL reflections.  The weighted R-factor wR and
 goodness of fit S are based on F^2^, conventional R-factors R are based
 on F, with F set to zero for negative F^2^. The threshold expression of
 F^2^ > 2sigma(F^2^) is used only for calculating R-factors(gt) etc. and is
 not relevant to the choice of reflections for refinement.  R-factors based
 on F^2^ are statistically about twice as large as those based on F, and R-
 factors based on ALL data will be even larger.
;

_refine_ls_structure_factor_coef  Fsqd
_refine_ls_matrix_type            full
_refine_ls_weighting_scheme       calc
_refine_ls_weighting_details
 'calc w=1/[\s^2^(Fo^2^)+(0.0950P)^2^+0.0000P] where P=(Fo^2^+2Fc^2^)/3'
_atom_sites_solution_primary      direct
_atom_sites_solution_secondary    difmap
_atom_sites_solution_hydrogens    geom
_refine_ls_hydrogen_treatment     mixed
_refine_ls_extinction_method      none
_refine_ls_extinction_coef        ?
_refine_ls_number_reflns          4716
_refine_ls_number_parameters      289
_refine_ls_number_restraints      0
_refine_ls_R_factor_all           0.0673
_refine_ls_R_factor_gt            0.0523
_refine_ls_wR_factor_ref          0.1485
_refine_ls_wR_factor_gt           0.1422
_refine_ls_goodness_of_fit_ref    1.010
_refine_ls_restrained_S_all       1.010
_refine_ls_shift/su_max           0.001
_refine_ls_shift/su_mean          0.000
_refine_diff_density_max          0.329
_refine_diff_density_min         -0.411
_refine_diff_density_rms          0.079

loop_
 _atom_site_label
 _atom_site_type_symbol
 _atom_site_fract_x
 _atom_site_fract_y
 _atom_site_fract_z
 _atom_site_U_iso_or_equiv
 _atom_site_adp_type
 _atom_site_occupancy
 _atom_site_symmetry_multiplicity
 _atom_site_calc_flag
 _atom_site_refinement_flags
 _atom_site_disorder_assembly
 _atom_site_disorder_group
O1A O 0.71787(12) 0.43630(12) -0.08040(11) 0.0233(3) Uani 1 1 d . . .
H1AA H 0.6306 0.4379 -0.0627 0.035 Uiso 1 1 calc R . .
O2A O 0.58105(12) 0.46420(12) 0.11109(10) 0.0214(3) Uani 1 1 d . . .
O3A O 0.74638(13) 0.42605(13) 0.25307(10) 0.0257(3) Uani 1 1 d . . .
N1A N 0.81741(14) 0.50267(13) 0.07024(11) 0.0165(3) Uani 1 1 d . . .
C1A C 0.78542(18) 0.53813(16) -0.05313(14) 0.0174(4) Uani 1 1 d . . .
H1AB H 0.7176 0.6170 -0.0724 0.021 Uiso 1 1 calc R . .
C2A C 0.95613(17) 0.53719(16) 0.10726(15) 0.0161(4) Uani 1 1 d . . .
H2AA H 0.9409(19) 0.5424(16) 0.1810(15) 0.015(4) Uiso 1 1 d . . .
```

```
C3A C 0.98608(19) 0.67645(16) 0.03207(15) 0.0209(4) Uani 1 1 d . . .
H3AA H 1.0834 0.6980 0.0494 0.025 Uiso 1 1 calc R . .
H3AB H 0.9168 0.7391 0.0524 0.025 Uiso 1 1 calc R . .
C4A C 0.97620(19) 0.69640(16) -0.09701(15) 0.0216(4) Uani 1 1 d . . .
H4AA H 1.0722 0.7163 -0.1320 0.026 Uiso 1 1 calc R . .
H4AB H 0.9104 0.7732 -0.1317 0.026 Uiso 1 1 calc R . .
C5A C 0.92243(18) 0.57585(16) -0.12492(14) 0.0179(4) Uani 1 1 d . . .
C6A C 0.70499(18) 0.46534(16) 0.14277(14) 0.0178(4) Uani 1 1 d . . .
C7A C 0.64226(19) 0.37201(18) 0.34522(15) 0.0246(4) Uani 1 1 d . . .
C8A C 0.5253(2) 0.47545(19) 0.34839(16) 0.0298(5) Uani 1 1 d . . .
H8AA H 0.5694 0.5562 0.3504 0.045 Uiso 1 1 calc R . .
H8AB H 0.4657 0.4425 0.4169 0.045 Uiso 1 1 calc R . .
H8AC H 0.4655 0.4942 0.2800 0.045 Uiso 1 1 calc R . .
C9A C 0.5808(2) 0.24791(19) 0.33143(18) 0.0355(5) Uani 1 1 d . . .
H9AA H 0.6592 0.1894 0.3187 0.053 Uiso 1 1 calc R . .
H9AB H 0.5158 0.2718 0.2658 0.053 Uiso 1 1 calc R . .
H9AC H 0.5280 0.2028 0.4009 0.053 Uiso 1 1 calc R . .
C10A C 0.7364(2) 0.3397(2) 0.45087(16) 0.0405(6) Uani 1 1 d . . .
H10A H 0.8125 0.2750 0.4460 0.061 Uiso 1 1 calc R . .
H10B H 0.6780 0.3033 0.5194 0.061 Uiso 1 1 calc R . .
H10C H 0.7795 0.4199 0.4553 0.061 Uiso 1 1 calc R . .
C11A C 0.8774(2) 0.61640(19) -0.25095(15) 0.0268(4) Uani 1 1 d . . .
H11A H 0.9581 0.6556 -0.2995 0.040 Uiso 1 1 calc R . .
H11B H 0.7962 0.6808 -0.2631 0.040 Uiso 1 1 calc R . .
H11C H 0.8490 0.5387 -0.2707 0.040 Uiso 1 1 calc R . .
O1B O 0.20668(12) 0.01685(13) 0.09287(11) 0.0244(3) Uani 1 1 d . . .
H1BA H 0.1219 0.0117 0.0733 0.037 Uiso 1 1 calc R . .
O2B O 0.08675(12) -0.00335(12) -0.10288(10) 0.0228(3) Uani 1 1 d . . .
O3B O 0.24702(12) 0.05996(13) -0.24965(10) 0.0252(3) Uani 1 1 d . . .
N1B N 0.32643(14) -0.02074(13) -0.06897(11) 0.0157(3) Uani 1 1 d . . .
C1B C 0.29730(17) -0.07074(16) 0.05497(14) 0.0170(4) Uani 1 1 d . . .
H1BB H 0.2491 -0.1561 0.0709 0.020 Uiso 1 1 calc R . .
C2B C 0.47371(17) -0.03088(16) -0.11202(15) 0.0156(4) Uani 1 1 d . . .
H2BA H 0.4661(17) -0.0310(14) -0.1888(13) 0.004(4) Uiso 1 1 d . . .
C3B C 0.53705(19) -0.16695(16) -0.04583(15) 0.0209(4) Uani 1 1 d . . .
H3BA H 0.6394 -0.1728 -0.0674 0.025 Uiso 1 1 calc R . .
H3BB H 0.4871 -0.2341 -0.0696 0.025 Uiso 1 1 calc R . .
C4B C 0.52622(19) -0.19998(16) 0.08503(15) 0.0219(4) Uani 1 1 d . . .
H4BA H 0.4817 -0.2859 0.1164 0.026 Uiso 1 1 calc R . .
H4BB H 0.6240 -0.2084 0.1171 0.026 Uiso 1 1 calc R . .
C5B C 0.43801(17) -0.09572(16) 0.12302(14) 0.0166(4) Uani 1 1 d . . .
C6B C 0.21070(17) 0.01063(16) -0.13830(14) 0.0180(4) Uani 1 1 d . . .
C7B C 0.1361(2) 0.11747(19) -0.33690(15) 0.0251(4) Uani 1 1 d . . .
C8B C 0.0309(2) 0.01606(19) -0.34376(16) 0.0294(5) Uani 1 1 d . . .
H8BA H 0.0840 -0.0629 -0.3502 0.044 Uiso 1 1 calc R . .
H8BB H -0.0303 0.0525 -0.4110 0.044 Uiso 1 1 calc R . .
H8BC H -0.0288 -0.0069 -0.2745 0.044 Uiso 1 1 calc R . .
C9B C 0.0619(2) 0.2359(2) -0.31212(18) 0.0368(5) Uani 1 1 d . . .
H9BA H 0.1341 0.2957 -0.3032 0.055 Uiso 1 1 calc R . .
H9BB H 0.0054 0.2066 -0.2415 0.055 Uiso 1 1 calc R . .
H9BC H -0.0018 0.2819 -0.3758 0.055 Uiso 1 1 calc R . .
C10B C 0.2262(2) 0.1590(2) -0.44587(16) 0.0409(6) Uani 1 1 d . . .
H10D H 0.2949 0.2228 -0.4394 0.061 Uiso 1 1 calc R . .
H10E H 0.1633 0.1991 -0.5115 0.061 Uiso 1 1 calc R . .
H10F H 0.2782 0.0817 -0.4568 0.061 Uiso 1 1 calc R . .
C11B C 0.3966(2) -0.15318(19) 0.24942(15) 0.0265(4) Uani 1 1 d . . .
H11D H 0.3428 -0.0860 0.2750 0.040 Uiso 1 1 calc R . .
H11E H 0.4837 -0.1815 0.2954 0.040 Uiso 1 1 calc R . .
H11F H 0.3370 -0.2288 0.2586 0.040 Uiso 1 1 calc R . .

loop_
 _atom_site_aniso_label
    _atom_site_aniso_U_11
```

```
   _atom_site_aniso_U_22
   _atom_site_aniso_U_33
   _atom_site_aniso_U_23
   _atom_site_aniso_U_13
   _atom_site_aniso_U_12
  O1A 0.0084(6) 0.0366(7) 0.0308(7) -0.0189(6) 0.0031(5) -0.0032(5)
  O2A 0.0077(6) 0.0324(7) 0.0237(7) -0.0082(5) 0.0006(5) 0.0007(5)
  O3A 0.0097(6) 0.0459(8) 0.0182(7) -0.0048(6) 0.0030(5) -0.0022(6)
  N1A 0.0072(7) 0.0240(8) 0.0189(7) -0.0070(6) 0.0006(6) -0.0012(6)
  C1A 0.0107(8) 0.0216(9) 0.0191(9) -0.0055(7) 0.0015(7) 0.0012(7)
  C2A 0.0070(8) 0.0235(9) 0.0206(9) -0.0108(7) 0.0013(7) 0.0001(7)
  C3A 0.0135(9) 0.0181(8) 0.0322(10) -0.0094(8) -0.0002(7) 0.0002(7)
  C4A 0.0149(9) 0.0173(9) 0.0303(10) -0.0043(8) 0.0053(8) 0.0011(7)
  C5A 0.0103(8) 0.0212(9) 0.0204(9) -0.0043(7) 0.0017(7) 0.0021(7)
  C6A 0.0108(8) 0.0227(9) 0.0204(9) -0.0074(7) 0.0005(7) 0.0013(7)
  C7A 0.0132(9) 0.0373(11) 0.0200(9) -0.0043(8) 0.0065(7) 0.0005(8)
  C8A 0.0254(11) 0.0368(11) 0.0269(10) -0.0103(9) 0.0051(8) 0.0034(9)
  C9A 0.0335(12) 0.0310(11) 0.0370(12) -0.0035(9) 0.0108(9) -0.0018(9)
  C10A 0.0259(11) 0.0659(15) 0.0216(10) -0.0016(10) 0.0020(9) 0.0014(10)
  C11A 0.0163(9) 0.0377(11) 0.0217(10) -0.0028(8) 0.0027(8) 0.0046(8)
  O1B 0.0043(6) 0.0442(8) 0.0297(7) -0.0196(6) 0.0004(5) 0.0040(5)
  O2B 0.0056(6) 0.0390(8) 0.0238(7) -0.0096(6) 0.0012(5) -0.0004(5)
  O3B 0.0071(6) 0.0459(8) 0.0188(7) -0.0042(6) -0.0012(5) 0.0011(5)
  N1B 0.0039(7) 0.0254(8) 0.0177(7) -0.0065(6) 0.0009(5) 0.0004(6)
  C1B 0.0086(8) 0.0225(9) 0.0198(9) -0.0062(7) 0.0019(7) -0.0008(7)
  C2B 0.0044(8) 0.0241(9) 0.0205(9) -0.0105(7) 0.0028(7) 0.0006(6)
  C3B 0.0122(9) 0.0177(9) 0.0343(11) -0.0103(8) 0.0036(7) 0.0005(7)
  C4B 0.0162(9) 0.0172(8) 0.0322(10) -0.0074(8) -0.0063(8) 0.0027(7)
  C5B 0.0089(8) 0.0197(8) 0.0199(9) -0.0038(7) -0.0010(7) 0.0003(6)
  C6B 0.0088(8) 0.0250(9) 0.0209(9) -0.0080(7) 0.0008(7) -0.0005(7)
  C7B 0.0158(9) 0.0382(11) 0.0187(9) -0.0047(8) -0.0061(7) 0.0026(8)
  C8B 0.0215(10) 0.0402(11) 0.0274(11) -0.0117(9) -0.0052(8) 0.0014(9)
  C9B 0.0366(12) 0.0352(11) 0.0366(12) -0.0086(9) -0.0120(10) 0.0075(9)
  C10B 0.0278(12) 0.0634(15) 0.0234(11) -0.0008(10) -0.0006(9) -0.0039(11)
  C11B 0.0183(10) 0.0316(10) 0.0250(10) -0.0006(8) -0.0035(8) -0.0063(8)

 _geom_special_details
 ;
  All esds (except the esd in the dihedral angle between two l.s. planes)
  are estimated using the full covariance matrix.  The cell esds are taken
  into account individually in the estimation of esds in distances, angles
  and torsion angles; correlations between esds in cell parameters are only
  used when they are defined by crystal symmetry.  An approximate
 (isotropic)
  treatment of cell esds is used for estimating esds involving l.s. planes.
 ;

 loop_
  _geom_bond_atom_site_label_1
  _geom_bond_atom_site_label_2
  _geom_bond_distance
  _geom_bond_site_symmetry_2
  _geom_bond_publ_flag
 O1A C1A 1.409(2) . ?
 O1A H1AA 0.8400 . ?
 O2A C6A 1.229(2) . ?
 O3A C6A 1.347(2) . ?
 O3A C7A 1.474(2) . ?
 N1A C6A 1.357(2) . ?
 N1A C1A 1.476(2) . ?
 N1A C2A 1.479(2) . ?
 C1A C5A 1.538(2) . ?
 C1A H1AB 1.0000 . ?
```

```
C2A C3A 1.531(2) . ?
C2A C5A 1.583(2) 2_765 ?
C2A H2AA 0.929(17) . ?
C3A C4A 1.535(2) . ?
C3A H3AA 0.9900 . ?
C3A H3AB 0.9900 . ?
C4A C5A 1.537(2) . ?
C4A H4AA 0.9900 . ?
C4A H4AB 0.9900 . ?
C5A C11A 1.534(2) . ?
C5A C2A 1.583(2) 2_765 ?
C7A C10A 1.521(3) . ?
C7A C8A 1.523(2) . ?
C7A C9A 1.525(3) . ?
C8A H8AA 0.9800 . ?
C8A H8AB 0.9800 . ?
C8A H8AC 0.9800 . ?
C9A H9AA 0.9800 . ?
C9A H9AB 0.9800 . ?
C9A H9AC 0.9800 . ?
C10A H10A 0.9800 . ?
C10A H10B 0.9800 . ?
C10A H10C 0.9800 . ?
C11A H11A 0.9800 . ?
C11A H11B 0.9800 . ?
C11A H11C 0.9800 . ?
O1B C1B 1.4054(18) . ?
O1B H1BA 0.8400 . ?
O2B C6B 1.228(2) . ?
O3B C6B 1.349(2) . ?
O3B C7B 1.475(2) . ?
N1B C6B 1.353(2) . ?
N1B C2B 1.474(2) . ?
N1B C1B 1.475(2) . ?
C1B C5B 1.538(2) . ?
C1B H1BB 1.0000 . ?
C2B C3B 1.530(2) . ?
C2B C5B 1.587(2) 2_655 ?
C2B H2BA 0.945(15) . ?
C3B C4B 1.537(2) . ?
C3B H3BA 0.9900 . ?
C3B H3BB 0.9900 . ?
C4B C5B 1.530(2) . ?
C4B H4BA 0.9900 . ?
C4B H4BB 0.9900 . ?
C5B C11B 1.534(2) . ?
C5B C2B 1.587(2) 2_655 ?
C7B C8B 1.518(3) . ?
C7B C9B 1.520(3) . ?
C7B C10B 1.524(3) . ?
C8B H8BA 0.9800 . ?
C8B H8BB 0.9800 . ?
C8B H8BC 0.9800 . ?
C9B H9BA 0.9800 . ?
C9B H9BB 0.9800 . ?
C9B H9BC 0.9800 . ?
C10B H10D 0.9800 . ?
C10B H10E 0.9800 . ?
C10B H10F 0.9800 . ?
C11B H11D 0.9800 . ?
C11B H11E 0.9800 . ?
C11B H11F 0.9800 . ?
```

```
loop_
 _geom_angle_atom_site_label_1
 _geom_angle_atom_site_label_2
 _geom_angle_atom_site_label_3
 _geom_angle
 _geom_angle_site_symmetry_1
 _geom_angle_site_symmetry_3
 _geom_angle_publ_flag
C1A O1A H1AA 109.5 . . ?
C6A O3A C7A 120.49(13) . . ?
C6A N1A C1A 116.27(13) . . ?
C6A N1A C2A 122.85(14) . . ?
C1A N1A C2A 119.37(13) . . ?
O1A C1A N1A 111.55(13) . . ?
O1A C1A C5A 111.09(13) . . ?
N1A C1A C5A 110.70(13) . . ?
O1A C1A H1AB 107.8 . . ?
N1A C1A H1AB 107.8 . . ?
C5A C1A H1AB 107.8 . . ?
N1A C2A C3A 107.24(13) . . ?
N1A C2A C5A 113.64(13) . 2_765 ?
C3A C2A C5A 119.63(14) . 2_765 ?
N1A C2A H2AA 105.9(11) . . ?
C3A C2A H2AA 106.4(10) . . ?
C5A C2A H2AA 102.8(11) 2_765 . ?
C2A C3A C4A 114.38(13) . . ?
C2A C3A H3AA 108.7 . . ?
C4A C3A H3AA 108.7 . . ?
C2A C3A H3AB 108.7 . . ?
C4A C3A H3AB 108.7 . . ?
H3AA C3A H3AB 107.6 . . ?
C3A C4A C5A 113.00(14) . . ?
C3A C4A H4AA 109.0 . . ?
C5A C4A H4AA 109.0 . . ?
C3A C4A H4AB 109.0 . . ?
C5A C4A H4AB 109.0 . . ?
H4AA C4A H4AB 107.8 . . ?
C11A C5A C4A 109.08(14) . . ?
C11A C5A C1A 106.78(14) . . ?
C4A C5A C1A 105.95(13) . . ?
C11A C5A C2A 107.49(13) . 2_765 ?
C4A C5A C2A 111.71(14) . 2_765 ?
C1A C5A C2A 115.61(14) . 2_765 ?
O2A C6A O3A 124.26(16) . . ?
O2A C6A N1A 123.80(16) . . ?
O3A C6A N1A 111.90(14) . . ?
O3A C7A C10A 101.62(14) . . ?
O3A C7A C8A 110.62(15) . . ?
C10A C7A C8A 110.84(16) . . ?
O3A C7A C9A 110.27(14) . . ?
C10A C7A C9A 110.96(16) . . ?
C8A C7A C9A 112.07(17) . . ?
C7A C8A H8AA 109.5 . . ?
C7A C8A H8AB 109.5 . . ?
H8AA C8A H8AB 109.5 . . ?
C7A C8A H8AC 109.5 . . ?
H8AA C8A H8AC 109.5 . . ?
H8AB C8A H8AC 109.5 . . ?
C7A C9A H9AA 109.5 . . ?
C7A C9A H9AB 109.5 . . ?
H9AA C9A H9AB 109.5 . . ?
C7A C9A H9AC 109.5 . . ?
H9AA C9A H9AC 109.5 . . ?
```

```
H9AB C9A H9AC 109.5 . . ?
C7A C10A H10A 109.5 . . ?
C7A C10A H10B 109.5 . . ?
H10A C10A H10B 109.5 . . ?
C7A C10A H10C 109.5 . . ?
H10A C10A H10C 109.5 . . ?
H10B C10A H10C 109.5 . . ?
C5A C11A H11A 109.5 . . ?
C5A C11A H11B 109.5 . . ?
H11A C11A H11B 109.5 . . ?
C5A C11A H11C 109.5 . . ?
H11A C11A H11C 109.5 . . ?
H11B C11A H11C 109.5 . . ?
C1B O1B H1BA 109.5 . . ?
C6B O3B C7B 120.60(13) . . ?
C6B N1B C2B 122.86(14) . . ?
C6B N1B C1B 116.47(13) . . ?
C2B N1B C1B 119.60(13) . . ?
O1B C1B N1B 111.87(13) . . ?
O1B C1B C5B 109.06(13) . . ?
N1B C1B C5B 110.63(13) . . ?
O1B C1B H1BB 108.4 . . ?
N1B C1B H1BB 108.4 . . ?
C5B C1B H1BB 108.4 . . ?
N1B C2B C3B 107.05(14) . . ?
N1B C2B C5B 113.20(12) . 2_655 ?
C3B C2B C5B 119.73(13) . 2_655 ?
N1B C2B H2BA 106.9(10) . . ?
C3B C2B H2BA 106.0(9) . . ?
C5B C2B H2BA 103.0(9) 2_655 . ?
C2B C3B C4B 114.59(13) . . ?
C2B C3B H3BA 108.6 . . ?
C4B C3B H3BA 108.6 . . ?
C2B C3B H3BB 108.6 . . ?
C4B C3B H3BB 108.6 . . ?
H3BA C3B H3BB 107.6 . . ?
C5B C4B C3B 112.71(13) . . ?
C5B C4B H4BA 109.0 . . ?
C3B C4B H4BA 109.0 . . ?
C5B C4B H4BB 109.0 . . ?
C3B C4B H4BB 109.0 . . ?
H4BA C4B H4BB 107.8 . . ?
C4B C5B C11B 109.04(14) . . ?
C4B C5B C1B 106.45(13) . . ?
C11B C5B C1B 106.47(14) . . ?
C4B C5B C2B 111.96(14) . 2_655 ?
C11B C5B C2B 107.32(13) . 2_655 ?
C1B C5B C2B 115.37(13) . 2_655 ?
O2B C6B O3B 124.22(15) . . ?
O2B C6B N1B 123.30(16) . . ?
O3B C6B N1B 112.48(14) . . ?
O3B C7B C8B 111.53(15) . . ?
O3B C7B C9B 109.29(14) . . ?
C8B C7B C9B 112.28(16) . . ?
O3B C7B C10B 101.60(14) . . ?
C8B C7B C10B 110.49(15) . . ?
C9B C7B C10B 111.17(17) . . ?
C7B C8B H8BA 109.5 . . ?
C7B C8B H8BB 109.5 . . ?
H8BA C8B H8BB 109.5 . . ?
C7B C8B H8BC 109.5 . . ?
H8BA C8B H8BC 109.5 . . ?
   H8BB C8B H8BC 109.5 . . ?
```

```
 C7B C9B H9BA 109.5 . . ?
 C7B C9B H9BB 109.5 . . ?
 H9BA C9B H9BB 109.5 . . ?
 C7B C9B H9BC 109.5 . . ?
 H9BA C9B H9BC 109.5 . . ?
 H9BB C9B H9BC 109.5 . . ?
 C7B C10B H10D 109.5 . . ?
 C7B C10B H10E 109.5 . . ?
 H10D C10B H10E 109.5 . . ?
 C7B C10B H10F 109.5 . . ?
 H10D C10B H10F 109.5 . . ?
 H10E C10B H10F 109.5 . . ?
 C5B C11B H11D 109.5 . . ?
 C5B C11B H11E 109.5 . . ?
 H11D C11B H11E 109.5 . . ?
 C5B C11B H11F 109.5 . . ?
 H11D C11B H11F 109.5 . . ?
 H11E C11B H11F 109.5 . . ?

 loop_
  _geom_torsion_atom_site_label_1
  _geom_torsion_atom_site_label_2
  _geom_torsion_atom_site_label_3
  _geom_torsion_atom_site_label_4
  _geom_torsion
  _geom_torsion_site_symmetry_1
  _geom_torsion_site_symmetry_2
  _geom_torsion_site_symmetry_3
  _geom_torsion_site_symmetry_4
  _geom_torsion_publ_flag
C6A N1A C1A O1A -54.72(18) . . . . ?
C2A N1A C1A O1A 138.90(14) . . . . ?
C6A N1A C1A C5A -178.97(13) . . . . ?
C2A N1A C1A C5A 14.64(19) . . . . ?
C6A N1A C2A C3A -123.52(16) . . . . ?
C1A N1A C2A C3A 41.93(18) . . . . ?
C6A N1A C2A C5A 101.97(17) . . . 2_765 ?
C1A N1A C2A C5A -92.58(17) . . . 2_765 ?
N1A C2A C3A C4A -52.16(18) . . . . ?
C5A C2A C3A C4A 79.11(19) 2_765 . . . ?
C2A C3A C4A C5A 6.1(2) . . . . ?
C3A C4A C5A C11A 164.77(14) . . . . ?
C3A C4A C5A C1A 50.15(17) . . . . ?
C3A C4A C5A C2A -76.55(17) . . . 2_765 ?
O1A C1A C5A C11A 57.82(17) . . . . ?
N1A C1A C5A C11A -177.67(13) . . . . ?
O1A C1A C5A C4A 174.00(13) . . . . ?
N1A C1A C5A C4A -61.49(16) . . . . ?
O1A C1A C5A C2A -61.69(18) . . . 2_765 ?
N1A C1A C5A C2A 62.82(17) . . . 2_765 ?
C7A O3A C6A O2A 2.8(2) . . . . ?
C7A O3A C6A N1A -175.32(13) . . . . ?
C1A N1A C6A O2A -2.5(2) . . . . ?
C2A N1A C6A O2A 163.35(15) . . . . ?
C1A N1A C6A O3A 175.58(13) . . . . ?
C2A N1A C6A O3A -18.6(2) . . . . ?
C6A O3A C7A C10A 178.79(15) . . . . ?
C6A O3A C7A C8A -63.5(2) . . . . ?
C6A O3A C7A C9A 61.1(2) . . . . ?
C6B N1B C1B O1B -55.43(19) . . . . ?
C2B N1B C1B O1B 136.07(14) . . . . ?
C6B N1B C1B C5B -177.23(14) . . . . ?
C2B N1B C1B C5B 14.26(19) . . . . ?
```

```
C6B N1B C2B C3B -125.76(16) . . . . ?
C1B N1B C2B C3B 41.98(18) . . . . ?
C6B N1B C2B C5B 100.16(17) . . . 2_655 ?
C1B N1B C2B C5B -92.11(17) . . . 2_655 ?
N1B C2B C3B C4B -52.49(18) . . . . ?
C5B C2B C3B C4B 78.02(19) 2_655 . . . ?
C2B C3B C4B C5B 6.7(2) . . . . ?
C3B C4B C5B C11B 164.01(14) . . . . ?
C3B C4B C5B C1B 49.53(18) . . . . ?
C3B C4B C5B C2B -77.39(17) . . . 2_655 ?
O1B C1B C5B C4B 175.38(13) . . . . ?
N1B C1B C5B C4B -61.17(17) . . . . ?
O1B C1B C5B C11B 59.16(17) . . . . ?
N1B C1B C5B C11B -177.39(13) . . . . ?
O1B C1B C5B C2B -59.76(18) . . . 2_655 ?
N1B C1B C5B C2B 63.68(17) . . . 2_655 ?
C7B O3B C6B O2B 8.0(2) . . . . ?
C7B O3B C6B N1B -171.25(14) . . . . ?
C2B N1B C6B O2B 166.50(15) . . . . ?
C1B N1B C6B O2B -1.6(2) . . . . ?
C2B N1B C6B O3B -14.2(2) . . . . ?
C1B N1B C6B O3B 177.71(13) . . . . ?
C6B O3B C7B C8B -62.5(2) . . . . ?
C6B O3B C7B C9B 62.2(2) . . . . ?
C6B O3B C7B C10B 179.75(15) . . . . ?

loop_
 _geom_hbond_atom_site_label_D
 _geom_hbond_atom_site_label_H
 _geom_hbond_atom_site_label_A
 _geom_hbond_distance_DH
 _geom_hbond_distance_HA
 _geom_hbond_distance_DA
 _geom_hbond_angle_DHA
 _geom_hbond_site_symmetry_A
O1A H1AA O2A  0.84 2.19 2.9263(17) 145.7 2_665
O1B H1BA O2B  0.84 1.98 2.7478(17) 152.4 2
```

X-ray crystal structure data for decalin ether (330)

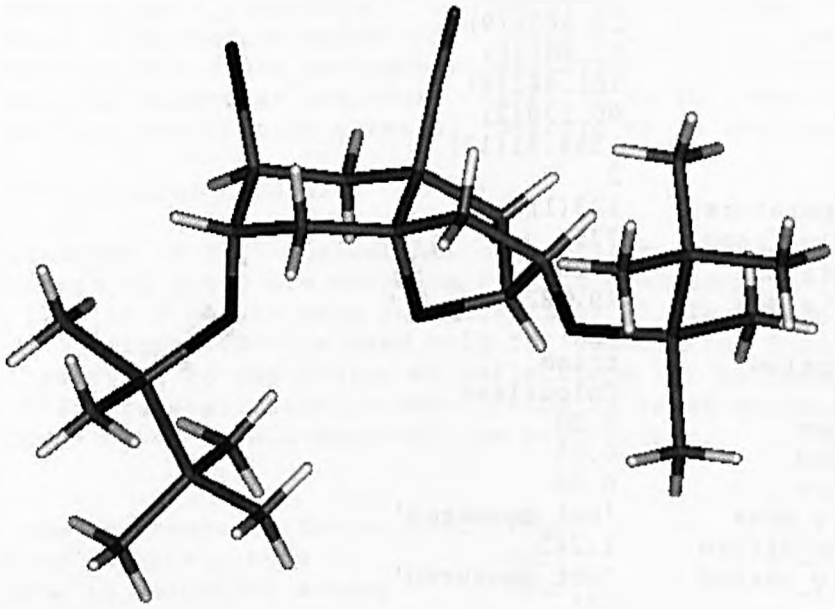

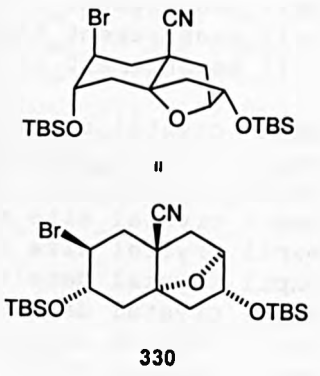

330

```
data_csf119s

_audit_creation_method            SHELXL-97
_chemical_name_systematic
;
 ?
;
_chemical_name_common             ?
_chemical_melting_point           ?
_chemical_formula_moiety          ?
_chemical_formula_sum
 'C23 H42 Br N O3 Si2'
_chemical_formula_weight          516.67

loop_
 _atom_type_symbol
 _atom_type_description
 _atom_type_scat_dispersion_real
 _atom_type_scat_dispersion_imag
 _atom_type_scat_source
 'C'  'C'   0.0033   0.0016
 'International Tables Vol C Tables 4.2.6.8 and 6.1.1.4'
 'H'  'H'   0.0000   0.0000
 'International Tables Vol C Tables 4.2.6.8 and 6.1.1.4'
 'N'  'N'   0.0061   0.0033
 'International Tables Vol C Tables 4.2.6.8 and 6.1.1.4'
 'O'  'O'   0.0106   0.0060
 'International Tables Vol C Tables 4.2.6.8 and 6.1.1.4'
 'Si'  'Si'   0.0817   0.0704
 'International Tables Vol C Tables 4.2.6.8 and 6.1.1.4'
 'Br'  'Br'  -0.2901   2.4595
 'International Tables Vol C Tables 4.2.6.8 and 6.1.1.4'

_symmetry_cell_setting            Triclinic
_symmetry_space_group_name_H-M    P-1

loop_
 _symmetry_equiv_pos_as_xyz
```

```
 'x, y, z'
 '-x, -y, -z'

_cell_length_a                    7.3353(4)
_cell_length_b                    11.9856(7)
_cell_length_c                    15.8601(9)
_cell_angle_alpha                 95.406(2)
_cell_angle_beta                  101.841(2)
_cell_angle_gamma                 90.139(2)
_cell_volume                      1358.31(13)
_cell_formula_units_Z             2
_cell_measurement_temperature     123(1)
_cell_measurement_reflns_used     7757
_cell_measurement_theta_min       2.256
_cell_measurement_theta_max       29.222

_exptl_crystal_description        prism
_exptl_crystal_colour             Colourless
_exptl_crystal_size_max           0.30
_exptl_crystal_size_mid           0.25
_exptl_crystal_size_min           0.15
_exptl_crystal_density_meas       'not measured'
_exptl_crystal_density_diffrn     1.263
_exptl_crystal_density_method     'not measured'
_exptl_crystal_F_000              548
_exptl_absorpt_coefficient_mu     1.624
_exptl_absorpt_correction_type    none
_exptl_absorpt_correction_T_min   ?
_exptl_absorpt_correction_T_max   ?
_exptl_absorpt_process_details    ?

_exptl_special_details
;
 ?
;

_diffrn_ambient_temperature            123(1)
_diffrn_radiation_wavelength           0.71073
_diffrn_radiation_type                 MoK\a
_diffrn_radiation_source               'fine-focus sealed tube'
_diffrn_radiation_monochromator        graphite
_diffrn_measurement_device_type        'Bruker AXS 1K CCD area detector'
_diffrn_measurement_method             'narrow frame \w scans'
_diffrn_detector_area_resol_mean       8.192
_diffrn_standards_number               'see text'
_diffrn_standards_interval_count       ?
_diffrn_standards_interval_time        ?
_diffrn_standards_decay_%              none
_diffrn_reflns_number                  11831
_diffrn_reflns_av_R_equivalents        0.0164
_diffrn_reflns_av_sigmaI/netI          0.0270
_diffrn_reflns_limit_h_min             -9
_diffrn_reflns_limit_h_max             9
_diffrn_reflns_limit_k_min             -14
_diffrn_reflns_limit_k_max             14
_diffrn_reflns_limit_l_min             -19
_diffrn_reflns_limit_l_max             19
_diffrn_reflns_theta_min               1.32
_diffrn_reflns_theta_max               26.37
_diffrn_reflns_theta_full              26.37
_diffrn_measured_fraction_theta_full   0.990
_reflns_number_total                   5493
   _reflns_number_gt                      4719
```

```
_reflns_threshold_expression          >2sigma(I)

_computing_data_collection      'SMART V5.056 (Bruker AXS, 1997)'
_computing_cell_refinement      'SMART V5.056/SAINT V6.01 (Bruker AXS,
1997)'
_computing_data_reduction       'SAINT V6.01 (Bruker AXS, 1997)'
_computing_structure_solution   'SHELXTL V5.10 (Sheldrick, 1997)'
_computing_structure_refinement 'SHELXTL V5.10 (Sheldrick, 1997)'
_computing_molecular_graphics   'SHELXTL V5.10 (Sheldrick, 1997)'
_computing_publication_material 'SHELXTL V5.10 (Sheldrick, 1997)'

_refine_special_details
;
 Refinement of F^2^ against ALL reflections.  The weighted R-factor wR and
 goodness of fit S are based on F^2^, conventional R-factors R are based
 on F, with F set to zero for negative F^2^. The threshold expression of
 F^2^ > 2sigma(F^2^) is used only for calculating R-factors(gt) etc. and is
 not relevant to the choice of reflections for refinement.  R-factors based
 on F^2^ are statistically about twice as large as those based on F, and R-
 factors based on ALL data will be even larger.
;

_refine_ls_structure_factor_coef  Fsqd
_refine_ls_matrix_type            full
_refine_ls_weighting_scheme       calc
_refine_ls_weighting_details
 'calc w=1/[\s^2^(Fo^2^)+(0.0585P)^2^+0.0000P] where P=(Fo^2^+2Fc^2^)/3'
_atom_sites_solution_primary      direct
_atom_sites_solution_secondary    difmap
_atom_sites_solution_hydrogens    geom
_refine_ls_hydrogen_treatment     mixed
_refine_ls_extinction_method      none
_refine_ls_extinction_coef        ?
_refine_ls_number_reflns          5493
_refine_ls_number_parameters      281
_refine_ls_number_restraints      0
_refine_ls_R_factor_all           0.0333
_refine_ls_R_factor_gt            0.0280
_refine_ls_wR_factor_ref          0.0852
_refine_ls_wR_factor_gt           0.0803
_refine_ls_goodness_of_fit_ref    1.004
_refine_ls_restrained_S_all       1.004
_refine_ls_shift/su_max           0.003
_refine_ls_shift/su_mean          0.000
_refine_diff_density_max          0.640
_refine_diff_density_min         -0.323
_refine_diff_density_rms          0.051

loop_
 _atom_site_label
 _atom_site_type_symbol
 _atom_site_fract_x
 _atom_site_fract_y
 _atom_site_fract_z
 _atom_site_U_iso_or_equiv
 _atom_site_adp_type
 _atom_site_occupancy
 _atom_site_symmetry_multiplicity
 _atom_site_calc_flag
 _atom_site_refinement_flags
 _atom_site_disorder_assembly
 _atom_site_disorder_group
Br1 Br 0.73887(3) 0.250924(18) 0.208585(13) 0.03343(8) Uani 1 1 d . . .
```

```
Si1 Si 1.48911(7) 0.80847(4) 0.16918(3) 0.02128(12) Uani 1 1 d . . .
Si2 Si 1.29203(6) 0.25540(4) 0.47566(3) 0.01766(12) Uani 1 1 d . . .
O1 O 1.35746(16) 0.47324(10) 0.27265(8) 0.0194(3) Uani 1 1 d . . .
O2 O 1.42379(18) 0.70516(11) 0.21957(8) 0.0235(3) Uani 1 1 d . . .
O3 O 1.23442(17) 0.31254(11) 0.38320(8) 0.0248(3) Uani 1 1 d . . .
N1 N 0.8220(3) 0.43108(15) 0.05371(11) 0.0331(4) Uani 1 1 d . . .
C1 C 1.3005(3) 0.40882(15) 0.12585(12) 0.0227(4) Uani 1 1 d . . .
H1A H 1.3748 0.3403 0.1227 0.027 Uiso 1 1 calc R . .
H1B H 1.2661 0.4356 0.0676 0.027 Uiso 1 1 calc R . .
C2 C 1.4055(3) 0.50033(16) 0.19282(12) 0.0218(4) Uani 1 1 d . . .
H2A H 1.5427 0.5031 0.1952 0.026 Uiso 1 1 calc R . .
C3 C 1.3104(3) 0.61179(15) 0.17570(12) 0.0219(4) Uani 1 1 d . . .
H3A H 1.2743 0.6192 0.1122 0.026 Uiso 1 1 calc R . .
C4 C 1.1371(3) 0.59687(15) 0.21452(12) 0.0212(4) Uani 1 1 d . . .
H4A H 1.1361 0.6539 0.2638 0.025 Uiso 1 1 calc R . .
H4B H 1.0212 0.6020 0.1704 0.025 Uiso 1 1 calc R . .
C5 C 1.0514(2) 0.45736(15) 0.31399(11) 0.0203(4) Uani 1 1 d . . .
H5A H 0.9203 0.4784 0.2939 0.024 Uiso 1 1 calc R . .
H5B H 1.1037 0.5075 0.3667 0.024 Uiso 1 1 calc R . .
C6 C 1.0529(2) 0.33736(16) 0.33858(12) 0.0212(4) Uani 1 1 d . . .
H6A H 0.9618 0.3288 0.3767 0.025 Uiso 1 1 calc R . .
C7 C 1.0070(3) 0.25117(16) 0.25958(12) 0.0235(4) Uani 1 1 d . . .
H7A H 1.0362 0.1756 0.2801 0.028 Uiso 1 1 calc R . .
C8 C 1.1255(3) 0.26898(15) 0.19382(12) 0.0229(4) Uani 1 1 d . . .
H8A H 1.0819 0.2153 0.1421 0.027 Uiso 1 1 calc R . .
H8B H 1.2557 0.2506 0.2188 0.027 Uiso 1 1 calc R . .
C9 C 1.1246(2) 0.38823(15) 0.16431(11) 0.0192(4) Uani 1 1 d . . .
C10 C 1.1585(2) 0.47872(14) 0.24460(11) 0.0172(4) Uani 1 1 d . . .
C11 C 0.9521(3) 0.40996(15) 0.10225(12) 0.0226(4) Uani 1 1 d . . .
C12 C 1.5784(3) 0.75079(19) 0.07266(14) 0.0329(5) Uani 1 1 d . . .
H12A H 1.6762 0.6970 0.0901 0.049 Uiso 1 1 calc R . .
H12B H 1.6297 0.8120 0.0472 0.049 Uiso 1 1 calc R . .
H12C H 1.4762 0.7129 0.0299 0.049 Uiso 1 1 calc R . .
C13 C 1.6790(3) 0.88399(19) 0.25115(14) 0.0344(5) Uani 1 1 d . . .
H13A H 1.7854 0.8347 0.2642 0.052 Uiso 1 1 calc R . .
H13B H 1.6335 0.9058 0.3042 0.052 Uiso 1 1 calc R . .
H13C H 1.7178 0.9512 0.2282 0.052 Uiso 1 1 calc R . .
C14 C 1.2876(3) 0.90468(16) 0.13656(12) 0.0237(4) Uani 1 1 d . . .
C15 C 1.1256(3) 0.84246(19) 0.07200(17) 0.0427(6) Uani 1 1 d . . .
H15A H 1.0282 0.8957 0.0527 0.064 Uiso 1 1 calc R . .
H15B H 1.0742 0.7840 0.1003 0.064 Uiso 1 1 calc R . .
H15C H 1.1712 0.8080 0.0220 0.064 Uiso 1 1 calc R . .
C16 C 1.3527(4) 1.0024(2) 0.09355(18) 0.0446(6) Uani 1 1 d . . .
H16A H 1.2496 1.0537 0.0789 0.067 Uiso 1 1 calc R . .
H16B H 1.3933 0.9734 0.0407 0.067 Uiso 1 1 calc R . .
H16C H 1.4568 1.0427 0.1335 0.067 Uiso 1 1 calc R . .
C17 C 1.2142(3) 0.9511(2) 0.21630(15) 0.0409(6) Uani 1 1 d . . .
H17A H 1.1093 1.0000 0.1986 0.061 Uiso 1 1 calc R . .
H17B H 1.3138 0.9941 0.2572 0.061 Uiso 1 1 calc R . .
H17C H 1.1727 0.8889 0.2441 0.061 Uiso 1 1 calc R . .
C18 C 1.2381(3) 0.35047(17) 0.56627(13) 0.0288(4) Uani 1 1 d . . .
H18A H 1.1033 0.3614 0.5569 0.043 Uiso 1 1 calc R . .
H18B H 1.3021 0.4230 0.5689 0.043 Uiso 1 1 calc R . .
H18C H 1.2804 0.3172 0.6209 0.043 Uiso 1 1 calc R . .
C19 C 1.1639(3) 0.11960(17) 0.46926(14) 0.0283(4) Uani 1 1 d . . .
H19A H 1.0298 0.1329 0.4607 0.042 Uiso 1 1 calc R . .
H19B H 1.2052 0.0847 0.5232 0.042 Uiso 1 1 calc R . .
H19C H 1.1891 0.0697 0.4206 0.042 Uiso 1 1 calc R . .
C20 C 1.5490(2) 0.23562(15) 0.48526(11) 0.0192(4) Uani 1 1 d . . .
C21 C 1.6413(3) 0.34989(17) 0.48159(14) 0.0299(4) Uani 1 1 d . . .
H21A H 1.7756 0.3407 0.4859 0.045 Uiso 1 1 calc R . .
H21B H 1.6200 0.4021 0.5298 0.045 Uiso 1 1 calc R . .
   H21C H 1.5873 0.3797 0.4267 0.045 Uiso 1 1 calc R . .
```

```
 C22 C 1.6344(3) 0.18910(18) 0.57141(12) 0.0284(4) Uani 1 1 d . . .
 H22A H 1.7692 0.1820 0.5763 0.043 Uiso 1 1 calc R . .
 H22B H 1.5783 0.1153 0.5732 0.043 Uiso 1 1 calc R . .
 H22C H 1.6104 0.2404 0.6196 0.043 Uiso 1 1 calc R . .
 C23 C 1.5820(3) 0.15402(18) 0.41012(13) 0.0275(4) Uani 1 1 d . . .
 H23A H 1.7161 0.1485 0.4123 0.041 Uiso 1 1 calc R . .
 H23B H 1.5209 0.1813 0.3552 0.041 Uiso 1 1 calc R . .
 H23C H 1.5300 0.0800 0.4147 0.041 Uiso 1 1 calc R . .

 loop_
  _atom_site_aniso_label
  _atom_site_aniso_U_11
  _atom_site_aniso_U_22
  _atom_site_aniso_U_33
  _atom_site_aniso_U_23
  _atom_site_aniso_U_13
  _atom_site_aniso_U_12
 Br1 0.02727(12) 0.03944(14) 0.03139(13) 0.00993(9) -0.00185(9) -0.00978(9)
 Si1 0.0229(3) 0.0220(3) 0.0193(3) 0.0017(2) 0.0054(2) -0.0026(2)
 Si2 0.0168(2) 0.0214(3) 0.0156(2) 0.00522(19) 0.00352(19) 0.00196(19)
 O1 0.0176(6) 0.0243(7) 0.0166(6) 0.0044(5) 0.0032(5) 0.0034(5)
 O2 0.0290(7) 0.0208(7) 0.0191(7) 0.0026(5) 0.0008(5) -0.0051(5)
 O3 0.0190(6) 0.0364(8) 0.0199(7) 0.0129(6) 0.0015(5) 0.0055(6)
 N1 0.0385(10) 0.0330(10) 0.0240(9) 0.0070(8) -0.0044(8) -0.0045(8)
 C1 0.0296(10) 0.0202(9) 0.0197(9) 0.0017(7) 0.0088(8) 0.0048(8)
 C2 0.0228(9) 0.0247(10) 0.0195(9) 0.0046(8) 0.0071(7) 0.0023(7)
 C3 0.0268(9) 0.0201(9) 0.0166(9) 0.0023(7) -0.0008(7) -0.0014(7)
 C4 0.0227(9) 0.0171(9) 0.0220(9) 0.0010(7) 0.0006(7) 0.0026(7)
 C5 0.0196(9) 0.0235(9) 0.0167(9) -0.0009(7) 0.0026(7) 0.0039(7)
 C6 0.0174(8) 0.0294(10) 0.0174(9) 0.0068(8) 0.0029(7) 0.0038(7)
 C7 0.0252(9) 0.0210(10) 0.0235(10) 0.0067(8) 0.0013(8) 0.0019(8)
 C8 0.0309(10) 0.0174(9) 0.0198(9) 0.0020(7) 0.0039(8) 0.0036(8)
 C9 0.0251(9) 0.0171(9) 0.0151(9) 0.0011(7) 0.0036(7) 0.0014(7)
 C10 0.0174(8) 0.0174(9) 0.0150(8) 0.0008(7) -0.0003(7) 0.0018(7)
 C11 0.0328(10) 0.0170(9) 0.0170(9) 0.0022(7) 0.0028(8) -0.0018(8)
 C12 0.0343(11) 0.0378(12) 0.0293(11) 0.0009(9) 0.0138(9) 0.0035(9)
 C13 0.0307(11) 0.0368(12) 0.0339(12) 0.0020(10) 0.0032(9) -0.0104(9)
 C14 0.0293(10) 0.0203(9) 0.0219(10) 0.0027(8) 0.0054(8) -0.0019(8)
 C15 0.0390(12) 0.0303(12) 0.0493(15) 0.0030(11) -0.0123(11) 0.0059(10)
 C16 0.0491(14) 0.0322(12) 0.0609(16) 0.0220(11) 0.0226(13) 0.0047(10)
 C17 0.0446(13) 0.0458(14) 0.0362(13) 0.0067(11) 0.0158(11) 0.0178(11)
 C18 0.0307(10) 0.0328(11) 0.0247(10) 0.0020(8) 0.0105(8) 0.0065(9)
 C19 0.0220(9) 0.0295(11) 0.0336(11) 0.0088(9) 0.0038(8) -0.0021(8)
 C20 0.0181(8) 0.0223(9) 0.0168(9) 0.0033(7) 0.0020(7) -0.0006(7)
 C21 0.0229(10) 0.0324(11) 0.0343(12) 0.0037(9) 0.0054(9) -0.0060(8)
 C22 0.0239(10) 0.0390(12) 0.0215(10) 0.0072(9) 0.0010(8) 0.0066(8)
 C23 0.0210(9) 0.0364(11) 0.0252(10) 0.0000(9) 0.0065(8) 0.0039(8)

 _geom_special_details
 ;
  All esds (except the esd in the dihedral angle between two l.s. planes)
  are estimated using the full covariance matrix.  The cell esds are taken
  into account individually in the estimation of esds in distances, angles
  and torsion angles; correlations between esds in cell parameters are only
  used when they are defined by crystal symmetry.  An approximate
(isotropic)
  treatment of cell esds is used for estimating esds involving l.s. planes.
 ;

 loop_
  _geom_bond_atom_site_label_1
  _geom_bond_atom_site_label_2
  _geom_bond_distance
```

```
 _geom_bond_site_symmetry_2
 _geom_bond_publ_flag
Br1 C7 1.9672(18) . ?
Si1 O2 1.6560(13) . ?
Si1 C12 1.861(2) . ?
Si1 C13 1.865(2) . ?
Si1 C14 1.894(2) . ?
Si2 O3 1.6536(13) . ?
Si2 C18 1.857(2) . ?
Si2 C19 1.862(2) . ?
Si2 C20 1.8773(18) . ?
O1 C10 1.440(2) . ?
O1 C2 1.447(2) . ?
O2 C3 1.428(2) . ?
O3 C6 1.420(2) . ?
N1 C11 1.141(2) . ?
C1 C2 1.538(3) . ?
C1 C9 1.565(3) . ?
C1 H1A 0.9900 . ?
C1 H1B 0.9900 . ?
C2 C3 1.530(3) . ?
C2 H2A 1.0000 . ?
C3 C4 1.539(3) . ?
C3 H3A 1.0000 . ?
C4 C10 1.535(2) . ?
C4 H4A 0.9900 . ?
C4 H4B 0.9900 . ?
C5 C10 1.517(2) . ?
C5 C6 1.525(3) . ?
C5 H5A 0.9900 . ?
C5 H5B 0.9900 . ?
C6 C7 1.527(3) . ?
C6 H6A 1.0000 . ?
C7 C8 1.517(3) . ?
C7 H7A 1.0000 . ?
C8 C9 1.545(2) . ?
C8 H8A 0.9900 . ?
C8 H8B 0.9900 . ?
C9 C11 1.475(3) . ?
C9 C10 1.571(2) . ?
C12 H12A 0.9800 . ?
C12 H12B 0.9800 . ?
C12 H12C 0.9800 . ?
C13 H13A 0.9800 . ?
C13 H13B 0.9800 . ?
C13 H13C 0.9800 . ?
C14 C16 1.532(3) . ?
C14 C17 1.532(3) . ?
C14 C15 1.539(3) . ?
C15 H15A 0.9800 . ?
C15 H15B 0.9800 . ?
C15 H15C 0.9800 . ?
C16 H16A 0.9800 . ?
C16 H16B 0.9800 . ?
C16 H16C 0.9800 . ?
C17 H17A 0.9800 . ?
C17 H17B 0.9800 . ?
C17 H17C 0.9800 . ?
C18 H18A 0.9800 . ?
C18 H18B 0.9800 . ?
C18 H18C 0.9800 . ?
C19 H19A 0.9800 . ?
   C19 H19B 0.9800 . ?
```

```
C19 H19C 0.9800 . ?
C20 C23 1.528(3) . ?
C20 C21 1.538(3) . ?
C20 C22 1.538(3) . ?
C21 H21A 0.9800 . ?
C21 H21B 0.9800 . ?
C21 H21C 0.9800 . ?
C22 H22A 0.9800 . ?
C22 H22B 0.9800 . ?
C22 H22C 0.9800 . ?
C23 H23A 0.9800 . ?
C23 H23B 0.9800 . ?
C23 H23C 0.9800 . ?

loop_
 _geom_angle_atom_site_label_1
 _geom_angle_atom_site_label_2
 _geom_angle_atom_site_label_3
 _geom_angle
 _geom_angle_site_symmetry_1
 _geom_angle_site_symmetry_3
 _geom_angle_publ_flag
O2 Si1 C12 110.20(9) . . ?
O2 Si1 C13 104.26(8) . . ?
C12 Si1 C13 110.67(10) . . ?
O2 Si1 C14 110.37(8) . . ?
C12 Si1 C14 110.58(9) . . ?
C13 Si1 C14 110.60(10) . . ?
O3 Si2 C18 110.75(8) . . ?
O3 Si2 C19 110.51(8) . . ?
C18 Si2 C19 109.03(10) . . ?
O3 Si2 C20 102.04(7) . . ?
C18 Si2 C20 112.45(9) . . ?
C19 Si2 C20 111.93(9) . . ?
C10 O1 C2 97.01(12) . . ?
C3 O2 Si1 123.21(11) . . ?
C6 O3 Si2 127.54(11) . . ?
C2 C1 C9 101.17(14) . . ?
C2 C1 H1A 111.5 . . ?
C9 C1 H1A 111.5 . . ?
C2 C1 H1B 111.5 . . ?
C9 C1 H1B 111.5 . . ?
H1A C1 H1B 109.4 . . ?
O1 C2 C3 104.05(14) . . ?
O1 C2 C1 102.92(14) . . ?
C3 C2 C1 108.04(15) . . ?
O1 C2 H2A 113.6 . . ?
C3 C2 H2A 113.6 . . ?
C1 C2 H2A 113.6 . . ?
O2 C3 C2 111.83(15) . . ?
O2 C3 C4 111.40(15) . . ?
C2 C3 C4 100.27(14) . . ?
O2 C3 H3A 111.0 . . ?
C2 C3 H3A 111.0 . . ?
C4 C3 H3A 111.0 . . ?
C10 C4 C3 103.19(14) . . ?
C10 C4 H4A 111.1 . . ?
C3 C4 H4A 111.1 . . ?
C10 C4 H4B 111.1 . . ?
C3 C4 H4B 111.1 . . ?
H4A C4 H4B 109.1 . . ?
C10 C5 C6 115.77(15) . . ?
C10 C5 H5A 108.3 . . ?
```

```
C6 C5 H5A 108.3 . . ?
C10 C5 H5B 108.3 . . ?
C6 C5 H5B 108.3 . . ?
H5A C5 H5B 107.4 . . ?
O3 C6 C5 109.45(15) . . ?
O3 C6 C7 106.04(14) . . ?
C5 C6 C7 112.48(15) . . ?
O3 C6 H6A 109.6 . . ?
C5 C6 H6A 109.6 . . ?
C7 C6 H6A 109.6 . . ?
C8 C7 C6 112.10(15) . . ?
C8 C7 Br1 112.17(13) . . ?
C6 C7 Br1 110.10(12) . . ?
C8 C7 H7A 107.4 . . ?
C6 C7 H7A 107.4 . . ?
Br1 C7 H7A 107.4 . . ?
C7 C8 C9 115.69(15) . . ?
C7 C8 H8A 108.4 . . ?
C9 C8 H8A 108.4 . . ?
C7 C8 H8B 108.4 . . ?
C9 C8 H8B 108.4 . . ?
H8A C8 H8B 107.4 . . ?
C11 C9 C8 112.36(15) . . ?
C11 C9 C1 111.03(15) . . ?
C8 C9 C1 110.36(14) . . ?
C11 C9 C10 111.04(14) . . ?
C8 C9 C10 110.59(14) . . ?
C1 C9 C10 100.90(14) . . ?
O1 C10 C5 113.75(14) . . ?
O1 C10 C4 101.59(13) . . ?
C5 C10 C4 114.41(15) . . ?
O1 C10 C9 100.52(13) . . ?
C5 C10 C9 114.76(15) . . ?
C4 C10 C9 110.21(14) . . ?
N1 C11 C9 177.0(2) . . ?
Si1 C12 H12A 109.5 . . ?
Si1 C12 H12B 109.5 . . ?
H12A C12 H12B 109.5 . . ?
Si1 C12 H12C 109.5 . . ?
H12A C12 H12C 109.5 . . ?
H12B C12 H12C 109.5 . . ?
Si1 C13 H13A 109.5 . . ?
Si1 C13 H13B 109.5 . . ?
H13A C13 H13B 109.5 . . ?
Si1 C13 H13C 109.5 . . ?
H13A C13 H13C 109.5 . . ?
H13B C13 H13C 109.5 . . ?
C16 C14 C17 109.16(18) . . ?
C16 C14 C15 108.27(18) . . ?
C17 C14 C15 108.07(19) . . ?
C16 C14 Si1 109.65(14) . . ?
C17 C14 Si1 110.21(14) . . ?
C15 C14 Si1 111.43(14) . . ?
C14 C15 H15A 109.5 . . ?
C14 C15 H15B 109.5 . . ?
H15A C15 H15B 109.5 . . ?
C14 C15 H15C 109.5 . . ?
H15A C15 H15C 109.5 . . ?
H15B C15 H15C 109.5 . . ?
C14 C16 H16A 109.5 . . ?
C14 C16 H16B 109.5 . . ?
H16A C16 H16B 109.5 . . ?
   C14 C16 H16C 109.5 . . ?
```

```
  H16A C16 H16C 109.5 . . ?
  H16B C16 H16C 109.5 . . ?
  C14 C17 H17A 109.5 . . ?
  C14 C17 H17B 109.5 . . ?
  H17A C17 H17B 109.5 . . ?
  C14 C17 H17C 109.5 . . ?
  H17A C17 H17C 109.5 . . ?
  H17B C17 H17C 109.5 . . ?
  Si2 C18 H18A 109.5 . . ?
  Si2 C18 H18B 109.5 . . ?
  H18A C18 H18B 109.5 . . ?
  Si2 C18 H18C 109.5 . . ?
  H18A C18 H18C 109.5 . . ?
  H18B C18 H18C 109.5 . . ?
  Si2 C19 H19A 109.5 . . ?
  Si2 C19 H19B 109.5 . . ?
  H19A C19 H19B 109.5 . . ?
  Si2 C19 H19C 109.5 . . ?
  H19A C19 H19C 109.5 . . ?
  H19B C19 H19C 109.5 . . ?
  C23 C20 C21 109.62(16) . . ?
  C23 C20 C22 109.42(15) . . ?
  C21 C20 C22 109.31(16) . . ?
  C23 C20 Si2 109.37(12) . . ?
  C21 C20 Si2 108.53(12) . . ?
  C22 C20 Si2 110.59(12) . . ?
  C20 C21 H21A 109.5 . . ?
  C20 C21 H21B 109.5 . . ?
  H21A C21 H21B 109.5 . . ?
  C20 C21 H21C 109.5 . . ?
  H21A C21 H21C 109.5 . . ?
  H21B C21 H21C 109.5 . . ?
  C20 C22 H22A 109.5 . . ?
  C20 C22 H22B 109.5 . . ?
  H22A C22 H22B 109.5 . . ?
  C20 C22 H22C 109.5 . . ?
  H22A C22 H22C 109.5 . . ?
  H22B C22 H22C 109.5 . . ?
  C20 C23 H23A 109.5 . . ?
  C20 C23 H23B 109.5 . . ?
  H23A C23 H23B 109.5 . . ?
  C20 C23 H23C 109.5 . . ?
  H23A C23 H23C 109.5 . . ?
  H23B C23 H23C 109.5 . . ?

  loop_
   _geom_torsion_atom_site_label_1
   _geom_torsion_atom_site_label_2
   _geom_torsion_atom_site_label_3
   _geom_torsion_atom_site_label_4
   _geom_torsion
   _geom_torsion_site_symmetry_1
   _geom_torsion_site_symmetry_2
   _geom_torsion_site_symmetry_3
   _geom_torsion_site_symmetry_4
   _geom_torsion_publ_flag
 C12 Si1 O2 C3 -47.01(16) . . . . ?
 C13 Si1 O2 C3 -165.80(14) . . . . ?
 C14 Si1 O2 C3 75.41(15) . . . . ?
 C18 Si2 O3 C6 -66.06(17) . . . . ?
 C19 Si2 O3 C6 54.87(17) . . . . ?
 C20 Si2 O3 C6 174.05(15) . . . . ?
 C10 O1 C2 C3 55.22(15) . . . . ?
```

```
C10 O1 C2 C1 -57.42(15) . . . . ?
C9 C1 C2 O1 32.21(16) . . . . ?
C9 C1 C2 C3 -77.46(17) . . . . ?
Si1 O2 C3 C2 122.81(14) . . . . ?
Si1 O2 C3 C4 -125.89(14) . . . . ?
O1 C2 C3 O2 85.85(17) . . . . ?
C1 C2 C3 O2 -165.26(14) . . . . ?
O1 C2 C3 C4 -32.32(17) . . . . ?
C1 C2 C3 C4 76.58(16) . . . . ?
O2 C3 C4 C10 -120.19(15) . . . . ?
C2 C3 C4 C10 -1.71(17) . . . . ?
Si2 O3 C6 C5 131.06(14) . . . . ?
Si2 O3 C6 C7 -107.38(15) . . . . ?
C10 C5 C6 O3 69.48(19) . . . . ?
C10 C5 C6 C7 -48.1(2) . . . . ?
O3 C6 C7 C8 -68.76(18) . . . . ?
C5 C6 C7 C8 50.8(2) . . . . ?
O3 C6 C7 Br1 165.62(11) . . . . ?
C5 C6 C7 Br1 -74.78(16) . . . . ?
C6 C7 C8 C9 -53.1(2) . . . . ?
Br1 C7 C8 C9 71.36(18) . . . . ?
C7 C8 C9 C11 -76.5(2) . . . . ?
C7 C8 C9 C1 159.02(15) . . . . ?
C7 C8 C9 C10 48.2(2) . . . . ?
C2 C1 C9 C11 120.89(16) . . . . ?
C2 C1 C9 C8 -113.85(15) . . . . ?
C2 C1 C9 C10 3.12(16) . . . . ?
C2 O1 C10 C5 -178.41(15) . . . . ?
C2 O1 C10 C4 -54.96(15) . . . . ?
C2 O1 C10 C9 58.42(14) . . . . ?
C6 C5 C10 O1 -70.03(19) . . . . ?
C6 C5 C10 C4 173.82(14) . . . . ?
C6 C5 C10 C9 45.0(2) . . . . ?
C3 C4 C10 O1 35.13(16) . . . . ?
C3 C4 C10 C5 158.13(15) . . . . ?
C3 C4 C10 C9 -70.78(17) . . . . ?
C11 C9 C10 O1 -155.31(14) . . . . ?
C8 C9 C10 O1 79.24(16) . . . . ?
C1 C9 C10 O1 -37.55(15) . . . . ?
C11 C9 C10 C5 82.23(18) . . . . ?
C8 C9 C10 C5 -43.2(2) . . . . ?
C1 C9 C10 C5 -160.01(14) . . . . ?
C11 C9 C10 C4 -48.68(19) . . . . ?
C8 C9 C10 C4 -174.13(14) . . . . ?
C1 C9 C10 C4 69.08(16) . . . . ?
C8 C9 C11 N1 -172(4) . . . . ?
C1 C9 C11 N1 -48(4) . . . . ?
C10 C9 C11 N1 63(4) . . . . ?
O2 Si1 C14 C16 177.59(14) . . . . ?
C12 Si1 C14 C16 -60.21(17) . . . . ?
C13 Si1 C14 C16 62.74(17) . . . . ?
O2 Si1 C14 C17 57.41(16) . . . . ?
C12 Si1 C14 C17 179.61(15) . . . . ?
C13 Si1 C14 C17 -57.44(17) . . . . ?
O2 Si1 C14 C15 -62.55(17) . . . . ?
C12 Si1 C14 C15 59.64(18) . . . . ?
C13 Si1 C14 C15 -177.41(15) . . . . ?
O3 Si2 C20 C23 -62.94(14) . . . . ?
C18 Si2 C20 C23 178.36(13) . . . . ?
C19 Si2 C20 C23 55.23(15) . . . . ?
O3 Si2 C20 C21 56.61(14) . . . . ?
C18 Si2 C20 C21 -62.09(15) . . . . ?
   C19 Si2 C20 C21 174.78(13) . . . . ?
```

```
O3 Si2 C20 C22 176.50(13) . . . . ?
C18 Si2 C20 C22 57.80(16) . . . . ?
C19 Si2 C20 C22 -65.33(16) . . . . ?
```

X-ray crystal structure data for *bis*-acetonide (311)

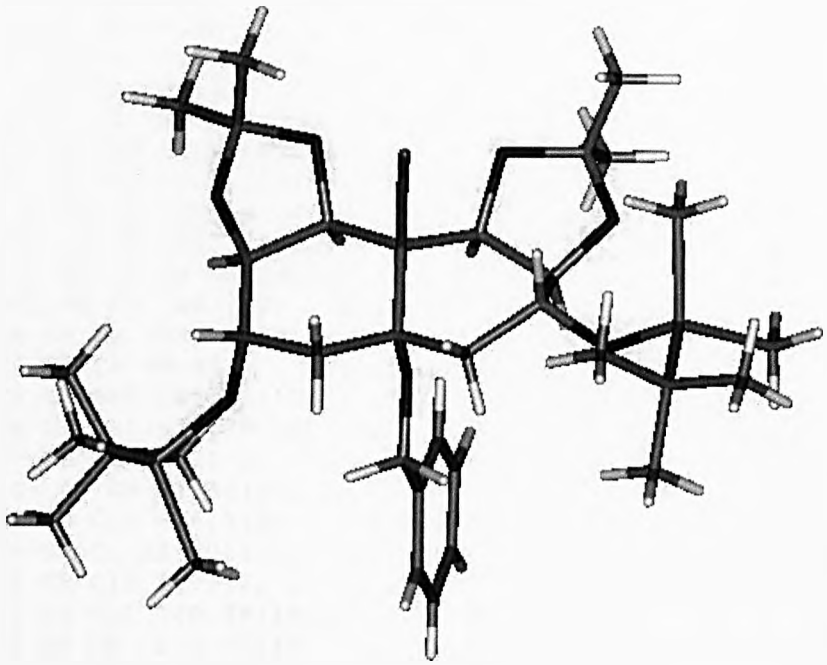

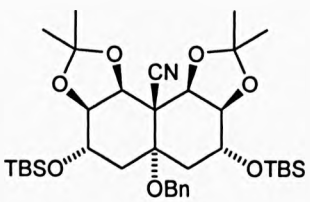

311

```
data_csf132s

_audit_creation_method            SHELXL-97
_chemical_name_systematic
;
 ?
;
_chemical_name_common             ?
_chemical_melting_point           ?
_chemical_formula_moiety          ?
_chemical_formula_sum
 'C36 H59 N O7 Si2'
_chemical_formula_weight          674.02

loop_
 _atom_type_symbol
 _atom_type_description
 _atom_type_scat_dispersion_real
 _atom_type_scat_dispersion_imag
 _atom_type_scat_source
 'C'  'C'   0.0033   0.0016
 'International Tables Vol C Tables 4.2.6.8 and 6.1.1.4'
 'H'  'H'   0.0000   0.0000
 'International Tables Vol C Tables 4.2.6.8 and 6.1.1.4'
 'N'  'N'   0.0061   0.0033
 'International Tables Vol C Tables 4.2.6.8 and 6.1.1.4'
 'O'  'O'   0.0106   0.0060
 'International Tables Vol C Tables 4.2.6.8 and 6.1.1.4'
 'Si'  'Si'   0.0817   0.0704
 'International Tables Vol C Tables 4.2.6.8 and 6.1.1.4'

_symmetry_cell_setting            Triclinic
_symmetry_space_group_name_H-M    P-1

loop_
 _symmetry_equiv_pos_as_xyz
```

```
  'x, y, z'
  '-x, -y, -z'

_cell_length_a                    11.7021(8)
_cell_length_b                    14.0933(9)
_cell_length_c                    14.3609(9)
_cell_angle_alpha                 118.628(2)
_cell_angle_beta                  95.055(2)
_cell_angle_gamma                 105.704(2)
_cell_volume                      1933.7(2)
_cell_formula_units_Z             2
_cell_measurement_temperature     123(1)
_cell_measurement_reflns_used     992
_cell_measurement_theta_min       2.656
_cell_measurement_theta_max       29.083

_exptl_crystal_description        prism
_exptl_crystal_colour             colourless
_exptl_crystal_size_max           0.35
_exptl_crystal_size_mid           0.30
_exptl_crystal_size_min           0.20
_exptl_crystal_density_meas       'not measured'
_exptl_crystal_density_diffrn     1.158
_exptl_crystal_density_method     'not measured'
_exptl_crystal_F_000              732
_exptl_absorpt_coefficient_mu     0.136
_exptl_absorpt_correction_type    none
_exptl_absorpt_correction_T_min   ?
_exptl_absorpt_correction_T_max   ?
_exptl_absorpt_process_details    ?

_exptl_special_details
;
 ?
;

_diffrn_ambient_temperature            123(1)
_diffrn_radiation_wavelength           0.71073
_diffrn_radiation_type                 MoK\a
_diffrn_radiation_source               'fine-focus sealed tube'
_diffrn_radiation_monochromator        graphite
_diffrn_measurement_device_type        'Bruker AXS 1K CCD area detector'
_diffrn_measurement_method             'narrow frame \w scans'
_diffrn_detector_area_resol_mean       8.192
_diffrn_standards_number               'see text'
_diffrn_standards_interval_count       ?
_diffrn_standards_interval_time        ?
_diffrn_standards_decay_%              'none'
_diffrn_reflns_number                  16779
_diffrn_reflns_av_R_equivalents        0.0116
_diffrn_reflns_av_sigmaI/netI          0.0137
_diffrn_reflns_limit_h_min             -14
_diffrn_reflns_limit_h_max             14
_diffrn_reflns_limit_k_min             -12
_diffrn_reflns_limit_k_max             17
_diffrn_reflns_limit_l_min             -17
_diffrn_reflns_limit_l_max             17
_diffrn_reflns_theta_min               1.76
_diffrn_reflns_theta_max               26.37
_diffrn_reflns_theta_full              26.37
_diffrn_measured_fraction_theta_full   0.967

_reflns_number_total                   7637
```

```
_reflns_number_gt                    6750
_reflns_threshold_expression         >2sigma(I)

_computing_data_collection      'SMART V5.060 (Bruker AXS, 1999)'
_computing_cell_refinement      'SMART V5.060/SAINT V6.02a (Bruker AXS,
1999)'
_computing_data_reduction       'SAINT V6.02a (Bruker AXS, 1997)'
_computing_structure_solution   'SHELXTL V5.10 (Sheldrick, 1997)'
_computing_structure_refinement 'SHELXTL V5.10 (Sheldrick, 1997)'
_computing_molecular_graphics   'SHELXTL V5.10 (Sheldrick, 1997)'
_computing_publication_material 'SHELXTL V5.10 (Sheldrick, 1997)'

_refine_special_details
;
 Refinement of F^2^ against ALL reflections.  The weighted R-factor wR and
 goodness of fit S are based on F^2^, conventional R-factors R are based
 on F, with F set to zero for negative F^2^. The threshold expression of
 F^2^ > 2sigma(F^2^) is used only for calculating R-factors(gt) etc. and is
 not relevant to the choice of reflections for refinement.  R-factors based
 on F^2^ are statistically about twice as large as those based on F, and R-
 factors based on ALL data will be even larger.
;

_refine_ls_structure_factor_coef  Fsqd
_refine_ls_matrix_type            full
_refine_ls_weighting_scheme       calc
_refine_ls_weighting_details
 'calc w=1/[\s^2^(Fo^2^)+(0.0675P)^2^+1.0000P] where P=(Fo^2^+2Fc^2^)/3'
_atom_sites_solution_primary      direct
_atom_sites_solution_secondary    difmap
_atom_sites_solution_hydrogens    geom
_refine_ls_hydrogen_treatment     mixed
_refine_ls_extinction_method      none
_refine_ls_extinction_coef        none
_refine_ls_number_reflns          7637
_refine_ls_number_parameters      429
_refine_ls_number_restraints      0
_refine_ls_R_factor_all           0.0450
_refine_ls_R_factor_gt            0.0401
_refine_ls_wR_factor_ref          0.1165
_refine_ls_wR_factor_gt           0.1123
_refine_ls_goodness_of_fit_ref    1.008
_refine_ls_restrained_S_all       1.008
_refine_ls_shift/su_max           0.002
_refine_ls_shift/su_mean          0.000
_refine_diff_density_max          0.643
_refine_diff_density_min         -0.447
_refine_diff_density_rms          0.045

loop_
 _atom_site_label
 _atom_site_type_symbol
 _atom_site_fract_x
 _atom_site_fract_y
 _atom_site_fract_z
 _atom_site_U_iso_or_equiv
 _atom_site_adp_type
 _atom_site_occupancy
 _atom_site_symmetry_multiplicity
 _atom_site_calc_flag
 _atom_site_refinement_flags
 _atom_site_disorder_assembly
    _atom_site_disorder_group
```

```
Si1 Si 0.26867(4) 0.92694(4) 1.00339(3) 0.02251(11) Uani 1 1 d . . .
Si2 Si 0.33061(4) 0.45060(3) 0.25793(3) 0.02155(11) Uani 1 1 d . . .
O1 O 0.12127(9) 0.94980(8) 0.64899(8) 0.0229(2) Uani 1 1 d . . .
O2 O 0.23944(11) 1.03155(10) 0.82079(9) 0.0333(3) Uani 1 1 d . . .
O3 O 0.30876(10) 0.88544(11) 0.88644(8) 0.0309(3) Uani 1 1 d . . .
O4 O 0.01473(10) 0.74415(9) 0.40208(8) 0.0241(2) Uani 1 1 d . . .
O5 O -0.02039(10) 0.55124(9) 0.31611(9) 0.0272(2) Uani 1 1 d . . .
O6 O 0.28592(9) 0.55237(9) 0.34694(8) 0.0234(2) Uani 1 1 d . . .
O7 O 0.35105(9) 0.77023(8) 0.56655(8) 0.0206(2) Uani 1 1 d . . .
N1 N -0.05797(12) 0.69213(11) 0.59839(11) 0.0264(3) Uani 1 1 d . . .
C1 C 0.21128(13) 0.89728(12) 0.63441(11) 0.0200(3) Uani 1 1 d . . .
H1A H 0.2717 0.9290 0.6022 0.024 Uiso 1 1 calc R . .
C2 C 0.27648(14) 0.93738(12) 0.75211(12) 0.0245(3) Uani 1 1 d . . .
H2A H 0.3676 0.9653 0.7633 0.029 Uiso 1 1 calc R . .
C3 C 0.23717(14) 0.84492(13) 0.78080(11) 0.0236(3) Uani 1 1 d . . .
H3A H 0.1487 0.8278 0.7816 0.028 Uiso 1 1 calc R . .
C4 C 0.25357(14) 0.73296(13) 0.69767(12) 0.0244(3) Uani 1 1 d . . .
H4A H 0.1926 0.6671 0.6954 0.029 Uiso 1 1 calc R . .
H4B H 0.3363 0.7361 0.7243 0.029 Uiso 1 1 calc R . .
C5 C 0.23937(12) 0.70869(12) 0.57949(11) 0.0188(3) Uani 1 1 d . . .
C6 C 0.19143(13) 0.57800(12) 0.49734(11) 0.0196(3) Uani 1 1 d . . .
H6A H 0.2500 0.5460 0.5146 0.024 Uiso 1 1 calc R . .
H6B H 0.1122 0.5431 0.5084 0.024 Uiso 1 1 calc R . .
C7 C 0.17211(12) 0.53990(12) 0.37659(11) 0.0192(3) Uani 1 1 d . . .
H7A H 0.1186 0.4562 0.3317 0.023 Uiso 1 1 calc R . .
C8 C 0.11007(13) 0.60752(12) 0.34656(11) 0.0219(3) Uani 1 1 d . . .
H8A H 0.1355 0.6072 0.2818 0.026 Uiso 1 1 calc R . .
C9 C 0.12710(13) 0.73242(12) 0.43371(11) 0.0200(3) Uani 1 1 d . . .
H9A H 0.1962 0.7867 0.4269 0.024 Uiso 1 1 calc R . .
C10 C 0.15063(12) 0.76409(11) 0.55557(11) 0.0176(3) Uani 1 1 d . . .
C11 C 0.17112(14) 1.05587(13) 0.75305(13) 0.0262(3) Uani 1 1 d . . .
C12 C 0.06541(16) 1.08407(15) 0.79894(15) 0.0354(4) Uani 1 1 d . . .
H12A H 0.0129 1.0183 0.8011 0.053 Uiso 1 1 calc R . .
H12B H 0.0172 1.0996 0.7521 0.053 Uiso 1 1 calc R . .
H12C H 0.0975 1.1526 0.8734 0.053 Uiso 1 1 calc R . .
C13 C 0.25539(18) 1.15162(14) 0.74278(17) 0.0412(4) Uani 1 1 d . . .
H13A H 0.3238 1.1298 0.7156 0.062 Uiso 1 1 calc R . .
H13B H 0.2876 1.2236 0.8149 0.062 Uiso 1 1 calc R . .
H13C H 0.2091 1.1632 0.6913 0.062 Uiso 1 1 calc R . .
C14 C 0.11630(15) 0.94243(17) 0.99070(15) 0.0368(4) Uani 1 1 d . . .
H14A H 0.1189 0.9982 0.9679 0.055 Uiso 1 1 calc R . .
H14B H 0.0961 0.9701 1.0618 0.055 Uiso 1 1 calc R . .
H14C H 0.0536 0.8672 0.9358 0.055 Uiso 1 1 calc R . .
C15 C 0.38524(16) 1.07108(15) 1.10671(14) 0.0378(4) Uani 1 1 d . . .
H15A H 0.3864 1.1257 1.0827 0.057 Uiso 1 1 calc R . .
H15B H 0.4664 1.0646 1.1145 0.057 Uiso 1 1 calc R . .
H15C H 0.3645 1.0991 1.1776 0.057 Uiso 1 1 calc R . .
C16 C 0.26870(19) 0.81568(16) 1.04099(16) 0.0392(4) Uani 1 1 d . . .
C17 C 0.2612(4) 0.8616(3) 1.1598(3) 0.0915(11) Uani 1 1 d . . .
H17A H 0.2545 0.8010 1.1767 0.137 Uiso 1 1 calc R . .
H17B H 0.1888 0.8841 1.1695 0.137 Uiso 1 1 calc R . .
H17C H 0.3354 0.9291 1.2093 0.137 Uiso 1 1 calc R . .
C18 C 0.1570(4) 0.7070(2) 0.9689(3) 0.1013(12) Uani 1 1 d . . .
H18A H 0.1509 0.6542 0.9957 0.152 Uiso 1 1 calc R . .
H18B H 0.1647 0.6693 0.8932 0.152 Uiso 1 1 calc R . .
H18C H 0.0831 0.7272 0.9709 0.152 Uiso 1 1 calc R . .
C19 C 0.3860(3) 0.7898(3) 1.0300(3) 0.0854(10) Uani 1 1 d . . .
H19A H 0.3855 0.7326 1.0505 0.128 Uiso 1 1 calc R . .
H19B H 0.4569 0.8611 1.0786 0.128 Uiso 1 1 calc R . .
H19C H 0.3913 0.7588 0.9539 0.128 Uiso 1 1 calc R . .
C20 C -0.06926(15) 0.63227(14) 0.31306(13) 0.0293(3) Uani 1 1 d . . .
C21 C -0.19497(15) 0.60830(16) 0.33423(16) 0.0386(4) Uani 1 1 d . . .
H21A H -0.1890 0.6105 0.4038 0.058 Uiso 1 1 calc R . .
```

```
H21B H -0.2505 0.5316 0.2743 0.058 Uiso 1 1 calc R . .
H21C H -0.2271 0.6672 0.3384 0.058 Uiso 1 1 calc R . .
C22 C -0.0712(2) 0.62943(18) 0.20540(14) 0.0441(5) Uani 1 1 d . . .
H22A H 0.0121 0.6444 0.1950 0.066 Uiso 1 1 calc R . .
H22B H -0.1010 0.6890 0.2078 0.066 Uiso 1 1 calc R . .
H22C H -0.1259 0.5531 0.1443 0.066 Uiso 1 1 calc R . .
C23 C 0.46753(18) 0.45212(18) 0.33610(15) 0.0408(4) Uani 1 1 d . . .
H23A H 0.4451 0.4365 0.3929 0.061 Uiso 1 1 calc R . .
H23B H 0.5329 0.5282 0.3707 0.061 Uiso 1 1 calc R . .
H23C H 0.4966 0.3924 0.2859 0.061 Uiso 1 1 calc R . .
C24 C 0.20570(18) 0.30622(15) 0.18835(16) 0.0405(4) Uani 1 1 d . . .
H24A H 0.1863 0.2854 0.2427 0.061 Uiso 1 1 calc R . .
H24B H 0.2326 0.2482 0.1330 0.061 Uiso 1 1 calc R . .
H24C H 0.1324 0.3090 0.1527 0.061 Uiso 1 1 calc R . .
C25 C 0.37580(15) 0.49098(15) 0.15559(13) 0.0294(3) Uani 1 1 d . . .
C26 C 0.46189(19) 0.61807(17) 0.21611(17) 0.0456(5) Uani 1 1 d . . .
H26A H 0.4872 0.6380 0.1625 0.068 Uiso 1 1 calc R . .
H26B H 0.5346 0.6294 0.2653 0.068 Uiso 1 1 calc R . .
H26C H 0.4188 0.6679 0.2592 0.068 Uiso 1 1 calc R . .
C27 C 0.4427(2) 0.4126(2) 0.08558(17) 0.0489(5) Uani 1 1 d . . .
H27A H 0.4628 0.4304 0.0296 0.073 Uiso 1 1 calc R . .
H27B H 0.3892 0.3312 0.0498 0.073 Uiso 1 1 calc R . .
H27C H 0.5184 0.4263 0.1330 0.073 Uiso 1 1 calc R . .
C28 C 0.2627(2) 0.4750(2) 0.07948(16) 0.0473(5) Uani 1 1 d . . .
H28A H 0.2887 0.4980 0.0280 0.071 Uiso 1 1 calc R . .
H28B H 0.2186 0.5232 0.1233 0.071 Uiso 1 1 calc R . .
H28C H 0.2083 0.3935 0.0384 0.071 Uiso 1 1 calc R . .
C29 C 0.03231(13) 0.72274(11) 0.57844(11) 0.0192(3) Uani 1 1 d . . .
C30 C 0.45540(13) 0.73918(13) 0.57775(13) 0.0246(3) Uani 1 1 d . . .
H30A H 0.4376 0.6575 0.5202 0.030 Uiso 1 1 calc R . .
H30B H 0.4749 0.7473 0.6503 0.030 Uiso 1 1 calc R . .
C31 C 0.56360(13) 0.81738(14) 0.56703(12) 0.0252(3) Uani 1 1 d . . .
C32 C 0.55690(17) 0.9074(2) 0.5553(2) 0.0596(7) Uani 1 1 d . . .
H32A H 0.4813 0.9198 0.5509 0.071 Uiso 1 1 calc R . .
C33 C 0.6601(2) 0.9802(3) 0.5498(3) 0.0824(11) Uani 1 1 d . . .
H33A H 0.6545 1.0430 0.5433 0.099 Uiso 1 1 calc R . .
C34 C 0.76965(17) 0.9626(2) 0.55348(19) 0.0509(6) Uani 1 1 d . . .
H34A H 0.8390 1.0113 0.5475 0.061 Uiso 1 1 calc R . .
C35 C 0.77796(15) 0.87393(17) 0.56587(15) 0.0393(4) Uani 1 1 d . . .
H35A H 0.8536 0.8614 0.5695 0.047 Uiso 1 1 calc R . .
C36 C 0.67599(15) 0.80249(15) 0.57313(16) 0.0374(4) Uani 1 1 d . . .
H36A H 0.6832 0.7419 0.5825 0.045 Uiso 1 1 calc R . .

loop_
 _atom_site_aniso_label
 _atom_site_aniso_U_11
 _atom_site_aniso_U_22
 _atom_site_aniso_U_33
 _atom_site_aniso_U_23
 _atom_site_aniso_U_13
 _atom_site_aniso_U_12
Si1 0.0198(2) 0.0259(2) 0.01820(19) 0.00777(17) 0.00587(15) 0.01010(16)
Si2 0.0245(2) 0.0225(2) 0.0212(2) 0.01177(17) 0.01008(15) 0.01146(16)
O1 0.0241(5) 0.0160(5) 0.0260(5) 0.0078(4) 0.0077(4) 0.0092(4)
O2 0.0409(7) 0.0251(6) 0.0234(5) 0.0028(5) 0.0056(5) 0.0174(5)
O3 0.0248(5) 0.0476(7) 0.0172(5) 0.0114(5) 0.0057(4) 0.0196(5)
O4 0.0271(5) 0.0215(5) 0.0229(5) 0.0100(4) 0.0034(4) 0.0115(4)
O5 0.0242(5) 0.0209(5) 0.0283(5) 0.0078(4) -0.0013(4) 0.0093(4)
O6 0.0218(5) 0.0215(5) 0.0250(5) 0.0098(4) 0.0111(4) 0.0083(4)
O7 0.0169(5) 0.0196(5) 0.0247(5) 0.0108(4) 0.0065(4) 0.0069(4)
N1 0.0260(7) 0.0232(6) 0.0305(7) 0.0146(6) 0.0107(5) 0.0073(5)
C1 0.0190(6) 0.0159(6) 0.0229(7) 0.0085(6) 0.0076(5) 0.0060(5)
   C2 0.0227(7) 0.0191(7) 0.0218(7) 0.0034(6) 0.0045(6) 0.0080(6)
```

```
C3 0.0223(7) 0.0291(8) 0.0166(6) 0.0088(6) 0.0043(5) 0.0116(6)
C4 0.0302(8) 0.0276(8) 0.0199(7) 0.0131(6) 0.0086(6) 0.0148(6)
C5 0.0194(7) 0.0190(7) 0.0192(6) 0.0103(6) 0.0068(5) 0.0076(5)
C6 0.0218(7) 0.0172(6) 0.0225(7) 0.0112(6) 0.0083(5) 0.0084(5)
C7 0.0186(6) 0.0162(6) 0.0206(7) 0.0075(5) 0.0074(5) 0.0068(5)
C8 0.0249(7) 0.0214(7) 0.0186(6) 0.0090(6) 0.0060(5) 0.0099(6)
C9 0.0231(7) 0.0197(7) 0.0208(7) 0.0121(6) 0.0077(5) 0.0095(6)
C10 0.0186(6) 0.0153(6) 0.0190(6) 0.0089(5) 0.0064(5) 0.0058(5)
C11 0.0276(8) 0.0173(7) 0.0276(8) 0.0069(6) 0.0090(6) 0.0084(6)
C12 0.0350(9) 0.0286(8) 0.0382(9) 0.0108(7) 0.0169(7) 0.0159(7)
C13 0.0442(10) 0.0187(8) 0.0517(11) 0.0121(8) 0.0215(9) 0.0080(7)
C14 0.0256(8) 0.0509(11) 0.0367(9) 0.0219(8) 0.0136(7) 0.0182(8)
C15 0.0312(9) 0.0327(9) 0.0295(8) 0.0042(7) 0.0051(7) 0.0077(7)
C16 0.0502(11) 0.0386(10) 0.0402(10) 0.0239(8) 0.0207(8) 0.0230(9)
C17 0.167(3) 0.114(2) 0.083(2) 0.082(2) 0.084(2) 0.100(3)
C18 0.124(3) 0.0426(15) 0.118(3) 0.0462(17) 0.005(2) 0.0030(16)
C19 0.096(2) 0.111(2) 0.139(3) 0.102(2) 0.070(2) 0.081(2)
C20 0.0322(8) 0.0244(8) 0.0252(7) 0.0080(6) -0.0011(6) 0.0140(7)
C21 0.0263(8) 0.0332(9) 0.0453(10) 0.0136(8) -0.0020(7) 0.0124(7)
C22 0.0624(13) 0.0468(11) 0.0249(8) 0.0140(8) 0.0022(8) 0.0340(10)
C23 0.0487(11) 0.0553(12) 0.0371(9) 0.0277(9) 0.0160(8) 0.0366(10)
C24 0.0449(10) 0.0220(8) 0.0452(10) 0.0097(7) 0.0243(8) 0.0101(7)
C25 0.0334(8) 0.0351(9) 0.0244(7) 0.0177(7) 0.0117(6) 0.0135(7)
C26 0.0496(11) 0.0438(11) 0.0461(11) 0.0300(9) 0.0168(9) 0.0064(9)
C27 0.0646(13) 0.0618(13) 0.0400(10) 0.0303(10) 0.0360(10) 0.0359(11)
C28 0.0552(12) 0.0610(13) 0.0300(9) 0.0272(9) 0.0046(8) 0.0226(10)
C29 0.0230(7) 0.0148(6) 0.0188(6) 0.0080(5) 0.0053(5) 0.0071(5)
C30 0.0198(7) 0.0219(7) 0.0278(7) 0.0095(6) 0.0034(6) 0.0092(6)
C31 0.0206(7) 0.0317(8) 0.0181(7) 0.0095(6) 0.0044(5) 0.0091(6)
C32 0.0259(9) 0.1037(19) 0.1070(19) 0.0932(18) 0.0262(11) 0.0282(11)
C33 0.0353(11) 0.139(3) 0.157(3) 0.136(3) 0.0355(15) 0.0330(14)
C34 0.0269(9) 0.0866(16) 0.0618(13) 0.0571(13) 0.0176(9) 0.0147(10)
C35 0.0203(8) 0.0437(10) 0.0391(9) 0.0111(8) 0.0090(7) 0.0106(7)
C36 0.0243(8) 0.0272(8) 0.0489(10) 0.0115(8) 0.0068(7) 0.0099(7)

_geom_special_details
;
 All esds (except the esd in the dihedral angle between two l.s. planes)
 are estimated using the full covariance matrix.  The cell esds are taken
 into account individually in the estimation of esds in distances, angles
 and torsion angles; correlations between esds in cell parameters are only
 used when they are defined by crystal symmetry.  An approximate
(isotropic)
 treatment of cell esds is used for estimating esds involving l.s. planes.
;

loop_
 _geom_bond_atom_site_label_1
 _geom_bond_atom_site_label_2
 _geom_bond_distance
 _geom_bond_site_symmetry_2
 _geom_bond_publ_flag
Si1 O3 1.6519(11) . ?
Si1 C15 1.8558(17) . ?
Si1 C14 1.8578(17) . ?
Si1 C16 1.8873(19) . ?
Si2 O6 1.6528(11) . ?
Si2 C24 1.8600(18) . ?
Si2 C23 1.8625(18) . ?
Si2 C25 1.8812(16) . ?
O1 C1 1.4190(18) . ?
O1 C11 1.4289(18) . ?
O2 C11 1.426(2) . ?
```

```
O2 C2 1.4334(18) . ?
O3 C3 1.4199(17) . ?
O4 C9 1.4308(17) . ?
O4 C20 1.4473(18) . ?
O5 C20 1.4249(19) . ?
O5 C8 1.4302(18) . ?
O6 C7 1.4251(16) . ?
O7 C30 1.4251(18) . ?
O7 C5 1.4417(16) . ?
N1 C29 1.1443(19) . ?
C1 C2 1.544(2) . ?
C1 C10 1.5523(18) . ?
C1 H1A 1.0000 . ?
C2 C3 1.517(2) . ?
C2 H2A 1.0000 . ?
C3 C4 1.533(2) . ?
C3 H3A 1.0000 . ?
C4 C5 1.5453(19) . ?
C4 H4A 0.9900 . ?
C4 H4B 0.9900 . ?
C5 C6 1.5299(19) . ?
C5 C10 1.5618(19) . ?
C6 C7 1.5229(19) . ?
C6 H6A 0.9900 . ?
C6 H6B 0.9900 . ?
C7 C8 1.528(2) . ?
C7 H7A 1.0000 . ?
C8 C9 1.5362(19) . ?
C8 H8A 1.0000 . ?
C9 C10 1.5612(18) . ?
C9 H9A 1.0000 . ?
C10 C29 1.4804(19) . ?
C11 C12 1.510(2) . ?
C11 C13 1.520(2) . ?
C12 H12A 0.9800 . ?
C12 H12B 0.9800 . ?
C12 H12C 0.9800 . ?
C13 H13A 0.9800 . ?
C13 H13B 0.9800 . ?
C13 H13C 0.9800 . ?
C14 H14A 0.9800 . ?
C14 H14B 0.9800 . ?
C14 H14C 0.9800 . ?
C15 H15A 0.9800 . ?
C15 H15B 0.9800 . ?
C15 H15C 0.9800 . ?
C16 C18 1.511(4) . ?
C16 C19 1.515(3) . ?
C16 C17 1.528(3) . ?
C17 H17A 0.9800 . ?
C17 H17B 0.9800 . ?
C17 H17C 0.9800 . ?
C18 H18A 0.9800 . ?
C18 H18B 0.9800 . ?
C18 H18C 0.9800 . ?
C19 H19A 0.9800 . ?
C19 H19B 0.9800 . ?
C19 H19C 0.9800 . ?
C20 C21 1.509(2) . ?
C20 C22 1.525(2) . ?
C21 H21A 0.9800 . ?
C21 H21B 0.9800 . ?
   C21 H21C 0.9800 . ?
```

```
 C22 H22A 0.9800 . ?
 C22 H22B 0.9800 . ?
 C22 H22C 0.9800 . ?
 C23 H23A 0.9800 . ?
 C23 H23B 0.9800 . ?
 C23 H23C 0.9800 . ?
 C24 H24A 0.9800 . ?
 C24 H24B 0.9800 . ?
 C24 H24C 0.9800 . ?
 C25 C28 1.531(2) . ?
 C25 C26 1.535(2) . ?
 C25 C27 1.545(3) . ?
 C26 H26A 0.9800 . ?
 C26 H26B 0.9800 . ?
 C26 H26C 0.9800 . ?
 C27 H27A 0.9800 . ?
 C27 H27B 0.9800 . ?
 C27 H27C 0.9800 . ?
 C28 H28A 0.9800 . ?
 C28 H28B 0.9800 . ?
 C28 H28C 0.9800 . ?
 C30 C31 1.511(2) . ?
 C30 H30A 0.9900 . ?
 C30 H30B 0.9900 . ?
 C31 C32 1.379(3) . ?
 C31 C36 1.389(2) . ?
 C32 C33 1.394(3) . ?
 C32 H32A 0.9500 . ?
 C33 C34 1.372(3) . ?
 C33 H33A 0.9500 . ?
 C34 C35 1.370(3) . ?
 C34 H34A 0.9500 . ?
 C35 C36 1.386(3) . ?
 C35 H35A 0.9500 . ?
 C36 H36A 0.9500 . ?

 loop_
  _geom_angle_atom_site_label_1
  _geom_angle_atom_site_label_2
  _geom_angle_atom_site_label_3
  _geom_angle
  _geom_angle_site_symmetry_1
  _geom_angle_site_symmetry_3
  _geom_angle_publ_flag
 O3 Si1 C15 106.90(8) . . ?
 O3 Si1 C14 111.00(7) . . ?
 C15 Si1 C14 108.29(9) . . ?
 O3 Si1 C16 107.22(7) . . ?
 C15 Si1 C16 111.45(9) . . ?
 C14 Si1 C16 111.88(9) . . ?
 O6 Si2 C24 110.97(7) . . ?
 O6 Si2 C23 107.09(7) . . ?
 C24 Si2 C23 110.73(10) . . ?
 O6 Si2 C25 107.40(7) . . ?
 C24 Si2 C25 110.91(8) . . ?
 C23 Si2 C25 109.61(8) . . ?
 C1 O1 C11 106.10(11) . . ?
 C11 O2 C2 108.79(11) . . ?
 C3 O3 Si1 129.21(10) . . ?
 C9 O4 C20 108.76(11) . . ?
 C20 O5 C8 105.09(11) . . ?
 C7 O6 Si2 128.48(9) . . ?
 C30 O7 C5 117.54(11) . . ?
```

```
O1 C1 C2 104.18(11) . . ?
O1 C1 C10 110.57(11) . . ?
C2 C1 C10 114.97(11) . . ?
O1 C1 H1A 109.0 . . ?
C2 C1 H1A 109.0 . . ?
C10 C1 H1A 109.0 . . ?
O2 C2 C3 108.82(12) . . ?
O2 C2 C1 103.99(12) . . ?
C3 C2 C1 113.47(12) . . ?
O2 C2 H2A 110.1 . . ?
C3 C2 H2A 110.1 . . ?
C1 C2 H2A 110.1 . . ?
O3 C3 C2 109.74(12) . . ?
O3 C3 C4 108.40(12) . . ?
C2 C3 C4 111.63(12) . . ?
O3 C3 H3A 109.0 . . ?
C2 C3 H3A 109.0 . . ?
C4 C3 H3A 109.0 . . ?
C3 C4 C5 115.32(12) . . ?
C3 C4 H4A 108.4 . . ?
C5 C4 H4A 108.4 . . ?
C3 C4 H4B 108.4 . . ?
C5 C4 H4B 108.4 . . ?
H4A C4 H4B 107.5 . . ?
O7 C5 C6 113.38(11) . . ?
O7 C5 C4 111.85(11) . . ?
C6 C5 C4 109.74(11) . . ?
O7 C5 C10 100.58(10) . . ?
C6 C5 C10 110.48(11) . . ?
C4 C5 C10 110.52(11) . . ?
C7 C6 C5 116.09(11) . . ?
C7 C6 H6A 108.3 . . ?
C5 C6 H6A 108.3 . . ?
C7 C6 H6B 108.3 . . ?
C5 C6 H6B 108.3 . . ?
H6A C6 H6B 107.4 . . ?
O6 C7 C6 111.02(11) . . ?
O6 C7 C8 107.94(11) . . ?
C6 C7 C8 113.14(12) . . ?
O6 C7 H7A 108.2 . . ?
C6 C7 H7A 108.2 . . ?
C8 C7 H7A 108.2 . . ?
O5 C8 C7 109.48(11) . . ?
O5 C8 C9 102.01(11) . . ?
C7 C8 C9 119.83(12) . . ?
O5 C8 H8A 108.3 . . ?
C7 C8 H8A 108.3 . . ?
C9 C8 H8A 108.3 . . ?
O4 C9 C8 103.55(11) . . ?
O4 C9 C10 110.01(11) . . ?
C8 C9 C10 116.52(11) . . ?
O4 C9 H9A 108.8 . . ?
C8 C9 H9A 108.8 . . ?
C10 C9 H9A 108.8 . . ?
C29 C10 C1 109.08(11) . . ?
C29 C10 C9 109.40(11) . . ?
C1 C10 C9 110.19(11) . . ?
C29 C10 C5 109.40(11) . . ?
C1 C10 C5 107.47(11) . . ?
C9 C10 C5 111.26(11) . . ?
O2 C11 O1 105.13(11) . . ?
O2 C11 C12 109.03(14) . . ?
   O1 C11 C12 108.02(13) . . ?
```

```
O2 C11 C13 110.11(14) . . ?
O1 C11 C13 110.96(13) . . ?
C12 C11 C13 113.25(14) . . ?
C11 C12 H12A 109.5 . . ?
C11 C12 H12B 109.5 . . ?
H12A C12 H12B 109.5 . . ?
C11 C12 H12C 109.5 . . ?
H12A C12 H12C 109.5 . . ?
H12B C12 H12C 109.5 . . ?
C11 C13 H13A 109.5 . . ?
C11 C13 H13B 109.5 . . ?
H13A C13 H13B 109.5 . . ?
C11 C13 H13C 109.5 . . ?
H13A C13 H13C 109.5 . . ?
H13B C13 H13C 109.5 . . ?
Si1 C14 H14A 109.5 . . ?
Si1 C14 H14B 109.5 . . ?
H14A C14 H14B 109.5 . . ?
Si1 C14 H14C 109.5 . . ?
H14A C14 H14C 109.5 . . ?
H14B C14 H14C 109.5 . . ?
Si1 C15 H15A 109.5 . . ?
Si1 C15 H15B 109.5 . . ?
H15A C15 H15B 109.5 . . ?
Si1 C15 H15C 109.5 . . ?
H15A C15 H15C 109.5 . . ?
H15B C15 H15C 109.5 . . ?
C18 C16 C19 111.0(2) . . ?
C18 C16 C17 107.4(3) . . ?
C19 C16 C17 108.5(2) . . ?
C18 C16 Si1 109.83(17) . . ?
C19 C16 Si1 110.08(15) . . ?
C17 C16 Si1 110.03(15) . . ?
C16 C17 H17A 109.5 . . ?
C16 C17 H17B 109.5 . . ?
H17A C17 H17B 109.5 . . ?
C16 C17 H17C 109.5 . . ?
H17A C17 H17C 109.5 . . ?
H17B C17 H17C 109.5 . . ?
C16 C18 H18A 109.5 . . ?
C16 C18 H18B 109.5 . . ?
H18A C18 H18B 109.5 . . ?
C16 C18 H18C 109.5 . . ?
H18A C18 H18C 109.5 . . ?
H18B C18 H18C 109.5 . . ?
C16 C19 H19A 109.5 . . ?
C16 C19 H19B 109.5 . . ?
H19A C19 H19B 109.5 . . ?
C16 C19 H19C 109.5 . . ?
H19A C19 H19C 109.5 . . ?
H19B C19 H19C 109.5 . . ?
O5 C20 O4 104.74(11) . . ?
O5 C20 C21 108.46(14) . . ?
O4 C20 C21 110.24(13) . . ?
O5 C20 C22 111.67(14) . . ?
O4 C20 C22 108.83(14) . . ?
C21 C20 C22 112.62(15) . . ?
C20 C21 H21A 109.5 . . ?
C20 C21 H21B 109.5 . . ?
H21A C21 H21B 109.5 . . ?
C20 C21 H21C 109.5 . . ?
H21A C21 H21C 109.5 . . ?
H21B C21 H21C 109.5 . . ?
```

```
C20 C22 H22A 109.5 . . ?
C20 C22 H22B 109.5 . . ?
H22A C22 H22B 109.5 . . ?
C20 C22 H22C 109.5 . . ?
H22A C22 H22C 109.5 . . ?
H22B C22 H22C 109.5 . . ?
Si2 C23 H23A 109.5 . . ?
Si2 C23 H23B 109.5 . . ?
H23A C23 H23B 109.5 . . ?
Si2 C23 H23C 109.5 . . ?
H23A C23 H23C 109.5 . . ?
H23B C23 H23C 109.5 . . ?
Si2 C24 H24A 109.5 . . ?
Si2 C24 H24B 109.5 . . ?
H24A C24 H24B 109.5 . . ?
Si2 C24 H24C 109.5 . . ?
H24A C24 H24C 109.5 . . ?
H24B C24 H24C 109.5 . . ?
C28 C25 C26 108.71(16) . . ?
C28 C25 C27 108.88(15) . . ?
C26 C25 C27 109.48(16) . . ?
C28 C25 Si2 111.01(12) . . ?
C26 C25 Si2 109.78(11) . . ?
C27 C25 Si2 108.95(12) . . ?
C25 C26 H26A 109.5 . . ?
C25 C26 H26B 109.5 . . ?
H26A C26 H26B 109.5 . . ?
C25 C26 H26C 109.5 . . ?
H26A C26 H26C 109.5 . . ?
H26B C26 H26C 109.5 . . ?
C25 C27 H27A 109.5 . . ?
C25 C27 H27B 109.5 . . ?
H27A C27 H27B 109.5 . . ?
C25 C27 H27C 109.5 . . ?
H27A C27 H27C 109.5 . . ?
H27B C27 H27C 109.5 . . ?
C25 C28 H28A 109.5 . . ?
C25 C28 H28B 109.5 . . ?
H28A C28 H28B 109.5 . . ?
C25 C28 H28C 109.5 . . ?
H28A C28 H28C 109.5 . . ?
H28B C28 H28C 109.5 . . ?
N1 C29 C10 178.58(14) . . ?
O7 C30 C31 109.14(12) . . ?
O7 C30 H30A 109.9 . . ?
C31 C30 H30A 109.9 . . ?
O7 C30 H30B 109.9 . . ?
C31 C30 H30B 109.9 . . ?
H30A C30 H30B 108.3 . . ?
C32 C31 C36 117.71(16) . . ?
C32 C31 C30 122.33(14) . . ?
C36 C31 C30 119.91(15) . . ?
C31 C32 C33 120.56(19) . . ?
C31 C32 H32A 119.7 . . ?
C33 C32 H32A 119.7 . . ?
C34 C33 C32 120.9(2) . . ?
C34 C33 H33A 119.6 . . ?
C32 C33 H33A 119.6 . . ?
C35 C34 C33 119.22(18) . . ?
C35 C34 H34A 120.4 . . ?
C33 C34 H34A 120.4 . . ?
C34 C35 C36 120.00(17) . . ?
   C34 C35 H35A 120.0 . . ?
```

```
C36 C35 H35A 120.0 . . ?
C35 C36 C31 121.60(18) . . ?
C35 C36 H36A 119.2 . . ?
C31 C36 H36A 119.2 . . ?

loop_
 _geom_torsion_atom_site_label_1
 _geom_torsion_atom_site_label_2
 _geom_torsion_atom_site_label_3
 _geom_torsion_atom_site_label_4
 _geom_torsion
 _geom_torsion_site_symmetry_1
 _geom_torsion_site_symmetry_2
 _geom_torsion_site_symmetry_3
 _geom_torsion_site_symmetry_4
 _geom_torsion_publ_flag
C15 Si1 O3 C3 -128.78(14) . . . . ?
C14 Si1 O3 C3 -10.87(16) . . . . ?
C16 Si1 O3 C3 111.60(14) . . . . ?
C24 Si2 O6 C7 3.08(14) . . . . ?
C23 Si2 O6 C7 -117.88(13) . . . . ?
C25 Si2 O6 C7 124.46(12) . . . . ?
C11 O1 C1 C2 30.78(13) . . . . ?
C11 O1 C1 C10 154.82(11) . . . . ?
C11 O2 C2 C3 -127.46(13) . . . . ?
C11 O2 C2 C1 -6.22(15) . . . . ?
O1 C1 C2 O2 -15.05(14) . . . . ?
C10 C1 C2 O2 -136.21(12) . . . . ?
O1 C1 C2 C3 103.03(13) . . . . ?
C10 C1 C2 C3 -18.14(18) . . . . ?
Si1 O3 C3 C2 107.05(14) . . . . ?
Si1 O3 C3 C4 -130.80(13) . . . . ?
O2 C2 C3 O3 -69.69(15) . . . . ?
C1 C2 C3 O3 175.06(12) . . . . ?
O2 C2 C3 C4 170.11(12) . . . . ?
C1 C2 C3 C4 54.86(17) . . . . ?
O3 C3 C4 C5 -151.20(12) . . . . ?
C2 C3 C4 C5 -30.21(18) . . . . ?
C30 O7 C5 C6 -59.41(15) . . . . ?
C30 O7 C5 C4 65.33(15) . . . . ?
C30 O7 C5 C10 -177.35(11) . . . . ?
C3 C4 C5 O7 82.62(15) . . . . ?
C3 C4 C5 C6 -150.65(13) . . . . ?
C3 C4 C5 C10 -28.56(17) . . . . ?
O7 C5 C6 C7 -54.31(16) . . . . ?
C4 C5 C6 C7 179.82(12) . . . . ?
C10 C5 C6 C7 57.71(16) . . . . ?
Si2 O6 C7 C6 116.79(12) . . . . ?
Si2 O6 C7 C8 -118.68(11) . . . . ?
C5 C6 C7 O6 77.98(15) . . . . ?
C5 C6 C7 C8 -43.56(17) . . . . ?
C20 O5 C8 C7 167.78(11) . . . . ?
C20 O5 C8 C9 39.85(14) . . . . ?
O6 C7 C8 O5 147.95(11) . . . . ?
C6 C7 C8 O5 -88.79(14) . . . . ?
O6 C7 C8 C9 -94.84(14) . . . . ?
C6 C7 C8 C9 28.41(18) . . . . ?
C20 O4 C9 C8 7.05(14) . . . . ?
C20 O4 C9 C10 -118.16(12) . . . . ?
O5 C8 C9 O4 -28.44(13) . . . . ?
C7 C8 C9 O4 -149.44(12) . . . . ?
O5 C8 C9 C10 92.48(13) . . . . ?
C7 C8 C9 C10 -28.52(18) . . . . ?
```

```
O1 C1 C10 C29 -38.91(15) . . . . ?
C2 C1 C10 C29 78.69(15) . . . . ?
O1 C1 C10 C9 81.20(14) . . . . ?
C2 C1 C10 C9 -161.20(12) . . . . ?
O1 C1 C10 C5 -157.42(11) . . . . ?
C2 C1 C10 C5 -39.82(15) . . . . ?
O4 C9 C10 C29 36.94(15) . . . . ?
C8 C9 C10 C29 -80.48(15) . . . . ?
O4 C9 C10 C1 -82.97(13) . . . . ?
C8 C9 C10 C1 159.61(12) . . . . ?
O4 C9 C10 C5 157.94(11) . . . . ?
C8 C9 C10 C5 40.52(16) . . . . ?
O7 C5 C10 C29 -172.89(10) . . . . ?
C6 C5 C10 C29 67.06(14) . . . . ?
C4 C5 C10 C29 -54.59(14) . . . . ?
O7 C5 C10 C1 -54.59(12) . . . . ?
C6 C5 C10 C1 -174.64(11) . . . . ?
C4 C5 C10 C1 63.71(14) . . . . ?
O7 C5 C10 C9 66.11(12) . . . . ?
C6 C5 C10 C9 -53.93(14) . . . . ?
C4 C5 C10 C9 -175.59(11) . . . . ?
C2 O2 C11 O1 25.27(15) . . . . ?
C2 O2 C11 C12 140.88(13) . . . . ?
C2 O2 C11 C13 -94.31(15) . . . . ?
C1 O1 C11 O2 -35.31(14) . . . . ?
C1 O1 C11 C12 -151.62(13) . . . . ?
C1 O1 C11 C13 83.70(15) . . . . ?
O3 Si1 C16 C18 -74.8(2) . . . . ?
C15 Si1 C16 C18 168.5(2) . . . . ?
C14 Si1 C16 C18 47.1(2) . . . . ?
O3 Si1 C16 C19 47.7(2) . . . . ?
C15 Si1 C16 C19 -69.0(2) . . . . ?
C14 Si1 C16 C19 169.62(19) . . . . ?
O3 Si1 C16 C17 167.2(2) . . . . ?
C15 Si1 C16 C17 50.6(2) . . . . ?
C14 Si1 C16 C17 -70.9(2) . . . . ?
C8 O5 C20 O4 -36.25(15) . . . . ?
C8 O5 C20 C21 -153.95(13) . . . . ?
C8 O5 C20 C22 81.37(16) . . . . ?
C9 O4 C20 O5 17.17(16) . . . . ?
C9 O4 C20 C21 133.65(13) . . . . ?
C9 O4 C20 C22 -102.38(14) . . . . ?
O6 Si2 C25 C28 -71.56(14) . . . . ?
C24 Si2 C25 C28 49.86(16) . . . . ?
C23 Si2 C25 C28 172.43(13) . . . . ?
O6 Si2 C25 C26 48.66(14) . . . . ?
C24 Si2 C25 C26 170.08(13) . . . . ?
C23 Si2 C25 C26 -67.35(15) . . . . ?
O6 Si2 C25 C27 168.55(12) . . . . ?
C24 Si2 C25 C27 -70.04(15) . . . . ?
C23 Si2 C25 C27 52.54(15) . . . . ?
C1 C10 C29 N1 -46(6) . . . . ?
C9 C10 C29 N1 -167(6) . . . . ?
C5 C10 C29 N1 71(6) . . . . ?
C5 O7 C30 C31 -177.17(11) . . . . ?
O7 C30 C31 C32 3.6(2) . . . . ?
O7 C30 C31 C36 -178.85(14) . . . . ?
C36 C31 C32 C33 0.0(4) . . . . ?
C30 C31 C32 C33 177.6(2) . . . . ?
C31 C32 C33 C34 1.4(5) . . . . ?
C32 C33 C34 C35 -1.8(5) . . . . ?
C33 C34 C35 C36 0.8(3) . . . . ?
   C34 C35 C36 C31 0.7(3) . . . . ?
```

```
C32 C31 C36 C35 -1.1(3) . . . . ?
C30 C31 C36 C35 -178.69(16) . . . . ?
```